UNIVERSITA' DEGLI STUDI DI SALERNO

Dipartimento di Medicina, Chirurgia e Odontoiatria

"*Scuola Medica Salernitana*"

MEDICINA TRASLAZIONALE DELLO SVILUPPO E DELL'INVECCHIAMENTO ATTIVO

XXXII Ciclo

Curriculum
TECNOLOGIE INNOVATIVE IN MEDICINA TRASLAZIONALE

Tesi di Dottorato

Ph.D. Thesis

Post-transcriptional gene regulatory networks in chronic airway inflammation: role of RNA-binding proteins

Relatore	**Candidato**
Ch. Prof.ssa Cristiana STELLATO	Luca RICCIARDI
Coordinatore	Matricola 8800900017
Ch. Prof. Palmiero MONTELEONE	

Anno Accademico 2018/19

Index

ABSTRACT

Background. RNA-binding proteins (RBPs) play a key role in post-transcriptional gene regulation (PTGR) of genes involved in numerous biological processes. These proteins act through the binding to specific *cis*-elements present in their RNA targets and by forming, with other regulatory factors, dynamic ribonucleoprotein complexes (RNPs) that ultimately determine the fate of different type of RNAs. There are several families of RBPs classified according to the type of RNA target that they bind and this thesis focused on the study of RBPs that regulate the turnover and translation of messenger RNA (mRBPs). Multiple studies in the last decade have established that aberrant expression and function of RBPs participate to cancer pathogenesis by altering the stability and translation of genes involved in many mechanism of neoplastic transformation. Many of the cancer-related pathways for which PTGR mediated by RBPs has been established are also critically involved in chronic inflammation; to this end, many important basic and preclinical studies and gene ablation animal models indicate that RBPs are critically involved also in inflammatory responses and immunity. In contrast to the growing number of studies on the role pf RBPs in human cancer, translational studies based on chronic inflammatory disease are still scarce.

Aims. In this thesis we aimed at studying the expression profile of mRBPs in two major human chronic lung inflammatory diseases: chronic obstructive pulmonary disease (COPD) and bronchial asthma and to proceed with the characterization of their functional role in disease pathogenesis. On these studies, our long-term aim is to explore mRBP therapeutic targeting, for which we plan to develop dedicated experimental models.

Results. . In our first study we focused on three RBPs, Tristetraprolin (TTP), AU-binding factor 1 (AUF-1) and Human Antigen R (HuR). These proteins recognize core sequences mostly present in the 3'-Untraslated Region (UTR) of numerous mRNAs involved in inflammatory process. HuR acts mainly as a positive regulator of mRNA stability and translation, while TTP and AUF-1 appear to limit these functions. RBPs expression was evaluated by immunohistochemistry in bronchial and peripheral lung samples from mild-to-moderate stable COPD patients and age/smoking history-matched smoker with normal lung function as controls (n=12 both cohorts)*. For the first time, selective downregulation of AUF-1 was identified in airway epithelium of COPD patients vs. controls. Results were confirmed in a publicly available microarray database of primary epithelial cells obtained from bronchial brushing of COPD patients and non-smoking and smoking subjects as controls (n=6/12/12 each). Results were also validated in *in vitro* studies, using the normal human airway epithelial BEAS-2B cell line stimulated with hydrogen peroxide, cytokine combination (Cytomix), cigarette smoke extract (CSE) - which are well-established models of chronic inflammation and oxidative stress occurring in COPD - also following siRNA-mediated silencing. The chosen i*n vitro* stimulations recapitulate the selective decrease of AUF-1. We also observed, in the public transcriptomic database previously probed, that decrease in AUF-1 in epithelial cells of COPD patients paralleled significant alteration of a curated list of AUF-1-regulated inflammatory transcripts.

Based on these results, the investigation continued in two directions: in one study, the analysis of RBP profile was broadened, by performing an *in silico* analysis of the expression profile of ~ 600 mRBPs, derived from a published RBP census, in stable COPD and severe bronchial asthma. The mRBP list was searched in two selected transcriptomic datasets of primary airway epithelium, isolated by bronchial brushing in patients vs control cohorts. *In silico* analysis revealed a peculiar mRBPs modulation in COPD patients compared with non-smoking and smoking controls, with predominant RBP downregulation. Cluster analysis identified a group of disease-related coexpressed RBPs. Genome ontology identified in the RBP profile the involvement in important COPD pathogenic processes. Strikingly, no significant modulation of RBPs was found in the dataset of patients with severe asthma versus controls.

As for the second direction, we focused on further characterization of the role of AUF-I in airway epithelium. Using an RNA immunoprecipitation and sequencing (RIP-Seq) approach, we identified AUF-1 targets in the airway epithelial cell line BEAS-2B and identified specific interacting sequences in targeted transcripts. The list of AUF-1 targeted transcripts was then searched within the public transcriptomic database of COPD patients and controls previously probed. Dysregulation of AUF1-trascripts in COPD patients compared to no-smoker and smoker controls was therefore identified and used to guide the selection of the transcripts to perform validation studies (ongoing).

Conclusions. The studies performed for this thesis have identified novel expression profiles of RBPs in COPD and severe asthma. In particular, significant changes in RBPs expression characterize the bronchial epithelial response elicited by the COPD pathophysiology, while surprisingly lacking in epithelial transcriptomics of severe asthma patients compared to healthy controls. Among the RBPs, AUF-1 may play a pathogenic role in COPD by altering post-transcriptional control of epithelial gene expression, thus contributing to increased airway inflammation. Overall,

identification of these changes can be used to infer putative pathogenetic roles of mRBPs and identify novel disease-related regulatory networks.

Complete list of study subjects' clinical characteristics are in Study #1 (page 83, Table 1)

Part 1.

RNA-Binding Proteins and Their Role
in Post-Transcriptional Gene Regulation

1. Posttrancriptional gene regulation (PTGR): definition and relationship with other gene regulatory mechanims

Gene expression is a set of integrated processes through which the information contained in a gene is converted into a functional protein. Regulatory mechanisms are in place from early nuclear events, that lead to transcription of DNA-encoded genes to messenger RNA (mRNA); the life cycle of mRNAs is then regulated through its nuclear and cytoplasmatic stages, followed by cytoplasmic-based mechanisms controlling protein translation and post-translational protein modifications (Figure 1). Based on this multi-step process, cells are able to conform gene expression to perform basic homeostatic functions (cell cycle, differentiation and programmed cell death) and to respond to environmental stimuli, shaping the phenotypic characteristics of various biological responses.

The multiple regulatory mechanisms overseeing gene expression act in a highly coordinated manner over time and space. In the last decades, a better understanding of fundamentals in RNA biology assigned a greater importance than previously recognized to the role that RNA metabolism plays within cellular mechanisms. These studies clear indicate that mRNA is not a simple intermediary between genes and proteins, but it is an important regulatory node for regulating the trimming and amplitude of protein expression.
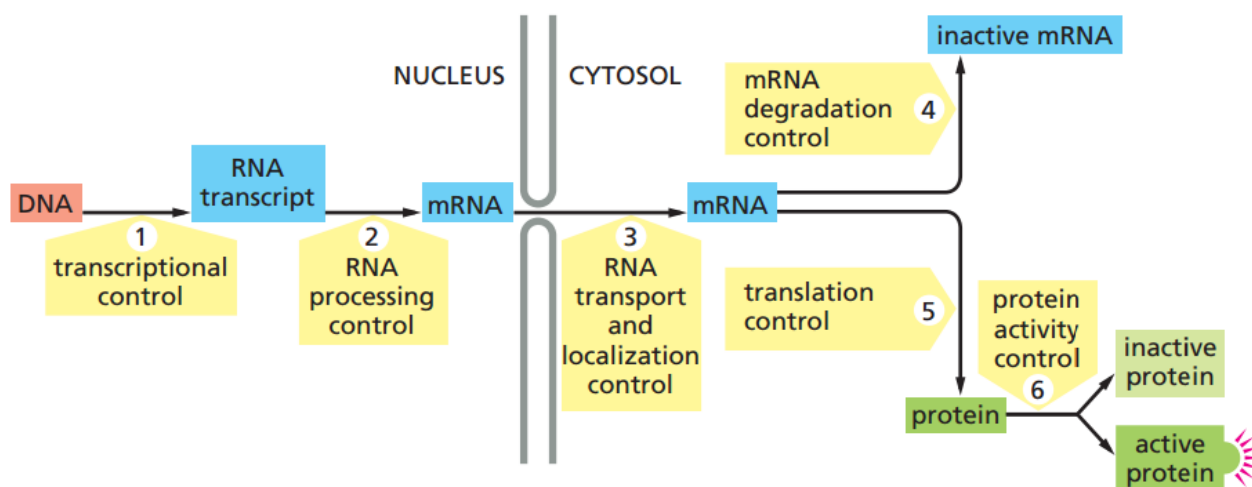
Figure 1 Regulatory steps of gene expression. Multi-step control of gene expression guards the flow of the information carried by a gene into successful translation in a fully functional protein. Control of RNA metabolism and translation (yellow boxes 2 to 5) is a multi-faceted regulatory component contributing to diversification of protein expression as well as modulation of its timing and amplitude.[1]

Gene expression starts with modifications of the chromatin structure that regulate access of the transcription machinery to DNA. During the cell cycle, chromatin is present in two forms: the transcriptionally active euchromatin and heterochromatin, which is more compact than euchromatin and transcriptionally inactive. Difference in chromatin packing determines the degree of accessibility of transcription factors (TFs),

regulatory proteins that activate or inhibit the transcription of genes through binding to specific DNA sequence called response elements. In the heterochromatin, DNA wraps around histone proteins, forming nucleosomes. Heterochromatin is composed mainly of repetitive sequences and is divided into two types: constitutive heterochromatin in which DNA is permanently inaccessible, present for example in the centromeres, and facultative heterochromatin. The latter can acquire the characteristics of euchromatin according to the cell type and stage of cell differentiation. Euchromatin, unlike heterochromatin, contains more non-histone proteins and consists of poorly repetitive sequences. In this configuration the chromatin is structurally loose to allow access to RNA and DNA polymerases that transcribe and replicate the DNA strand. The processes of acetylation, phosphorylation and methylation act on the tails of both types of chromatin, modifying its degree of spiralling and making it more or less available for transcription (Figure 2).
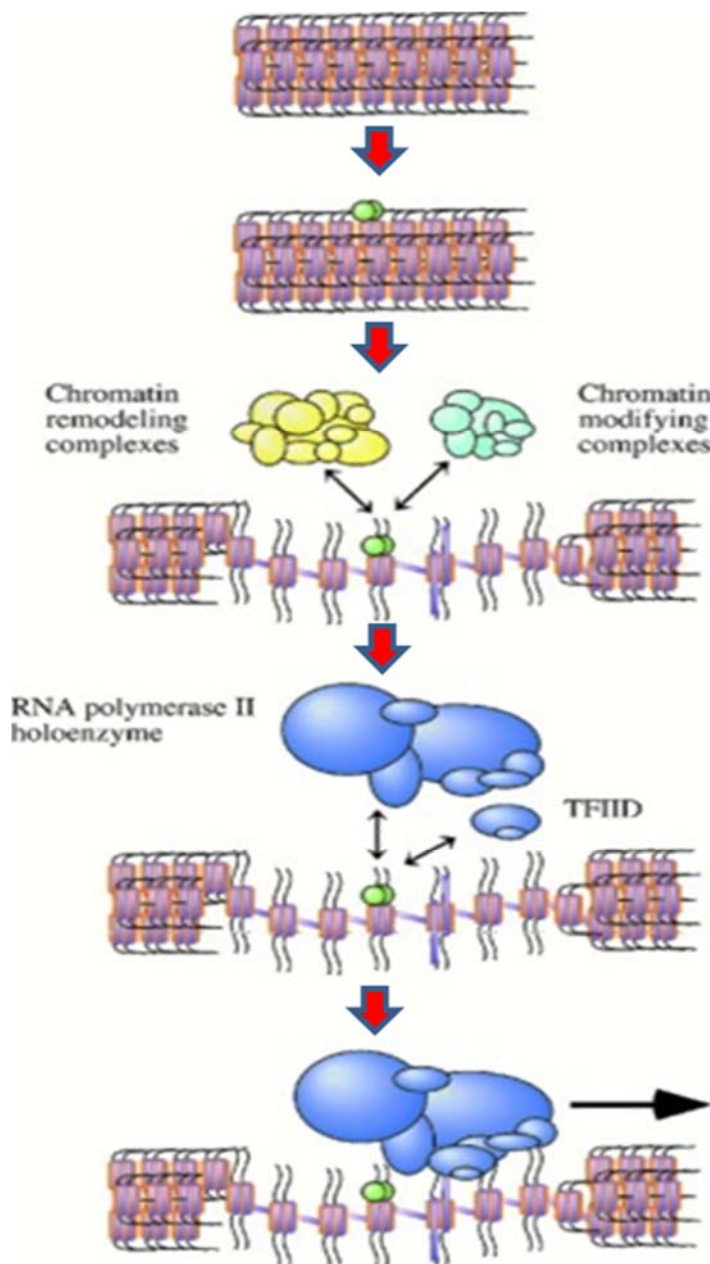
Figure 2. Model of chromatin changes during transcriptional gene activation. When not involved in active transcription, DNA is complexed with histone proteins in the form of heterochromatin. Following the cell's transcriptional requests, activating factors bind to specific DNA sequences and recruit both chromatin remodelling and modifying factors. These proteins bind to chromatin and alter its structure, forming the eucromatin and allow access to the promoter sequences for recruitment of the transcriptional machinery, such as RNA polymerase II (Pol II) holoenzyme, TATA-box binding protein (TBP) and other components of the transcriptional apparatus.[2]

Transcription allows the transfer of the gene-specific information into an mRNA molecule. Transcription occurs when RNA polymerases are recruited on specific DNA sequences, called promoters that act as regulatory hubs. In eukaryotes, in fact, RNA polymerase II (Pol II) is unable to bind DNA sequences directly and instead interacts with a series of regulatory proteins and TFs. These factors must bind to the promoter before RNA polymerase can dock and perform its function. Specific cis-regulatory elements, called enhancers and silencers, are able to significantly increase or inhibit, respectively, the rate of transcription for the gene under their control. Enhancers can be located far from the regulated gene, thus requiring a folding of the DNA to allow TF binding and proper assembly of the transcription machinery. Silencers determine instead inhibition of gene transcription by blocking the recruitment of RNA polymerase.[2-4]

Transcription leads to the synthesis of a precursor messenger RNA (pre-mRNA), which undergoes a series of modifications. Splicing is a key nuclear modification in which pre-RNA is transformed into a mature messenger RNA (mRNA). The splicing reaction is catalysed by a spliceosome, a protein complex formed by proteins and small molecules of nuclear RNA (snRNA, small nuclear RNA). At the end of splicing, the non-coding regions (introns) are removed while the coding regions (exons) are joined together. In alternative splicing, exons and introns can be combined in multiple ways to produce different mature mRNAs that encode different protein sequences. Through this crucial mechanism the cell can produce a greater number of proteins than that encoded by the genetic information, as part of the cellular response to the internal and external stimuli. The addition of a cap (capping) of 7-methylguanosine at the 5'-end and of a tail of poly-adenine (polyadenylation) at the 3'-end of the RNA chain protect the newly synthesized mature mRNA during transport from the nucleus to the cytosol; moreover, these structures guarantee protection from untimely decay and greater translation efficiency by assisting ribosome recognition.

Through the concerted action of different molecular species interacting with mRNA throughout the all stages of mRNA lifespan, post-transcriptional gene regulation (PTGR) regulates mRNA metabolism and protein translation rates. These regulatory factors are represented by RNA-binding proteins (RBPs) and by noncoding RNAs (ncRNA), mainly represented by microRNAs (miRNAs). These factors form dynamic ribonucleoprotein complexes (mRNPs) with targeted mRNAs via sequence-specific interactions.[5] Their concerted action on transcript localization, stability and translation critically influences the rate of protein output in fundamental process like cell cycle, proliferation and stress responses.[6-8] As further discussed in the following paragraphs, RBPs bind to sequence or structural elements in untranslated regions (UTRs) of protein-coding transcripts; specific control via base pairing to sequences mostly located in 3′-UTRs of target mRNAs is also exerted by miRNAs (Figure 3, paragraphs 2a and b).[9]
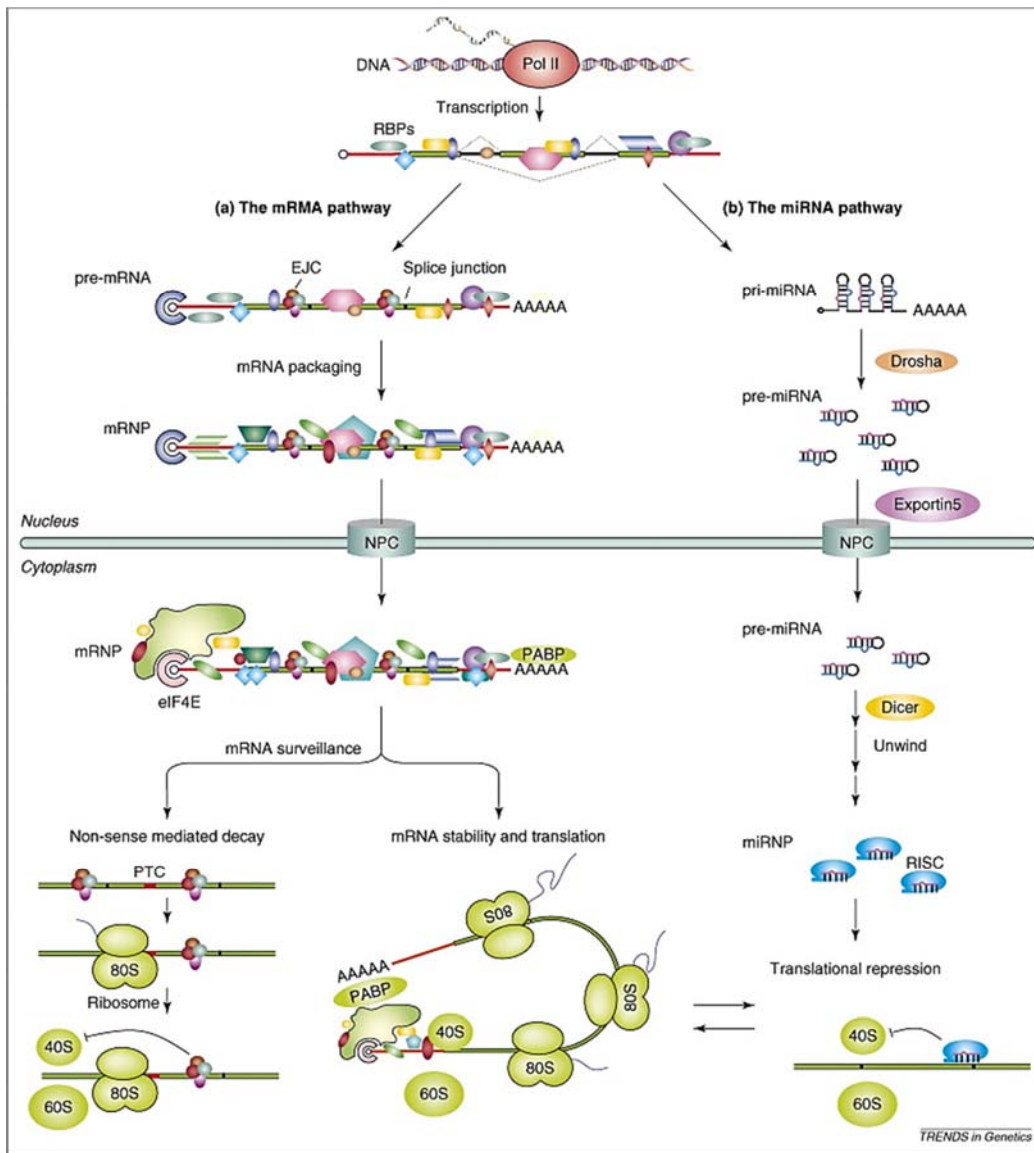
Figure 3. Pathways involved in post-transcriptional regulation. (a) In the mRNA pathway, the transcripts produced by RNA polymerase II (Pol II) are encoded in mature mRNAs. RBPs bind mRNAs, to which the exon junction complex (EJC) that regulates their cytoplasmic fate are also complexed. This first mechanism determines the formation of mRNPs over mature RNA. Then, transcripts are transported into the cytoplasm through the nuclear pores where new components are added to mRNPs. The function of mRNA surveillance further differentiates the fate of mRNA. Via Nonsense-mediated mRNA decay (NMD), mRNAs containing a premature stop codon (PTC) are rapidly and selectively degraded. mRNAs that have a normal stop codon are instead recognized by poly(A) binding protein (PABP) which binds the 3'end and promotes protein coding. (b) in the miRNA pathway, a primary transcript, pri-miRNA, is processed by the RNase Drosha which leads to the formation of the primary transcript, called pre-miRNA. Subsequently, the pre-miRNA is exported to the cytoplasm where becomes a mature miRNA upon processing by the endonuclease Dicer. One strand of the miRNA is then incorporated into the complex RNA-induced silencing complex (RISC) and allows the complex to recognize its target mRNAs and allow for its decay or translational suppression **(**see paragraphs 2a, 2b for further details).[10]

2. Pathways mediating PTGR

a. miRNA pathway

One of the main classes of sncRNAs, miRNAs are small endogenous single-stranded RNA molecules about 21-23n in length. They originate from primary double-stranded RNA transcripts, defined as pri-miRNA, produced by Pol II and characterized by the presence of a secondary structure rich in folds. The pri-miRNA is then processed in the nucleus by a microprocessor complex which includes Drosha, a type III RNase, and DGCR8 / Pasha.[11,12] This complex binds and cleaves double-stranded RNA to generate a second precursor, the pre-miRNA, about 70-80 nucleotides long with a hairpin structure and 3' protruding ends of two nucleotides. Pre-miRNAs are then exported to the cytoplasm in association with the nuclear membrane protein exportin 5, which mediates their translocation through the excision of the loop and subsequent maturation into pre-miRNA, through a RAN-GTP-mediated mechanism.[13] Once in the cytoplasm, pre-miRNAs undergo further processing done by Dicer, an RNase III endonuclease that recognizes the 3 'end deriving from the previous processing and produces the mature single-stranded miRNA, a molecule about 21 nucleotides long. Mature miRNAs will then be loaded into the RNA-induced silencing complex (RISC) to induce gene silencing. A key role in the regulatory activity mediated by the RISC complex is played by Argonaut proteins, 100 kDa-molecules containing two highly conserved RNA binding domains necessary for the formation of the RISC complex: the Piwi-Argonaute-Zwille (PAZ) domain (at the N-terminal end) and one PIWI domain at the C -terminal. The PAZ domain binds the 3' end to a single strand of the mature miRNA, while the PIWI domain binds the 5'-end. These interactions provide miRNA with the correct orientation for interaction with the target mRNA molecule. In mammalian cells, Argonaut proteins are divided into several subfamilies according to sequence similarity. The AGO family is composed of 4 members (AGO1, AGO2, AGO3 and AGO4) present in all mammalian cells and called E1F2C / hAgo in Homo Sapiens, and by the PIWI proteins which are present in germ line cells and in hematopoietic stem cells. Gene silencing can take place according to different mechanisms, according to the degree of complementarity between the miRNA and the 3'-UTR region of the target mRNA: a perfect complementarity promotes the endonucleotide cut and degradation of the mRNA, while a partial complementarity leads to repressed translation.

The substantial impact of miRNA-mediated post-transcriptional regulation is provided by studies indicating that a specific set of miRNAs was able to override a pre-existing transcriptional program: for example, somatic cells could be reprogrammed into induced pluripotent stem (iPS) cells via the ectopic expression of four miRNAs, mir-200c, mir-302, mir-369 and miR367.[14,15] Similarly, miR-9 and miR-124 were sufficient to mediate trans differentiation of human fibroblasts into neurons.[16]

b. mRNA pathway

Transcripts produced by Pol II are critically regulated by RBPs. As further discussed in the following paragraphs, these molecular species regulate all aspects of mRNA biogenesis, through sequence-specific interactions with the transcripts as well as by protein-protein interactions occurring among RBPs, forming functional units called ribonucleoprotein (RNP) complexes. Throughout the diverse phases of mRNA metabolism, RNP can dynamically change in composition by changes in expression and/or post-translational modifications (PTM) of RBP components. It is believed that these modifications, driven by homeostatic and pathological triggers, ultimately convey specificity of RBP-driven post-transcriptional regulation.

In order to be translated, a normal mature mRNA molecule has its 7-methylguanosine cap bound by the initiation factor eukaryotic translation initiation factor (eIF)-4E and its polyadenylated tail bound by the polyadenylate [poly(A)] binding protein (PABP). In particular, PABP is associated with the 3' end of the pre-mRNA and increases the affinity for transcript binding of the polyA polymerase that adds the poly (A) chain and promotes its translation.[17] Then, the ribosome removes the exon-exon junction complexes and begins amino acid chain elongation. Translation is complete when the ribosome reaches a termination codon. In this setting, RNPs modulate mRNA throughout the multi-step process of mRNA turnover and translation. The role of RBPs in this context will be further described in the following paragraphs and constitute the main focus of many studies, along with those performed for the present thesis, evaluating alteration of RBP-mediated PTGR in shaping protein expression in disease pathogenesis.

RBPs also participate to nonsense-mediated mRNA decay (NMD), in which mRNAs carrying premature termination codon (PTC) are selectively recognized and destroyed. The NMD is control mechanism ubiquitously present in eukaryotic cells and several pathologies and tumors are correlate to genetic mutations that determine the formation of PTC.[18] In the presence of a PTC, the ribosome is released before reaching the exon-exon junction complexes present downstream of a stop codon (Figure 4). The core NMD machinery comprises three trans-acting factors, called up-frameshift (UPF) proteins, which belong to the helicase family, recruited to mRNAs upon recognition of stop codons by the translation apparatus.[19-21]
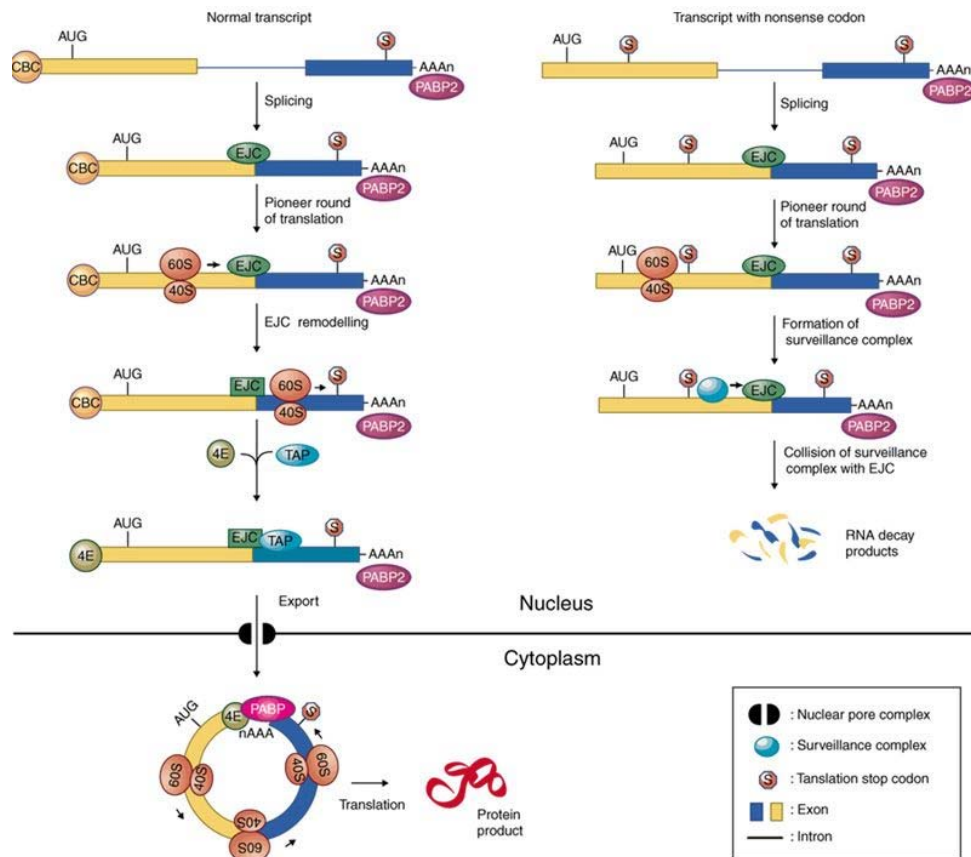
Figure 4. mRNA fate: differences between normal and nonsense codon-bearing transcripts (NMD). mRNA can undergo two different fates, depending on the presence or absence of the normal stop codon. During the splicing events, several proteins associate into an exon junction complex (EJC) on the exon – exon junctions. During the translation of mRNAs containing a normal stop codon, the EJC is reshaped and promotes the export of mRNA to the cytoplasm where protein synthesis takes place. On the contrary, in the presence of nonsense codons the ribosome suspends synthesis at this point and is converted into a surveillance complex. The interaction between this complex and the EJC leads to the decay of the mRNA.[22]

Termination of translation leads to the activation of the NMD and the assembly of a RNP complex called exon junction complex (EJC). This complex is located 24 nucleotides upstream of exon–exon junctions and remains associated with the mature mRNA until this is translated in the cytoplasm.[10,23] In the EJC complex, UPF1 is allowed to interact with the other two UPF proteins, UPF2 and UPF3. The PTC causes retention of EJC on mRNA and subsequent phosphorylation of UPF1 by interaction with UPF2 and UPF3. Subsequently, UPF1 phosphorylation triggers its dephosphorylation by various factors. Among these, the endonuclease heterodimer SMG5/SMG7 recruits phosphorylated UPF1 to cytoplasmic mRNA decay bodies and promotes deadenylation followed by decapping and exonucleolytic RNA decay. However, the interaction between the endonuclease SMG6 and phosphorylated UPF1 determines the endonucleolytic cut near the termination site and subsequent exonucleolytic degradation of the two fragments. The eukaryotic cells therefore succeed - through exoribonuclease degradation from 5′-to-3′ mediated by 5'-3' exoribonuclease 1 (XRN1) and exoribonuclease degradation 3′-to-5, mediated by the multiprotein ribonuclease complex exosome - to quickly eliminate the mRNA containing the PTC.[24]

c. Crosstalk between PTGR regulatory factors: miRNAs and RNA Binding Proteins (RBPs)

The miRNA- and RBP-mediated pathways of regulation may collaborate or compete on specific mRNA substrates for a particular binding site on an mRNA, indicating important synergistic or antagonistic functions, respectively. Complex and diverse combinations of regulatory molecules (miRNA/RBP, RBP/RBP, miRNA/miRNA) (Figure 5) entail functional outcomes highly dependent form the biological context[7]. Crosstalk between RBPs will be further discussed in subsequent paragraph (3b/iii).
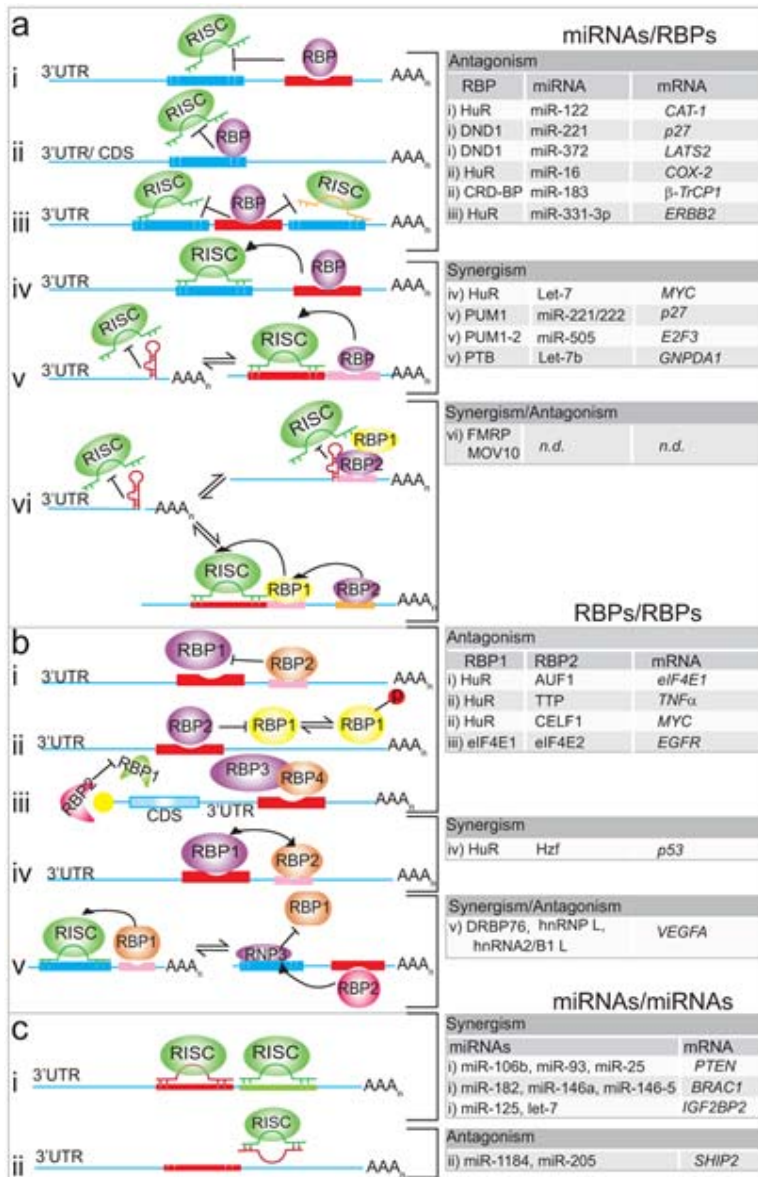
Figure 5. Crosstalk between miRNAs and RBPs. (a): interactions RBP/miRNA. Left upper panel: when in antagonism, the binding of the RBP to the transcript prevents the binding of the miRNAs. The RBP can bind the transcript next to the RISC binding site (i), overlap in 3'-UTRs or coding sequences (CDS) (ii), or in between sites (iii). Left middle panel: when in synergism, RBPs can promote the link between RISC and transcript (iv), modifying local RNA structures (v). Left lower panel: Different ways of interacting between RBPs can influence RISC activity in either synergistic or antagonistic manner (vi). **(b): interactions RBP/RBP.** Left upper panel: two RBPs can compete with each other for distinct binding sites (i) or for the same (ii). Furthermore, the translation initiation factors can also compete for a region in the cap end of the transcript (iii). Left middle panel: The export of mature mRNA and protein synthesis can be promoted by a cooperative mechanism among RBPs (iv). Left lower panel: example of possible antagonistic or synergistic interaction of RBP on a target transcript (VEGF-α) (v). **(c): interactions miRNA/miRNA.** RISCs can also act synergistically or antagonistically. Left upper panel: as a result of synergism (i), a greater inhibition of the expression of the transcript is possible. Left lower panel: (ii) antagonistic interplay between RISC determine an increase of target expression.[7]

3. Determinants of posttranscriptional regulation: focus on RBPs

a. General view of RBPs

Over the past two decades the development of large-scale analytic methods, as next-generation sequencing and advanced application of mass spectrometry, has enabled the genome-wide identification of RBPs, of their protein cofactors and many of their RNA targets. However, many questions remain to be answered. An authoritative study conducted by Gerstberger et al[25] presented a manually curated census of 1,542 RBPs that interact with all known classes of RNAs, evaluating their evolutionary conservation, their abundance and their tissue-specific expression, as previously done by others for TFs, another fundamental category of proteins involved in gene regulation.[26]

From a phylogenetic point of view, important distinctions exist between RBPs and TFs. Since TFs control distinctive and specific cell functions, such as cell differentiation, they are poorly conserved between species and are rather configured as species- and tissue-specific. On the other side, RBPs control basal and stereotyped cellular functions such as inflammation and stress response and are therefore remarkably conserved among the species and ubiquitously expressed. Although TFs and RBPs are encoded by a similar number of genes (1704 and 1542 genes, respectively), it is important to note that in eukaryotes TFs represent just 3% of cell transcript against 20% of RBPs. Phylogenetic relationships of RBP have identified gene families that differentiated the RNA metabolic pathways during evolution. Many human RBP paralogues present binding sites identical or almost identical and could represent an alternative to the increase in protein synthesis and a mechanism that facilitates regulation between the various cell types.

At least six different classes of RBPs can be distinguished on the basis of their target RNA: there are RBPs binding mRNA and pre-mRNA(mRBPs), tRNA, snRNA (small nuclear RNA) and snoRNA (small nucleolar RNA) in addition to RBPs binding RNA sequences non-coding (ncRNA) such as miRNA, piRNA and lncRNA(Figure 6).[27] The class with the highest number of members was found in mRBPs (692 proteins), in line with the expansion of alternative splicing mechanisms and polyadenylation of mRNA during evolution in higher eukaryotes.
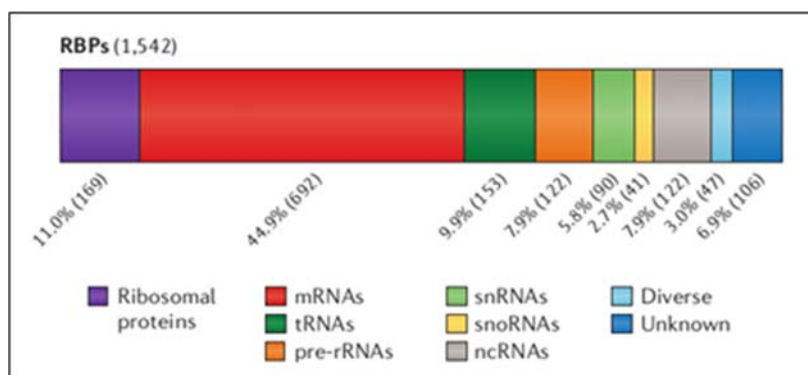
Figure 6. RBPs classification according to targeted RNA species. RBPs can be classified, according to the type of RNA species they bind, to into RBPs binding to messenger RNA (mRNA), transfer RNA (tRNA), pre-ribosomal RNA, small nuclear RNA (snRNA), small nucleolar RNA (snoRNA) and non-coding RNA (ncRNA). For some RBPs the target is not yet known or they can bind to diverse targets.[27]

b. RBPs regulating mRNA stability and translation (mRBPs)

i. RBP-regulated transcripts as functional operons

Several genome-wide studies using new methodologies of immunoprecipitation are increasingly identifying the profile of transcripts associated with RBPs.[28,29] Earlier studies proposed that multiple functionally related mRNAs that bear a conserved cis-element can be regulated by one or more cognate RBPs, thus creating subsets of transcripts whose fate is determined post-transcriptionally in a coordinate fashion, reminiscent of polycistronic mRNAs and bacterial higher-order DNA regulons. Like bacteria use these elements to coordinate protein production, RNA operons co-regulate monocistronic mRNAs that can function as members of more than one RNA operon, forming higher-order "RNA regimens". In this way the cell is able to respond more easily and quickly to environmental stimuli and regulate protein production by acting on the levels of stability and translation of the mRNA (Figure 7).
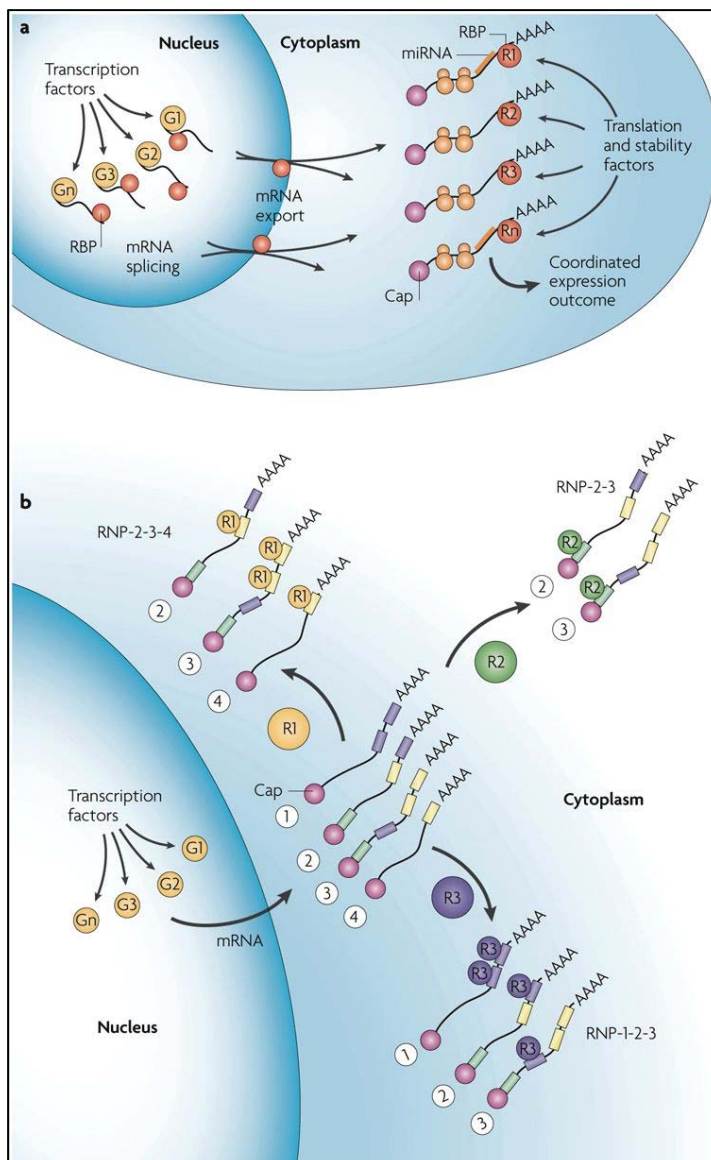
Figure 7. Coordination of subsets of mRNAs from transcription to translation. a) Transcription factors regulate the transcription of the different genes (G1 - Gn) in the nucleus. Subsequently, RBPs recognize their target RNAs and transport them to the cytoplasm after splicing events. In this way the RNA operon modulates stability and translation of mature mRNAs and allows the simultaneous expression of proteins functionally related or belonging to the same complex. b) With a different mechanism, the transcription factors determine the transcription of different genes (G1 - Gn) in the nucleus which are then exported to the cytoplasm in the form of mature mRNA. Here they are grouped into different RNA operons (RNP-ns), whose composition depends on the binding of RBP to the recognized sequence elements. This mechanism determines both coordination between the operons and co-regulation of the operons to form a higher-order combinatorial regulons.[30]

The trans-acting factors interact with multiple regulatory elements within the non-coding regions of mRNAs, called untranslated sequence elements for regulation (USERs). However, some USERs have also been found in the coding portions of the mRNAs. Their presence is of considerable importance for the association of the trans-factor with a specific mRNA, determining its regulation mode. Each mRNA can combine several RNA operons that regulate its fate through "USER codes". If a protein performs more than one function, its transcript can be a member of more than one RNA operon and be co-regulated with a different subset of mRNAs when exerting a different biological function. In the same way, regardless of the information of the gene, the instructions transferred to multiple copies of each mRNA can be regulated simultaneously or in sequence at several levels and in a combinatorial way by one or more RBPs. Therefore, RNA operons represent modular RNP units that coordinate multiple mRNAs to ensure efficient but flexible use of genetic information. Importantly, the regulation of RNA operons can be activated or repressed through PTM signals, such as phosphorylation.[31-33]

ii. Structural features guiding RNA-RBP interactions

The mechanisms by which RBPs recognize their targets can be implemented through specific USER, as previously described, but is also aided by formation of secondary structures (for example, stem-loop conformations). RBPs that are structurally different can share the same USER on a target or act in similar way, ensuring a high degree of redundancy to PTGR regulation. To identify specific roles of RBPs in regulatory pathways it is therefore necessary to take into consideration multiple aspects, such as the protein family they belong, their specific structural features, preferential subcellular localization, susceptibility to signalling pathways for PTM-dependent functions.[25]

Many RBPs have a common modular structure consisting of the repetition of a few basic domains. The combination of these domains is closely related to their functional activity. Through these domains, RBP can interact with specific sequences present mainly in the untranslated regions of the RNA strand; other domains are important for protein-protein interactions with other RNP components exerting regulatory or enzymatic activities.[34]

1. RBP binding domains

Many cellular processes rely on proteins that present in their primary structure multiple repeats of few basic modular units. Such modular architecture offers a high amount of versatility, providing a degree of specificity and affinity than would not be achievable with individual domains.[35] Increasingly, binding interfaces between RBPs and RNAs as well as among the components of RNP units are resolved at molecular level.[36] The main binding domains present in RBPs are listed in Table 1 and those closely related to our studies are briefly described in this paragraph and schematically illustrated in Figure 8:[37]

Table 1. Main RBDs in RBPs.[27]

Domain	Description
RRM	RNA recognition motif, single-strand RNA (ssRNA)-binding
RG/RGG	RG/RGG box repeats are arginine glycine rich low complexity regions, may bind RNA or act as protein-protein interaction domains in shuttling
DEAD	DEAD and DEAH box helicase motif, unwinds RNA (and DNA)
zf-CCCH	Zinc finger motif type C-x8-C-x5-C-x3-H, ssRNA-binding
KH	KH-homology domain, ssRNA-binding
GTP_EFTU, GTP_EFTU_D2, GTP_EFTU_D3	GTP-elongation factor family, proteins usually consist of 3 structural domains, 2 oligonucleotide binding domains (D2 and D3) and a GTP-binding domain
dsrm	Double-stranded RNA binding motif
zf-CCHC	Zinc knuckle, C-x2-C-x4-H-x4-C, ssRNA-binding
LSM	Like Sm domain is found in snRNP complexes, bind A/U rich regions
OB_NTP_bind	Oligonucleotide/oligosaccharide-binding (OB)-fold, found in DEAD-box helicases in association with HA2 domain, regulates helicase activity through RNA binding
HA2	Helicase-associated domain, found in RNA helicases
G-patch	G-patch domain, ~48 amino acids with 6 conserved glycines, found in RBPs
IBN_N	Importin-beta N-terminal domain, RNA transport or RBP transport proteins
SAP	(SAF-A/B, Acinus and PIAS) motif, RNA/DNA-binding domain
TUDOR	Tudor domain, found in Tudor proteins, Tudor proteins are in complexes with RBPs
RnaseA	RNase A domain, ssRNA endonuclease
zf-C2H2_jaz	JAZ dsRNA-binding protein zinc-fingers, dsRNA-binding
MMR_HSR1	50S ribosome-binding GTPase domain, found in RBPs
KOW	KOW (Kyprides, Ouzounis, Woese) motif, found in a variety of ribosomal proteins
RNase_T	RNase T ssRNA exonuclease domain
MIF4G	MIF4G (Middle domain of eukaryotic initiation factor 4G (eIF4G)), RNA- (and DNA-) binding
zf-RanBP	RNA-binding Ran-binding-protein-like zinc finger
NTF2	Nuclear transport factor 2 (NTF2) domain, found in RNA export factors
PAZ	Piwi Argonaut and Zwille (PAZ) domain, posttranscriptional silencing domain, binds siRNAs
RBM1CTR	C-terminal region found in hnRNPs
PAM2	PABP-interacting motif PAM2, found in RBPs
Xpo1	exportin 1 domain, RNA transport or RBP transport proteins
S1	S1 ssRNA-binding domain
HGTP_anticodon	Anticodon binding domain, found in aminoacyl-tRNA synthetases
tRNA-synt_2b	tRNA synthetase class II core domain (G, H, P, S and T), core catalytic domain of tRNA synthetases
Piwi	Piwi domain (P-element induced wimpy testis), posttranscriptional silencing domain, dsRNA guide hydrolysis of ssRNA
CSD	cold-shock domain, ssRNA/ssDNA binding
Ribosomal_L7Ae	domain found in ribosomal proteins L7Ae/L30e/S12e/Gadd45
RNase_Zc3h12a	ssRNA endonuclease domain found in Zc3h12a proteins, member of the NYN domain family
Anticodon_1	tRNA anticodon-binding domain, found in tRNA synthetases
R3H	R3H domain, R-x3-H conserved core, binds ssRNA/ssDNA

❖ **RNA-recognition motif (RRM).** It is a small domain of 70–75 aa and is the most common RNA binding motif. Due to their small size, these domains generally have a limited ability to interact with RNA in a specific fashion. For this reason, multiple copies of RRMs - typically two of them - are often tethered together on a single polypeptide to create a larger binding interface that recognizes a longer sequence. All the RRM domains have in common four β-sheets and two orthogonal α-helices, whose charged residues protrude externally forming hydrogen bonds with the nucleotide residues of ribonucleic acid. The main protein surface of the RRM involved in the interaction with RNA is the four-layer β-sheet, which usually contacts two or three nucleotides. For example, in the Pumilio (Puf) family of proteins each protein domain is able to recognize a single nucleotide. However, the affinity and specificity of the protein increases to eight nucleotides by combining multiple repetitions.[37,38]

❖ **Zinc finger motif.** There are many different types of zinc finger motifs but they all share the presence of one or more Zn^{2+} ions. They consist of ββα protein fold in which a β-hairpin and a α-helix are joined together via a Zn^{2+} ion. They were initially described as DNA binding motifs of transcriptional activators or repressors. Subsequently, proteins carrying zinc finger motifs with RNA-binding properties were also found. Zinc finger motifs are typically classified based on the residues used to coordinate the zinc ion: Cys2His2 (C2H2), CCCH, or CCHC and are generally present in multiple repeats within a protein. C2H2 zinc fingers interact with DNA primarily by forming direct hydrogen bonds to Watson–Crick base pairs in the major groove, using residues within their recognition α-helix. A second family of CCCH motives recognize specific sequence of single-stranded RNA through an interaction between intermolecular hydrogen bonds and Watson-Crick edges of the RNA bases. Several zinc fingers are utilized in a modular fashion in order to attain high sequence-specific recognition. Both DNA and RNA can be recognized by the same residues as zinc fingers. However, the different nucleic acid structures allow for a distinct structural arrangement of the zinc fingers on the nucleic acid template.[35,37,39]

❖ **Double-stranded RNA-binding motif (dsRBM).** They are small αβ domains of 70–90 amino acids that recognize the shape of the RNA rather than its sequence, interacting mainly with double-stranded (ds) RNA without making specific contacts with the nucleobases. In particular, dsRBM make contact with the sugar-phosphate backbone of the major groove and of one minor groove, which is mediated by the β1-β2 loop along with the N-terminus region of the alpha helix 2. This interaction is a unique adaptation for the shape of an RNA double helix as it involves 2'-hydroxyls and phosphate oxygen. Although the dsRBM have common structural characteristics, the chemical models are different and determine a different specificity for the different RNAs, such as inner rings, bulges or helices containing, misalignments, stem rings. For this reason they are involved in multiple functions such as RNP localization, RNA interference, RNA processing, RNA localization, RNA editing and translational control.[37,40]

❖ **K Homology Motif (KH).** This motif is structurally similar to RRMs and binds to both ssDNA and ssRNA. It is composed of about 70 amino acids with a signature sequence of (I/L/V)-I-G-X-X-G-X-X-(I/L/V) near the center of the domain that is functionally essential. Mutations within this region of the Fragile X Mental Retardation protein (FMRP) cause Fragile X mental retardation syndrome.[41] All KH domains form a three-layer β sheet packed against three α helices. Based on their topology, they are classified into type I (βααββα) and type II (αββααβ) subfamilies. Unlike RRM, there are no aromatic amino acids in the chemical structure and the recognition takes place through chemical bonds, such as shape complementarity, electrostatic interactions and hydrogen bonding.[10,39,42,43]

Through the specific motif combination, RBPs can bind to their targets with high affinity, remaining associated until their final destination of decay or translation, or have more transient association within the RNP, according to PTM or other cellular perturbations.[44]

Systematic investigation of RBPs has been performed in various cell types by interactome capture assays.[45,46] This technique is based on the creation of covalent bonds between RBP and its targets by crosslinking with UV light. The mRNA is then recovered through the use of oligo-desoxymethidine (dT) resins which bind to the poly A tail of the mRNA. Subsequently, the bound proteins are identified by means of quantitative mass spectrometry in tandem for liquid chromatography (LC-MS/MS).[47,48] An interesting finding of these studies is that about half of the detected RBPs has no conventional RBD.[45,49,50]
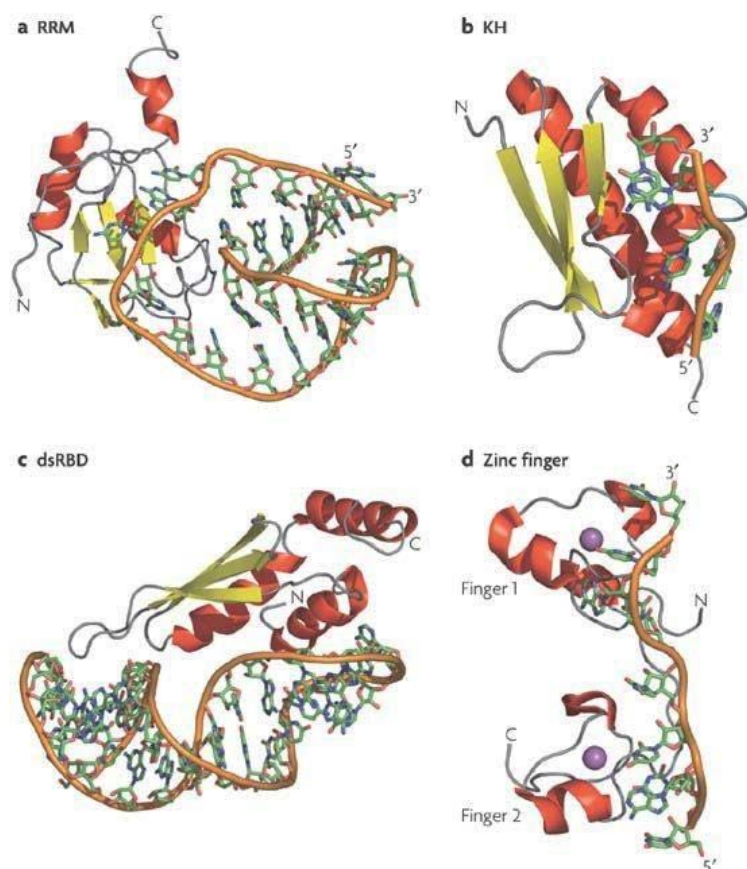
Figure 8. Representation of four main RNA binding domains. Representation of the structure of a) RNA-recognition motif (RRM); b) The K-homology-3 (KH3); c) double-stranded RNA-binding domain (dsRBD); d) two zinc fingers. See text for details.[34]

2. Regulatory elements conserved on targeted mRNAs

Transcripts coding for proteins involved in biological functions requiring rapid and coordinated changes of gene expression (as in cell cycle or inflammatory responses) are particularly rich of the USER sequences, mostly located in their 3'-UTR or 5'-UTR but also found in coding regions (Table 2: examples of USER) that serve as binding sites for trans-acting RBPs that can influence positively or negatively their stability and/or translation,[51] as described in previous paragraphs.

Table 2. Main cis-elements mediating mRNA stability and example of transcript bearing the element. For full description see [52].

a. ARE

The adenylate/uridylate-rich elements, called AU-rich elements or AREs, is the most well-characterized family of USER sequences. They are highly conserved throughout evolution, generally spanning 40-150 nucleotides. AREs are classified according to the type and number of motifs they contain and are divided into: Class I, Class II and Class III, with subclasses according to specific AU composition and patterns (Table 3).

Table 3. Classification of Adenylate-uridylate-rich elements as described by [53].

Group	Motif	Representative transcripts
I	WAUUUAW with U-rich region	c-fos, c-myc
IIA	AUUUAUUUAUUUAUUUAUUUA	GM-CSF, TNF-α
IIB	AUUUAUUUAUUUAUUUA	IFN-α
IIC	WAUUUAUUUAUUUAW	COX-2, IL-2, VEGF
IID	WWAUUUAUUUAWW	FGF2
IIE	WWWWAUUUAWWWW	u-PA receptor
III	U-rich region, non-AUUUA	c-jun

GM-CSF: granulocyte macrophage-colony stimulating factor; TNF: tumour necrosis factor; IFN: interferon; COX: cyclooxygenase; IL: interleukin; VEGF: vascular endothelial growth factor; FGF: fibroblast growth factor; u-Pa: urokinase plasminogen activator. [#]: proposed classification by WILUSZ et al.

These elements mediate RNA binding for multiple RBPs that are collectively defined as ARE-binding proteins (ARE-BP) (Table 4), which are key effectors of PTGR in inflammatory responses and will be further defined in the following paragraphs.[54,55] Bioinformatic analysis estimate that 5–8% of human genes contain ARE sequences.[30] In general, the presence of AREs indicates the need of a rapid mRNA turnover.

Table 4. Selected list of major ARE-binding proteins.[56]

Protein	Gene symbol	Nucleus/ cytoplasm	cDNA RefSeq ID	Protein RefSeq	Domain (motifs)	ARE-mRNA targets (examples)	C[a]	Role in mRNA decay
HuA (HuR)	ELAVL1	Nucleus Cytoplasm (ubiquitous)	NM_001419	NP_001410	3 RRMs	TNF, IL3, PTSG2 FOS, VEGF CCND1, SERPINB2	I III IV V	Stabilizing
HuB (Hel-N1)	ELAVL2	Cytoplasm Nucleus (neural, sex glands)	NM_004432	NP_004423	3 RRMs	GLUT1	IV	Stabilizing Translational Enhancing
HuC	ELAV3	Nucleus (neural)	NM_001420	NP_001411	3 RRMs	VEGF	IV	Stabilizing
HuD	ELAV4	Nucleus (neural)	NM_021952	NP_068771	3 RRMs	MYCN	IV	Stabilizing
KSRP	KHSRP	Nucleus Cytoplasm	NM_003685	NP_003676	4 KH domains	TNF, FOS	I IV	Destabilizing
AUF1 (hnRNP D)	HNRPD	Nucleus Cytoplasm (ubiquitous)	NM_000657	NP_000648	2 RRMS	GRO2, TNF GRO1, IL8 BCL2, FOS SERPINB2P	I II III V	Destabilizing Stabilizing Isoforms
TIA1	TIA1	Nucleus Cytoplasm	NM_022037	NP_071320	3 RRMs	TNF, GMCSF	I	Translational Silencing
TIAR	TIAL1	Cytoplasm	NM_003252 NM_022333	NP_003243 NP_071728	3 RRMs	TNF	I	Translational Silencing
HnRNPA1	HNRPA1	Nucleus (PBMCs)	NM_002136	NP_002127	2 RRMs	I-2	III	Destabilizing
HnRNPA2	HNRPA2/ B1	Cytoplasm	NM_002137	NP_002128	2 RRMs	GLUT1		Destabilizing
HnRNPC	HNRPC	Nucleus	NM_004500	NP_004491	1 RRM	IL2	III	Destabilizing
TTP	ZFP36	Nucleus Cytoplasm (fibroblasts, macrophage)	NM_003407	NP_003398	2 C₃H zinc fingers	TNF, GMC-SF PAI2	I V	Destabilizing
BRF1 CMG1 Berg36	ZFP36L1	Nucleus Cytoplasm	NM_004926	NP_004917	2 C₃H zinc fingers	IL3	III	Destabilizing

Notes to Table: C[a] ARE clusters are based on;[54,57] Hu (A, B, C, D) = Human antigen A, B, C, D, KSRP= KH-type splicing regulatory protein, AUF-1 = AU-binding Factor 1, TIA1 = T-cell-restricted intracellular antigen, TIAR = TIA-related, HnRNP = Heterogeneous Nuclear Ribonucleoprotein (A1, A2, C), TTP = Tristetraprolin, BRF1 = Butyrate-response factor 1. For full ARE-mRNA targets acronym list see [56].

The RNA-binding domains of ARE-BPs are very diverse and include RNA Recognition Motifs (RRMs), zinc fingers and K homology (KH)-domains. Simultaneous interaction of ARE-BPs with multiple targets (or with multiple sites within a target) can be mediated by several of these motifs in a single protein.[58] ARE-RBPs bind with different affinity according to the specific ARE sequence and the binding motifs involved.

For example, in the interaction between TIA-1 and its target mRNA, RRM2 confers maximum binding affinity for pyrimidine-rich sequences, while RRM3 improves the overall affinity by interacting preferentially with C-rich motifs.[59-61] HuR and TIAR interact with high affinity U and AU rich elements.[62,63] Additionally, the KH domains of KSRP have different affinities for AU-rich sequences in mRNAs. This is due to the combination

of its first three KH domains which act as independent binding modules. All of its domains have a negative selection for C-rich sequences. The KH3 domain recognizes the sequences rich in AU and G, while the KH4 domain is involved in binding with the mRNA. It is also involved in its decay by means of an essential structural element in its β4 sheet.[64]

Functional outcomes of ARE-bound RNPs are determined by multiple factors. Some ARE-RBPs mediate mRNA destabilization (e.g., TTP and other TIS11 family members, AUF-1 and KSRP), while others stabilize the transcript to which they are bound (e.g., HuR). Likewise, subset of ARE-BPs represses translation of their mRNA targets (TIA-1, TIAR). These outcomes are linked to the specific subcellular distribution of the ARE-RBPs via stimulus-dependent shuttling between nucleus and cytoplasm.[65] Moreover, factors controlling the relative abundance of RBP isoforms, their conformational state or their post-translational modifications can critically shape the fate of the ARE BP-RNA complexes.[66] In conclusion, the fate of an ARE-bearing transcript targetable by several ARE-BPs is subjected to different outcomes through the dynamic conditions shaping preferential access of one RBP over another.

b.   GRE

Another USER is composed of GU-enriched sequences and is therefore defined as GU-rich element (GRE).[67] The GREs are classified into five clusters according to GUUUG pentamers in the 3'-UTR of mRNA (Table 5). Transcripts containing GRE are involved in multiple cell functions, such as cell growth and activation and regulation of apoptosis. GREs can be seen in mRNAs of transcription factors and inflammatory proteins, such as c-jun, jun-b and Tumor necrosis factor (TNF-receptor)-1B. Introduction of the GRE into the 3'-UTR of a beta-globin reporter conferred instability to the otherwise stable reporter transcript, demonstrating that the GRE is a functional mediator of mRNA decay.[68] The BP CUGBP Elav-Like Family Member 1 (CUGBP1), a member of the abnormal embryonic lethal CELF (CELF factor) family, was the first reported GRE-BP and was characterized as a destabilizer for the myotonin protein kinase mRNA. In subsequent studies, CUGBP1 has been associated with various post-transcriptional regulatory functions, such as regulation of deadenylation, alternative splicing and stabilization and decay of mRNAs.[69,70]

Table 5. GRE Motifs and abundance in human genes.[71]

GRE Motif	Cluster	3'UTR	5'UTR	CDS
GUUUGUUUGUUUGUUUGUUUG	I	0.12%	0.01%	0.01%
GUUUGUUUGUUUGUUUG	II	0.24%	0.02%	0.01%
GUUUGUUUGUUUG	III	0.73%	0.07%	0.07%
KK[GUUUGUUUG]KK	IV	0.30%	0.03%	0.11%
KKKU[GUU UG]UKKK	V	4.15%	0.44%	1.41%

c. Other USERs

As shown in Table 3, there are numerous RNA cis-acting elements beyond ARE and GRE, in some cases related to specific biological process or involved in fundamental responses to stress, as for the integrated stress response (ISR). Some of these additional USERs are briefly described in this paragraph.

❖ Internal ribosome entry sequence (IRES) represents an important element usually present in 5′-UTRs but also found within the coding region of mRNAs. The presence of IRES in the 5′-cap of the mRNAs confers the ability to be translated into proteins even in conditions where the cap-dependent translation is compromised, for example in different forms of cellular stress or apoptosis.[72]

❖ Hairpin or higher order intramolecular mRNA structures, such as Pseudoknot, can modulate translation without the aid of binding factors. They intervene in various stages of translation. For example, if they are included near the CAP structure in the 5'-UTR they can modulate translation start, while they can be involved in frame-displacement events, influencing the elongation phase.[73-75]

❖ Selenocysteine insertion sequence (SECIS) is an RNA element around 60 nucleotides in length that adopts a stem-loop structure. This structural motif recruits proteins involved in selenium metabolism and directs the cell to translate UGA codons as selenocysteines instead of the normal stop codon. The SECIS elements are specific to the organism in that they contain non-canonical A-G base pairs which are not common in nature but which are of high importance for the correct function of SECIS.[76,77] Furthermore, these elements are a fundamental aspect of the messenger RNAs that encode selenoproteins, which contain selenocysteine residues.[78]

❖ Iron-responsive element (IRE) (shown in Table 2) is a short conserved stem-loop which is bound by iron response proteins (IRPs, also named IRE-BP or IRBP). This element is found in UTRs of mRNA coding for proteins involved in iron metabolism – such as ferritin and the transferrin receptor - and it has been well characterized both in its sequence and in its secondary structure. The mRNA encoding ferritin, an intracellular iron storage protein, contains an IRE located in its 5'-UTR, while the transferrin receptor, which is involved in the cellular uptake of plasmatic iron, contains multiple IREs in the 3'-UTR. At low iron concentrations, the IRPs reduce the synthesis of ferritin protein by binding to the specific IRE on the 5'-UTR of its mRNA. At the same time, they bind to the IREs located in the 3'-UTR of the transferrin receptor mRNA and determine an increase in the stability of the transcript. This complex increases downstream translation of the transferrin receptor, favouring iron uptake from the bloodstream.[49,79-85]

❖ Upstream open reading frames (uORFs). uORFs are present in the genome of eukaryotic cells and their presence in transcripts is estimated to be greater than 40%. Their main function is the regulation of protein synthesis.[86,87] They can be present in single or multiple repeats within the 5′-UTRs of numerous mRNAs and exert a predominantly negative influence on the translation regulated downstream by the major ORF. In eukaryotes the first step of protein synthesis consists in the association of multiple

factors including eIF3, eIF1, eIF1A, the ternary complex eIF2-GTP-Met-tRNAiMet and the small ribosomal subunit 40S for the formation of the pre-start 43S complex.[88] Subsequently, the complex binds to the 5'-cap of the mRNA and moves along the RNA filament to begin the translation from the first start codon.[89] The presence of a uORF has a constitutive inhibitory effect as it appears to be connected to the dissociation of the eIF2 ternary complex and other critical initiation factors during the translation phase and therefore determine low levels of subsequent translation reinitiation at downstream coding sequences. However, there are also uORFs that do not have a constitutive effect or can promote the start of translation at the CDS in response to environmental stress, which can be implemented by the element itself or be mediated by RBPs.[84,86,90,91] For example, inhibition of the activity of the nucleotide exchange factor guanine eIF2 is caused by the phosphorylation of eIF2 on its α subunit to serine 51 (eIF2α-P) and causes a decrease in the exchange of GDP for GTP, decreasing the formation of the complex pre-initial 43S and then stopping the initiation of translation.[92,93] Since eIF2α-P is involved in translational control in response to environmental stress, this path is often referred to as integrated stress response (ISR).[94] In conditions of stress damage, the reduction of protein synthesis allows cells to store nutrients and energy and would facilitate the reprogramming of gene expression to limit its damage. To facilitate reprogramming of gene expression in the presence of eIF2α-P, a subset of mRNA is preferentially translated through uORF-mediated mechanisms. uORFs are widely present in the transcripts of genes that are activated in response to stress and regulate their translation. Included among the preferentially translated ISR gene transcripts are DNA damage-inducible transcript 3, also known as C/EBP homologous protein (CHOP), Activating Transcription Factor 4 (ATF4 or CREB2), Activating Transcription Factor 5 (ATF5) and also CCAAT-enhancer-binding proteins α (C/EBPα) and CCAAT-enhancer-binding proteins β (C/EBPβ) which encode the leucine hinge transcription factors activated in response to stress.[95-98]

3. Modification of RNA: adenosine methylation

Several RBPs can recognize methylated adenosine in RNA molecules (N^6-Methyladenosine or m^6A) and mediate the functions associated to this modification. N^6-methyladenosine (m^6A) is the most prevalent post-transcriptional RNA modification on eukaryote mRNA; this modification is present in 0.1–0.4% of all cellular adenosines, accounting for ~50% of all methylated ribonucleotides.[99,100] Adenosine methilation occurs predominantly in two consensus sequence motifs: G m^6A C (~70%) and A m^6A C (~30%).[101,102] The m^6A are mostly localized in highly conserved regions: long internal exons, locations upstream of stop codons, and the 3′-UTR of mRNA. The biological functions of m^6A are mediated by special binding proteins (i.e., methyltransferases, demethyltransferases, and effectors) that can install, remove or recognize this modification, respectively. Through RBP recognition and binding, this modification affects several cellular processes, such as mRNA stability and translation, splicing, miRNA biogenesis, X-chromosome inactivation,

sometimes as part of a pathogenetic process.[103,104] In fact, alterations in m[6]A patterns are present in pathologies such as cancer, obesity.[100,105] Some evidence suggest that proteins of the YT521-B homology (YTH) domain family (YTHDF) act as reader of m[6]A with a specific YTH domain.[106] Some RBPs use KH domains to recognize m[6]A-containing RNAs to promote their translation and stability. Of note, HNRNP proteins – which we found downregulated in our study *in silico*, see pag. 107 - have also been shown to recognize m[6]A: for example, in *in vitro* studies on HeLa cell line, alteration of splicing events was due to binding of HNRNPA2B1 to G m[6]A C containing sites.[107]

iii. Ribonucleoprotein complex: a dynamic regulatory module foundamental for PTGR

Besides the RNA-protein interactions mediated by the cis/trans recognitions previously described, the protein interactions occurring in the context of RNP complexes give rise to regulatory networks in which two or more RBPs contribute to regulating a common RNA target. In integration with transcriptional activation, their combined action ultimately defines post-transcriptionally the steady-state levels of RNAs and their availability for translation (for mRNAs) or the ability to exert its role (for non-coding RNAs). Interactions between RBPs can either be synergistic (cooperative), aim for a different regulatory outcome (competitive), or regulate one another (mutual control) (Figure 9).[108]
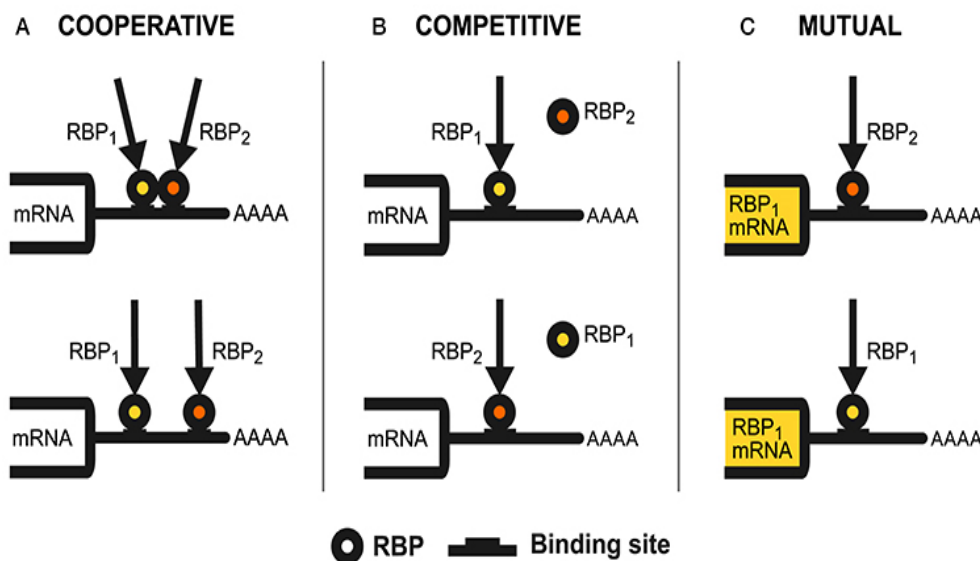
Figure 9. RBPs regulatory interplay modes. Different patterns of regulatory interaction experimentally described between RBPs in a generic mRNA 3′-UTR as the interaction substrate. (A) Cooperative interaction. Two RBPs can recognize binding sites on the target mRNA that can be close to each other, or distant but brought to proximity by the secondary structure of RNA. Two RBPs can also cooperate on distant sites without direct interaction between them. In this case (below) there is independent cooperation. (B) Competitive interaction. Two RBPs compete for the superimposed binding on the same target mRNA. The regulation of the transcript is given by the balance between the two RBPs. (C) Mutual interaction. Two RBPs control mutual expression, either to favor or limit expression.[108]

1. Cooperative regulation

The interplay of two RBPs having a common target and whose action is synergistic is said to be cooperative. This mechanism intervenes in the different phases of PTGR and provides a balance among the competing RBPs on the target mRNA, which ultimately defines the outcome of the regulation. In <u>nuclear export and alternative polyadenylation</u> for example, HuR and ZNF385A co-regulate the export of p53 mRNA.[109] For <u>control of the mRNA stability,</u> HuR binding to ARE can be increased through a synergistic mechanism with other RBPs, such as RBM38.[110] Similarly, AUF-1 interacts with ZFP36, whose binding improves the association of AUF-1 with the target mRNAs; AUF-1 can also serve as co-activator of RNA binding for ZFP36 family proteins (characterized in the following paragraph iv).[111,112] The <u>translational control</u> of the Annexin A2 Receptor (ANXA2R) mRNA occurs through a complex mechanism in which HuR, HNRNPA0 and HNRNPA2B1 cooperatively bind the 5'-UTR of the transcript. They act on the translation on its first uORF leading to inhibition of the protein synthesis.[113] <u>RBP synergism in the post-transcriptional regulation in human cancers</u> occurs for example between HuR and the p42^{AUF-1}. These two RBPs compete for binding to the 3'-UTR of eIF4E mRNA at non-overlapping sites. A distinct ARE in the 3'-UTR of eIF4E mRNA was found to be responsible for HuR-binding and mRNA stabilisation and could correlate with enhanced expression of both eIF4E and HuR in malignant cancer specimens.[7,114]

2. Competitive regulation

Due to the similarity between both structure and target recognition mechanism of different RBPs, it is likely that many of them may end up competing for the same target binding sites.[115] Competitive regulation by RBPs is more common than synergistic/cooperative interaction. It provides a balance among competing RBPs on the transcript targets and has been found in various steps of post-transcriptional control, such as RNA processing, mRNA stability and translation.[116-118] The antagonistic control of mRNA stability by RBPs, of particular relevance for our studies, above all involves AREs. For example, TTP, HuR and KSRP share common AREs on target mRNAs, such as enzyme cyclooxygenase-2 (COX-2), TNF-α and c-fos, and act through a competitive mechanism that determines the fate of the transcript. Target recognition by TTP and KSRP determines a negative regulation of its stability, while the HuR bond promotes its stabilization.[119-124] Similarly, Cyclin Dependent Kinase Inhibitor 1A (CDKN1A) and Cyclin D1 (CCND1) mRNA present binding sites that are subject to a competitive mechanism between the RBP AUF-1 and HuR. For p21 and CCND1 mRNA, the binding of the two RBPs on overlapping sites determines as well an opposite modulation on the stability of the transcripts. In particular, HuR promotes its stabilization, while AUF-1 promotes its decay.[125] HuR can also compete with TIA-1 for a binding site present at the 3′-UTR of the Programmed Cell Death 4 (PDCD4) mRNA. In this case, however, the two RBPs have a redundant function which determines the stabilization of the transcript.[126] Also, HuR and ZFP36 share numerous targets on which they play an opposite role.[127]

ARE-BP can also modulate the process of <u>translation</u> through an antagonistic model. For example, CUGBP Elav-Like Family Member 1 (CELF1) and HuR compete for the 3'-UTR binding site of the Occludin (OCLN) mRNA. As before, CELF1 represses its translation by directing the mRNA towards the P-bodies, while HuR stabilizes the transcript thus improving its translation.[128] P-bodies are small cytoplasmic foci that contain many of the enzymes required for mRNA decay.

3. Mutual control

An example of a mutual control among RBPs is represented by TTP which can negatively self-regulate its own mRNA and HuR, which antagonizes this effect by stabilizing TTP mRNA.[129,130] HuR has also a positive effect towards translational regulation both on its own mRNA and on that of KSRP.[115,131] In turn, HuR and KSRP regulate the stability of their own mRNAs.[132] Along the same lines, HuR can stabilize the TIA-1 mRNA and in turn, TIA-1 causes a decrease in cellular HuR levels. In fact, TIA-1 knockdown determines an increase of HuR expression levels in human HeLa cervical carcinoma cells. This is an important mutual control, since HuR is an anti-apoptotic factor and TIA-1 a pro-apoptotic factor, and this balance also regulates programmed cell death.[133]

iv. Control of mRNA turnover (stabilization and decay) and translation by RBPs

1. mRNA stabilization

<u>mRNA Stabilization: the RBP HuR as key mediator.</u> Human antigen R (HuR or HuA) is the sole ubiquitously expressed member of the Embryonic Lethal, Abnormal Vision, Drosophila-Like (ELAVL) family along with HuB (ELAVL2), HuC (ELAVL3), and HuD proteins that are primarily found in neurons, though their expression was also found in the serum of patients with encephalomyelitis, sensory neuronopathy, small cell lung cancer and paraneoplastic manifestations.[134,135] Their ELAVL gene name refers to early mortality and other alterations of the embryo caused by gene ablation in animal models.

HuR contains three RMMs, of which RRM1 and RRM2 are separated by a short linker of 7 amino acid residues and bind with high affinity to U/AU-rich sequences, while RMM3 contributes to HuR's interaction with target poly (A) tails.[136] Additionally, the HuR structure contains the Nucleocytoplasmic Shuttling (HNS) sequence, which allows shuttling from the nucleus to the cytoplasm of the protein (Figure 10).

Figure 10. Schematic representation of HuR protein domains. The domains RRM1 and RRM2 are connected by a short linker of 7 residuals. Between RMM2 and RRM3 is the Nucleocytoplasmic Shuttling (HNS) which allows the protein to shuttle between the cytoplasm and the nucleus.[137]

HuR is functionally characterized mainly as a positive regulator of mRNA stability and translation, counteracting the mRNA-destabilizing effects of TTP, BRF-1, KSRP and AUF-1. HuR resides in the nucleus and shuttles into the cytoplasm upon cell activation by stressful stimuli - such as exposure to UV rays, thermal shock, nutrient deprivation, cytokine stimulation - where it coordinates the turnover of mRNAs participating to cell cycle, apoptosis, and inflammatory responses. The cellular distribution between the nucleus and cytoplasm depends by phosphorylation at different sites and changes also according to the stage of the cell cycle.[138] One of the functions attributed to HuR is the coordination of pro-survival cellular program as it sustains the expression of various anti-apoptotic proteins, such as prothymosin α, an inhibitor of the apoptosome.[139,140] At the same time, HuR has also been described as an essential regulator in the cell death processes, promoting caspase-mediated apoptosis.[141,142] These studies suggest that while HuR has an anti-apoptotic function during early cell stress response, it may promote apoptosis when cell death is unavoidable.

The mechanism of HuR-dependent mRNA stabilization is not fully understood: it mostly relies on preventing mRNA decay by competitive binding to sites shared with mRNA-destabilizing RBPs. Several direct HuR target mRNAs were identified by immunoprecipitation followed by transcriptomic analysis. HuR stabilizes mRNAs encoding BCL2 Apoptosis Regulator (BCL2), MCL1 Apoptosis Regulator, BCL2 Family Member (MCL1), cyclin A, cyclin B1, CCND1, lymphotoxin-α, granulocyte-macrophage colony stimulating factor (GM-CSF), interleukin IL-4, IL-13, vascular endothelium growth factor (VEGF), CD3ζ, Fas Ligand (CD95L), GATA Binding Protein 3 (GATA-3) and X-Linked Inhibitor Of Apoptosis (XIAP).[143] In leukemogenesis, overexpression of HuR results in a stabilization of the p53 mRNA which in turn leads to inhibition of the p53-dependent transcription of mRNA encoding the survivin protein. This finding were confirmed in experiments where p53 silencing cause an increase in both levels and stability of survivin mRNA.[143] Therefore, it has been suggested that the mutational state of p53 may influence modulation in survivin levels which are in turn dependent on HuR levels.[144] HuR has also been shown to interact with, and be regulated by miRNAs. The biological impact of this joint regulation is related also to the type of targeted mRNA: for example, in colon cancer cells the expression of mRNA coding for the pro-inflammatory COX-2 has been described to be subjected to competitive regulation between the HuR and miR-16 for an overlapping binding site located in the mRNA 3'-UTR. In non-transformed colonic cells HuR is mainly localised in the nucleus, allowing miR-

16 to bind to the mRNA and suppress COX-2 expression; however, the predominant cytoplasmic localization of HuR in these cells (which reflects its activation state) leads to binding site occupancy, making it less accessible to miR-16 and determining the stabilisation of COX-2 mRNA.[145] With analogous mechanism, in prostate cancer cells receptor tyrosine kinase 2 (ERBB-2) mRNA is controlled by HuR. The interaction between HuR and 3'-UTR of ERBB-2 determines a steric hindrance and blocks the association of two miR-331-3p/RISC molecules adjacent to the HuR binding site. This mechanism leads the stabilisation of ERBB-2 mRNAs. In prostate cancer cells, the accumulation of ERBB-2 has a pathological role in that it leads to the activation of pathways that are related to resistance to cell therapy and therefore to cancer progression. One of the activated pathways is the phosphatidylinositol-3-kinase (PI3K) / AKT signalling pathway.[146] In contrast, in HeLa cells HuR recruits let-7-loaded RISC in a synergistic manner, and loads this complex on 3'-UTR of c-myc mRNA to inhibit its expression.[147]

2. mRNA decay

<u>TPA-induced sequence (TIS11) proteins: Tristetraprolin and its family members.</u> Tristetraprolin (TTP), also known as Zinc finger protein 36 homolog (ZFP36), is the prototypic member of the TPA-induced sequence (TIS11) family along with Butyrate-response factor (BRF)-1 (TIS11b, ZFP36L1) and BRF-2 (TIS11d, ZFP36L2).[148] The *ZFP36* gene encodes a proline-rich, zinc finger protein of about 36 kDa with three repetitions of the PPPP motif that determine its name. The protein contains two zinc finger domains that bind to class II ARE of several mRNAs to promote their decay[148] (Figure 11). The sequence UUAUUUAUU is the core destabilizing element of many ARE-containing mRNAs.[125,149,150] TTP is expressed as an early-response gene in various cell types upon cell stimulation by phorbol ester, insulin, serum and other mitogenic stimuli.
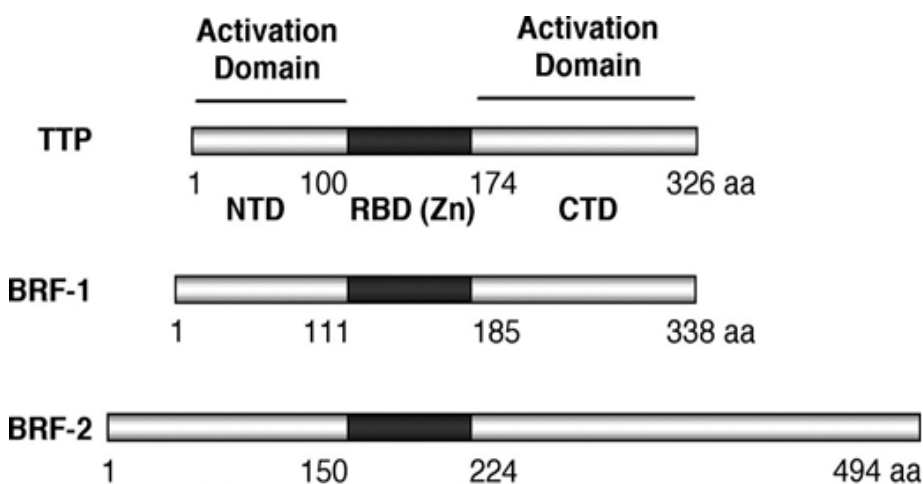
Figure 11. Functional domains structure of TIS11 family. Schematic structure of TIS11 proteins structure and common characteristics. The central region contains the zinc finger domain (RBD-Zn). Activation and decay domains are present at the N-terminal (NTD) and C-terminal (CTD), respectively.[151]

Characterization of the 5'-proximal region of *ZPF36* gene had identified various promoter elements that are essential for the serum-inducibility of TTP in response to different stimuli through binding of transcription factors such as Sp1 Transcription Factor (SP1), Early Growth Response 1 (EGR-1), and Activator protein 1 (AP1).[152,153] Ogawa and colleagues showed that treatment of human T cells with transforming growth factor-β (TGF-β) induced expression of TTP mRNA through the binding of Smad3/4 transcription factors to the putative Smad-responsive binding elements present in the TTP promoter.[154] The induction of TTP was also confirmed in other studies through the use of various growth-inhibiting cytokines, such as interferons, anti-inflammatory compounds and glucocorticoids. Therefore, the expression of TTP has been correlated with the control of the inflammatory and immune response.[155-158] As previously described, TTP self-regulates its mRNA through the link with its ARE in a negative feedback loop.[129,159]

Rapid transcriptional induction was also observed for another member of the TIS11 family, <u>BRF-1</u>. In particular, its induction appears to be cell type- and stimulus-dependent.[160] Additionally, in some organs, such as the heart and liver, BRF-1 expression can be regulated by the circadian clock. In turn, this mechanism influences the circadian expression of target transcripts.[161,162] The transcripts of BRF-1 and BRF-2 also contain ARE in their 3′-UTR and their mRNAs were found to be part of the pool of mRNA associated with TTP in a possible cross-regulatory mechanism.[163]

<u>The mechanism of action by which TIS11 members accelerate the degradation of mRNA</u> is complex (Figure 12). It occurs by first promoting the removal of the polyadenylated tail from the mRNA (deadenylation). Three major deadenylation complexes have been reported in vertebrates, the carbon catabolite repressor 4/ Ccr4p-associated factor 1/ CCR4-NOT Transcription Complex (CCR4/CAF1/NOT) complex, the Pan2/Pan3 complex, and the poly A-specific ribonuclease (PARN) complex.[164-166] The CCR4 component of the CCR4/CAF1/NOT complex was found associated with TTP and BRF-1 in NIH3T3 cells for the destabilization of ARE-containing targets; depletion of CAF1 from the complex determined their stabilization, indicating a non-redundant role.[151] The mRNA deadenylation activity conducted by PARN can be promoted *in vitro* by members of the TIS11 family, although the association between TTP and PARN to activate deadenylation seems to be indirect, mediated by other as yet unidentified factors.[167] The deadenylation of the target mRNAs allows the rapid decay of the transcript, promoted by the members of the TIS11 family through two primary decay pathways: the first according to a 5′ to 3′ direction occurring in the cytoplasmic P-bodies, while the 3′ to 5′ decay is mediated by the multienzymatic complex of the exosome.[168,169]

In addition to its role as a posttranscriptional regulator, TTP interferes also with the nuclear import of the p65 subunit of NF-κB through direct interaction and determines the inhibition of the transcription and activity of NF-κB.[170,171] TTP can inhibit NF-κB activity also through histone deacetylases (HDACs) recruitment, in particular HDAC-1, HDAC-3, and HDAC-7.[172]
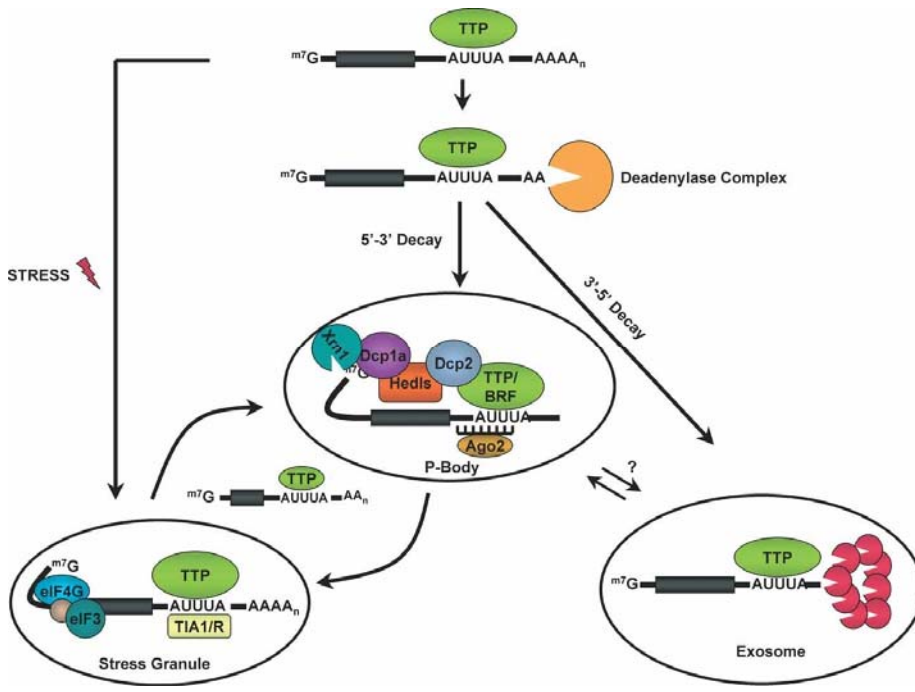
Figure 12. Mechanisms of TTP-mediated mRNA decay. TTP recognizes specific ARE sequences present on the 3'-UTR of the targeted mRNA and associates with members of the deadenylase complex, such as PARN, CCr4 and CAF1. This association can take place through direct or indirect association and promotes the deadenylation of the transcript. Subsequently, the mRNA is directed to the P-bodies, where the 5'-cap is also removed through the interaction of TTP and the decapping complex. At this point, the mRNA can undergo a 5′-to-3' exonucleolytic decay. Furthermore, TTP can also intervene in the transport of translationally repressed transcripts from P-bodies to stress granules (SGs) for decay. In the 3′-to-5'decay, the degradation process of the mRNA occurs through the association between TTP and the components of the exosome.[148]

Among the mRNA targeted by TTP there are several transcripts encoding key proteins in immune responses, such as interleukin TNF-α, (IL) -2, IL-3, IL-6, IL-10, IFN-γ, GM-CSF and COX-2.[148,173] TTP also downregulates the stability of the mRNA encoding VEGF, assuming a potential role in tumor angiogenesis processes.[174]

Heterogeneous nuclear ribonucleoprotein (hnRNP) family: AUF-1. The RBP AUF-1 (AU-binding Factor 1) also named hnRNPD, belongs to a family of ubiquitously expressed hnRNPs. The first *in vitro* evidence of AUF-1 function was an increase in the decay of the c-myc mRNA associated with the polysome, thus assigning a cytoplasmic mRNA decay role to this RBP.[175,176]

Four AUF-1 protein isoforms are known, named according to their molecular weight (Figure 13). The differential inclusion during alternative splicing events of exons 2 and/or 7, encoding 19- and 49 amino acid-long inserts near the N- and C-termini, respectively, is responsible for the different length of the four isoforms. The p45[AUF-1] isoform contains both exons 2 and 7; p42[AUF-1] contains only exon 7; p40[AUF-1] contains only exon 2 and p37[AUF-1] has neither of the two exons.[177]. Differently from the majority of genes, AUF-1 gene contains 10 exons but the translational termination codon is located whitin exon 8. Exon 9 is a 107-nucleotide-long, alternatively spliced region of the 3′-UTR; exon 10 contains the remainder of the 3′-UTR starting in exon 8 and the poly(A) signal. The role of these additional exons and introns is not well established but they could provide additional means of regulation. Indeed, AUF-1 binds these intron sequences, suggesting self-

regulatory RNP interactions.[115,178] All the isoforms share a glutamine-rich (Q-rich) domain and two non-identical RRM domains arranged in tandem, but they display a different binding affinity for their transcripts.[179,180] The four isoforms show a different binding specificity and affinity for their targets, such as COX-2, TNF-α, VEGF, c-myc and c-fos:[175,179,181-183] in fact, the p37^{AUF-1} and p42^{AUF-1} isoforms have a binding affinity towards the ARE sequence from three to five times greater than that of the other two isoforms. The Q-rich domain appears to be involved in protein-protein interactions but a complete understanding of its role is still lacking. All AUF-1 proteins form stable dimers in solution that can bind sequentially to form oligomeric structures on RNA substrates.[184,185] These oligomers are significantly more stable when formed by the p42^{AUF-1} and p45^{AUF-1} isoforms, suggesting that sequences encoded by exon 7 enhance secondary binding events required to form these higher-order complexes.[178] Furthermore, the interaction between AUF-1 and RNAs appears to be more complex than that of other classic hnRNP proteins. Earlier studies using homology modelling of AUF-1's RRM2 to that of RRMs of other hnRNP proteins and electromobility shift assays demonstrated that AUF-1 binding to the RNA is achieved mainly through interactions with conserved amino acids with no base-specific recognition.[186] A more recent global analysis of AUF-1-bound targets and binding sites performed by photoactivatable ribonucleoside-enhanced cross-linking and immunoprecipitation (PAR-CLIP) analysis[187] revealed instead that AUF-1 recognizes also GRE sequences in mRNAs and noncoding RNAs and influences target transcript's fate in different ways: first, AUF-1 lowers the steady-state levels of the majority of its target RNAs;[188] second, AUF-1 does not change the abundance of a different subset of target RNAs but instead promotes their translation, as shown by ribosome profiling experiments; third, AUF-1 enhances the steady-state levels of a subset of target mRNAs mostly encoding DNA-maintenance proteins.[187] AUF-1 can also participate to transcriptional process, as it was shown to be required for telomere maintenance via transcriptional activation of the telomerase reverse transcriptase (TERT) gene[189,190] and direct interaction with telomeric repeat sequences.[191,192]

AUF-1 expression itself can also be regulated by PTM such as phosphorylation, methylation, ubiquitination or protein isomerization, which leads to mRNA decay or alternative splicing events in the 3-′UTR of its mRNA.[193,194] For example, the retaining of exon 9 forces the junction between exon 9 and exon 10 to be positioned well over 50–55 nucleotides downstream of the translational termination codon, and this configuration activates mRNA degradation via NMD pathway in mammalian cells.[195] The cellular concentrations of AUF-1 are modulated through ubiquitin-proteasome degradation. Both p37^{AUF-1} and p40^{AUF-1} can be poly-ubiquitinated, while inclusion of the exon 7-encoded domain in p42^{AUF-1} and p45^{AUF-1} appears to inhibit this modification.[196]

The isoforms p42^{AUF-1} and p45^{AUF-1} have been found in many cell types to be mainly located in the nucleus, while p37^{AUF-1} and p40^{AUF-1} move between the nucleus and the cytoplasm, influenced by the presence or absence of exons containing nuclear localization signals. Subcellular localization also affects the functions of

the four isoforms.[197-199] In particular, the nuclear import signal (NIS) contained in the C-terminal domain of p37[AUF-1] and p40[AUF-1] is responsible for their nuclear location. On the other hand, the insertion of exon 7-encoded amino acids in p42[AUF-1] and p45[AUF-1] disrupt the NIS to promote cytoplasmic localization. Exon 7 contains instead a nuclear export signal which allows shuttling of p42[AUF-1] and p45[AUF-1] isoforms in a nuclear matrix-independent manner.[200,201] This complex configuration has been studied in particular for p37[AUF-1] through the deletion of its C-terminal domain. In this system, after entering the nucleus in which binds to the mRNA target, the transcript-bound p37[AUF-1] returns to the cytoplasm to exert its function.[202] Subsequent studies with p40[AUF-1] identified a C-terminal sequence consisting of 19 amino acids (SGYGKVSRRGGHQNSYKPY) as the one is responsible for nucleocytoplasmic shuttling. During transport in the nucleus, the isoform interacts with the nuclear import receptor transportin 1 (Trn-1).[203] Another AUF-1 interactor, 14-3-3σ belongs to the acid protein family. This protein interacts mainly with p37[AUF-1] and to a lesser extent with p40[AUF-1]. The interaction between 14-3-3σ and p37[AUF-1] leads to retention of AUF-1 in the cytoplasm. No interaction with 14-3-3σ was shown for the other two isoforms.[204]

Collectively, these data show that there is a very organized and rigorous control over the localization and shuttling of the different AUF-1 isoforms, thus guaranteeing a diversified expression which also determines greater functional versatility.[111]

Figure 13. Structure and cellular localization of AUF-1 family isoforms. (a) Domain organization of peptide sequences encoded by alternatively spliced exons 2 and 7. Glutamine-rich (Q-rich) for nucleocytoplasmic shuttling and RRMs domains of proteins are also shown. (b) p37[AUF-1] and p40[AUF-1] isoform are predominantly cytoplasmatic and shuttle more actively between the nucleus and cytoplasm compared with the larger p42[AUF-1] and p45[AUF-1] isoforms.[111]

Rapid turnover of AUF-1 targets is the result of protein–ARE/GRE interactions as well as protein–protein interactions involving AUF-1 and other proteins within the RNP. As most RBPs, AUF-1 proteins have no intrinsic nucleolithic function but they recruit downstream components of the mRNA decay machinery, such as eukaryotic eIF4G, PABP, and heat shock proteins Hsp70, Hsc70, and Hsp27 (Figure 14).[193,205,206]

The possible mechanism of action of AUF-1 foresees that in the absence of an ARE, AUF-1 can be found as homodimer or heterodimer. Dimerization requires the presence of an alanine-rich N-terminus. Following the recognition of an ARE, oligomers are formed which can act as a platform for other factors to form an ARE-BP and signal transduction regulated complex (ASTRC). Finally, this complex is responsible for the recruitment of mRNA degradation machinery.[207] Two models for the mechanism of decay are proposed: in the first model, AUF-1 can be degraded by proteasome after its ubiquitination while the decay of mRNA is performed by recruiting the exosome;[120,193] in the second model, mRNAs can be shuttled to discrete cytoplasmic foci, such as P-bodies or stress granules (SGs) for their decay.[111]
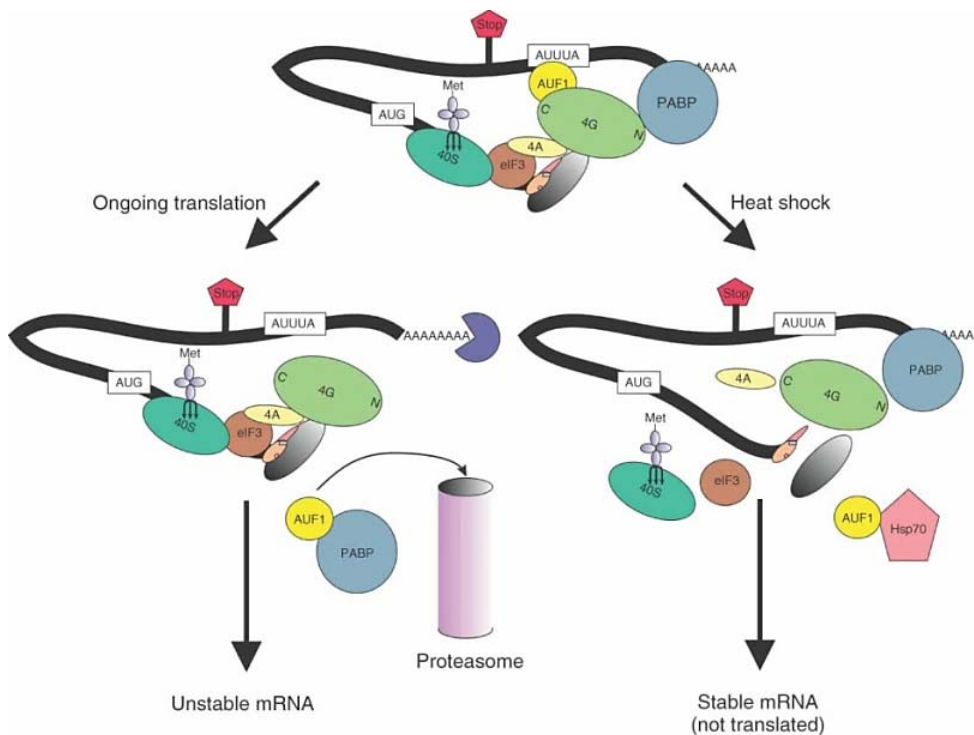
Figure 14. Mechanisms of AUF-1-mediated mRNA decay and stabilization upon heat shock. Initially, AUF-1 interacts with eIF4G and the target ARE but the regulatory outcome depends on external cell signaling. During ongoing translation, AUF-1 is removed from ARE sequence in a complex with PABP. Following the exposure of a poly A tail, the transcript is probably destined for degradation by proteasome, leading to unstable mRNA. During heat shock, hsp70 can associate instead with AUF-1 and disrupt or block the interaction between AUF-1 and PABP, leaving PABP free to remain bound to the poly(A) tail, thus masking it from ribonucleases and stabilizing the transcript.[208]

AUF-1 may also stabilize or modulate the translational efficiency of specific ARE-containing mRNAs upon cellular stress, like heat shock (Figure 14). This stabilizing effect occurs in an isoform-specific manner. For example, the p40[AUF-1] isoform is involved in transcript stabilization of the anti-inflammatory cytokine IL-10.[51,199,209] The decay activity of AUF-1 mRNA appears to be mainly mediated by the isoforms normally present in the cytoplasm (p37[AUF-1] and p40[AUF-1]).[210,211] In agreement with the diverse functional outcomes

mediated by AUF-1, in human monocytes AUF-1 promotes translation of the mRNA encoding transforming growth factor-β-activated kinase 1 (TAK1), a member of the NF-kB signaling pathway that is needed to induce expression of IL-10. Along the same lines, AUF-1 binds ARE-like sequences in the 3′-UTR of IL-10 transcript and enhances its expression levels subsequent cell stimulation with lipopolysaccharide (LPS).[209]

KH-type splicing regulatory protein (KSRP) KSRP is a multi-functional protein that converts extracellular signals into changes of gene expression by participation to multiple layers of gene regulation: it is involved in transcription, alternative pre-mRNA splicing, mRNA localization, mRNA decay of unstable mRNAs and maturation of miRNAs, including the prototypical tumor suppressor let-7.

The amino acidic sequence of KSRP consists of a central region comprising four KH domains, two of which have additional secondary structure elements. The N-terminus contains putative α-helix involved in protein-protein recognition. This structure consists of a proline-glycine (PG)-rich region and a nuclear localization signal. Instead, the carboxy-terminal includes four tyrosine-rich repeats that are important for up-regulating some targets, such as c-myc.[212] Both KH domains and sequences are necessary for efficient mRNA decay.[213] Moreover, post-translational modifications sites allow regulation of protein functions have been identified. These sites are located both in the domain KH 1 (KH1) and in the C-terminal of the protein. (Figure 15).
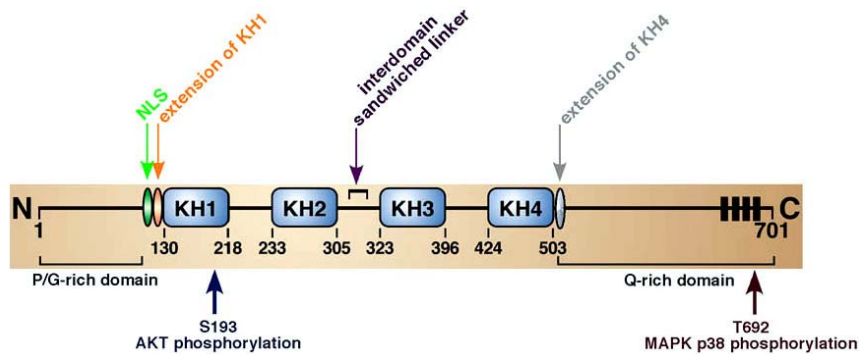
Figure 15. Schematic of KSRP structure. The structure of KSRP features four tandem KH domains. The C-terminal contains the sequence rich in Q (Q-rich), while the N-terminal contains the proline-glycine (PG)-rich region and nuclear localization signal. S193 and T692 are the phosphorylation sites for AKT and mitogen-activated protein kinase (MAPK) p38, respectively. The vertical bars show the Y-rich repetitions.[214]

Similar to other ARE-BPs, KSRP binding to ARE-containing mRNAs leads to recruitment of the exosome and other enzymes necessary to mRNA degradation.[120,215] KSRP is required in the PI3K/AKT-mediated maturation of a group of miRNAs highly enriched in skeletal muscle, collectively referred to as myomiRs, during myogenic differentiation of multipotent mesenchymal C2C12 cells.[216]

The four KH domains recognize targets in a combinatorial manner and each domain is capable of binding ARE with low affinity over a short sequence of mRNA.[217] In particular, *in vitro* studies on HeLa and HT1080 cells have shown that simultaneous binding of at least two KH domains is required to increase the binding affinity of this RBP. For example, KH3 required the collaboration of the KH2 or KH4 domains to increase the degradation function.[64,214]

Some key targets of KSRP that are relevant to hematopoiesis include ZFP36, Phorbol-12-Myristate-13-Acetate-Induced Protein 1 (NOXA), Blimp-1 variant 1 (PRDM1 variant 1), BTB Domain And CNC Homolog 2 (BACH2), Baculoviral IAP repeat-containing protein 3 (cIAP2), Bone Morphogenetic Protein 2 (BMP2), Bone morphogenetic protein 6 (BMP6), cyclin D3, CCL20, CCR1, CCR3, CCR7, CXCL2, CXCL3, CXCL10, CXCL11, ID2, IL-6, Suppressor of cytokine signaling 2 (SOCS2), E-selectin, and Toll-like receptor 4 (TLR4).[143] Immunoprecipitation studies found KSRP associated with Drosha and DGCR8 proteins and involved in regulation of maturation of let7a, miR-15b, miR-16, miR-20, miR-21, miR-26b, miR-27b, miR-98, miR-106a, miR-125b, miR-196a, miR-199a, miR-301, and miR-595. Furthermore, KSRP seems to promote the association of Drosha with pri-miRNA and of Dicer with pre-miRNA, at least for let-7a and miR-2151, and to promote their maturation. Others studies report found that KSRP is involved in the maturation of miR-155 from pri- and pre-miR-155 after LPS stimulation in macrophages.[218,219]

3. Translational control

<u>T-cell-restricted intracellular antigen (TIA)-1 and TIA-related (TIAR)</u>**.** The TIA family comprises approximately 375 ubiquitously expressed proteins with predominant expression in brain, testicle and spleen. Consistent with their functional redundancy, their translation levels are negatively cross-regulated by each other.[220-222]

TIA-1 and TIAR share more than 80% of sequence homology. Their structure is composed of three N-terminal RRMs mediating binding to mRNA targets and a C-terminal Q-rich prion-related domain (PRD) (Figure 16). The three domains RRM1, RRM2 and RRM3 have an identity of 79%, 89% and 91%, respectively, while the PRD is shared for 51%. PRD also plays an essential role, as together with the associated Q-rich domain it is essential for the SG formation. Indeed, TIA-1 KO in mouse embryonic fibroblasts (MEF) shows a reduced ability to form SG. In the same models, TIA-1 proteins without PRD do not induce spontaneous SG and are not recruited into SG induced by challenge with arsenite.[223] The RRM2 and RRM3 motifs both intervene directly in binding to the recognized target sequence, but RRM2 has a greater affinity for pyrimidine-rich sequences and drives the interaction. Specifically, RRM2 guides protein-RNA interaction while RRM3 improves overall binding affinity through its interaction with C-rich motifs.[60,61] Variations in pH may also have an effect on TIA-1 binding interactions, acting as pH-dependent molecular switch.[224] Deletional studies indicate that TIAR binding with U-rich RNA mainly relies on RRM2.[225,226]

Both TIA-1 and TIAR occur with two isoforms (a and b) as result of alternative splicing. The inclusion/exclusion of an 11 amino acid-long peptide at the beginning of RRM2 of TIA-1 forms TIA-1a and TIA-1b isoforms, respectively. Similarly for TIAR, inclusion/exclusion of a 17 amino acids fragment within RRM1 discriminates TIARa from TIARb (Figure 16).[220] These amino acids are important because they confer to the two RBPs distinct functional properties on their targets. For example, TIARa is the only isoform that shows a translational silencing activity on the proteolytic enzyme Human Matrix Metalloproteinase-13

(HMMP13) in HEK293 cells. TIARb, TIA-1a and TIA-1b do not have this activity. Some tumors show an increase of the expression levels of the HMMP13 protein, therefore its negative modulation by TIARa can act as tumor suppression.[227]
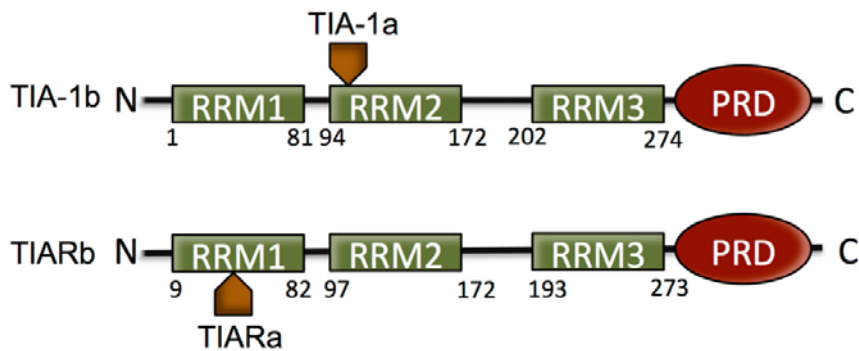
The function of translational repressors of TIA-1 and TIAR is linked to their ability to recruit target mRNAs into SGs in cells responding to external stressors, such as oxidative damage.[228,229] In unstressed cells, a preinitiation complex comprising eukaryotic translation initiation factors (eIFs) forms at the 5' end of capped mRNAs and is subsequently displaced upon assembly of the 60S subunit to initiate translation. In cells exposed to damaging stimuli, including oxidants, phosphorylation of eIF2a by a family of kinases, Protein kinase R (PKR), Eukaryotic Translation Initiation Factor 2 Alpha Kinase 3 (PERK), Eukaryotic Translation Initiation Factor 2 Alpha Kinase 4 (GCN2), Eukaryotic Translation Initiation Factor 2-alpha Kinase 1 (HRI), reduces the levels of functional preinitiation complex.[230] Under these conditions, TIAR and TIA-1 accumulate in the cytoplasm and associate with the 40S ribosomal subunit, forming inactive preinitiation complexes that function as translational repressors. The self-aggregating properties of TIA-1 and TIAR further facilitate the accumulation of the non-functional preinitiation complexes into SGs. Because other RBPs are recruited to SGs, these cytoplasmic foci are believed to function as dynamic sites of mRNA triage during stress, wherein the composition of RNP complexes and their subsequent engagement with the translation or degradation machineries are decided.[228,231] According to this regulatory paradigm, eIF2a kinases directly influence the stability or translation of TIA-target mRNAs, even though TIA proteins are not direct substrates of these kinases.

TIA-1 and TIAR can also act during the translation initiation phase to stop protein synthesis of upstream regulators. For example, during stress they can bind the terminal oligopyrimidine (TOP) mRNA, which contains a 5' terminal oligopyrimidine tract (5'-TOP) that occurs mainly in transcripts coding for ribosomal proteins as well as for elongation factors (elF1alpha and elF2) which are not required in stress condition.[225] TIA-1 and TIAR are key participants of in the SGs formation. These structures' half-life is limited in time: after their formation, the cells activate the pathways that determine the heat shock/chaperone proteins (Hsp70) production and reverse the self-association of TIA proteins. This mechanism allows to protect the proteins from denaturation; the disassembly of the SG, after several hours once the stress is lessened, allows the cell to

resume protein synthesis.[232-234] As example of stress-induced SG metabolism, under hypoxic conditions the ARE-containing hypoxia inducible factor (HIF)-1α mRNA is targeted by TIA-1 and TIAR. When both RBPs are localized in the SG, a decrease of the HIF-1α expression is observed.[235] Also HuR can aggregate in SG and modulate the translation of specific housekeeping mRNA under stress conditions.[236] SG deregulation results in cytoplasmic accumulation and is related to some diseases, such as Alzheimer's and Parkinson's disease.[237] Furthermore, TIA-1 and TIAR are able to compensate each other for negative translational regulation of c-myc, TNF-α, VEGF and COX-2.[66,238]

As described for AUF-1, several ARE-RBPs can also bind DNA sequences and influence transcription. Among these, TIA-1 and TIAR have shown higher affinity for DNA than RNA sequences. Therefore it has been hypothesized that the two RBPs could be a link between transcription and splicing.[61,239,240] To this end, splicing control over the Fas gene sequence by TIA-1 and TIAR causes the expression of the pro-apoptotic membrane-bound form in detriment of the anti-apoptotic soluble one.[241]

To summarize, it is now well established that the control of mRNA metabolism begins immediately following its transcription and continues through the distribution to different cellular compartments, up to the final translation or transcript degradation. The role of RBPs is to guide their target mRNAs along the way. As described in this paragraph, many RBPs shuttle between nucleus and cytoplasm and their functions are linked to their specific subcellular distribution. The information of RBP binding sites derived from experimental studies provide valuable functional insights about regulatory site recognition and their subcellular localization. For instance, an RBP that acts as a nuclear splicing factor rather than a cytoplasmic translation factor will have interaction sites that fall within intronic sequences or adjacent to the splicing sites.[242]

v. Elements affecting RBP function

1. Intracellular localization and post-translational modification

Similar to transcription factors and other regulatory molecules, RBPs are subjected to post-translational modifications (PTMs) that link triggers and signals from the extracellular environment to gene regulation pathways, integrating transcriptional and posttranscriptional events into a coordinated regulatory flow. The determination of target binding affinity, cellular localization of the RBPs and the functions that are consequent to this compartmentalization are all critically defined by the PTM following intracellular/extracellular signals. Phosphorylation of RBPs has been better characterized (Table 6) but others PTMs such as methylation, acetylation, ubiquitination, isomerization and NEDDylation, are also important.[66] An examplary list of the main phosphorylation sites for a selected group of mRBPs is shown in Table 6.

Table 6. List of main phosphorylation sites on RBPs.[243]

RBP	Kinase	Phosphorylation site	Type of cell
TIS11	MK2	Ser52	3T3
TIS11	CAMK2	Ser52	CD8 T
TIS11	PKB	Ser248	CD8 T
TIS11	PKA	Ser197	HEK-293
TIS11	GSK3	Ser218	HEK-293
TIS11	ERK	Ser228	HEK-293
TIS11b	PKA/PKB	Ser54/92	CD8 T
TIS11b	mTOR	Ser334	MEF
TIS11d	PKB	Ser98	3T3
TIS11d	PKA/PKB	Ser28/98	CD8 T
TIS11d	mTOR	Ser57/73/416/464	MEF
KSRP	mTOR	Ser182, Ser185	MEF
KSRP	PKA	Ser481	CD8 T
Nucleolin	mTOR	Ser28/34/40/41/145/157/616/189/403/212/460, Thr121	MEF
Roquin	ERK/MAPK	Ser770	CD8 T
Roquin	mTOR	Ser531/535	MEF
hnRNPk	CDK2	Ser284	CD8 T
hnRNPu	CK1	Ser187	CD8 T
hnRNPu	CAMK2	Ser247	CD8 T
hnRNPF	mTOR	Ser63	MEF
hnRNPA3	mTOR	Ser356/359/367	MEF
hnRNPA3	CK1	Ser359	CD8 T
hnRNPA3	PKA	Ser357	CD8 T
hnRNPAb	PKA	Ser260	CD8 T
AUF1	mTOR	Ser82/83, Thr177	MEF
hnRNPA2B1	mTOR	Ser245/247/266/272, Tyr254	MEF
hnRNPK	mTOR	Ser284/379	MEF
hnRNPC	mTOR	Ser229/232/241/268/306/313	MEF
hnRNPUL1	mTOR	Ser513	MEF
hnRNPUL1	CAMK2	Ser195	CD8 T
hnRNPA1	mTOR	Ser6/257	MEF
hnRNPA1	CDK1	Ser6	CD8 T
hnRNPH2	mTOR	Ser104	MEF
HuR	mTOR	Ser202	MEF
IMP2	mTOR	Ser102	MEF
IMP2	mTOR	Ser160/161/163	MEF

The phosphorylation sites on RBPs for respective kinases in a specific cell are obtained from published phospho-proteomic studies. In Yu et al. (2011)), mTOR phosphorylation sites on RBP in MEFs are derived using inhibitors rapamycin and KU-0063794 against mTOR in a SILAC experiment. Similarly in Hsu et al. (2011), mTOR regulated phosphosites on RBPs in MEFs were verified using Torin1 (mTOR) inhibitor in an iTRAQ experiment. By employing SILAC technology, Navarro et al. (2011) identified phosphorylation sites on different RBPs for the respective kinases in TCR stimulated CD8 T cells. Wang et al. (2008) identified phosphorylation sites on RBPs in 3T3 cells using iTRAQ.

HuR. An example of stimulus-regulated RBP compartmentalization is given by the response of HuR. As previously described, HuR is an RBP which resides mainly in the nucleus. To date, its role in this compartment is not fully clear, except for its involvement in pre-mRNA splicing. The transport of HuR through the nuclear envelope takes place via the HNS and several components of transport machinery, such as the chromosome region maintenance 1 (CRM1), importin-1α, transportins 1 and transportins 2.[136,244,245] HuR nucleocytoplasmic transport and subcellular localization has been reported to be regulated by phosphorylation induced by several kinases such as cell cycle-dependent kinase (Cdk)-1, AMP-activated protein kinase (AMPK), protein kinase C (PKC), and p38 and by methylation, via the coactivator-associated arginine methyltransferase 1 (CARM1).[246,247] In general, the type of modification determines an alteration of HuR association with the target transcripts, or a change in subcellular localization. In particular, the PTM that occurs within the RRM sequence determines an increase of the binding affinity, while PTMs close to the HNS lead to a change in localization. For example, phosphorylation of a Ser-202 by Cdk1 phosphatase leads to inhibition of 14-3-3-mediated cytoplasmic export of HuR. Cdk1 is instead inactivated under stress conditions thus determining the release of HuR in the cytoplasm.[248] Additionally, it has been shown in human mesangial cells (HMC) that HuR may undergo double phosphorylation in two different Ser residues following treatment with ATP or angiotensin II (AngII). This determines cytoplasmic export and promotes target binding activity. Upon challenge with ATP, PKC-α acts on Ser-158 and Ser-221, while AngII triggers PKC-δ action on Ser-221 and Ser-318.[249,250] Although HuR is not a direct substrate of p38 kinase, activation of MAPK p38 causes an increase in the cytoplasmic level of HuR in response to oxidants, such as taxanes and sulindac.[251] The same effect also occurs after MAPK phosphorylation in a Thr-118 in response to DNA cell damage following γ irradiation. In this specific case, an increase in the association between HuR and p21, cyclin A2 and cyclin B1 mRNAs was also found.[246,252] Methylation of HuR to Asp-271 by CARM1 and subsequent stabilization of TNF-α mRNA occurs in macrophages after LPS treatment.[253,254] Additionally, HuR's NEDDylation causes an increase in the stability of HuR, which can therefore increase stabilization of its target transcripts.[255,256]

TIS11 family. Nucleo-cytoplasmic shuttling affects also members of the TIS11 family and is controlled by PTMs. Among them, TTP has been shown to be a downstream target of phosphorylation through major kinase pathways, such as mitogen-activated protein kinases/ extracellular-signal-regulated kinase (MAPK/ERK), p38 mitogen-activated protein kinases (p38) MAPK, c-Jun N-terminal kinases (JNK), glycogen synthase kinase (GSK)-3β, Protein kinase A (PKA), PKB/AKT, and PKC.[257-259] In particular, the export of TTP from the nucleus to the cytoplasm depends on its phosphorylation of TTP at conserved serine residues by MAPK-activated protein kinase 2 (MK2), downstream to p38 MAPK.[260] In the unphosphorylated state, TTP binds ARE-containing mRNAs targeting them for decay. The limitation of its activity is provided by the proteasomal degradation that occurs in these conditions. Upon activation by p38 MAPK/MK2, protein phosphorylation of nuclear TTP at Ser-52 and Ser-178 increases the association with 14-3-3 protein.[261] This interaction protects TTP from proteosomal degradation and promotes enhanced cytoplasmic localization, but the complex remains

functionally inactive.[262-264] The restoration of TTP activity occurs through its dephosphorylation by phosphatase PP2A following the cessation of the p38-mediated stabilization signal.[148] A similar mechanism was proposed to mediate the stabilization of TNF-α in response to LPS treatment.[229] Also the interaction between nuclear pore protein Nup214 and TTP may regulate intracellular trafficking of TTP.[265]

Another member of the TIS-11 family, BRF-1 was shown to be phosphorylated by Akt at Ser-92 and Ser-203. Phosphorylated BRF-1 was still capable of binding to target mRNAs, but formed a complexes with 14-3-3 that could not be recruited to the exosome. Consequently, labile target mRNAs were stabilized following BRF-1 phosphorylation. Further studies showed that BRF-1 phosphorylation by Akt rendered BRF-1 more stable and increased its association with the cytoskeleton.[229,262]

AUF-1. Modulation of subcellular translocation of AUF-1 isoforms is regulated by MAP kinase phosphatase 1 (MKP-1), a negative regulator of the host inflammatory response to infection. This phosphatase promotes AUF-1 redistribution to the cytoplasm.[266] AUF-1 was shown to be phosphorylated *in vitro* by the anaplastic lymphoma kinase (ALK) and was found hyperphosphorylated in cells expressing a chimeric protein (nucleophosmin-ALK or NPM-ALK) whose presence is linked to anaplastic large cell lymphoma. AUF-1 phosphorylation was further correlated with an increase in the stability of several AUF-1 target mRNAs encoding proteins with roles in cell proliferation and survival.[267] *In vitro* kinase assays indicated that Ser-87 was phosphorylated by PKA and Ser-83 by GSK-3β.[268] The sequential binding of the p40^{AUF-1} dimers to the TNF-α transcript can also be modulated by phosphorylation in Ser-83 and Ser-87. In particular, the phosphorylation of Ser-83 alone is able to inhibit the binding of the dimer by 40%, while the phosphorylation of Ser-87 determines a 2-fold increase in the affinity of the second binding event. In combination of the two events, the negative effect of Ser-83 phosphorylation has a greater impact than the positive effect of Ser-87 phosphorylation.[269]

KSRP. This RBP has numerous phosphorylation sites in its structure, of which Thr-692 and Ser-193 have been shown to be especially relevant.[270] Phosphorylation of KSRP has been linked to an inhibition of its mRNA decay-promoting function by two different mechanisms. In the first mechanism, PI3K-Akt signaling phosphorylates KSRP at Ser-193. This modification promoted the assembly of KSRP with 14-3-3. The resulting complex could not be recruited to the exosome, resulting in the stabilization of a subset of KSRP target transcripts including the β-catenin mRNA.[271] KSRP was also shown to be a substrate of phosphorylation by p38, a modification that did not affect KSRP's ability to interact with the degradation machinery, but did abrogate the binding of KSRP to target mRNAs, rendering them stable.[272]

4. PGTR in inflammation: role of RBPs

a. PTGR in inflammation: a crucial rheostatic mechanism

Various endogenous and exogenous stimuli, such as damaged cells and pathogens, can cause tissue damage and trigger an inflammatory response that removes damaging causes and restore tissue integrity; importantly, inflammation 'begins with the end in mind' and damage-limiting cellular programs start as soon as inflammation begins, to avoid uncontrolled and prolonged inflammatory response that can worsen tissue damage. Mechanisms of resolution of inflammation modify cell survival and differentiation programs, regulate gene expression of pro-/anti-inflammatory cytokines, chemokines, enzymes acting both on transcriptional and post-transcriptional level.[273] While epigenetic and transcriptional events shape cell response qualitatively, deciding the pattern of gene expression to 'switch on or off' in response to endogenous or environmental triggers, PTGR rather acts a 'rheostat' and rapidly adapt the cell response by controlling the appropriate amplitude and timing of protein expression patterns. The rate-limiting control provided by PTGR is particularly critical in inflammatory and immune responses, where changes in amplitude and duration of expression for dangerous and protective genes are in dynamic balance and become critical in determining either successful resolution of acute inflammation or chronic overexpression of the adaptive immune response.[274,275]

Many inflammatory cytokine mRNAs are enriched in USER and targeted by post-transcriptional regulatory factors.[6] As described in the previous paragraphs, also in regulating inflammatory responses the specificity of PTGR is provided by the combination of multiple elements – structural features of RBPs and related binding sequences, coexpression of regulatory molecules, signalling-induced PTM changes in RNP composition and binding affinity, and so on - that ultimately regulate protein expression by stabilizing or degrading target mRNAs, and modulating translation rates.[30,276] This complex regulatory web is yet to be fully characterized in inflammatory responses in human diseases. Table 7 summarizes some of the experimental evidence for RBPs-dependent regulation of mRNA stability and translation of proteins involved in immune and inflammatory responses. (for full review and more detailed lists, see[277]).

Table 7. Short list of AU-rich elements (ARE)-RBP and their functional effect on mRNA target stability and translational efficiency of genes relevant in inflammatory responses (see [277] also for full list of acronyms).[277]

ARE-BPs	mRNA stability		Protein expression			
	Increase	Decrease	Translational efficiency		Abundance	
			Increase	Decrease	Up regulated	Down regulated
AUF-1	c-myc	c-myc				GM–CSF
	c-fos	c-fos				IL-3
	PTH	p21				
	GM–CSF	Cyclin D1				
	TNF-α	GM–CSF				
		IL-3				
HuR	c-fos		p53	TNF-α	p21	TNF-α
	MyoD			COX-2	Cyclin A	
	p21				Cyclin B1	
	Cyclin A				NOS II/iNOS	
	Cyclin B1				GM–CSF	
	Cyclin D1				COX-2	
	NOS II/iNOS				IL-3	
	GM–CSF				VEGF	
	TNF-α				p53	
	COX-2					
	IL-3					
	VEGF					
	Myogenin					
Hel-N1	TNF-α		NF-M		NF-M	
	GLUT1		GLUT1		GLUT1	
HuD	GAP-43				GAP-43	
TTP		c-fos				GM–CSF
		GM–CSF				TNF-α
		TNF-α				IL-2
		COX-2				IL-3

		IL-2			
		IL-3			
BRF1		TNF-α			GM–CSF
		IL-3			IL-3
TIA-1			TNF-α		TNF-α
			COX-2		COX-2
KSRP		c-fos			NOS II/iNOS
		NOS II/iNOS			
		TNF-α			
		IL-2			
		c-jun			
CUG-BP2	COX-2		COX-2		COX-2
Nucleolin	BCL-2				
TINO		BCL-2			
PAIP2	VEGF			VEGF	

b. Main RBPs involved in inflammatory responses: main targets and experimental *in vitro*/animal models

Within the last decade, whole genome studies of RBP-bound transcriptome, obtained through protocols of immunoprecipitation of increasing complexity, have characterized on a global scale the mRNA targets of each RBP in several cell types: these studies have revealed both overlapping and discrete targets for each RBP, along with definition of an array of binding sites.[187,278] Various *in vitro* and animal models have been developed to study RBP-mediated mechanisms of gene regulation in inflammatory responses.

i. HuR

Several studies, performed in different cell types upon various inflammatory models, have indicated that a main function of HuR consists in the stabilization of inflammatory transcripts, such as TNFα, IL-3, IL-6, IL-8, GM-CSF, COX-2, VEGF, TGF-β, iNOS, CD154 (the CD40 ligand), the β-adrenergic receptor.[279] TNF-α and COX-2 mRNAs contain an HuR binding motif (HBM) and a type III ARE at the 3′-UTR; in a mouse model of HuR transgenics crossed with mice lacking the ARE region in TNF-α transcript, the TNF-α mRNA was no longer stabilized by HuR, confirming the importance of ARE in mediating HuR regulation of TNF-α expression. Similarly, TNF-α mRNA translation is reduced in crossbreeding between overexpressing *HuR* and *TIA-1⁻/⁻* mice suggesting an important co-operation of HuR and TIA-1 in translational regulation.[280] Through stabilization of pro-inflammatory transcripts, HuR has been postulated to play a pathogenic role in various

inflammatory disorders, such as rheumatoid arthritis, particularly by increasing the expression of TNF-α and COX-2, both involved in osteocartilage destruction,[281-283] or in inflammatory bowel disease by COX-2 upregulation in the colonic epithelium.[284] In patients infected by human immunodeficiency virus (HIV), the occurrence of atherosclerosis has been linked to HuR-mediated upregulation of TNF-α and IL-6 after protease inhibitor (PI) therapy.[285] HuR upregulates the expression of several pro-inflammatory cytokines and growth factors, such as TNF-α and GM-CSF, that have a role also in bronchial asthma:[286] increased stabilization of toll-like receptor 4 (TLR4) mRNA has been found in vascular smooth muscle hyperplasia during vascular inflammation.[287] Moreover, HuR plays an important role also in T cell biology: *HuR* ablation by *lox-cre* recombinase system causes various T cell abnormalities while the mouse model of tamoxifen-inducible *HuR* conditional KO displays atrophy of multiple organs due to increased apoptosis of progenitor thymic, bone marrow, and intestinal cells.[288,289] However, HuR might also indirectly exert anti-inflammatory functions: HuR transgenic mouse models show translational silencing of ARE-containing transcripts - including TNF-α - resulting in attenuation of acute inflammatory reaction.[123,290,291] HuR can also stabilize viral mRNAs, such as Sindbis virus by binding U-rich regions,[292] or HIV reverse transcriptase.[290,293] Mice lacking HuR display increased susceptibility to endotoxemia, rapid progression of chemical-induced colitis and colitis-associated cancer.[291]

ii. TTP & TIS11 family

Genome-wide analysis of TTP-associated transcripts indicate that this RBP is a crucial regulator of ARE-bearing immune transcriptome.[149,163] controlling the mRNA decay of major cytokines, chemokines, enzymes and other determinants of inflammation (Table 8). Mouse models of TTP ablation clearly indicate its crucial role as an endogenous downregulator of acute inflammatory responses. TTP-deficient mice develop a systemic autoimmune inflammatory syndrome characterized by cachexia, conjunctivitis, dermatitis, erosive polyarticular arthritis, and patchy alopecia after 1-8 weeks from birth.[294] This strong inflammatory phenotype is mainly caused by overexpression of TNF-α due to aberrant mRNA stabilization, as demonstrated in this model by the effect of treatment with anti-TNF-α, which almost fully prevented this phenotype. Other experiments in gene ablation models reinforced the key role of TTP in regulation of TNF-α production: in $TTP^{-/-}$ bone marrow-derived mouse macrophages, LPS stimulation increases TNF-α mRNA half-life and TNF-α secretion, and anti-TNF-α antibody treatment ameliorates experimental arthritis.[295,296] Moreover, $TTP^{-/-}$ mice show several abnormalities in various organs: i) hematopoietic abnormalities, such as extramedullary hematopoiesis, hypoplastic thymus with disorganization in cortical and medullary areas, and enlarged hyperplastic spleen; ii) presence of liver and heart inflammatory abscesses;[294] iii) severe left-side cardiac valvulitis with mitral and aortic valve stenosis.[297] Extramedullary hemopoiesis is caused by GM-CSF overproduction by bone marrow stromal cells leading to accumulation of mature neutrophils in the bone marrow, lymph nodes, spleen, and peripheral blood.[298] However, $TTP^{-/-}$ myeloid progenitor cells isolated from

spleen and bone marrow do not exhibit increased *in vitro* proliferation or different cellular responses to growth factors, suggesting that TPP is required but not essential for myeloid cells development and that it needs to co-operate *in vivo* with other regulatory factors.

Table 8. Short list of main TTP mRNA targets according to biological process. For full references and acronyms description see [148].

Biological Function	TTP - mRNA targets
Immune response and inflammation	CCL2
	CCL 3
	CD86
	COX-2
	DUSP1
	E47
	GM-CSF2
	IDO
	Interleukins (IL-2, IL-32, IL-6, IL-8, IL-10, IL-12)
	IFN-γ
	MHC (Class 1B and F)
	PAI-2
	SOD2
	TNF-α2
	TIS11 (TTP)
Cell cycle	Cyclin D1
	MIP-2
	p21
	Plk3
Carcinogenesis	c-myc
	c-fos
	E6-AP
Angiogenesis	VEGF1
Development	PITX2
Protein glycosylation	1,4-galactosyltransferase

Another TIS11 family member, BRF-1, plays an important role in embryogenesis: *BRF-1* KO embryos die at day 11[299] showing intraembryonic and extraembryonic vascular abnormalities and heart malformations, failure in chorioallantoic fusion, and placental dysfunctions.[300] *BRF-1* KO embryos, in particular embryonic fibroblasts display increased VEGF-A levels; however, VEGF-A mRNA stability is not changed, suggesting a BRF-1-dependent translational regulation.[299] BRF-2 is similarly important in organogenesis, as mice lacking the BRF-2 N-terminal are infertile due to loss in luteinizing hormone receptor (LHR) expression.[301,302] Moreover, BRF-2 also influence the expression of histone demethylases H3K4 and H3K9 and induces global transcriptional silencing in oocytes, hindering the oocyte-to-embryo transition.[303]

iii. AUF-1

AUF-1 is involved in multiple cellular processes by regulating, sometimes in opposite direction, the stability of hundreds of mRNAs containing AU- and GU-rich elements according to the isoforms involved, as described by recent PAR-CLIP studies (Table 9) and discussed previously herein.[187]

As also described for TTP, *AUF-1$^{-/-}$* mouse model display a strong inflammatory phenotype. In particular, deregulation of IL-10 has an important role in this phenotype. IL-10 is an important target of AUF-1: LPS (or endotoxin)-induced IL-10 mRNA is stabilized by the p40^{AUF-1} isoform and by knocking-down *AUF-1*, IL-10 levels decrease after LPS stimulation.[304] Moreover, *AUF-1$^{-/-}$* mice are highly susceptible to endotoxin-induced septic shock with increased mortality due to an extensive inflammatory response, mediated by an inadequate TNF-α and IL-1β mRNA degradation, chiefly mediated by AUF-1.[305] Mice lacking AUF-1 develop a spontaneous chronic, pruritic inflammatory skin dermatitis highly resembling atopic dermatitis, characterized by enhanced dermal infiltration of inflammatory cells, reduced wound healing, and elevated serum IgE levels. In addition, *AUF-1$^{-/-}$* T cells and macrophages have increased expression of inflammatory mediators, such as IL-2, TNF-α, and IL-1β.[306] Mice lacking *AUF-1* have also increased telomere erosion, enhanced cellular senescence, and early-onset aging, as p42^{AUF-1} and p45^{AUF-1} induce transcriptionally the expression of TERT mRNA.[189] Overall, the heterogeneous phenotype of *AUF-1* deficient mice is linked to the wide range of AUF-1-target mRNAs and to the type of isoform involved having different functions and localization (Figure 17).

Critical for immune responses, AUF-1 is also involved in germinal center B cell development through regulation of BCL2, A1 and B-cell lymphoma-extra large (BCL-XL) genes, ultimately influencing follicular and plasma cell maturation and IgG secretion.[307] AUF-1 can also interact with viral proteins, such as the internal ribosomal entry site at the 5′-UTR of the hepatitis C virus (HCV) mRNA,[308] or Epstein–Barr virus-encoded small RNAs (EBER)-1 RNA, a non-coding RNA expressed by Epstein–Barr virus. In particular, EBER1 can compete with p40^{AUF-1} for binding to ARE-containing mRNA targets, such as type 1 IFN (IFN1) cytokines, and interfere with AUF-1 in regulation of those specific targets.[309]

Table 9. Partial list of transcripts relevant to inflammatory process regulated by AUF-1. N.D.: Not Determined. (for full reference list and acronym description see [111]).

Gene	Mechanism of mRNA Regulation	Specific Isoform(s) Implicated
GROα	Decay	N.D.
GM-CSF	Decay	p40^{AUF-1}
IL-1β	Decay	p40^{AUF-1}
IL-10	Decay	p40^{AUF-1}
IL-6	Decay	p37^{AUF-1}, p42^{AUF-1}
MCL1	Decay	p40^{AUF-1}, p42^{AUF-1}, p45^{AUF-1}
TNF-α	Decay	p40^{AUF-1}
VEGF	Decay	N.D.
IL-2	Decay	N.D.
iNOS	Decay	p37^{AUF-1}, p40^{AUF-1}, p42^{AUF-1}, p40^{AUF-1}
COX-2	Stability	p42^{AUF-1}
CDKN2A	Promotion of translation	N.D.
c-myc	Decay	N.D.
Cyclin D1	Decay	p45^{AUF-1}
Dicer1	Decay	N.D.
E2F1	Decay	N.D.
B-AR	Decay	p37^{AUF-1}
B56α	Decay	p37^{AUF-1}
Kv4.3	Decay	N.D.
SERCA2A	Decay	N.D.
ENK	Transcription	p37^{AUF-1}, p40^{AUF-1}, p42^{AUF-1}
HCV	Translation	N.D.
BCL2	Decay e stability	p40^{AUF-1}, p42^{AUF-1}, p45^{AUF-1}
A1	Stability	N.D.
BCL	Stability	N.D.
p16Ink4	Decay	p37^{AUF-1}, p40^{AUF-1}
p21cip	Decay	p37^{AUF-1}, p40^{AUF-1}
p19ARF	Decay	p37^{AUF-1}, p40^{AUF-1}
TERT	Transcription	p42^{AUF-1}, p45^{AUF-1}

Diseases of the AUF1 knockout mouse

AUF1 locus — Exon 3

Targeting vector — Neo ... TK

AUF1 knockout mouse

m7G—TNF-α—AAA$_n$
m7G—IL-1β—AAA$_n$
→ Control of systemic inflammatory response

m7G—Bcl-2—AAA$_n$
m7G—A1—AAA$_n$
m7G—Bcl-X$_L$—AAA$_n$
→ Splenic follicular B-cell maintenance

m7G—TNF-α—AAA$_n$
m7G—IL-1β—AAA$_n$
m7G—IL-2—AAA$_n$
→ Pruitic skin inflammation and atopic dermatitis

m7G—p16^{ink4a}—AAA$_n$
m7G—p19^{Arf}—AAA$_n$
m7G—p21^{CIP}—AAA$_n$
mTERT
mTERC
→ Multifaceted control of aging and cellular senescence

Figure 17. **AUF-1 KO mouse model displays multiple abnormalities.** The AUF-1 KO mouse was generated by homologous recombination in mouse embryonic stem cells by targeting the RNA-binding motif containing the third exon of AUF-1, allowing for disruption of the remainder of the reading frame. Neo, neomycin-resistant cassette; TK, thymidine kinase cassette; filled box, coding region; open box, noncoding region. Loss of AUF-1 results in dysregulation of multiple mRNA targets and transcription of select genes leading to specific phenotypes observed in the AUF-1 KO mouse.[111]

iv. TIA-1/TIAR

TIA-1 and TIAR participate to TNF-α regulation together with HuR and AUF-1: mice KO for TIA-1 display a normal basal phenotype, but after LPS challenge *TIA-1$^{-/-}$* macrophages produced larger amounts of TNF-α compared to wild type controls and mice developed mild arthritis.[280,310] Mice lacking both TIA-1 and TTP have a more severe arthritis compared to mice lacking either TIA-1 or TTP, suggesting a coordination between mechanisms of mRNA turnover and translation in the control of pro-inflammatory gene expression.[148,276,311] TIAR can also bind to TNF-α mRNA in macrophages and inhibit TNF-α translation after LPS stimulation.[312,313] Finally, TIAR can target COX-2 and HMMP-13 mRNAs in primary murine fibroblasts and human mesangial cells.[313-315]

c. RBPs in human disease

Alterations in target mRNAs due to loss of function and/or reduced expression of RBPs can result in cell dysfunctions or death, with pathogenic alterations in cell cycle, apoptosis, inflammation and other biological functions. Diseases related to alterations in target mRNAs, such as mutations in splicing sites, regulatory sequences in mRNA processing or polyadenylation signals, are frequent (> 10% of all genetic diseases) but typically affect a small number of mRNAs. This is the case of β-thalassemia, where mutations in the splicing sites or polyadenylation signal of the β-globin mRNA result in reduced synthesis of the hemoglobin β-chain.[316,317] Diseases related instead to modifications in trans-acting factors are usually more complex and heterogeneous - and are critically understudied, especially among chronic inflammatory diseases. Several RBPs can be involved in disease pathogenesis: the fragile X syndrome is an example in which a CGG expansion at the 5′-UTR of the fragile X mental retardation (FMR)-1 gene causes loss-of-function of the RBP FMRP.[318] In neurons, FMRP binds and represses neuro-specific target mRNAs by binding with high affinity *via* two KH and one RGG-binding domains.[10,319,320] This condition is associated with impaired cognitive and neurological and neuromuscular disorders. This condition is associated with intellectual disability, seizures, characteristic facial features and behavioral problems.[321]

HuR has been indicated to play a role in neurological disorder development, such as neurofibromatosis, by modulating Neurofibromatosis type 1 (NF1) mRNA expression.[322] An important role for AUF-1 has been discovered in models of human heart disease: cardiac myocytes treated with angiotensin II show increased levels of AUF-1 that accelerates mRNA decay of Potassium voltage-gated channel subfamily D member 3 ($K_v4.3$), a potassium channel protein, contributing to cardiac hypertrophy.[323,324] In addition, AUF-1 can bind the mRNA of Sarco-Endoplasmic Reticulum Calcium ATPase (SERCA2A), a calcium-regulated ATPase, in the sarcoplasmic reticulum of cardiomyocytes and increase its degradation during cardiac hypertrophy and heart failure.[111,325]

TIA-1 and TIAR proteins are associated to abnormal phase separation by mutated Prion-Related Domain (PRD)-containing protein in neurodegenerative and aging-associated diseases.[66,223,326]

i. Cancer

In the last decade, alterations of RBP expression and intracellular localization have been increasingly identified as pathogenic in human neoplastic diseases, to the point that some RBPs are currently evaluated for therapeutic targeting in several cancers. For example, AUF-1 nucleocytoplasmic shuttling is augmented in human melanoma cells and linked to increased IL-10 levels and tumor escape.[208,327] In sarcoma mouse models, overexpressed p37[AUF-1] is deemed responsible for overexpression of several cell cycle regulators, such as cyclin D1, c-myc and c-fos oncogenes leading to increased vascularization.[51,328] AUF-1 is also implicated in proliferation and invasiveness of breast cancer cells through aberrant regulation of several targets: suppression of the cell cycle inhibitor cyclin-dependent kinase Inhibitor 2A (CDKN2A), increased secretion of stromal cell-derived factor 1 (SDF1) and matrix metalloproteinase-2 (MMP-2), and facilitation of the endothelial–mesenchymal transition (EMT).[51] In addition, AUF-1 can bind and stabilize BCL-2 leading to cell survival and resistance to radio- and chemotherapy.[329]

Along the same lines, altered biology of HuR have been documented in the pathogenesis of several solid tumors such as breast, lung, ovarian and prostate cancers, where increased levels and abnormal intracellular localization of HuR are related to poor prognosis. In human hepatocarcinoma, HuR migrates in the cytoplasm under stress conditions, where binds to and stabilizes the cationic amino acid transporter 1 (CAT1) mRNA inducing miR-122 functional repression and increasing its mRNA translation.[9] In colorectal cancer cells, HuR localization is massively predominant in the cytoplasm leading to increased stabilization of COX-2 mRNA, a key player in this cancer type, through impedance of miR-16 binding.[7,145] In anaplastic large cell lymphoma (ALCL), NMP-ALK phosphorylates HuR that moves to polysomes, where binds to and stabilizes CCAAT-enhancer-binding protein (c-EBP)-β mRNA, leading to increased resistance to apoptosis.[330,331]

In the last decade, loss of TTP in several cancers has been described and correlated to aggressive phenotype and poor prognosis.[332] In particular, altered balance between TTP/HuR expression is deemed pathogenic. TTP regulates mitotic signalling pathways through decreased expression of serine/threonine kinase Pim-1, a proto-oncogene, in pancreatic carcinoma, colorectal cancer, melanoma and malignant gliomas,[333] while promoting cyclin B1 mRNA degradation in lung carcinoma.[334] In breast and cervical cancers, suppression of TTP expression is related to poor clinical outcome and high tumor grade.[335-337] In hepatocellular carcinoma (HCC) cell lines, hypermethylation of a CpG site located in *ZFP36* promoter causes loss of TTP expression.[338] Regulation of mRNA stability of adhesion proteins and extracellular matrix components might play an important role in metastasis formation, as TTP and HuR might co-operate in varius ways in regulating the expression of metalloproteinase mRNAs.[333,339,340] These two RBPs can compete for binding sites on the same mRNA target in an agonistic or antagonistic manner: HuR and TTP show different expression levels in tumors as increased HuR levels usually occur in tandem with reduced TTP expression.[68,148,341,342] Thus, upregulation of TTP expression may be therapeutically advantageous (Figure 18).
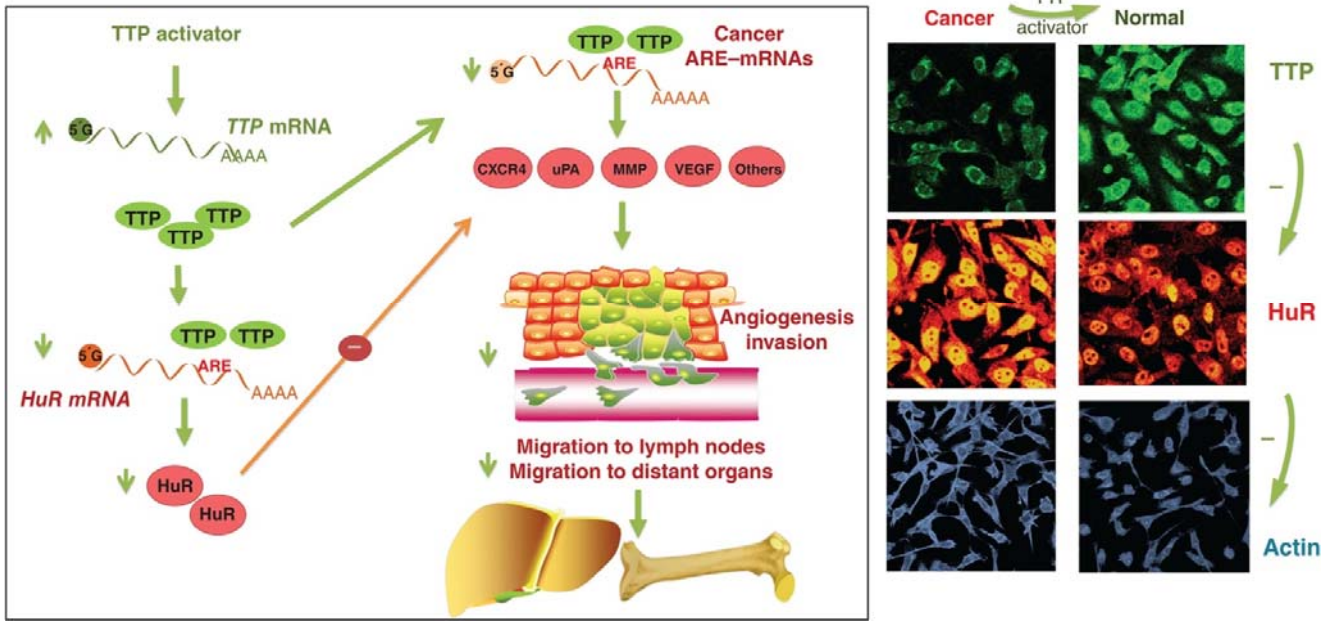
Figure 18. Graphical representation of potential modulation of the antagonistic effect between TTP and HuR in breast cancer. Through the use of a TTP activator, such as cell-permeable peptide-nucleic acid against miR-29a, TTP can act on HuR mRNA and induce a reduction in its expression while exerting mRNA-decaying effects on common targets. This combined effect determines a cascade of downstream events that leads to the modulation of several targets, previously stabilized by HuR, that promoted tumor progression and its metastasis. Right panel: changes in TTP and HuR expression levels are shown in both normal and tumor conditions through confocal microscopy. In blue the cytoskeletal polymerization of actin is shown.[343]

In malignant gliomas, HuR stabilizes and overexpresses VEGF and IL-8 promoting angiogenesis and cell proliferation;[344] on the contrary, *in vitro* ectopic TTP expression in human glioma cell lines destabilizes VEGF and IL-8 mRNA leading to growth inhibition.[345] In colorectal cancers, loss of TTP with high HuR expression impairs COX-2 mRNA expression in early stage diseases[346] while, loss of TIA-1 binding promotes COX-2 expression.[315]

ii. Chronic inflammatory diseases

Chronic lung diseases, diabetes, cardiovascular diseases are among the non-neoplastic, non-communicable diseases (NCD) underlying mortality and morbidity worldwide, along with neoplastic diseases. NCD appear to be associated with conditions that were not present during the vast majority of human history and are instead characteristic of post-industrial, western-world social structure: these include the continuous availability of high-calorie nutrients, a low level of physical activity, increased chronic exposure to pollutants and toxic compounds, changes in commensal microbiota. These conditions associate with a mal-adaptive inflammatory response expressing as a chronic low-grade inflammation that characterize all NCDs — including respiratory diseases such as chronic obstructive pulmonary disease (COPD) and asthma. This 'para-inflammation',

differently from the inflammation ensuing from tissue injury or infection, might not have any physiological counterpart and can, in turn, contribute to further disease progression.[347-349] Moreover, chronic inflammatory processes represent a major risk factor for development of many cancer types, by determining a microenvironment through which neoplastic transformation can develop. The complex combination of epigenetic, genetic and environmental factors ultimately determines whether chronic inflammation or cancer will ensue. Many signalling pathways, growth factors, citokines, chemokines, enzymes are involved in both inflammatory responses and neoplastic transformation and determine alterations along common biological responses, such proliferation/cell death, oxidative stress responses, inflammatory cell recruitment, angiogenesis. Importantly, the majority of these processes are mediated by proteins coded by ARE-bearing mRNAs, indicating the relevance of PTGR and its determinants also in inflammatory responses (Table 10). Despite numerous in-depth basic and preclinical studies - including several animal models with strong inflammatory phenotypes, as we briefly described - have clearly identified the mechanisms and unveiled a role for several mRBPs in inflammatory and immune responses,[6] translational studies in non-neoplastic NCDs are largely lagging behind those conducted in cancer, where studies on the pathogenic role of RBPs and potential therapeutic targetability are rapidly accumulating.[350-352] For example, expression level of AUF1 and HuR proteins in human peripheral blood T lymphocytes were found to be decresed in sarcoidosis patients compared to healthy individuals.[353]

Table 10. Representative ARE-rich genes involved in inflammation and in cancer.[342]

Symbol	Name	ARE*	Inflammation	Cancer
BCL2	B-cell CLL/lymphoma 2	III	Inflammatory response	Oncogenesis, apoptosis
CFOS	c-fos	III	Inflammatory response	Oncogenesis
CCND1	Cyclin D1	V		Oncogenesis, maintenance
CXCL-1	GRO-α	I	Chemotaxis	Oncogenesis, maintenance
ET2	Endothelin-2	IV	Chemotaxis, cell–cell signaling	Maintenance
EGF	Epidermal growth factor	V	Inflammatory response	Maintenance, angiogenesis, Invasion
EREG	Epiregulin	V	Cytokine response	Maintenance, angiogenesis
EGFR	EGF receptor	U-rich	Cytokine response	Cell growth, maintenance
FGF2	Fibroblastic growth factor 2	V	Chemotaxis	Cell growth, migration angiogenesis
CCL2	MCP-1	U-rich	Chemotaxis	Migration
CCL3	MIP-1α	IV	Chemotaxis	Migration
CSF2	GM-CSF	I	Cytokine response	Hematopoiesis, maintenance
CXCL-1	(Melanoma growth stimulating activity, alpha), GRO-α	II	Inflammatory response, chemotaxis	Cell growth, maintenance
ELAVL1	HuR	III	Cytokine response	RNA-binding, cell growth angiogenesis, metastasis
F3	Tissue factor	IV	Coagulation	Invasion, angiogenesis
SLC2A1	Glucose transporter 1 (Glut1)	U-rich	Inflammatory response	Maintenance
HIFA	Hypoxia induced factor-α	III	Transcription, inflammatory response	Hypoxia response, angiogenesis
IL-1β	Interleukin-1	II	Inflammatory response	Maintenance, metastasis
IL-6	Interleukin-6	IV	Inflammatory response	Cell growth, maintenance
IL8	Interleukin-8	III	Chemotaxis	Angiogenesis
LTA	Lymphotoxin	III	Inflammatory response	Oncogenesis
MMP13	Collagenase 3 (Matrix metalloproteinase-13)	V	Inflammatory response	Invasion, metastasis
NOS	Inducible nitric oxide synthase	V	Inflammatory response	DNA damage
PDGFB	Platelet-derived growth factor B	IV	Chemotaxis	Oncogenesis, maintenance
PFKB3	6-phosphofructo-2-kinase/fructose-2,6-iphosphatase 3	III	–	Carbohydrate metabolism, maintenance

PLAU	Urokinase plasminogen activator (uPA)	IV	Inflammatory response, chemotaxis	Invasion, metastasis, angiogenesis
PLAUR	UPA receptor	V	Chemotaxis	Invasion, metastasis
PTGS2	Cyclooxygenase (COX-2)	III	Inflammation, motility	Angiogenesis
PTHLH	Parathyroid hormone-like hormone	V	Inflammation	Maintenance
SCL2A1	Glut1 receptor	V	Inflammatory response	Glycolysis, maintenance
SERPINE	Plasminogen inhibitor activator 2	V	Adhesion, coagulation	Invasion, metastasis
SELE	E-selectin	III	Leukocyte adhesion, migration	Migration, metastasis
TNF	Tumor necrosis factor α	III	Inflammation, cell–cell communication	Cell growth, maintenance
VCAM	Vascular cell adhesion molecule-1	III	Leukocyte rolling	Metastasis
VEGF	Vascular endothelial growth factor	IV	Chemotaxis	Hypoxia response, angiogenesis

*ARE clusters are based on[352]

References - Part 1

1. Alberts B, Wilson J, Hunt T. Molecular biology of the cell. *Garland Science.* 2008.

2. Lee TI, Young RA. Transcription of Eukaryotic Protein-Coding Genes. *Annu Rev Genet.* 2000;34(1):77-137.

3. Roeder RG. The role of general initiation factors in transcription by RNA polymerase II. *Trends Biochem Sci.* 1996;21(9):327-335.

4. Nikolov DB, Burley SK. RNA polymerase II transcription initiation: A structural view. *Proc Natl Acad Sci U S A.* 1997;94(1):15-22.

5. Glisovic T, Bachorik JL, Yong J, Dreyfuss G. RNA-binding proteins and post-transcriptional gene regulation. *FEBS Lett.* 2008;582(14):1977-1986.

6. Anderson P. Post-transcriptional control of cytokine production. *Nat Immunol.* 2008;9(4):353-359.

7. Iadevaia V, Gerber AP. Combinatorial Control of mRNA Fates by RNA-Binding Proteins and Non-Coding RNAs. *Biomolecules.* 2015;5(4):2207-2222.

8. Ciafrè SA, Galardi S. microRNAs and RNA-binding proteins. *RNA Biol.* 2013;10(6):934-942.

9. Bhattacharyya SN, Habermacher R, Martine U, Closs EI, Filipowicz W. Relief of microRNA-Mediated Translational Repression in Human Cells Subjected to Stress. *Cell.* 2006;125(6):1111-1124.

10. Lukong KE, Chang K-w, Khandjian EW, Richard S. RNA-binding proteins in human genetic disease. *Trends Genet.* 2008;24(8):416-425.

11. Denli AM, Tops BBJ, Plasterk RHA, Ketting RF, Hannon GJ. Processing of primary microRNAs by the Microprocessor complex. *Nature.* 2004;432(7014):231-235.

12. Han J, Lee Y, Yeom KH, Kim YK, Jin H, Kim VN. The Drosha-DGCR8 complex in primary microRNA processing. *Genes Dev.* 2004;18(24):3016-3027.

13. Bartel DP. MicroRNAs: Genomics, Biogenesis, Mechanism, and Function. *Cell.* 2004;116(2):281-297.

14. Miyoshi N, Ishii H, Nagano H, et al. Reprogramming of Mouse and Human Cells to Pluripotency Using Mature MicroRNAs. *Cell Stem Cell.* 2011;8(6):633-638.

15. Anokye-Danso F, Trivedi Chinmay M, Juhr D, et al. Highly Efficient miRNA-Mediated Reprogramming of Mouse and Human Somatic Cells to Pluripotency. *Cell Stem Cell.* 2011;8(4):376-388.

16. Yuan J, Muljo SA. Exploring the RNA world in hematopoietic cells through the lens of RNA-binding proteins. *Immunol Rev.* 2013;253(1):290-303.

17. Kahvejian A, Svitkin YV, Sukarieh R, M'Boutchou M-N, Sonenberg N. Mammalian poly(A)-binding protein is a eukaryotic translation initiation factor, which acts via multiple mechanisms. *Genes Dev.* 2005;19(1):104-113.

18. Frischmeyer PA, Dietz HC. Nonsense-Mediated mRNA Decay in Health and Disease. *Hum Mol Genet.* 1999;8(10):1893-1900.

19. Chang Y-F, Imam JS, Wilkinson MF. The Nonsense-Mediated Decay RNA Surveillance Pathway. *Annu Rev Biochem.* 2007;76(1):51-74.

20. Yin S, Deng W, Zheng H, Zhang Z, Hu L, Kong X. Evidence that the nonsense-mediated mRNA decay pathway participates in X chromosome dosage compensation in mammals. *Biochem Biophys Res Commun.* 2009;383(3):378-382.

21. Kurosaki T, Maquat LE. Nonsense-mediated mRNA decay in humans at a glance. *J Cell Sci.* 2016;129(3):461-467.

22. Wilkinson MF, Shyu A-B. RNA surveillance by nuclear scanning? *Nat Cell Biol.* 2002;4(6):E144-E147.

23. Le Hir H, Séraphin B. EJCs at the Heart of Translational Control. *Cell.* 2008;133(2):213-216.

24. Nicholson P, Yepiskoposyan H, Metze S, Zamudio Orozco R, Kleinschmidt N, Mühlemann O. Nonsense-mediated mRNA decay in human cells: mechanistic insights, functions beyond quality control and the double-life of NMD factors. *Cell Mol Life Sci.* 2010;67(5):677-700.

25. Gerstberger S, Hafner M, Ascano M, Tuschl T. Evolutionary conservation and expression of human RNA-binding proteins and their role in human genetic disease. *Adv Exp Med Biol.* 2014;825:1-55.

26. Vaquerizas JM, Kummerfeld SK, Teichmann SA, Luscombe NM. A census of human transcription factors: function, expression and evolution. *Nat Rev Genet.* 2009;10(4):252-263.

27. Gerstberger S, Hafner M, Tuschl T. A census of human RNA-binding proteins. *Nat Rev Genet.* 2014;15:829.

28. Dasti A, Cid-Samper F, Bechara E, Tartaglia GG. RNA-centric approaches to study RNA-protein interactions in vitro and in silico. *Methods.* 2019.

29. Ramanathan M, Porter DF, Khavari PA. Methods to study RNA–protein interactions. *Nat Methods.* 2019;16(3):225-234.

30. Keene JD. RNA regulons: coordination of post-transcriptional events. *Nat Rev Gen.* 2007;8(7):533-543.

31. Abdelmohsen K, Pullmann R, Lal A, et al. Phosphorylation of HuR by Chk2 Regulates SIRT1 Expression. *Mol Cell.* 2007;25(4):543-557.

32. Intine RV, Tenenbaum SA, Sakulich AL, Keene JD, Maraia RJ. Differential Phosphorylation and Subcellular Localization of La RNPs Associated with Precursor tRNAs and Translation-Related mRNAs. *Mol Cell.* 2003;12(5):1301-1307.

33. Garbarino-Pico E, Niu S, Rollag MD, Strayer CA, Besharse JC, Green CB. Immediate early response of the circadian polyA ribonuclease nocturnin to two extracellular stimuli. *RNA.* 2007;13(5):745-755.

34. Lunde BM, Moore C, Varani G. RNA-binding proteins: modular design for efficient function. *Nat Rev Mol Cell Biol.* 2007;8(6):479-490.

35. Lunde BM, Moore C, Varani G. RNA-binding proteins: modular design for efficient function. *Nat Rev Mol Cell Biol.* 2007;8(6):479-490.

36. Kramer K, Sachsenberg T, Beckmann BM, et al. Photo-cross-linking and high-resolution mass spectrometry for assignment of RNA-binding sites in RNA-binding proteins. *Nat Methods.* 2014;11(10):1064-1070.

37. Stefl R, Skrisovska L, Allain FH-T. RNA sequence- and shape-dependent recognition by proteins in the ribonucleoprotein particle. *EMBO rep.* 2005;6(1):33-38.

38. Mattaj IW. RNA recognition: A family matter? *Cell.* 1993;73(5):837-840.

39. Cléry A, Allain F. From Structure to Function of RNA Binding Domains. *Landes Bioscience.* 2011.

40. Chang KY, Ramos A. The double-stranded RNA-binding motif, a versatile macromolecular docking platform. *FEBS J.* 2005;272(9):2109-2117.

41. De Boulle K, Verkerk AJMH, Reyniers E, et al. A point mutation in the FMR-1 gene associated with fragile X mental retardation. *Nate Gen.* 1993;3(1):31-35.

42. Lodish H, Berk A, Kaiser CA, Krieger M, Bretscher A, Ploegh H, Amon A, Martin KC. Mol Cell biology. *W. H. Freeman*. 2016.

43. Backe PH, Messias AC, Ravelli RBG, Sattler M, Cusack S. X-Ray Crystallographic and NMR Studies of the Third KH Domain of hnRNP K in Complex with Single-Stranded Nucleic Acids. *Structure*. 2005;13(7):1055-1067.

44. Dreyfuss G, Kim VN, Kataoka N. Messenger-RNA-binding proteins and the messages they carry. *Nat Rev Mol Cell Biol*. 2002;3(3):195-205.

45. Castello A, Fischer B, Eichelbaum K, et al. Insights into RNA Biol from an Atlas of Mammalian mRNA-Binding Proteins. *Cell*. 2012;149(6):1393-1406.

46. Beckmann BM, Castello A, Medenbach J. The expanding universe of ribonucleoproteins: of novel RNA-binding proteins and unconventional interactions. *Pflugers Arch*. 2016;468(6):1029-1040.

47. Ryder SP. Protein-mRNA interactome capture: cartography of the mRNP landscape. *F1000Res*. 2016;5:2627-2627.

48. Kastelic N, Landthaler M. mRNA interactome capture in mammalian cells. *Methods*. 2017;126:38-43.

49. Otsuka H, Fukao A, Funakami Y, Duncan KE, Fujiwara T. Emerging Evidence of Translational Control by AU-Rich Element-Binding Proteins. *Front Genet*. 2019;10(332).

50. Beckmann BM, Horos R, Fischer B, et al. The RNA-binding proteomes from yeast to man harbour conserved enigmRBPs. *Nat Commun*. 2015;6(1):10127.

51. White EJF, Brewer G, Wilson GM. Post-transcriptional control of gene expression by AUF-1: Mechanisms, physiological targets, and regulation. *Biochim Biophys Acta Gene Regul Mech*. 2013;1829(6):680-688.

52. Raghavan A, Bohjanen PR. Microarray-based analyses of mRNA decay in the regulation of mammalian gene expression. *Brief Funct Genomics*. 2004;3(2):112-124.

53. Wilusz CJ, Wilusz J. Bringing the role of mRNA decay in the control of gene expression into focus. *Trends Genet*. 2004;20(10):491-497.

54. Chen C-YA, Shyu A-B. AU-rich elements: characterization and importance in mRNA degradation. *Trends Biochem Sci*. 1995;20(11):465-470.

55. Zubiaga AM, Belasco JG, Greenberg ME. The nonamer UUAUUUAUU is the key AU-rich sequence motif that mediates mRNA degradation. *Mol Cell Biol*. 1995;15(4):2219-2230.

56. Khabar KSA. The AU-Rich Transcriptome: More Than Interferons and Cytokines, and Its Role in Disease. *J Interferon Cytokine Res*. 2005;25(1):1-10.

57. Bakheet T, Williams BRG, Khabar KSA. ARED 2.0: an update of AU-rich element mRNA database. *Nucleic Acids Res*. 2003;31(1):421-423.

58. Shen ZJ, Malter JS. Regulation of AU-Rich Element RNA Binding Proteins by Phosphorylation and the Prolyl Isomerase Pin1. *Biomolecules*. 2015;5(2):412-434.

59. Cruz-Gallardo I, Aroca Á, Gunzburg MJ, et al. The binding of TIA-1 to RNA C-rich sequences is driven by its C-terminal RRM domain. *RNA Biol*. 2014;11(6):766-776.

60. Wang I, Hennig J, Jagtap PKA, Sonntag M, Valcárcel J, Sattler M. Structure, dynamics and RNA binding of the multi-domain splicing factor TIA-1. *Nucleic Acids Res*. 2014;42(9):5949-5966.

61. Waris S, García-Mauriño SM, Sivakumaran A, et al. TIA-1 RRM23 binding and recognition of target oligonucleotides. *Nucleic Acids Res*. 2017;45(8):4944-4957.

62. Brennan CM, Steitz* JAJC, CMLS MLS. HuR and mRNA stability. *Cell Mol Life Sci.* 2001;58(2):266-277.

63. Kim HS, Wilce MCJ, Yoga YMK, et al. Different modes of interaction by TIAR and HuR with target RNA and DNA. *Nucleic Acids Res.* 2011;39(3):1117-1130.

64. García-Mayoral MF, Hollingworth D, Masino L, et al. The Structure of the C-Terminal KH Domains of KSRP Reveals a Noncanonical Motif Important for mRNA Degradation. *Structure.* 2007;15(4):485-498.

65. Gama-Carvalho M, Carmo-Fonseca M. The rules and roles of nucleocytoplasmic shuttling proteins. *FEBS Lett.* 2001;498(2-3):157-163.

66. García-Mauriño SM, Rivero-Rodríguez F, Velázquez-Cruz A, et al. RNA Binding Protein Regulation and Cross-Talk in the Control of AU-rich mRNA Fate. *Front Mol Biosci.* 2017;4(71).

67. Vlasova IA, Tahoe NM, Fan D, et al. Conserved GU-Rich Elements Mediate mRNA Decay by Binding to CUG-Binding Protein 1. *Mol Cell.* 2008;29(2):263-270.

68. Vlasova-St. Louis I, Bohjanen PR. Post-transcriptional regulation of cytokine and growth factor signaling in cancer. *Cytokine Growth Factor Rev.* 2017;33:83-93.

69. Rattenbacher B, Beisang D, Wiesner DL, et al. Analysis of CUGBP1 Targets Identifies GU-Repeat Sequences That Mediate Rapid mRNA Decay. *Mol Cell Biol.* 2010;30(16):3970-3980.

70. Timchenko LT, Miller JW, Timchenko NA, et al. Identification of a (CUG) n Triplet Repeat RNA-Binding Protein and Its Expression in Myotonic Dystrophy. *Nucleic Acids Res.* 1996;24(22):4407-4414.

71. Halees AS, Hitti E, Al-Saif M, et al. Global assessment of GU-rich regulatory content and function in the human transcriptome. *RNA Biol.* 2011;8(4):681-691.

72. Holcik M, Sonenberg N, Korneluk RG. Internal ribosome initiation of translation and the control of cell death. T*rends Genet.* 2000;16(10):469-473.

73. Pelletier J, Sonenberg N. Insertion mutagenesis to increase secondary structure within the 5′ noncoding region of a eukaryotic mRNA reduces translational efficiency. *Cell.* 1985;40(3):515-526.

74. Kozak M. Influences of mRNA secondary structure on initiation by eukaryotic ribosomes. *Proc Natl Acad Sci U S A.* 1986;83(9):2850-2854.

75. Namy O, Rousset JP, Napthine S, Brierley I. Reprogrammed genetic decoding in cellular gene expression. *Mol Cell.* 2004;13(2):157-168.

76. Walczak R, Westhof E, Carbon P, Krol A. A novel RNA structural motif in the selenocysteine insertion element of eukaryotic selenoprotein mRNAs. *RNA.* 1996;2(4):367-379.

77. Kryukov GV, Castellano S, Novoselov SV, et al. Characterization of mammalian selenoproteomes. *Science.* 2003;300(5624):1439-1443.

78. Gonzalez-Flores JN, Shetty SP, Dubey A, Copeland PR. The molecular biology of selenocysteine. *Biomol Concepts.* 2013;4(4):349-365.

79. Hentze M, Caughman S, Rouault T, et al. Identification of the iron-responsive element for the translational regulation of human ferritin mRNA. *Science.*1987;238(4833):1570-1573.

80. Casey J, Hentze M, Koeller D, et al. Iron-responsive elements: regulatory RNA sequences that control mRNA levels and translation. *Science.* 1988;240(4854):924-928.

81. Müllner EW, Kühn LC. A stem-loop in the 3′ untranslated region mediates iron-dependent regulation of transferrin receptor mRNA stability in the cytoplasm. *Cell.* 1988;53(5):815-825.

82. Constable A, Quick S, Gray NK, Hentze MW. Modulation of the RNA-binding activity of a regulatory protein by iron in vitro: switching between enzymatic and genetic function? *Proc Natl Acad Sci U S A.* 1992;89(10):4554-4558.

83. Gunshin H, Allerson CR, Polycarpou-Schwarz M, et al. Iron-dependent regulation of the divalent metal ion transporter. *FEBS Lett.* 2001;509(2):309-316.

84. Khan MA, Ma J, Walden WE, Merrick WC, Theil EC, Goss DJ. Rapid kinetics of iron responsive element (IRE) RNA/iron regulatory protein 1 and IRE-RNA/eIF4F complexes respond differently to metal ions. *Nucleic Acids Res.* 2014;42(10):6567-6577.

85. Ma J, Haldar S, Khan MA, et al. Fe2+ binds iron responsive element-RNA, selectively changing protein-binding affinities and regulating mRNA repression and activation. *Proc Natl Acad Sci U S A.* 2012;109(22):8417-8422.

86. Baird TD, Palam LR, Fusakio ME, et al. Selective mRNA translation during eIF2 phosphorylation induces expression of IBTKα. *Mol Biol Cell.* 2014;25(10):1686-1697.

87. Iacono M, Mignone F, Pesole G. uAUG and uORFs in human and rodent 5′untranslated mRNAs. *Gene.* 2005;349:97-105.

88. Jackson RJ, Hellen CUT, Pestova TV. The mechanism of eukaryotic translation initiation and principles of its regulation. *Nat Rev Mol Cell Biol.* 2010;11(2):113-127.

89. Kozak M. The scanning model for translation: an update. *J Cell Biol* 1989;108(2):229-241.

90. Gao X, Wan J, Liu B, Ma M, Shen B, Qian S-B. Quantitative profiling of initiating ribosomes in vivo. *Nat Met.* 2015;12(2):147-153.

91. Young SK, Wek RC. Upstream Open Reading Frames Differentially Regulate Gene-specific Translation in the Integrated Stress Response. *J Biol Chem.* 2016;291(33):16927-16935.

92. Jennings MD, Pavitt GD. A new function and complexity for protein translation initiation factor eIF2B. *Cell Cycle.* 2014;13(17):2660-2665.

93. Rowlands AG, Panniers R, Henshaw EC. The catalytic mechanism of guanine nucleotide exchange factor action and competitive inhibition by phosphorylated eukaryotic initiation factor 2. *J Biol Chem.* 1988;263(12):5526-5533.

94. Harding HP, Zhang Y, Zeng H, et al. An Integrated Stress Response Regulates Amino Acid Metabolism and Resistance to Oxidative Stress. *Mol Cell.* 2003;11(3):619-633.

95. Palam LR, Baird TD, Wek RC. Phosphorylation of eIF2 Facilitates Ribosomal Bypass of an Inhibitory Upstream ORF to Enhance CHOP Translation. *J Biol Chem.* 2011;286(13):10939-10949.

96. Vattem KM, Wek RC. Reinitiation involving upstream ORFs regulates ATF4 mRNA translation in mammalian cells. *Proc Natl Acad Sci U S A.* 2004;101(31):11269-11274.

97. Calkhoven CF, Müller C, Leutz A. Translational control of C/EBPα and C/EBPβ isoform expression.G*enRev.* 2000;14(15):1920-1932.

98. Zhou D, Palam LR, Jiang L, Narasimhan J, Staschke KA, Wek RC. Phosphorylation of eIF2 Directs ATF5 Translational Control in Response to Diverse Stress Conditions. *J Biol Chem.* 2008;283(11):7064-7073.

99. Zhang C, Fu J, Zhou Y. A Review in Research Progress Concerning m6A Methylation and Immunoregulation. *Front Immunol*. 2019;10:922.

100. Wei C-M, Gershowitz A, Moss B. Methylated nucleotides block 5′ terminus of HeLa cell messenger RNA. *Cell*. 1975;4(4):379-386.

101. Wei C-M, Moss B. Nucleotide sequences at the N6-methyladenosine sites of HeLa cell messenger ribonucleic acid. *Biochemistry*. 1977;16(8):1672-1676.

102. Wei CM, Gershowitz A, Moss B. 5'-Terminal and internal methylated nucleotide sequences in HeLa cell mRNA. *Biochemistry*. 1976;15(2):397-401.

103. Roignant J-Y, Soller M. m6A in mRNA: An Ancient Mechanism for Fine-Tuning Gene Expression. *Trends Genet*. 2017;33(6):380-390.

104. Yang Y, Fan X, Mao M, et al. Extensive translation of circular RNAs driven by N6-methyladenosine. *Cell Res*. 2017;27(5):626-641.

105. Wang S, Sun C, Li J, et al. Roles of RNA methylation by means of N6-methyladenosine (m6A) in human cancers. *Cancer Lett*. 2017;408:112-120.

106. Huang H, Weng H, Sun W, et al. Recognition of RNA N6-methyladenosine by IGF2BP proteins enhances mRNA stability and translation. *Nat Cell Biol*. 2018;20(3):285-295.

107. Alarcón Claudio R, Goodarzi H, Lee H, Liu X, Tavazoie S, Tavazoie Sohail F. HNRNPA2B1 Is a Mediator of m6A-Dependent Nuclear RNA Processing Events. *Cell*. 2015;162(6):1299-1308.

108. Dassi E. Handshakes and Fights: The Regulatory Interplay of RNA-Binding Proteins. *Front Mol Biosci*. 2017;4(67).

109. Nakamura H, Kawagishi H, Watanabe A, Sugimoto K, Maruyama M, Sugimoto M. Cooperative Role of the RNA-Binding Proteins Hzf and HuR in p53 Activation. *Mol Cell Biol*. 2011;31(10):1997-2009.

110. Cho SJ, Zhang J, Chen X. RNPC1 modulates the RNA-binding activity of, and cooperates with, HuR to regulate p21 mRNA stability. *Nucleic Acids Res*. 2010;38(7):2256-2267.

111. Moore AE, Chenette DM, Larkin LC, Schneider RJ. Physiological networks and disease functions of RNA-binding protein AUF-1. *Wiley Interdiscip Rev RNA*. 2014;5(4):549-564.

112. Kedar VP, Zucconi BE, Wilson GM, Blackshear PJ. Direct binding of specific AUF-1 isoforms to tandem zinc finger domains of tristetraprolin (TTP) family proteins. *J Biol Chem*. 2012;287(8):5459-5471.

113. Zhang J, Kong L, Guo S, et al. hnRNPs and ELAVL1 cooperate with uORFs to inhibit protein translation. *Nucleic Acids Res*. 2016;45(5):2849-2864.

114. Topisirovic I, Siddiqui N, Orolicki S, et al. Stability of Eukaryotic Translation Initiation Factor 4E mRNA Is Regulated by HuR, and This Activity Is Dysregulated in Cancer. *Mol Cell Biol*. 2009;29(5):1152-1162.

115. Pullmann R, Kim HH, Abdelmohsen K, et al. Analysis of Turnover and Translation Regulatory RNA-Binding Protein Expression through Binding to Cognate mRNAs. *Mol Cell Biol*. 2007;27(18):6265-6278.

116. Rahman MA, Masuda A, Ohe K, et al. HnRNP L and hnRNP LL antagonistically modulate PTB-mediated splicing suppression of CHRNA1 pre-mRNA. *Sci Rep*. 2013;3(1):2931.

117. Zhu J, Mayeda A, Krainer AR. Exon Identity Established through Differential Antagonism between Exonic Splicing Silencer-Bound hnRNP A1 and Enhancer-Bound SR Proteins. *Mol Cell*. 2001;8(6):1351-1361.

118. Gazzara MR, Mallory MJ, Roytenberg R, et al. Ancient antagonism between CELF and RBFOX families tunes mRNA splicing outcomes. *Genome Res.* 2017;27(8):1360-1370.

119. Chen C-YA, Xu N, Shyu A-B. Highly Selective Actions of HuR in Antagonizing AU-Rich Element-Mediated mRNA Destabilization. *Mol Cell Biol.* 2002;22(20):7268-7278.

120. Chen C-Y, Gherzi R, Ong S-E, et al. AU Binding Proteins Recruit the Exosome to Degrade ARE-Containing mRNAs. *Cell.* 2001;107(4):451-464.

121. Dean JLE, Wait R, Mahtani KR, Sully G, Clark AR, Saklatvala J. The 3′ Untranslated Region of Tumor Necrosis Factor Alpha mRNA Is a Target of the mRNA-Stabilizing Factor HuR. *Mol Cell Biol.* 2001;21(3):721-730.

122. Winzen R, Thakur BK, Dittrich-Breiholz O, et al. Functional Analysis of KSRP Interaction with the AU-Rich Element of Interleukin-8 and Identification of Inflammatory mRNA Targets. *Mol Cell Biol.* 2007;27(23):8388-8400.

123. Katsanou V, Papadaki O, Milatos S, et al. HuR as a Negative Posttranscriptional Modulator in Inflammation. *Mol Cell.* 2005;19(6):777-789.

124. Sawaoka H, Dixon DA, Oates JA, Boutaud O. Tristetraprolin Binds to the 3′-Untranslated Region of Cyclooxygenase-2 mRNA: A Polyadenylation Variant In A Cancer Cell Line Lacks The Binding Site. *J Biol Chem.* 2003;278(16):13928-13935.

125. Lal A, Mazan-Mamczarz K, Kawai T, Yang X, Martindale JL, Gorospe M. Concurrent versus individual binding of HuR and AUF-1 to common labile target mRNAs. *EMBO J..* 2004;23(15):3092-3102.

126. Wigington CP, Jung J, Rye EA, et al. Post-transcriptional Regulation of Programmed Cell Death 4 (PDCD4) mRNA by the RNA-binding Proteins Human Antigen R (HuR) and T-cell Intracellular Antigen 1 (TIA1). *J Biol Chem.* 2015;290(6):3468-3487.

127. Mukherjee N, Jacobs NC, Hafner M, et al. Global target mRNA specification and regulation by the RNA-binding protein ZFP36. *Genome Biol.* 2014;15(1):R12.

128. Yu T-X, Rao JN, Zou T, et al. Competitive binding of CUGBP1 and HuR to occludin mRNA controls its translation and modulates epithelial barrier function. *Mol Biol Cell.* 2013;24(2):85-99.

129. Tchen CR, Brook M, Saklatvala J, Clark AR. The Stability of Tristetraprolin mRNA Is Regulated by Mitogen-activated Protein Kinase p38 and by Tristetraprolin Itself. *J Biol Chem.* 2004;279(31):32393-32400.

130. Lin N-Y, Lin C-T, Chen Y-L, Chang C-J. Regulation of tristetraprolin during differentiation of 3T3-L1 preadipocytes. *FEBS J.* 2007;274(3):867-878.

131. Yi J, Chang N, Liu X, et al. Reduced nuclear export of HuR mRNA by HuR is linked to the loss of HuR in replicative senescence. *Nucleic Acids Res.* 2009;38(5):1547-1558.

132. Al-Ahmadi W, Al-Ghamdi M, Al-Haj L, Al-Saif M, Khabar KSA. Alternative polyadenylation variants of the RNA binding protein, HuR: abundance, role of AU-rich elements and auto-Regulation. *Nucleic Acids Res.* 2009;37(11):3612-3624.

133. Kawai T, Lal A, Yang X, Galban S, Mazan-Mamczarz K, Gorospe M. Translational Control of Cytochrome c by RNA-Binding Proteins TIA-1 and HuR. *Mol Cell Biol.* 2006;26(8):3295-3307.

134. Dalmau J, Furneaux HM, Cordon-Cardo C, Posner JB. The expression of the Hu (paraneoplastic encephalomyelitis/sensory neuronopathy) antigen in human normal and tumor tissues. *Am J Pathol.*1992;141(4):881-886.

135. Akamatsu W, Fujihara H, Mitsuhashi T, et al. The RNA-binding protein HuD regulates neuronal cell identity and maturation. *Proc Natl Acad Sci U S A.* 2005;102(12):4625-4630.

136. Fan XC, Steitz JA. HNS, a nuclear-cytoplasmic shuttling sequence in HuR. *Proc Natl Acad Sci U S A* 1998;95(26):15293-15298.

137. Lal P, Cerofolini L, D'Agostino VG, et al. Regulation of HuR structure and function by dihydrotanshinone-I. *Nucleic Acids Res.* 2017;45(16):9514-9527.

138. Kim HH, Abdelmohsen K, Lal A, et al. Nuclear HuR accumulation through phosphorylation by Cdk1. *Genes Dev.* 2008;22(13):1804-1815.

139. Lal A, Kawai T, Yang X, Mazan-Mamczarz K, Gorospe M. Antiapoptotic function of RNA-binding protein HuR effected through prothymosin α. *EMBO J.* 2005;24(10):1852-1862.

140. Abdelmohsen K, Lal A, Kim HH, Gorospe M. Posttranscriptional Orchestration of an Anti-Apoptotic Program by HuR. *Cell Cycle.* 2007;6(11):1288-1292.

141. Wang J, Guo Y, Chu H, Guan Y, Bi J, Wang B. Multiple Functions of the RNA-Binding Protein HuR in Cancer Progression, Treatment Responses and Prognosis. *Int J Mol Sci.* 2013;14(5):10015-10041.

142. Mazroui R, Di Marco S, Clair E, et al. Caspase-mediated cleavage of HuR in the cytoplasm contributes to pp32/PHAP-I regulation of apoptosis. *J Cell Biol.* 2008;180(1):113-127.

143. Baou M, Norton JD, Murphy JJ. AU-rich RNA binding proteins in hematopoiesis and leukemogenesis. *Blood.* 2011;118(22):5732-5740.

144. Donahue James M, Chang Elizabeth T, Xiao L, et al. The RNA-binding protein HuR stabilizes survivin mRNA in human oesophageal epithelial cells. *Biochem J.* 2011;437(1):89-96.

145. Young LE, Moore AE, Sokol L, Meisner-Kober N, Dixon DA. The mRNA Stability Factor HuR Inhibits MicroRNA-16 Targeting of COX-2. *Mol Cancer Res.* 2012;10(1):167-180.

146. Epis MR, Barker A, Giles KM, Beveridge DJ, Leedman PJ. The RNA-binding Protein HuR Opposes the Repression of ERBB-2 Gene Expression by MicroRNA miR-331-3p in Prostate Cancer Cells. *J Biol Chem.* 2011;286(48):41442-41454.

147. Kim HH, Kuwano Y, Srikantan S, Lee EK, Martindale JL, Gorospe M. HuR recruits let-7/RISC to repress c-Myc expression. *Genes Dev.* 2009;23(15):1743-1748.

148. Sanduja S, Blanco FF, Young LE, Kaza V, Dixon DA. The role of tristetraprolin in cancer and inflammation. *Front Biosci.* 2012;17:174-188.

149. Sanduja S, Blanco FF, Dixon DA. The roles of TTP and BRF proteins in regulated mRNA decay. *Wiley Interdiscip Rev RNA.* 2011;2(1):42-57.

150. Brewer BY, Malicka J, Blackshear PJ, Wilson GM. RNA Sequence Elements Required for High Affinity Binding by the Zinc Finger Domain of Tristetraprolin: Conformational Changes Coupled To The Bipartite Nature Of Au-Rich Mrna-Destabilizing Motifs. *J Biol Chem.* 2004;279(27):27870-27877.

151. Lykke-Andersen J, Wagner E. Recruitment and activation of mRNA decay enzymes by two ARE-mediated decay activation domains in the proteins TTP and BRF-1. *Genes Dev.* 2005;19(3):351-361.

152. Kaneda N, Murata T, Niimi Y, Minamiyama M. Cloning and characterization of the rat TIS11 gene. *Mol Cell Biochem.* 2000;213(1):119-126.

153. Lai WS, Thompson MJ, Taylor GA, Liu Y, Blackshear PJ. Promoter Analysis of Zfp-36, the Mitogen-inducible Gene Encoding the Zinc Finger Protein Tristetraprolin. *J Biol Chem.*1995;270(42):25266-25272.

154. Ogawa K, Chen F, Kim Y-J, Chen Y. Transcriptional Regulation of Tristetraprolin by Transforming Growth Factor-β in Human T Cells. *J Biol Chem.* 2003;278(32):30373-30381.

155. Cao H, Kelly MA, Kari F, et al. Green tea increases anti-inflammatory tristetraprolin and decreases pro-inflammatory tumor necrosis factor mRNA levels in rats. *J Inflamm.* 2007;4(1):1.

156. Ishmael FT, Fang X, Galdiero MR, et al. Role of the RNA-Binding Protein Tristetraprolin in Glucocorticoid-Mediated Gene Regulation. *J Immunol.* 2008;180(12):8342-8353.

157. Sauer I, Schaljo B, Vogl C, et al. Interferons limit inflammatory responses by induction of tristetraprolin. *Blood.* 2006;107(12):4790-4797.

158. Smoak K, Cidlowski JA. Glucocorticoids Regulate Tristetraprolin Synthesis and Posttranscriptionally Regulate Tumor Necrosis Factor Alpha Inflammatory Signaling. *Mol Cell Biol.* 2006;26(23):9126-9135.

159. Brooks SA, Connolly JE, Rigby WFC. The Role of mRNA Turnover in the Regulation of Tristetraprolin Expression: Evidence for an Extracellular Signal-Regulated Kinase-Specific, AU-Rich Element-Dependent, Autoregulatory Pathway. *J Immunol.* 2004;172(12):7263-7271.

160. Baou M, Jewell A, Murphy JJ. TIS11 family proteins and their roles in posttranscriptional gene regulation. *J Biomed Biotechnol.* 2009;2009:634520.

161. Storch K-F, Lipan O, Leykin I, et al. Extensive and divergent circadian gene expression in liver and heart. *Nature.* 2002;417(6884):78-83.

162. Panda S, Antoch MP, Miller BH, et al. Coordinated Transcription of Key Pathways in the Mouse by the Circadian Clock. *Cell.* 2002;109(3):307-320.

163. Stoecklin G, Tenenbaum SA, Mayo T, et al. Genome-wide Analysis Identifies Interleukin-10 mRNA as Target of Tristetraprolin. *J Biol Chem.* 2008;283(17):11689-11699.

164. Schwede A, Ellis L, Luther J, Carrington M, Stoecklin G, Clayton C. A role for Caf1 in mRNA deadenylation and decay in trypanosomes and human cells. *Nucleic Acids Res.* 2008;36(10):3374-3388.

165. Yamashita A, Chang T-C, Yamashita Y, et al. Concerted action of poly(A) nucleases and decapping enzyme in mammalian mRNA turnover. *Nat Struct Mol Biol.* 2005;12(12):1054-1063.

166. Parker R, Song H. The enzymes and control of eukaryotic mRNA turnover. *Nat Struct Mol Biol.* 2004;11(2):121-127.

167. Lai WS, Kennington EA, Blackshear PJ. Tristetraprolin and Its Family Members Can Promote the Cell-Free Deadenylation of AU-Rich Element-Containing mRNAs by Poly(A) Ribonuclease. *Mol Cell Biol.* 2003;23(11):3798-3812.

168. Eulalio A, Behm-Ansmant I, Izaurralde E. P bodies: at the crossroads of post-transcriptional pathways. *Nat Rev Mol Cell Biol.* 2007;8(1):9-22.

169. Garneau NL, Wilusz J, Wilusz CJ. The highways and byways of mRNA decay. *Nat Rev Mol Cell Biol.* 2007;8(2):113-126.

170. Liang J, Lei T, Song Y, Yanes N, Qi Y, Fu M. RNA-destabilizing Factor Tristetraprolin Negatively Regulates NF-κB Signaling. *J Biol Chem.* 2009;284(43):29383-29390.

171. Schichl YM, Resch U, Hofer-Warbinek R, de Martin R. Tristetraprolin Impairs NF-κB/p65 Nuclear Translocation. *J Biol Chem.* 2009;284(43):29571-29581.

172. Ashburner BP, Westerheide SD, Baldwin AS. The p65 (RelA) Subunit of NF-κB Interacts with the Histone Deacetylase (HDAC) Corepressors HDAC1 and HDAC2 To Negatively Regulate Gene Expression. *Mol Cell Biol.* 2001;21(20):7065-7077.

173. Tiedje C, Diaz-Muñoz MD, Trulley P, et al. The RNA-binding protein TTP is a global post-transcriptional regulator of feedback control in inflammation. *Nucleic Acids Res.* 2016;44(15):7418-7440.

174. Anderson P. Post-transcriptional regulons coordinate the initiation and resolution of inflammation. *Nat Rev Immunol.* 2010;10(1):24-35.

175. Brewer G. An A + U-rich element RNA-binding factor regulates c-myc mRNA stability in vitro. *Mol Cell Biol.*1991;11(5):2460-2466.

176. Brewer G, Ross J. Regulation of c-myc mRNA stability in vitro by a labile destabilizer with an essential nucleic acid component. *Mol Cell Biol.*1989;9(5):1996-2006.

177. White EJF, Matsangos AE, Wilson GM. AUF-1 regulation of coding and noncoding RNA. *Wiley Interdiscip Rev RNA.* 2017;8(2):e1393.

178. Wilson GM, Sun Y, Sellers J, et al. Regulation of AUF-1 Expression via Conserved Alternatively Spliced Elements in the 3′ Untranslated Region. *Mol Cell Biol.* 1999;19(6):4056-4064.

179. Wagner BJ, DeMaria CT, Sun Y, Wilson GM, Brewer G. Structure and Genomic Organization of the Human AUF-1 Gene: Alternative Pre-mRNA Splicing Generates Four Protein Isoforms. *Genomics.* 1998;48(2):195-202.

180. Zucconi BE, Wilson GM. Assembly of Functional Ribonucleoprotein Complexes by AU-rich Element RNA-binding Protein 1 (AUF-1) Requires Base-dependent and -independent RNA Contacts. *J Biol Chem.* 2013;288(39):28034-28048.

181. Lasa M, Mahtani KR, Finch A, Brewer G, Saklatvala J, Clark AR. Regulation of Cyclooxygenase 2 mRNA Stability by the Mitogen-Activated Protein Kinase p38 Signaling Cascade. *Mol Cell Biol.* 2000;20(12):4265-4274.

182. Loflin P, Chen C-YA, Shyu A-B. Unraveling a cytoplasmic role for hnRNP D in the in vivo mRNA destabilization directed by the AU-rich element. *Genes Dev.* 1999;13(14):1884-1897.

183. Fellows A, Griffin ME, Petrella BL, et al. AUF-1/hnRNP D represses expression of VEGF in macrophages. *Mol Biol Cell.* 2012;23(8):1414-1422.

184. Zucconi BE, Ballin JD, Brewer BY, et al. Alternatively Expressed Domains of AU-rich Element RNA-binding Protein 1 (AUF-1) Regulate RNA-binding Affinity, RNA-induced Protein Oligomerization, and the Local Conformation of Bound RNA Ligands. *J Biol Chem.* 2010;285(50):39127-39139.

185. DeMaria CT, Sun Y, Long L, Wagner BJ, Brewer G. Structural Determinants in AUF-1 Required for High Affinity Binding to A + U-rich Elements. *J Biol Chem.*1997;272(44):27635-27643.

186. Moraes Karen CM, Lee Wen H, Kobarg J. Analysis of the Structural Determinants for RNA Binding of the Human Protein AUF-1/hnRNP D. In. *Biol Chem.* 2002;383(5):831-837.

187. Yoon JH, De S, Srikantan S, et al. PAR-CLIP analysis uncovers AUF-1 impact on target RNA fate and genome integrity. *Nat Commun.* 2014;5:5248.

188. Fox AH, Lamond AI. Paraspeckles. *Cold Spring Harb Perspect Biol.* 2010;2(7).

189. Pont Adam R, Sadri N, Hsiao Susan J, Smith S, Schneider Robert J. mRNA Decay Factor AUF-1 Maintains Normal Aging, Telomere Maintenance, and Suppression of Senescence by Activation of Telomerase Transcription. *Mol Cell.* 2012;47(1):5-15.

190. Kang X, Chen W, Kim RH, Kang MK, Park NH. Regulation of the hTERT promoter activity by MSH2, the hnRNPs K and D, and GRHL2 in human oral squamous cell carcinoma cells. *Oncogene.* 2009;28(4):565-574.

191. Enokizono Y, Konishi Y, Nagata K, et al. Structure of hnRNP D complexed with single-stranded telomere DNA and unfolding of the quadruplex by heterogeneous nuclear ribonucleoprotein D. *J Biol Chem.* 2005;280(19):18862-18870.

192. Eversole A, Maizels N. In Vitro Properties of the Conserved Mammalian Protein hnRNP D Suggest a Role in Telomere Maintenance. *Mol Cellr Biol.* 2000;20(15):5425-5432.

193. Laroia G, Cuesta R, Brewer G, Schneider RJ. Control of mRNA Decay by Heat Shock-Ubiquitin-Proteasome Pathway. *Science.* 1999;284(5413):499-502.

194. Laroia G, Sarkar B, Schneider RJ. Ubiquitin-dependent mechanism regulates rapid turnover of AU-rich cytokine mRNAs. *Proc Natl Acad Sci U S A..* 2002;99(4):1842-1846.

195. Schoenberg DR, Maquat LE. Regulation of cytoplasmic mRNA decay. *Nat Rev Genet.* 2012;13(4):246-259.

196. Laroia G, Schneider RJ. Alternate exon insertion controls selective ubiquitination and degradation of different AUF-1 protein isoforms. *Nucleic Acids Res.* 2002;30(14):3052-3058.

197. Ing NH, Massuto DA, Jaeger LA. Estradiol up-regulates AUF-1p45 binding to stabilizing regions within the 3'-untranslated region of estrogen receptor alpha mRNA. *J Biol Chem.* 2008;283(3):1764-1772.

198. Paschoud S, Dogar AM, Kuntz C, Grisoni-Neupert B, Richman L, Kühn LC. Destabilization of Interleukin-6 mRNA Requires a Putative RNA Stem-Loop Structure, an AU-Rich Element, and the RNA-Binding Protein AUF-1. *Mol Cell Biol.* 2006;26(22):8228-8241.

199. Xu N, Chen CY, Shyu AB. Versatile role for hnRNP D isoforms in the differential regulation of cytoplasmic mRNA turnover. *Mol Cell Biol.* 2001;21(20):6960-6971.

200. Sarkar B, Lu J-Y, Schneider RJ. Nuclear Import and Export Functions in the Different Isoforms of the AUF-1/Heterogeneous Nuclear Ribonucleoprotein Protein Family. *J Biol Chem.* 2003;278(23):20700-20707.

201. Weighardt F, Cobianchi F, Cartegni L, et al. A novel hnRNP protein (HAP/SAF-B) enters a subset of hnRNP complexes and relocates in nuclear granules in response to heat shock. *J Cell Sci.* 1999;112(10):1465-1476.

202. Chen C-YA, Xu N, Zhu W, Shyu A-B. Functional dissection of hnRNP D suggests that nuclear import is required before hnRNP D can modulate mRNA turnover in the cytoplasm. *RNA.* 2004;10(4):669-680.

203. Suzuki M, Iijima M, Nishimura A, Tomozoe Y, Kamei D, Yamada M. Two separate regions essential for nuclear import of the hnRNP D nucleocytoplasmic shuttling sequence. *FEBS J.* 2005;272(15):3975-3987.

204. He C, Schneider R. 14-3-3sigma is a p37 AUF-1-binding protein that facilitates AUF-1 transport and AU-rich mRNA decay. *EMBO J.* 2006;25(16):3823-3831.

205. Lu JY, Bergman N, Sadri N, Schneider RJ. Assembly of AUF-1 with eIF4G-poly(A) binding protein complex suggests a translation function in AU-rich mRNA decay. *RNA.* 2006;12(5):883-893.

206. Sinsimer KS, Gratacós FM, Knapinska AM, et al. Chaperone Hsp27, a Novel Subunit of AUF-1 Protein Complexes, Functions in AU-Rich Element-Mediated mRNA Decay. *Mol Cell Biol.* 2008;28(17):5223-5237.

207. Wilson GM, Sun Y, Lu H, Brewer G. Assembly of AUF-1 Oligomers on U-rich RNA Targets by Sequential Dimer Association. *J Biol Chem.*1999;274(47):33374-33381.

208. Gratacós FM, Brewer G. The role of AUF-1 in regulated mRNA decay. *Wiley Interdiscip Rev RNA.* 2010;1(3):457-473.

209. Sarkar S, Han J, Sinsimer KS, et al. RNA-Binding Protein AUF-1 Regulates Lipopolysaccharide-Induced IL10 Expression by Activating IκB Kinase Complex in Monocytes. *Mol Cell Biol.* 2011;31(4):602-615.

210. Raineri I, Wegmueller D, Gross B, Certa U, Moroni C. Roles of AUF-1 isoforms, HuR and BRF1 in ARE-dependent mRNA turnover studied by RNA interference. *Nucleic Acids Res.* 2004;32(4):1279-1288.

211. Arao Y, Kikuchi A, Kishida M, et al. Stability of A+U-Rich Element Binding Factor 1 (AUF-1)-Binding Messenger Ribonucleic Acid Correlates with the Subcellular Relocalization of AUF-1 in the Rat Uterus upon Estrogen Treatment. *Mol Endocrinol.* 2004;18(9):2255-2267.

212. Davis-Smyth T, Duncan RC, Zheng T, Michelotti G, Levens D. The far upstream element-binding proteins comprise an ancient family of single-strand DNA-binding transactivators. *The J Biol Chem.* 1996;271(49):31679-31687.

213. Chou C-F, Mulky A, Maitra S, et al. Tethering KSRP, a Decay-Promoting AU-Rich Element-Binding Protein, to mRNAs Elicits mRNA Decay. *Mol Cell Biol.* 2006;26(10):3695-3706.

214. Briata P, Chen C-Y, Giovarelli M, et al. KSRP, many functions for a single protein. *Front biosci.* 2011;16:1787-1796.

215. Gherzi R, Lee K-Y, Briata P, et al. A KH Domain RNA Binding Protein, KSRP, Promotes ARE-Directed mRNA Turnover by Recruiting the Degradation Machinery. *Mol Cell.* 2004;14(5):571-583.

216. Briata P, Lin WJ, Giovarelli M, et al. PI3K/AKT signaling determines a dynamic switch between distinct KSRP functions favoring skeletal myogenesis. *Cell Death Differ.* 2012;19(3):478-487.

217. Gherzi R, Chen C-Y, Ramos A, Briata P. KSRP Controls Pleiotropic Cellular Functions. *Semin Cell Dev Biol.* 2014;34:2-8.

218. Zhang X, Wan G, Berger FG, He X, Lu X. The ATM Kinase Induces MicroRNA Biogenesis in the DNA Damage Response. *Mol Cell.* 2011;41(4):371-383.

219. Trabucchi M, Briata P, Garcia-Mayoral M, et al. The RNA-binding protein KSRP promotes the biogenesis of a subset of microRNAs. *Nature.* 2009;459(7249):1010-1014.

220. Beck ARP, Medley QG, O'Brien S, Anderson P, Streuli M. Structure, Tissue Distribution and Genomic Organization of the Murine RRM-Type RNA Binding Proteins TIA-1 and TIAR. *Nucleic Acids Res.* 1996;24(19):3829-3835.

221. Le Guiner C, Lejeune F, Galiana D, et al. TIA-1 and TIAR Activate Splicing of Alternative Exons with Weak 5′ Splice Sites followed by a U-rich Stretch on Their Own Pre-mRNAs. *J Biol Chem.* 2001;276(44):40638-40646.

222. Izquierdo JM, Valcárcel J. Two Isoforms of the T-cell Intracellular Antigen 1 (TIA-1) Splicing Factor Display Distinct Splicing Regulation Activities: Control of TIA-1 Isoform Ratio By TIA-1-Related Protein. *J Biol Chem.* 2007;282(27):19410-19417.

223. Gilks N, Kedersha N, Ayodele M, et al. Stress granule assembly is mediated by prion-like aggregation of TIA-1. *Mol Biol Cell.* 2004;15(12):5383-5398.

224. Cruz-Gallardo I, Del Conte R, Velázquez-Campoy A, García-Mauriño SM, Díaz-Moreno I. A Non-Invasive NMR Method Based on Histidine Imidazoles to Analyze the pH-Modulation of Protein–Nucleic Acid Interfaces. *Chemistry.* 2015;21(20):7588-7595.

225. Dember LM, Kim ND, Liu K-Q, Anderson P. Individual RNA Recognition Motifs of TIA-1 and TIAR Have Different RNA Binding Specificities. *J Biol Chem.* 1996;271(5):2783-2788.

226. Kim HS, Headey SJ, Yoga YMK, et al. Distinct binding properties of TIAR RRMs and linker region. *RNA Biol.* 2013;10(4):579-589.

227. Yu Q, Cok SJ, Zeng C, Morrison AR. Translational Repression of Human Matrix Metalloproteinases-13 by an Alternatively Spliced Form of T-cell-restricted Intracellular Antigen-related Protein (TIAR). *J Biol Chem.* 2003;278(3):1579-1584.

228. Kedersha N, Anderson P. Stress granules: sites of mRNA triage that regulate mRNA stability and translatability. *Biochem Soc Trans.* 2002;30(6):963-969.

229. Stoecklin G, Stubbs T, Kedersha N, et al. MK2-induced tristetraprolin:14-3-3 complexes prevent stress granule association and ARE-mRNA decay. *EMBO J.* 2004;23(6):1313-1324.

230. Holcik M, Sonenberg N. Translational control in stress and apoptosis. *Nat Rev Mol Cell Biol.* 2005;6(4):318-327.

231. Kedersha N, Stoecklin G, Ayodele M, et al. Stress granules and processing bodies are dynamically linked sites of mRNP remodeling. *J Cell Biol.* 2005;169(6):871-884.

232. Anderson P, Kedersha N. Stress granules: the Tao of RNA triage. *Trends Biochem Sci.* 2008;33(3):141-150.

233. Mazroui R, Marco SD, Kaufman RJ, Gallouzi I-E. Inhibition of the Ubiquitin-Proteasome System Induces Stress Granule Formation. *Mol Biol Cell.* 2007;18(7):2603-2618.

234. Waris S, Wilce MCJ, Wilce JA. RNA Recognition and Stress Granule Formation by TIA Proteins. *Int J Mol Sci.* 2014;15(12):23377-23388.

235. Gottschald OR, Malec V, Krasteva G, et al. TIAR and TIA-1 mRNA-Binding Proteins Co-aggregate under Conditions of Rapid Oxygen Decline and Extreme Hypoxia and Suppress the HIF-1α Pathway. *J Mol Cell Biol.* 2010;2(6):345-356.

236. Bergalet J, Fawal M, Lopez C, et al. HuR-Mediated Control of C/EBPβ mRNA Stability and Translation in ALK-Positive Anaplastic Large Cell Lymphomas. *Mol Cancer Res.* 2011;9(4):485-496.

237. Vanderweyde T, Yu H, Varnum M, et al. Contrasting Pathology of the Stress Granule Proteins TIA-1 and G3BP in Tauopathies. *J Neurosci.*2012;32(24):8270-8283.

238. Gueydan C, Droogmans L, Chalon P, Huez G, Caput D, Kruys V. Identification of TIAR as a Protein Binding to the Translational Regulatory AU-rich Element of Tumor Necrosis Factor α mRNA. *J Biol Chem*. 1999;274(4):2322-2326.

239. Suswam EA, Li YY, Mahtani H, King PH. Novel DNA-binding properties of the RNA-binding protein TIAR. *Nucleic Acids Res.* 2005;33(14):4507-4518.

240. McAlinden A, Liang L, Mukudai Y, Imamura T, Sandell LJ. Nuclear Protein TIA-1 Regulates COL2A1 Alternative Splicing and Interacts with Precursor mRNA and Genomic DNA. *J Biol Chem.* 2007;282(33):24444-24454.

241. Izquierdo JM, Valcárcel J. Fas-activated Serine/Threonine Kinase (FAST K) Synergizes with TIA-1/TIAR Proteins to Regulate Fas Alternative Splicing. *J Biol Chem.* 2007;282(3):1539-1543.

242. Mukherjee N, Wessels H-H, Lebedeva S, et al. Deciphering human ribonucleoprotein regulatory networks. *Nucleic Acids Res.* 2018;47(2):570-581.

243. Venigalla RK, Turner M. RNA-binding proteins as a point of convergence of the PI3K and p38 MAPK pathways. *Front Immunol.* 2012;3(398).

244. Gallouzi I-E, Steitz JA. Delineation of mRNA Export Pathways by the Use of Cell-Permeable Peptides. *Science.* 2001;294(5548):1895-1901.

245. Güttinger S, Mühlhäusser P, Koller-Eichhorn R, Brennecke J, Kutay U. Transportin2 functions as importin and mediates nuclear import of HuR. P*roc Natl Acad Sci U S A*.2004;101(9):2918-2923.

246. Wang W, Fan J, Yang X, et al. AMP-Activated Kinase Regulates Cytoplasmic HuR. *Mol Cell Biol.* 2002;22(10):3425-3436.

247. Doller A, Akool E-S, Huwiler A, et al. Posttranslational Modification of the AU-Rich Element Binding Protein HuR by Protein Kinase Cδ Elicits Angiotensin II-Induced Stabilization and Nuclear Export of Cyclooxygenase 2 mRNA. *Mol Cell Biol.* 2008;28(8):2608-2625.

248. Kim HH, Abdelmohsen K, Lal A, et al. Nuclear HuR accumulation through phosphorylation by Cdk1.*Genes Dev.* 2008;22(13):1804-1815.

249. Doller A, Huwiler A, Müller R, Radeke HH, Pfeilschifter J, Eberhardt W. Protein Kinase Cα-dependent Phosphorylation of the mRNA-stabilizing Factor HuR: Implications for Posttranscriptional Regulation of Cyclooxygenase-2. *Mol Cell Biol.* 2007;18(6):2137-2148.

250. Doller A, Pfeilschifter J, Eberhardt W. Signalling pathways regulating nucleo-cytoplasmic shuttling of the mRNA-binding protein HuR. *Cel Signal.* 2008;20(12):2165-2173.

251. Song I-S, Tatebe S, Dai W, Kuo MT. Delayed Mechanism for Induction of γ-Glutamylcysteine Synthetase Heavy Subunit mRNA Stability by Oxidative Stress Involving p38 Mitogen-activated Protein Kinase Signaling. *J Biol Chem.* 2005;280(31):28230-28240.

252. Lafarga V, Cuadrado A, Lopez de Silanes I, Bengoechea R, Fernandez-Capetillo O, Nebreda AR. p38 Mitogen-Activated Protein Kinase- and HuR-Dependent Stabilization of p21 Cip1 mRNA Mediates the G1S Checkpoint. *Mol Cell Biol.* 2009;29(16):4341-4351.

253. Li H, Park S, Kilburn B, et al. Lipopolysaccharide-induced Methylation of HuR, an mRNA-stabilizing Protein, by CARM1. *J Biol Chem.*2002;277(47):44623-44630.

254. Srikantan S, Gorospe M. HuR function in disease. *Front Biosci.* 2012;17:189-205.

255. Embade N, Fernández-Ramos D, Varela-Rey M, et al. Murine double minute 2 regulates Hu antigen R stability in human liver and colon cancer through NEDDylation. *Hepatology.* 2012;55(4):1237-1248.

256. Fernández-Ramos D, Martínez-Chantar ML. NEDDylation in liver cancer: The regulation of the RNA binding protein Hu antigen R. *Pancreatology.* 2015;15(S4):S49-S54.

257. Cao H, Deterding LJ, Blackshear PJ. Phosphorylation site analysis of the anti-inflammatory and mRNA-destabilizing protein tristetraprolin. *Expert Rev Proteomics.* 2007;4(6):711-726.

258. Chrestensen CA, Schroeder MJ, Shabanowitz J, et al. MAPKAP Kinase 2 Phosphorylates Tristetraprolin on in Vivo Sites Including Ser178, a Site Required for 14-3-3 Binding. *J Biol Chem.* 2004;279(11):10176-10184.

259. Mahtani KR, Brook M, Dean JLE, Sully G, Saklatvala J, Clark AR. Mitogen-Activated Protein Kinase p38 Controls the Expression and Posttranslational Modification of Tristetraprolin, a Regulator of Tumor Necrosis Factor Alpha mRNA Stability. *Mol Cell Biol.* 2001;21(19):6461-6469.

260. Brook M, Tchen CR, Santalucia T, et al. Posttranslational Regulation of Tristetraprolin Subcellular Localization and Protein Stability by p38 Mitogen-Activated Protein Kinase and Extracellular Signal-Regulated Kinase Pathways. *Mol Cell Biol.* 2006;26(6):2408-2418.

261. Mackintosh C. Dynamic interactions between 14-3-3 proteins and phosphoproteins regulate diverse cellular processes. *Biochem J.* 2004;381(2):329-342.

262. Benjamin D, Schmidlin M, Min L, Gross B, Moroni C. BRF1 Protein Turnover and mRNA Decay Activity Are Regulated by Protein Kinase B at the Same Phosphorylation Sites. *Mol Cell Biol.* 2006;26(24):9497-9507.

263. Sun L, Stoecklin G, Van Way S, et al. Tristetraprolin (TTP)-14-3-3 Complex Formation Protects TTP from Dephosphorylation by Protein Phosphatase 2a and Stabilizes Tumor Necrosis Factor-α mRNA. *J Biol Chem.* 2007;282(6):3766-3777.

264. Johnson BA, Stehn JR, Yaffe MB, Blackwell TK. Cytoplasmic Localization of Tristetraprolin Involves 14-3-3-dependent and -independent Mechanisms. *J Biol Chem.* 2002;277(20):18029-18036.

265. Carman JA, Nadler SG. Direct association of tristetraprolin with the nucleoporin CAN/Nup214. *Biochem Biophys Res Commun.* 2004;315(2):445-449.

266. Yu H, Sun Y, Haycraft C, Palanisamy V, Kirkwood KL. MKP-1 regulates cytokine mRNA stability through selectively modulation subcellular translocation of AUF-1. *Cytokine.* 2011;56(2):245-255.

267. Fawal M, Armstrong F, Ollier S, et al. A "liaison dangereuse" between AUF-1/hnRNPD and the oncogenic tyrosine kinase NPM-ALK. *Blood.* 2006;108(8):2780-2788.

268. Tolnay M, Juang Y-T, Tsokos GC. Protein kinase A enhances, whereas glycogen synthase kinase-3 beta inhibits, the activity of the exon 2-encoded transactivator domain of heterogeneous nuclear ribonucleoprotein D in a hierarchical fashion. *Biochem J.* 2002;363(1):127-136.

269. Wilson GM, Lu J, Sutphen K, et al. Phosphorylation of p40AUF-1 Regulates Binding to A + U-rich mRNA-destabilizing Elements and Protein-induced Changes in Ribonucleoprotein Structure. *J Biol Chem.* 2003;278(35):33039-33048.

270. Díaz-Moreno I, Hollingworth D, Kelly G, et al. Orientation of the central domains of KSRP and its implications for the interaction with the RNA targets. *Nucleic Acids Res.* 2010;38(15):5193-5205.

271. Ruggiero T, Trabucchi M, Ponassi M, et al. Identification of a set of KSRP target transcripts upregulated by PI3K-AKT signaling. *BMC Mol Biol.* 2007;8(1):28.

272. Briata P, Forcales SV, Ponassi M, et al. p38-Dependent Phosphorylation of the mRNA Decay-Promoting Factor KSRP Controls the Stability of Select Myogenic Transcripts. *Mol Cell.* 2005;20(6):891-903.

273. Hao S, Baltimore D. The stability of mRNA influences the temporal order of the induction of genes encoding inflammatory molecules. *Nat Immunol.* 2009;10(3):281-288.

274. Shyu A-B, Wilkinson MF. The Double Lives of Shuttling mRNA Binding Proteins. *Cell.* 2000;102(2):135-138.

275. Anderson P, Phillips K, Stoecklin G, Kedersha N. Post-transcriptional regulation of proinflammatory proteins. *J Leukoc Biol.* 2004;76(1):42-47.

276. Stoecklin G, Anderson P. Posttranscriptional Mechanisms Regulating the Inflammatory Response. *Adv Immunol.* 2006;89:1-37.

277. Barreau C, Paillard L, Osborne HB. AU-rich elements and associated factors: are there unifying principles? *Nucleic Acids Res.* 2005;33(22):7138-7150.

278. Hafner M, Landthaler M, Burger L, et al. Transcriptome-wide Identification of RNA-Binding Protein and MicroRNA Target Sites by PAR-CLIP. *Cell.* 2010;141(1):129-141.

279. Fan J, Ishmael FT, Fang X, et al. Chemokine transcripts as targets of the RNA-binding protein HuR in human airway epithelium. *J Immunol.* 2011;186(4):2482-2494.

280. Khera TK, Dick AD, Nicholson LB. Mechanisms of TNFα regulation in uveitis: Focus on RNA-binding proteins. *Prog Retin Eye Res.* 2010;29(6):610-621.

281. Nieminen R, Vuolteenaho K, Riutta A, et al. Aurothiomalate inhibits COX-2 expression in chondrocytes and in human cartilage possibly through its effects on COX-2 mRNA stability. *Eur J Pharmacol.* 2008;587(1):309-316.

282. Sugihara M, Tsutsumi A, Suzuki E, et al. Effects of infliximab therapy on gene expression levels of tumor necrosis factor α, tristetraprolin, T cell intracellular antigen 1, and Hu antigen R in patients with rheumatoid arthritis. *Arthritis Rheum.* 2007;56(7):2160-2169.

283. Suzuki E, Tsutsumi A, Sugihara M, et al. Expression of TNF-alpha, tristetraprolin, T-cell intracellular antigen-1 and Hu antigen R genes in synovium of patients with rheumatoid arthritis. *Int J Mol Med.* 2006;18(2):273-278.

284. Mari JFD, Saada JI, Mifflin RC, Valentich JD, Powell DW. HETEs enhance IL-1-mediated COX-2 expression via augmentation of message stability in human colonic myofibroblasts. 2 *Am J Physiol Gastrointest Liver Physiol.* 2007;293(4):G719-G728.

285. Zhou H, Jarujaron S, Gurley EC, et al. HIV protease inhibitors increase TNF-α and IL-6 expression in macrophages: Involvement of the RNA-binding protein HuR. *Atherosclerosis.* 2007;195(1):e134-e143.

286. Esnault S, Malter JS. Hyaluronic Acid or TNF-α Plus Fibronectin Triggers Granulocyte Macrophage-Colony-Stimulating Factor mRNA Stabilization in Eosinophils Yet Engages Differential Intracellular Pathways and mRNA Binding Proteins. *J Immol.* 2003;171(12):6780-6787.

287. Lin F-Y, Chen Y-H, Lin Y-W, et al. The role of human antigen R, an RNA-binding protein, in mediating the stabilization of toll-like receptor 4 mRNA induced by endotoxin: a novel mechanism involved in vascular inflammation. *Arterioscler Thromb Vasc Biol.* 2006;26(12):2622-2629.

288. Papadaki O, Milatos S, Grammenoudi S, Mukherjee N, Keene JD, Kontoyiannis DL. Control of Thymic T Cell Maturation, Deletion and Egress by the RNA-Binding Protein HuR. *J Immunol.* 2009;182(11):6779-6788.

289. Stellato C, Gubin MM, Magee JD, et al. Coordinate Regulation of GATA-3 and Th2 Cytokine Gene Expression by the RNA-Binding Protein HuR. *J Immunol.* 2011;187(1):441-449.

290. Srikantan S, Gorospe M. HuR function in disease. *Front biosci.* 2012;17:189-205.

291. Yiakouvaki A, Dimitriou M, Karakasiliotis I, Eftychi C, Theocharis S, Kontoyiannis DL. Myeloid cell expression of the RNA-binding protein HuR protects mice from pathologic inflammation and colorectal carcinogenesis. *J Clin Invest.* 2012;122(1):48-61.

292. Sokoloski KJ, Dickson AM, Chaskey EL, Garneau NL, Wilusz CJ, Wilusz J. Sindbis Virus Usurps the Cellular HuR Protein to Stabilize Its Transcripts and Promote Productive Infections in Mammalian and Mosquito Cells. *Cell Host Microbe.* 2010;8(2):196-207.

293. Lemay J, Maidou-Peindara P, Bader T, et al. HuR interacts with human immunodeficiency virus type 1 reverse transcriptase, and modulates reverse transcription in infected cells. *Retrovirology.* 2008;5(1):47.

294. Taylor GA, Carballo E, Lee DM, et al. A Pathogenetic Role for TNFα in the Syndrome of Cachexia, Arthritis, and Autoimmunity Resulting from Tristetraprolin (TTP) Deficiency. *Immunity.* 1996;4(5):445-454.

295. Carballo E, Blackshear PJ. Roles of tumor necrosis factor-α receptor subtypes in the pathogenesis of the tristetraprolin-deficiency syndrome. *Blood.* 2001;98(8):2389-2395.

296. Keffer J, Probert L, Cazlaris H, et al. Transgenic mice expressing human tumour necrosis factor: a predictive genetic model of arthritis. *EMBO J.* 1991;10(13):4025-4031.

297. Ghosh S, Hoenerhoff MJ, Clayton N, et al. Left-Sided Cardiac Valvulitis in Tristetraprolin-Deficient Mice: The Role of Tumor Necrosis Factor α. *Am J Pathol.* 2010;176(3):1484-1493.

298. Carballo E, Lai WS, Blackshear PJ. Evidence that tristetraprolin is a physiological regulator of granulocyte-macrophage colony-stimulating factor messenger RNA deadenylation and stability. *Blood.* 2000;95(6):1891-1899.

299. Bell SE, Sanchez MJ, Spasic-Boskovic O, et al. The RNA binding protein Zfp36l1 is required for normal vascularisation and post-transcriptionally regulates VEGF expression. *Dev Dyn.* 2006;235(11):3144-3155.

300. Stumpo DJ, Byrd NA, Phillips RS, et al. Chorioallantoic Fusion Defects and Embryonic Lethality Resulting from Disruption of Zfp36L1, a Gene Encoding a CCCH Tandem Zinc Finger Protein of the Tristetraprolin Family. *Mol Cell Biol .* 2004;24(14):6445-6455.

301. Ramos SBV, Stumpo DJ, Kennington EA, et al. The CCCH tandem zinc-finger protein Zfp36l2 is crucial for female fertility and early embryonic development. *Development.* 2004;131(19):4883-4893.

302. Ball CB, Rodriguez KF, Stumpo DJ, et al. The RNA-Binding Protein, ZFP36L2, Influences Ovulation and Oocyte Maturation. *PLOS ONE.* 2014;9(5):e97324.

303. Dumdie JN, Cho K, Ramaiah M, et al. Chromatin Modification and Global Transcriptional Silencing in the Oocyte Mediated by the mRNA Decay Activator ZFP36L2. *Dev Cell.* 2018;44(3):392-402.e397.

304. Sarkar S, Sinsimer KS, Foster RL, Brewer G, Pestka S. AUF-1 Isoform-Specific Regulation of Anti-inflammatory IL10 Expression in Monocytes. *J Interferon Cytokine Res.* 2008;28(11):679-691.

305. Lu J-Y, Sadri N, Schneider RJ. Endotoxic shock in AUF-1 knockout mice mediated by failure to degrade proinflammatory cytokine mRNAs. *Genes Dev.* 2006;20(22):3174-3184.

306. Sadri N, Schneider RJ. AUF-1/Hnrnpd-Deficient Mice Develop Pruritic Inflammatory Skin Disease. *J Invest Dermatol.* 2009;129(3):657-670.

307. Sadri N, Lu J-Y, Badura ML, Schneider RJ. AUF-1 is involved in splenic follicular B cell maintenance. *BMC Immunology.* 2010;11(1):1.

308. Paek KY, Kim CS, Park SM, Kim JH, Jang SK. RNA-Binding Protein hnRNP D Modulates Internal Ribosome Entry Site-Dependent Translation of Hepatitis C Virus RNA. *J Virol.* 2008;82(24):12082-12093.

309. Lee N, Pimienta G, Steitz JA. AUF-1/hnRNP D is a novel protein partner of the EBER1 noncoding RNA of Epstein-Barr virus. *RNA.* 2012;18(11):2073-2082.

310. Piecyk M, Wax S, Beck ARP, et al. TIA-1 is a translational silencer that selectively regulates the expression of TNF-α. *EMBO J.* 2000;19(15):4154-4163.

311. Phillips K, Kedersha N, Shen L, Blackshear PJ, Anderson P. Arthritis suppressor genes TIA-1 and TTP dampen the expression of tumor necrosis factor α, cyclooxygenase 2, and inflammatory arthritis. *Proc Natl Acad Sci U S A.* 2004;101(7):2011-2016.

312. Lewis T, Gueydan C, Huez G, Toulmé J-J, Kruys V. Mapping of a Minimal AU-rich Sequence Required for Lipopolysaccharide-induced Binding of a 55-kDa Protein on Tumor Necrosis Factor-α mRNA. *J Biol Chem.* 1998;273(22):13781-13786.

313. Ostareck DH, Ostareck-Lederer A. RNA-Binding Proteins in the Control of LPS-Induced Macrophage Response. *Front Genet.* 2019;10(31).

314. Cok SJ, Acton SJ, Morrison AR. The Proximal Region of the 3′-Untranslated Region of Cyclooxygenase-2 is Recognized by a Multimeric Protein Complex Containing HuR, TIA-1, TIAR, and the Heterogeneous Nuclear Ribonucleoprotein U. *J Biol Chem.* 2003;278(38):36157-36162.

315. Dixon DA, Balch GC, Kedersha N, et al. Regulation of Cyclooxygenase-2 Expression by the Translational Silencer TIA-1. *J Exp Med.* 2003;198(3):475-481.

316. Gehring NH, Wahle E, Fischer U. Deciphering the mRNP Code: RNA-Bound Determinants of Post-Transcriptional Gene Regulation. *Trends Biochem Sci.* 2017;42(5):369-382.

317. Galanello R, Origa R. Beta-thalassemia. *Orphanet J Rare Dis.* 2010;5(1):11.

318. Chelly J, Mandel J-L. Monogenic causes of X-linked mental retardation. *Nat Rev Genet.* 2001;2(9):669-680.

319. Darnell JC, Fraser CE, Mostovetsky O, et al. Kissing complex RNAs mediate interaction between the Fragile-X mental retardation protein KH2 domain and brain polyribosomes. *Genes Dev.* 2005;19(8):903-918.

320. Bardoni B, Davidovic L, Bensaid M, Khandjian EW. The fragile X syndrome: exploring its molecular basis and seeking a treatment. *Expert Rev Mol Med.* 2006;8(8):1-16.

321. Sitzmann AF, Hagelstrom RT, Tassone F, Hagerman RJ, Butler MG. Rare FMR1 gene mutations causing fragile X syndrome: A review. *Am J Med Genet A.* 2018;176(1):11-18.

322. Haeussler J, Haeusler J, Striebel AM, et al. Tumor Antigen HuR Binds Specifically to One of Five Protein-Binding Segments in the 3′-Untranslated Region of the Neurofibromin Messenger RNA. *Biochem Biophys Res Commun.* 2000;267(3):726-732.

323. Tomaselli GF, Marbán E. Electrophysiological remodeling in hypertrophy and heart failure. *Cardiovasc Res.* 1999;42(2):270-283.

324. Zhou C, Vignere CZ, Levitan ES. AUF-1 is upregulated by angiotensin II to destabilize cardiac Kv4.3 channel mRNA. *J Mol Cell Cardiol.* 2008;45(6):832-838.

325. Blum JL, Samarel AM, Mestril R. Phosphorylation and binding of AUF-1 to the 3′-untranslated region of cardiomyocyte SERCA2a mRNA. *Am J Physiol Heart Circ Physiol.* 2005;289(6):H2543-H2550.

326. Kai M. Kai, M. Roles of RNA-Binding Proteins in DNA Damage Response. *Int. J. Mol. Sci.* 2016;17(4):604.

327. Brewer G, Saccani S, Sarkar S, Lewis A, Pestka S. Increased Interleukin-10 mRNA Stability in Melanoma Cells Is Associated with Decreased Levels of A + U-Rich Element Binding Factor AUF-1. *J Interferon Cytokine Res.* 2003;23(10):553-564.

328. Gouble A, Grazide S, Meggetto F, Mercier P, Delsol G, Morello D. A new player in oncogenesis: AUF-1/hnRNPD overexpression leads to tumorigenesis in transgenic mice. *Cancer Res.* 2002;62(5):1489-1495.

329. Cory S, Adams JM. The Bcl2 family: regulators of the cellular life-or-death switch. *Nat Rev Cancer.* 2002;2(9):647-656.

330. Bergalet J, Fawal M, Lopez C, et al. HuR-Mediated Control of C/EBPβ mRNA Stability and Translation in ALK-Positive Anaplastic Large Cell Lymphomas. *Mol Cancer Res. 2*011;9(4):485-496.

331. Piva R, Pellegrino E, Mattioli M, et al. Functional validation of the anaplastic lymphoma kinase signature identifies CEBPB and Bcl2A1 as critical target genes. *J Clin Invest.* 2006;116(12):3171-3182.

332. Wang H, Ding N, Guo J, Xia J, Ruan Y. Dysregulation of TTP and HuR plays an important role in cancers. *Tumor Biol.* 2016;37(11):14451-14461.

333. Guo J, Qu H, Chen Y, Xia J. The role of RNA-binding protein tristetraprolin in cancer and immunity. *Med Oncol.* 2017;34(12):196.

334. Zheng X-T, Xiao X-Q. Sodium butyrate down-regulates tristetraprolin-mediated cyclin B1 expression independent of the formation of processing bodies. *Int J Biochem Cell Biol.* 2015;69:241-248.

335. Carrick DM, Blackshear PJ. Comparative expression of tristetraprolin (TTP) family member transcripts in normal human tissues and cancer cell lines. *Arch Biochem Biophys.* 2007;462(2):278-285.

336. Sanduja S, Kaza V, Dixon DA. The mRNA decay factor tristetraprolin (TTP) induces senescence in human papillomavirus-transformed cervical cancer cells by targeting E6-AP ubiquitin ligase. *Aging.* 2009;1(9):803-817.

337. Brennan SE, Kuwano Y, Alkharouf N, Blackshear PJ, Gorospe M, Wilson GM. The mRNA-Destabilizing Protein Tristetraprolin Is Suppressed in Many Cancers, Altering Tumorigenic Phenotypes and Patient Prognosis. *Cancer Res. 2*009;69(12):5168-5176.

338. Sohn BH, Park IY, Lee JJ, et al. Functional Switching of TGF-β1 Signaling in Liver Cancer via Epigenetic Modulation of a Single CpG Site in TTP Promoter. *Gastroenterology.* 2010;138(5):1898-1908.e1812.

339. Govindaraju S, Lee BS. Adaptive and maladaptive expression of the mRNA regulatory protein HuR. *World J Biol Chem.* 2013;4(4):111-118.

340. Vikesaa J, Hansen TV, Jønson L, et al. RNA-binding IMPs promote cell adhesion and invadopodia formation. *EMBO J.* 2006;25(7):1456-1468.

341. Kotta-Loizou I, Giaginis C, Theocharis S. Clinical significance of HuR expression in human malignancy. *Med Oncol.* 2014;31(9):161.

342. Khabar KSA. Post-transcriptional control during chronic inflammation and cancer: a focus on AU-rich elements. *Cell Mol Life Sci.* 2010;67(17):2937-2955

343. Khabar KSA. Hallmarks of cancer and AU-rich elements. *Wiley Interdiscip Rev RNA.* 2017;8(1):e1368.

344. Nabors LB, Gillespie GY, Harkins L, King PH. HuR, a RNA Stability Factor, Is Expressed in Malignant Brain Tumors and Binds to Adenine- and Uridine-rich Elements within the 3′ Untranslated Regions of Cytokine and Angiogenic Factor mRNAs. *Cancer Res.* 2001;61(5):2154-2161.

345. Suswam E, Li Y, Zhang X, et al. Tristetraprolin Down-regulates Interleukin-8 and Vascular Endothelial Growth Factor in Malignant Glioma Cells. *Cancer Res.* 2008;68(3):674-682.

346. Young LE, Sanduja S, Bemis–Standoli K, Pena EA, Price RL, Dixon DA. The mRNA Binding Proteins HuR and Tristetraprolin Regulate Cyclooxygenase 2 Expression During Colon Carcinogenesis. *Gastroenterology.* 2009;136(5):1669-1679.

347. Medzhitov R. Inflammation 2010: New Adventures of an Old Flame. *Cell.* 2010;140(6):771-776.

348. Medzhitov R. Origin and physiological roles of inflammation. *Nature.* 2008;454(7203):428-435.

349. Nathan C, Ding A. Nonresolving Inflammation. *Cell.* 2010;140(6):871-882.

350. Muralidharan R, Panneerselvam J, Chen A, Zhao YD, Munshi A, Ramesh R. HuR-targeted nanotherapy in combination with AMD3100 suppresses CXCR4 expression, cell growth, migration and invasion in lung cancer. *Cancer Gene Ther.* 2015;22(12):581-590.

351. Hitti E, Bakheet T, Al-Souhibani N, et al. Systematic Analysis of AU-Rich Element Expression in Cancer Reveals Common Functional Clusters Regulated by Key RNA-Binding Proteins. *Cancer Res.* 2016;76(14):4068-4080.

352. Bakheet T, Frevel M, Williams BRG, Greer W, Khabar KSA. ARED: human AU-rich element-containing mRNA database reveals an unexpectedly diverse functional repertoire of encoded proteins. *Nucleic Acids Res*. 2001;29(1):246-254.

353. Navratilova Z, Novosadova E, Hagemann-Jensen M, et al. Expression Profile of Six RNA-Binding Proteins in Pulmonary Sarcoidosis. PLOS ONE. 2016;11(8):e0161669.

Part 2.

General Aim and Studies
of the PhD Research Project

1. <u>General aim and specific studies of the PhD project</u>

The general aim of this thesis is to study the RBPs that regulate the fate and translation of protein-coding genes involved in two major human chronic lung inflammatory diseases: COPD and asthma.

In the initial study we selected three major inflammation-related RBPs – AUF-1, TTP and HuR - to evaluate their expression profile in well-characterized COPD patients and appropriate controls, and identified for the first time a specific loss of AUF-1 in small airway epithelium of COPD patients. Based on the results of this first work, we bifurcated our investigation: in one study we focused on the biology of AUF-1 using the airway epithelial cell line BEAS-2B. Using AUF-1 immunoprecipitation coupled with high-throughput sequencing, we definined epithelial AUF-1 mRNA targets and identified their binding interface. We are currently characterizing the functional role of AUF-1 binding to selected targets. In a separate study, we broadened instead our evaluation using an *in silico* approach. We conductied airway epithelial expression profiling of a large curated list of RBPs in transcriptomic databases of COPD patients and controls. Moreover, we extended this search for the first time to transcriptomic databases of severe asthma patients and relevant controls.

Differential expression of RNA-binding proteins in bronchial epithelium of stable COPD patients

Luca Ricciardi[1]*, Jessica Dal Col[1]*, Paolo Casolari[2], Domenico Memoli[1], Valeria Conti[1], Alessandro Vatrella[1], Becky M. Vonakis[3], Alberto Papi[2], Gaetano Caramori[4], Cristiana Stellato[1,3]

[1]Department of Medicine, Surgery and Dentistry "*Scuola Medica Salernitana*", University of Salerno, Salerno, Italy

[2]Interdipartimental Study Center for Inflammatory and Smoke-related Airway Diseases (CEMICEF), Cardiorespiratory and Internal Medicine Section, University of Ferrara, Ferrara, Italy

[3]Division of Allergy and Clinical Immunology, Johns Hopkins University School of Medicine, Baltimore, MD, USA

[4]Department of Biomedical Sciences, Dentistry and Morphological and Functional Imaging (BIOMORF), University of Messina, Messina, Italy

*Contributed equally

Abstract

Purpose: Inflammatory gene expression is modulated by posttranscriptional regulation via RNA-binding proteins (RBPs), which regulate mRNA turnover and translation by binding to conserved mRNA sequences. Their role in COPD is only partially defined. This study evaluated RBPs tristetraprolin (TTP), human antigen R (HuR), and AU-rich element-binding factor 1 (AUF-1) expression using lung tissue from COPD patients and control subjects and probed their function in epithelial responses *in vitro*.

Patients and methods: RBPs were detected by immunohistochemistry in bronchial and peripheral lung samples from mild-to-moderate stable COPD patients and age/smoking history-matched controls; RBPs and RBP-regulated genes were evaluated by Western blot, ELISA, protein array, and real-time PCR in human airway epithelial BEAS-2B cell line stimulated with hydrogen peroxide, cytokine combination (cytomix), cigarette smoke extract (CSE), and following siRNA-mediated silencing. Results were verified in a microarray database from bronchial brushings of COPD patients and controls. RBP transcripts were measured in peripheral blood mononuclear cell samples from additional stable COPD patients and controls.

Results: Specific, primarily nuclear immunostaining for the RBPs was detected in structural and inflammatory cells in bronchial and lung tissues. Immunostaining for AUF-1, but not TTP or HuR, was significantly decreased in bronchial epithelium of COPD samples vs controls. In BEAS-2B cells, cytomix and CSE stimulation reproduced the RBP pattern while increasing expression of AUF-1-regulated genes, interleukin-6, CCL2, CXCL1, and CXCL8. Silencing expression of AUF-1 reproduced, but not enhanced, target upregulation induced by cytomix compared to controls. Analysis of bronchial brushing-derived transcriptomic confirmed the selective decrease of AUF-1 in COPD vs controls and revealed significant changes in AUF-1-regulated genes by genome ontology.

Conclusion: Downregulated AUF-1 may be pathogenic in stable COPD by altering posttranscriptional control of epithelial gene expression.

Keywords: AUF-1; COPD; airway epithelium; inflammation; posttranscriptional gene regulation

Introduction

Posttranscriptional gene regulation (PTR) critically controls immune and inflammatory responses through coordinated changes in mRNA turnover and translation rates, adapting the amplitude and timing of protein expression to cell environment changes.1 Regulated mRNA degradation of effector genes – cytokines, chemokines, and enzymes – as well as transcription and signaling factors contributes to the physiological cessation of acute inflammatory reactions; conversely, aberrant mRNA stabilization and sustained translation can support inflammatory gene overexpression and failed resolution of inflammatory responses, leading to chronic disease.[1,2].

During inflammatory responses, triggered signaling pathways coordinate transcriptional regulation with posttranscriptional events by targeting downstream factors – RNA-binding proteins (RBPs), microRNA (miRNA), and other small noncoding RNAs (sncRNA) – that associate with mRNA through conserved sequences mainly present in their untranslated regions to form dynamic ribonucleoprotein (RNP) complexes.[2] Competitive or cooperative transcript binding of the different factors, as well as stimulus-driven remodeling of RBP composition, regulates mRNA stability and translation and ultimately conveys stimulus-specific PTR.[3,4].

Regulated responses to oxidative stress and aging are fundamental biological processes that are critically influenced by PTR regulation;[5] importantly, alterations of these processes are also key pathogenic determinants of COPD.[6] This disease affects over 350 million individuals globally (www.goldcopd.org), with 44 million cases in Europe (http://www.europeanlung.org/en/). It is the only chronic noncommunicable disease showing increasing morbidity and mortality, projected to become the third cause of death worldwide by 2020, and it is one of the strongest independent risk factors for the development of lung cancer among long-term smokers.[7] However, while investigation of RBP-driven regulation and even its therapeutic targeting is well under way in human lung cancer,[8–10] the role of RBPs in COPD pathogenesis is, by comparison, less explored.[11,12]

The etiology of COPD features a complex interplay of genetic and environmental factors, such as atmospheric pollution and cigarette smoking: the latter is involved in >90% of COPD cases in Westernized countries.[13] The progressive chronic airflow limitation in COPD is due to two major pathological processes: remodeling and narrowing of small airways and destruction of the lung parenchyma with consequent loss of the airways' alveolar attachments as a result of pulmonary emphysema. These changes determine diminished lung recoil, higher resistance to flow, and closure of small airways at higher lung volumes during expiration, with consequent air trapping in the lung. Hyperinflation of the lungs develops subsequently, which gives rise to the sensation of dyspnea and decrease exercise tolerance.[14]

Both the small-airway remodeling and the pulmonary emphysema are likely the results of chronic inflammation. Chronic lung inflammation in stable COPD is characterized by infiltration of neutrophils, monocytes, CD8+ cytotoxic, and CD4+ Th1 and Th17 T lymphocytes. Cell recruitment is initially triggered

by chemotactic signals elicited in macrophages and epithelial cells by smoke and air pollutants, through oxidative stress- and toll-like receptor-mediated signaling.[15] Driven by a globally defective response to the increased oxidative burden upon the respiratory system,[16] epigenetic changes in immune and epithelial cells maintain overexpression of cytokines, chemokines, and enzymes leading to tissue destruction and accelerated lung aging process, defined as inflammaging.[15,17,18].

Many of the key genes orchestrating this process, deregulated in COPD and in large part expressed in the epithelium – such as tumor necrosis factor-α (TNF-α), interleukin-1β (IL-1β), IL-6, interferon-γ (IFN-γ), granulocyte-monocyte colony stimulating factor, TGF-β, and VEGF, and chemokines such as CXCL1, CXCL5, CXCL8, CCL2, CCL11[19,20] – are subjected to PTR in which the RBPs human antigen R (HuR), tristetraprolin (TTP), and AU-rich element binding factor 1 (AUF-1, also denominated heteronuclear ribonucleoprotein D [HRNPD]) take part;[21–24] yet, the involvement of these factors has not been evaluated to date in COPD pathophysiology.

Genome-wide profiling of RBP-associated mRNAs indicated that functionally related mRNAs bearing shared conserved sequences (such as adenylate/uridylate-rich elements [ARE]) can be coordinately regulated by one or more RBPs.[25] In particular, studies consistently identified HuR, TTP, and AUF-1 as the three ARE-binding proteins mainly regulating genes involved in proliferation/apoptosis, oxidative stress responsiveness, angiogenesis, immune response skewing in immune cells, and their targets.[26–28] This points at the relevance of these RBPs as master regulators of homeostatic and pathologic immune responses and lends a strong rationale for investigating their expression and role in COPD pathogenesis.

HuR is the ubiquitous member of the Hu RBP family and acts mainly as a positive regulator of mRNA stability, partially by competing with ARE-binding RBPs, such as TTP and AUF-1, that limit gene expression by increasing the rate of mRNA decay of their targets.[26] TTP, encoded by the ZFP-36 gene, is an immediate/early response gene inducible by inflammatory signaling that promotes rapid decay of TNF-α and many other inflammatory and immune genes.[29] Function of AUF-1 is carried out by four isoforms – p37, p40, p42, p45 – generated from alternative splicing of the AUF/HRNPD gene, which mediate mRNA stabilization or decay according to the isoforms involved, their expression levels, and nucleocytoplasmic distribution.[30] Animal models indicate that TTP and AUF-1 are critically involved in the resolution of inflammation by accelerating the decay of overexpressed inflammatory genes: mouse knockout for TTP show early onset of severe inflammatory arthritis, myeloid hyperplasia, autoimmune dysfunction, and cachexia through overexpression of TNF-α and GM-CSF, due to their aberrant transcript stabilization;[31] similarly, aberrantly stable TNFα mRNA is found in AUF-1$^{-/-}$ mice in which endotoxin challenge provokes high mortality rates,[32] along with spontaneous onset of chronic pruritic eczema resembling atopic dermatitis, coupled with a Th2-skewed response with hypereosinophilia and increased immunoglobulin E (IgE) levels.[33]

This study investigates the expression of HuR, TTP, and AUF-1 in COPD with *ex vivo*, *in vitro*, and *in silico* approaches. The RBPs were evaluated by immunohistochemistry (IHC) in the lower airways of stable COPD

patients and control subjects; regulation of RBPs and RBP-regulated genes by inflammatory stimuli modeling COPD milieu was evaluated in the human bronchial epithelial cell line BEAS-2B and, based on the results, further probed with selective silencing of the RBP AUF-1. Transcripts of RBPs were also measured in peripheral blood mononuclear cell (PBMC) samples from additional stable COPD and control smokers to probe whether changes in RBPs were specific to lung inflammation or traceable as a potential marker of systemic inflammation in COPD.[34,35] Lastly, expression profiling of RBPs and RBP-dependent genes in primary bronchial epithelial cells was investigated using a published microarray database obtained from cells isolated by bronchial brushings of stable COPD patients and control subjects.[36]

Methods

Study population. Bronchial rings and peripheral lung samples were obtained from subjects recruited from the Respiratory Unit of the University Hospital of Ferrara, Italy, among patients undergoing lung resection for peripheral lung carcinoma (Table 1). Smokers with mild-to-moderate stable COPD (n=12) were compared with age- and smoke history-matched smokers with normal lung function (NLF) (n=12). Diagnosis of COPD was defined according to international guidelines as the presence of post-bronchodilator FEV1/FVC ratio <70% or the presence of cough and sputum production for at least 3 months in each of 2 consecutive years.[6] All patients were in stable condition at the time of the surgery and had not suffered acute exacerbations or upper respiratory tract infections in the preceding 2 months. None had received glucocorticoids or antibiotics within the month preceding surgery, or inhaled bronchodilators within the previous 48 hours. Patients had no history of asthma or other allergic diseases. All former smokers had stopped smoking for >1 year. Each patient was subjected to medical history, physical examination, chest radiography, electrocardiogram, routine blood tests, and pulmonary function tests during the week prior to surgery. Pulmonary function tests (Biomedin Spirometer, Padova, Italy) were performed as previously described[37] according to published guidelines.

Table I Study population providing bronchial and lung samples for immunohistochemical study

Participants	N	Age, years	Sex	Smoking history	Pack-years	FEV$_1$/FVC%
Smokers	12	68.6 (2.3)	10 M/2 F	6 ex, 6 current	48.2 (9.7)	79.3 (1.3)
COPD	12	71.9 (1.9)	11 M/1 F	6 ex, 6 current	52.9 (8.7)	65.7 (1.0)*

Notes: Predicted FEV$_1$% and FEV$_1$/FVC% are post-bronchodilator values. Data are expressed as mean (SD). *$P<0.01$ compared to smokers. M, male; F, female.

PBMC samples were obtained at the pulmonary outpatient clinic of the University Hospital in Salerno, Italy, from stable COPD and control smokers with NLF (Table S1). The study was approved by the local ethics committees of the University Hospitals of Ferrara and Salerno, and the participating patients and control subjects signed the approved informed consent forms.

Lung sample preparation and Immunohistochemistry (IHC). Collection, processing, and immunohistochemical analysis of bronchial rings and lung tissue samples as well as data analysis were performed as published.[16] The primary Abs (anti-human) used were rabbit polyclonal anti-AUF-1 (HPA004911; Atlas Antibodies, Bromma, Sweden); mouse monoclonal anti-HuR (sc-5261; Santa Cruz Biotechnology Inc., Dallas, TX, USA); and rabbit polyclonal anti-TTP (LS-B1572; LSBio, Seattle, WA). Negative Ab controls were carried using nonspecific isotype-matched Ig at their respective primary Ab concentrations. Image analysis was performed[16] using an integrated microscope (Olympus, Albertslund,

Denmark), video camera (JVC Digital color, Tatstrup, Denmark), automated microscope stage (Olympus), and PC running Image-Pro Plus software (Media Cybernetics) to quantify the RBP staining areas. Immunostaining counting and interpretation were done blinded without prior knowledge of clinicopathologic parameters. The scoring system for IHC is described in the Supplementary materials.

Cell culture and experimental protocols. The SV40-immortalized human tracheal epithelial cell line BEAS-2B (ATCC) was cultured in F12/DMEM (EuroClone) containing 5% heat-inactivated FBS (EuroClone), 2 mM L-glutamine (Lonza), penicillin (100 U/mL)–streptomycin (100 mg/mL) (Lonza), and 0.2% fungizone (EuroClone).[38] For cell challenge protocols, cells were kept in medium only or stimulated using 200 μM hydrogen peroxide (H2O2) or cytomix (10 nM each rHuIL-1β, TNFα, IFN-γ, GoldBio) (n=3 each) for increasing time points (1, 3, 6, 24, and 48 hours). Cigarette smoke extract (CSE) was prepared as described.[39] Briefly, smoke from one full-strength Marlboro cigarette (Phillip Morris, London, UK), with filter removed, was extracted in 1.5 minutes by controlled vacuum and bubbled into 10 mL of F12/DMEM. The solution was passed through a 0.2 μm filter, and the optical density (OD) was measured at 320 λ wavelength; the OD was then adjusted with culture medium to a reading of 0.85 considered as the 100% stock, which was then diluted with culture medium to a range of CSE solution percentages (see "Results" section) that were used within 30 minutes from preparation. Cells were serum-starved overnight prior to challenge with CSE, carried out for 24 hours. As a negative control, medium was obtained by the same procedure but with unlit cigarette, in which OD was unchanged from that of unprocessed medium.

For AUF-1 gene silencing, cells were seeded in six-well plates and transfected at 50%–60% confluency with 100 nM AUF-1 siRNA (5′-AAGAUC CUAUCACAGGGCGATdTdT-3′)[40] or a scrambled control siRNA (5′-GAGUCAACCUUAUGAUACUdTdT-3′) using the nonliposomal cationic vehicle FuGENE HD (Promega). After 48 hours, cells were exposed to cytomix or medium for additional 48 hours.

All cell monolayers were harvested using trypsin/EDTA (Lonza). The cells were counted, and viability was assessed by trypan blue exclusion in all conditions and found to be consistently >95% of total cell count. Supernatants of all experiments were collected, centrifuged, and stored at −80°C for subsequent analysis. Isolation of PBMC was performed by standard Ficoll gradient separation (Sigma).

RNA extraction, cDNA synthesis and qPCR. Total RNA was extracted using TriFast reagent (EuroClone) and reverse transcription was prepared using the Moloney murine leukemia virus reverse transcriptase (Applied Biological Materials) following the manufacturer's protocol. Template cDNA was subjected to quantitative real-time PCR (qRT-PCR) with the FluoCycle II SYBR Master Mix (Euroclone) according to the manufacturer's protocol. Primer sequences were: GAPDH forward: 5′-GAAGGTGAAGGTCGGAGTC-3′, reverse: 5′-GAAGATGGTGATGGGATTTC-3′; AUF-1 5′-GATCCTAAAAGGGCCAAAGC-3′, reverse: 5′-CCACTGTTGCTGTTGCTGAT-3; HuR 5′-CGCAGAGATTCAGGTTCTCC-3′, reverse: 5′-

CCAAACCCTTTGCACTTGTT-3′; TTP 5′-CGCTACAAGACTGAGCTATG-3′, reverse: 5′-CCTGGAGGTAGAACTTGTG-3. Primers were published[38,41] or designed with Primer-BLAST software (https://www.ncbi.nlm.nih.gov/tools/primer-blast/). Reactions were run in duplicate on a LightCycler 480 II (Roche), using the following setup: 5 minutes, 95°C; 15 seconds at 95°C, 45 cycles; 15 seconds, 60°C. Target expression was normalized to GAPDH by the cycle threshold (Ct) method and expressed using the $2^{-\Delta\Delta Ct}$ calculation as fold over control and in selected cases, $2^{-\Delta\Delta Ct}$ as fold over housekeeping gene levels.

Protein extraction and Western Blot. Nuclear and cytoplasmic proteins were separated, quantified, and subjected to Western blot analysis as described.[42,43] Briefly, proteins were fractionated using SDS-PAGE and transferred onto nitrocellulose membranes. After blocking with 5% milk for 1 hour, membranes were stained with primary antibodies (anti-RBP Abs as in IHC; mouse monoclonals anti-Lamin A/C [SAB420023; Sigma-Aldrich Co., St Louis, MO, USA], anti-tubulin [2128; Cell Signaling Technology], anti-PARP-1 [F-2, Sc-8007; Santa Cruz Biotechnology Inc.], anti-Cleaved Caspase-3 [Asp175, #9661; Cell Signaling Technology]) at 4°C overnight, then labeled with horseradish peroxidase-conjugated secondary antibodies. Immunoblotting analysis and densitometry were performed via digital image system (ChemiDoc MP; Bio-Rad Laboratories Inc., Hercules, CA, USA) using the enhanced chemiluminescent substrate ECL (#32106; Thermo Fisher Scientific, Waltham, MA, USA).

Analysis of secreted proteins. BEAS-2B supernatants were screened for secreted proteins using specific IL-6 and CCL2 ELISA kits (Elabscience; detection threshold 0.122 pg/mL, and Cloud-Clone Corp., Kathy, TX, USA; detection threshold 15 pg/mL, respectively) and using the Proteome Profiler Human Cytokine Array Kit (R&D Systems, Inc., Minneapolis, MN, USA), following the manufacturer's protocol. Absorbance values were measured using an Infinite M200 PRO plate reader (Tecan).

Bioinformatics analysis. We interrogated a microarray database originated from epithelial cells obtained by bronchial brushings of stable COPD patients (n=6), and smokers and nonsmokers (n=12 each) as NLF controls,[36] deposited in the Gene Expression Omnibus (GEO) repository (GEO ID: GSE5058). Fluorescence intensity data from individual data sets were extracted and normalized on the medians for fold change (FC) comparison of RBP expression among groups. For RBPs, FCs were set at ≥2.0 with a false discovery rate (FDR) ≤0.05. Data sets were subsequently analyzed for expression of AUF-1-associated transcripts and annotated according to genome-wide RNP-IP and PAR-CLIP analysis.[40,44] For this analysis, FC was set at ≥2.0 with FDR ≤0.05. Heatmaps were generated using tMEV tools v4_9_0.[45]

Genome Ontology Analysis. Characterization of the AUF-1-dependent gene clustering according to the database comparison was performed using NCBI PANTHER version 11 (www.pantherdb.org) with Bonferroni correction for multiple testing. The system clusters genes based on functional properties, using published studies and evolutionary relationships as sources.[46]

Statistical analysis. To determine differences for IHC data between groups, analyses of variance were used for clinical data and unpaired t-test with post hoc Mann–Whitney U-test. Categorical values were compared by chi-squared test.16 Data from qRT-PCR, Western blot densitometry, and ELISA were analyzed using Student's paired t-test; time- and concentration-dependent responses were analyzed using ANOVA test with Fisher's post hoc multiple comparison analysis. P<0.05 was considered significant. Statistical analysis was performed using GraphPad Prism 5 (GraphPad Software, Inc. La Jolla, CA, USA).

Results

Characterization of RBP expression in human lung tissue and PBMC in stable COPD patients and control subjects

Expression of HuR, TTP, and AUF-1 was first evaluated by IHC in bronchial rings and peripheral lung tissue samples obtained from patients with mild-to-moderate stable COPD and control smokers with NLF. The clinical characteristics of the study population are described in Table 1 and in the "Methods" section. As expected, smokers with COPD had significantly lower FEV1 (percent of predicted) and FEV1/FVC ratio compared to controls ($P < 0.01$).

Specific immunostaining was detected for all three RBPs in bronchial tissue (Figure 1) and peripheral lung (Figure 2), with mainly nuclear localization in both structural and inflammatory cells. In bronchial tissue, the number of bronchial epithelial cells with nuclei positively stained for AUF-1 was significantly lower in patients with COPD compared to control smokers (Figure 1), whereas no statistically significant difference in other AUF-1-positive cells was found between the two groups in bronchial tissue and peripheral lung samples (Figures 1 and 2). In contrast, the localization and global expression of HuR and TTP were not significantly different between stable COPD patients and control subjects in both bronchial and peripheral lung tissues (Figures 1 and 2). No statistical difference was found in RBP expression patterns between current and former smokers.
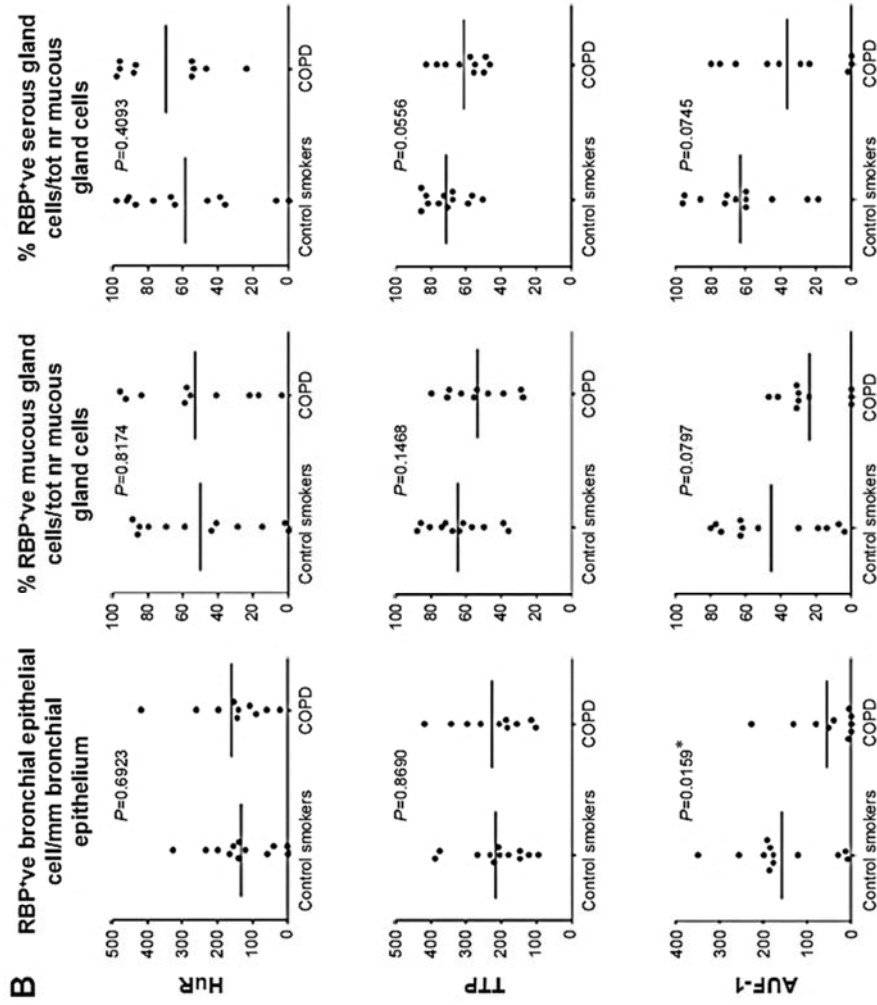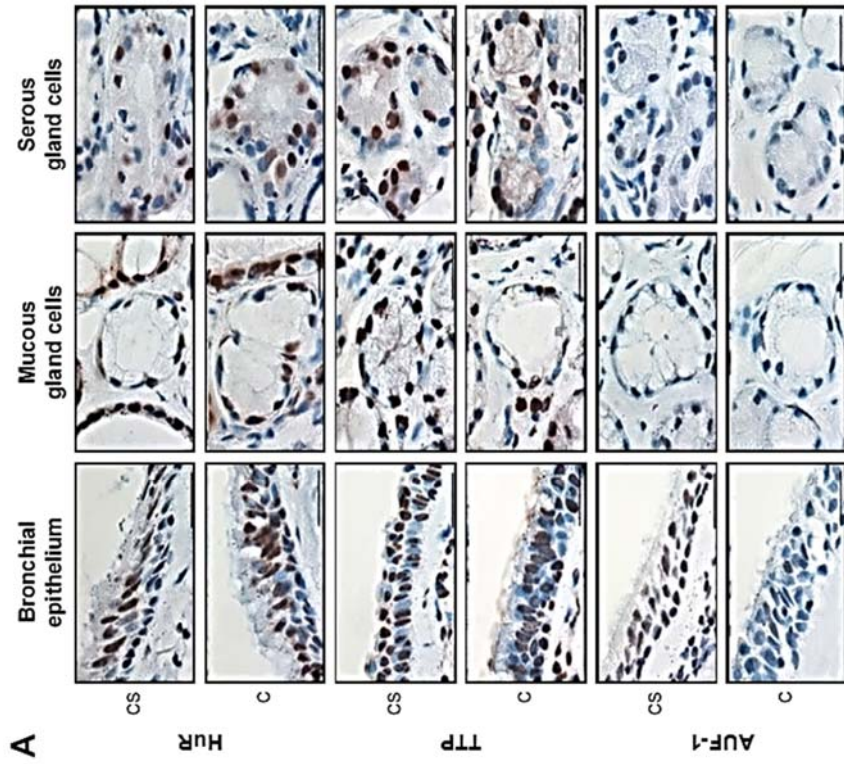
Figure 1 Expression of RNA-binding proteins in human bronchial rings.

Notes: (**A**) Photomicrographs showing immunostaining for HuR, TTP, and AUF-1 in bronchial epithelium, mucous gland cells, and serous gland cells (left to right) from a CS with NLF and a patient with mild-to-moderate COPD (C) (representative of n=12 for each group, see the "Methods" section). Scale bar set at 20 μm. (**B**) Individual and median (line) cell counts of nuclear immunostaining for HuR, TTP, and AUF-1 in bronchial epithelial cells, mucous gland cells, and serous gland cells (left to right) of CS and COPD, normalized as indicated. Student's *t*-test *P*-value for COPD vs CS is indicated in all panels. *P<0.05 vs CS. Scale bar set at 20 μm, magnification 1,000×.

Abbreviations: C, patients with COPD; HuR, human antigen R; TTP, tristetraprolin; AUF-1, AU-rich element-binding factor 1; NLF, normal lung function; CS, control smoker.

88
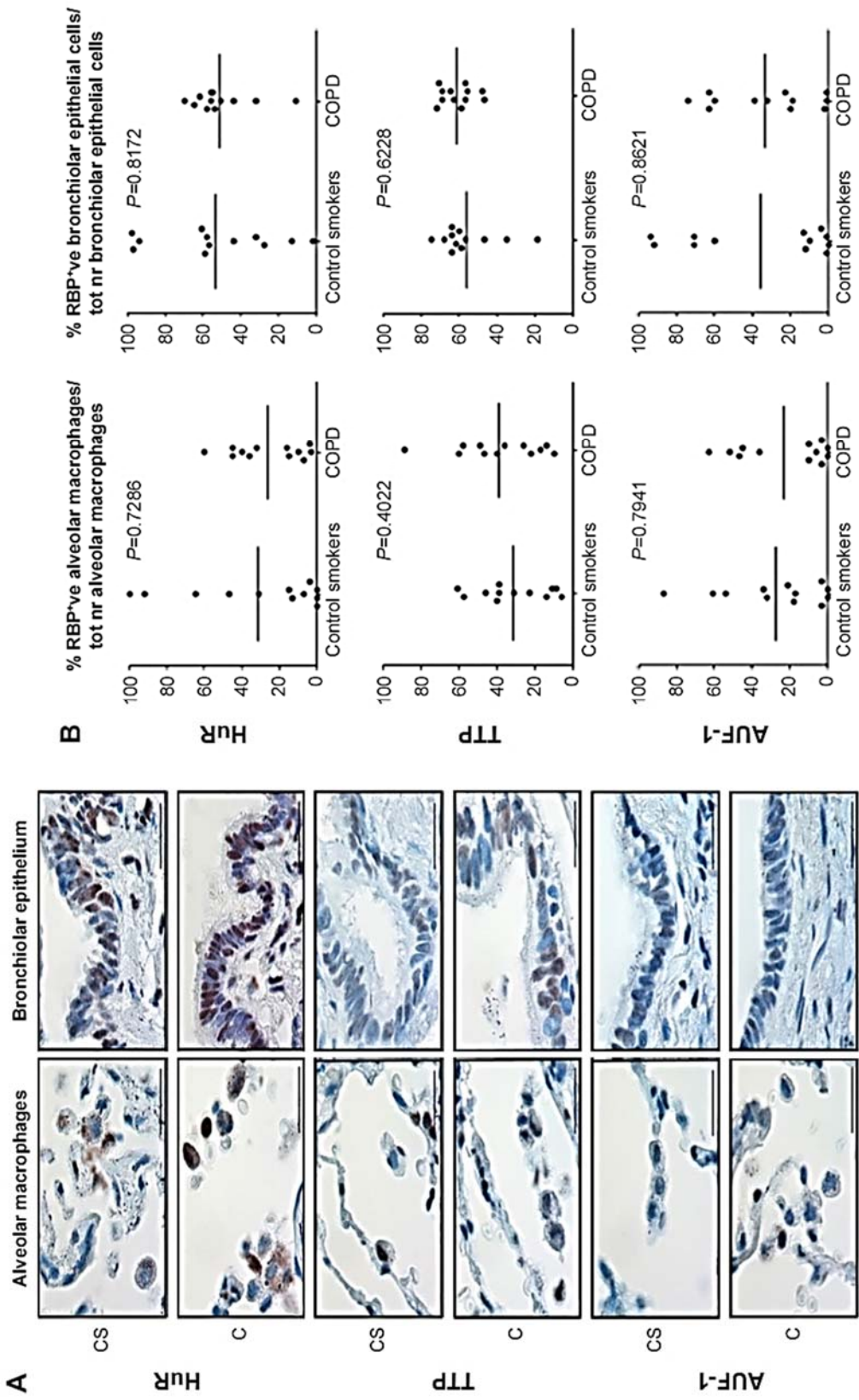
Figure 2 Expression of RNA-binding proteins in human peripheral lung.

Notes: (**A**) Photomicrographs showing immunostaining for HuR, TTP, and AUF-1 in alveolar macrophages and bronchiolar epithelium (left to right) from a control smoker and a patient with mild-to-moderate COPD (C) (representative of n=12 for each group, see the "Methods" section). Scale bar set at 20 μm, magnification 1,000×. (**B**) Individual and median (line) cell counts of nuclear immunostaining for HuR, TTP, and AUF-1 in alveolar macrophages and bronchiolar epithelium (left to right) of control smokers and COPD, normalized as indicated. Student's t-test P-value for COPD vs CS comparison is indicated in all panels.

Abbreviations: C, patients with COPD; HuR, human antigen R; TTP, tristetraprolin; AUF-1, AU-rich element-binding factor 1; CS, control smoker.

Evaluation of RBP mRNA levels in PBMCs obtained from additional stable COPD patients and control smokers with NLF (n=5 and 4, respectively; Table S1) by RT-PCR showed no differences between the two groups (Figure S1).

in vitro modulation of RBP expression in BEAS-2B cells by proinflammatory and oxidant stimuli

To investigate whether epithelial RBP expression could be modulated by a Th1-skewed cytokine milieu and oxidative stress, we evaluated HuR, TTP, and AUF-1 levels by Western blot analysis in BEAS-2B cells following challenge with cytomix or hydrogen peroxide (200 μM) (Figure 3). Cytomix induced a time-dependent, statistically significant decrease of the expression of main AUF-1 isoforms compared to unstimulated control (to a maximum of 60% decrease at 48 hours for p42 isoform in nuclear fraction, shown in bar graph (Figure 3) and 49% decrease in cytoplasmic fraction, $P<0.05$ in both cases). Such effect was stimulus-specific, as AUF-1 levels were unchanged by hydrogen peroxide stimulation. By contrast, HuR and TTP expressions were not affected by cell treatments beyond consistent but small variations. Cleavage of PARP-1 and caspase 3 as markers of apoptosis was not detected upon any cell treatment (Figure S2). RT-PCR analysis (Figure S3A) confirmed at mRNA level the lack of stimulus-induced changes in HuR and TTP expression; interestingly, AUF-1 mRNA was unchanged by cytomix despite clear protein downregulation. Instead, in line with protein results, hydrogen peroxide treatment did not change RBP transcript levels (Figure S3B).
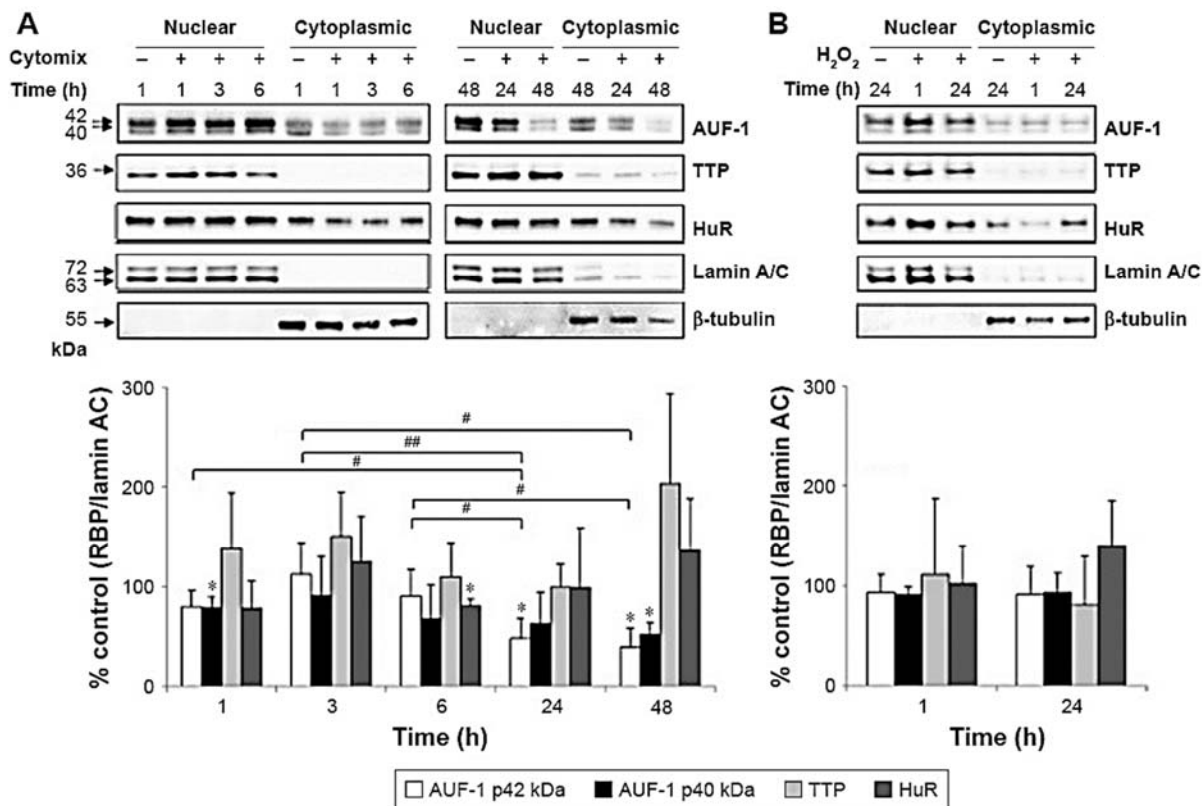
Figure 3. Modulation of the expression of RNA-binding proteins in the human bronchial epithelial cell line BEAS-2B. Western blot analysis of AUF-1, TTP, and HuRexpression in nucleocytoplasmic lysates of BEAS-2B cells cultured with (A) cytomix (n=4, n=3 for HuR) and (B) 200 μM H2O2 (n=3, n=4 for AUF-1) for the indicated times. Upper panels show representative immunoblots for the RBPs and for lamin A/C and β-tubulin as nuclear and cytoplasmic loading controls, respectively; bar graphs show densitometric analysis of nuclear fraction (mean ± SEM of indicated n). *$P <$ 0.05 vs unstimulated cells; # $P < 0.05$, ## $P < 0.01$ between indicated time points.

Abbreviations: HuR, human antigen R; TTP, tristetraprolin; AUF-1, AU-rich element-binding factor 1; RBP, RNA-binding protein; SEM, standard error of mean.

To test whether the RBP pattern induced by cytomix could be recapitulated by a broader COPD inflammatory modeling encompassing both inflammatory and oxidant-driven triggers, BEAS-2B cells were exposed to CSE for 24 hours, as described[39,47] (Figure 4). Expression of AUF-1 was downregulated in a concentration-dependent fashion, but a marked decrease in cell viability at the highest CSE concentration tested (20% and 10%) (Figure 4A) has led to exclusion of these two points from densitometric analysis; however, expression of AUF-1 main isoforms remained significantly decreased also by exposure to 3% CSE, a concentration displaying close to 90% cell viability (mean ± SEM, 88±2), to a maximum decrease of 54% in cytoplasmic extracts (P < 0.05, Figure 4B and C). Lack of cleavage of PARP-1 in all samples indicated absence of apoptosis (not shown).
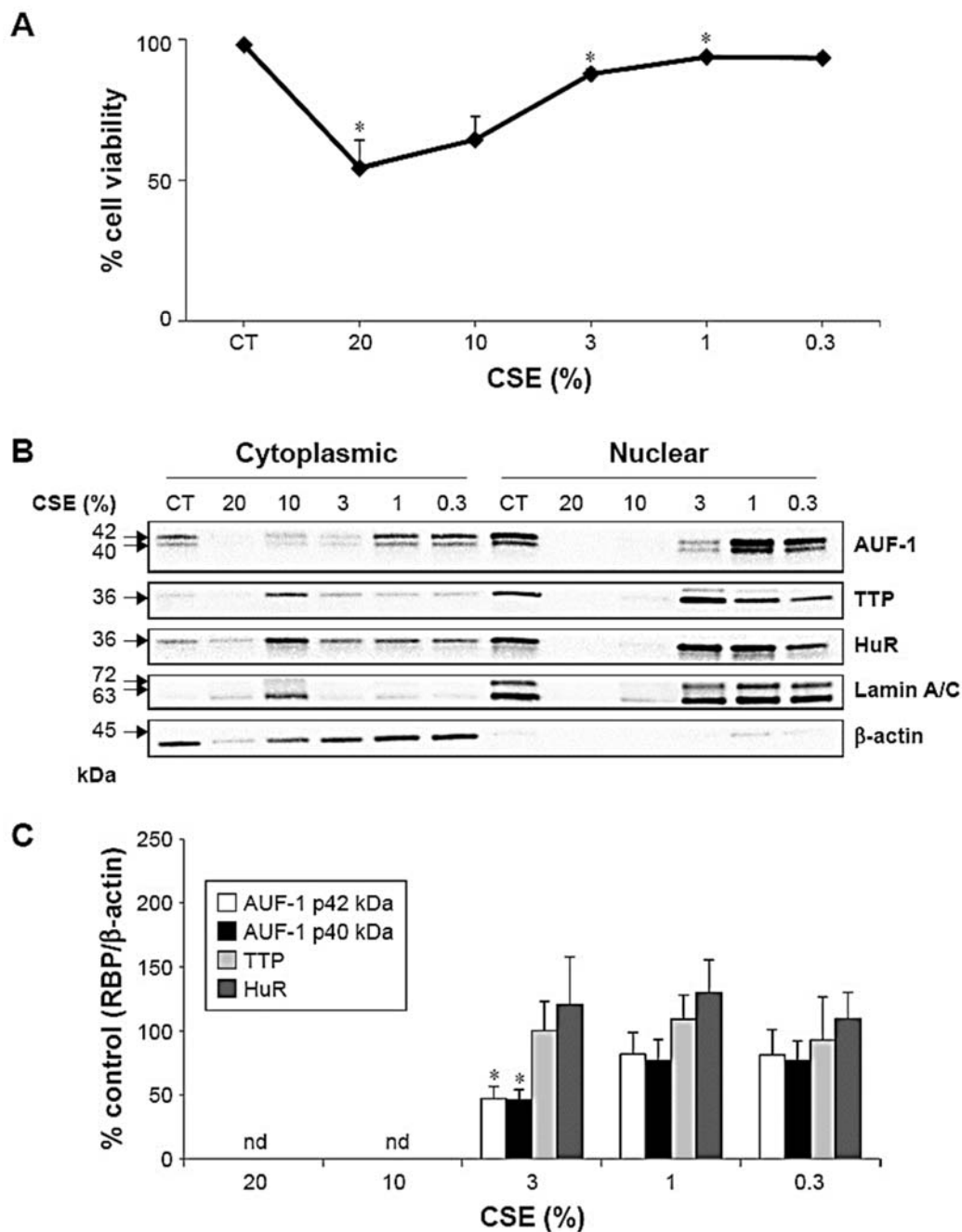
Figure 4. Effect of CSEon RBP expression in BEAS-2B cells. (A) Cell viability following 24-hour exposure to indicated CSEconcentrations (n=3, *$P < 0.05$ vs unstimulated [CT] cells). (B) Representative immunoblots of AUF-1, TTP, and HuRexpression; lamin A/C and β-tubulin as nuclear and cytoplasmic loading controls, respectively. (C) Densitometric analysis of cytoplasmic fraction (mean ± SEM of n=3). *$P < 0.05$ vs unstimulated cells; changes among concentrations not statistically significant. **Abbreviations:** CSE, cigarette smoke extract; HuR, human antigen R; TTP, tristetraprolin; AUF-1, AU-rich element-binding factor 1; ND, not determined; RBP, RNA-binding protein; SEM, standard error of mean.

Effect of cytomix-induced and siRNA-mediated loss of AUF-1 on RBP and inflammatory gene expression in BEAS-2B cells.

We then implemented silencing of AUF-1 expression in BEAS-2B cells (Figure 5) to investigate its potential effects on RBPs and the expression of their downstream targets. Following transfection with a specific AUF-1 siRNA,40 levels of AUF-1 protein in unstimulated cells were significantly, although partially, diminished compared to both mock (Fugene only)- and scrambled siRNA-transfected cells (Figure 5A) up to 49% and 58%, respectively, according to densitometric analysis (P>0.05 for both comparisons). Furthermore, cytomix treatment further lowered AUF-1 levels to a maximum average of 27% compared to unstimulated, AUF-1 silenced cells (Figure 5B, P<0.05). Levels of TTP protein in AUF-1-silenced cells displayed a small (close to twofold) yet significant increase in conditions of maximal AUF-1 loss induced by cytomix in these cells, while HuR levels were not affected by AUF-1 silencing (Figure 5B). In these experiments, AUF-1 mRNA, detected by RT-PCR, remained unchanged in cytomix-stimulated untransfected cells (Figure S3C) as in the previous experiment set (Figure S3A), while a consistent but small decrease in AUF-1 mRNA (25% of control, P<0.05) was detected in scrambled-transfected cells and, predictably, in cells transfected with AUF-1 siRNA (48% of control, P<0.05). Regarding the other RBPs, while HuR mRNA levels were unchanged among conditions, cytomix induced a consistent reduction in TTP mRNA (58% and 51% of control in untransfected and scrambled-transfected cells, respectively; P<0.05 in both cases) that was lost in AUF-1-silenced cells (Figure S3C). Interestingly, a small but significant increase in TTP protein was indeed detectable in these cells (Figure 5B). Furthermore, silencing of AUF-1 did not induce cell apoptosis, as verified by lack of cleavage of PARP-1 (Figure S4) or of caspase 3 (data not shown).
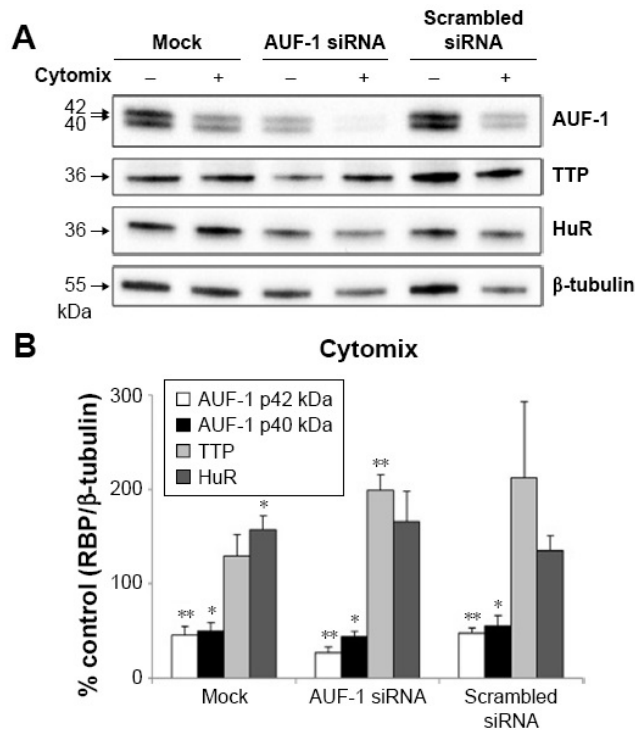
Figure 5. Expression of RNA-binding proteins in BEAS-2B cells following AUF-1 silencing. (A) Representative Western blot analysis (of n=4) of AUF-1, TTP, and HuRexpression in cells transfected with mock (Fugene only), AUF-1 siRNA, or scrambled siRNA, and treated for 48 hours with cytomix or medium control. (B) Densitometric analysis of cytomix-induced response (mean ± SEM of n=4 blots). *$P < 0.05$; **$P < 0.01$ compared to the corresponding medium control. Abbreviations: HuR, human antigen R; TTP, tristetraprolin; AUF-1, AU-rich element-binding factor 1; SEM, standard error of mean.

We then evaluated changes in AUF-1-regulated genes in conditions of relative loss of AUF-1 (Figure 6), first by assessing the expression of IL-6 and of the chemokine CCL2, chosen as readouts as they are overexpressed in airway epithelium in COPD and significantly increased as well in the AUF-1-deficient animal model.[19,33] RT-PCR analysis indicated that both transcripts were upregulated upon treatment in untransfected cells (Figure 6A) although not in a statistically significant fashion compared to unstimulated cells, likely due to variability in small sample size (n=4). Following AUF-1 silencing, basal mRNA levels did not change significantly compared to scrambled siRNA-transfected cells and upon cytomix stimulation, their increase was comparable to that caused by treatment in scrambled- and mock-transfected cells (Figure 6A), in which a similar decrease in AUF-1 protein was present (Figure 5). Levels of IL-6 and CCL2 proteins, detected by ELISA in the supernatants (Figure 6B), were instead significantly upregulated by cytomix, but also in this case without additional potentiation of cytokine secretion in AUF-1-silenced cells. Levels of both proteins following cytomix were comparable in scrambled and AUF-1-silenced cells also when normalized on cell number/condition (data not shown).
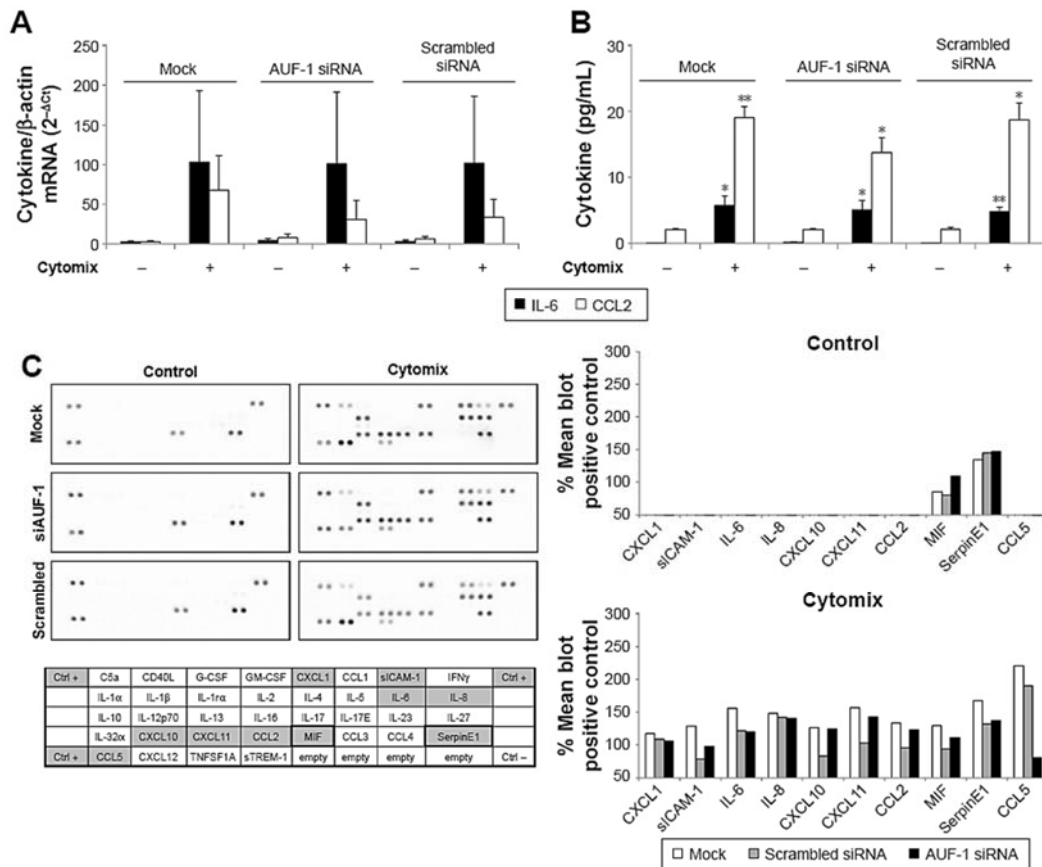
Figure 6. Expression of AUF-1-targeted cytokines in BEAS-2B cells following AUF-1 silencing. (A) CCL2 and IL-6 mRNAlevels measured by real-time PCR(mean ± SEM of n=4) in cells transfected with mock (Fugene only), AUF-1 siRNA, or scrambled siRNAand then treated 48 hours with cytomix or medium control. To show the comparison of mRNAlevels in unstimulated cells, results are expressed as fold over housekeeping mRNAlevels ($2^{-\Delta Ct}$). (B) Levels of IL-6 and CCL2 protein detected by ELISAin cell supernatants of experiments shown in A(mean ± SEM of n=4). *$P <$ 0.05; ** $P <$ 0.01 compared to the corresponding medium control. (**C**) BEAS-2B supernatants of a representative experiment from data set shown in A and B were screened using the Human Cytokine R&D Protein Arrays. Left: arrays for the indicated conditions; the grid identifies proteins as displayed on the array; in gray, proteins expressed in cytomix-treated cells; circled, proteins expressed also at baseline (all above arbitrary 5,000 densitometry unit cutoff). Right: bar graphs show densitometric analysis for the indicated conditions, expressed as percent of each blot's positive control (mean of densitometry reading of the six spots). **Abbreviations:** AUF-1, AU-rich element-binding factor 1; IL-6, interleukin 6.

To gain a broader view of potential differences in cytomix-induced epithelial responses upon loss of AUF-1, supernatants of a representative experiment were further screened with an inflammatory cytokine protein array carrying additional RBP targets, as well as cytokines and chemokines involved in COPD pathogenesis (Figure 6C). As for IL-6 and CCL2, stimulus-induced upregulation of COPD-relevant chemokines such as CXCL1, CXCL8, and CXCL10, as well as other proteins was densitometrically comparable among conditions with the exception of CCL5, which was markedly reduced in AUF-1 siRNA-transfected cells.

Validation of decreased AUF-1 levels and changes in AUF-1-regulated genes in COPD patients vs control subjects in primary airway epithelial cell transcriptome database.

In order to verify the overall RBP profile in primary airway epithelial cells, including the decreased AUF-1 expression and the potential downstream effects on target expression, we interrogated a public microarray database originated from primary airway epithelium obtained by bronchial brushings of COPD patients, and smokers and nonsmokers with NLF (GEO ID: GSE5058)[36] (Figure 7). Bronchial epithelial AUF-1 expression was found to be significantly lower in COPD vs both controls (FC =−2.7 and −3.5 vs nonsmokers and smokers, respectively), while FC levels for HuR and TTP did not change significantly among groups, showing however a trend toward reciprocal changes in COPD. We then evaluated in the same database a compiled list of 152 validated AUF-1 target genes.[40,44] Thirty of them were significantly upregulated and 22 were downregulated in COPD patients compared to both control groups, with greatest changes vs control smokers (Figure 8). Genome ontology analysis indicates that AUF-1 regulation has a potentially significant impact on several pathogenic pathways of stable COPD.
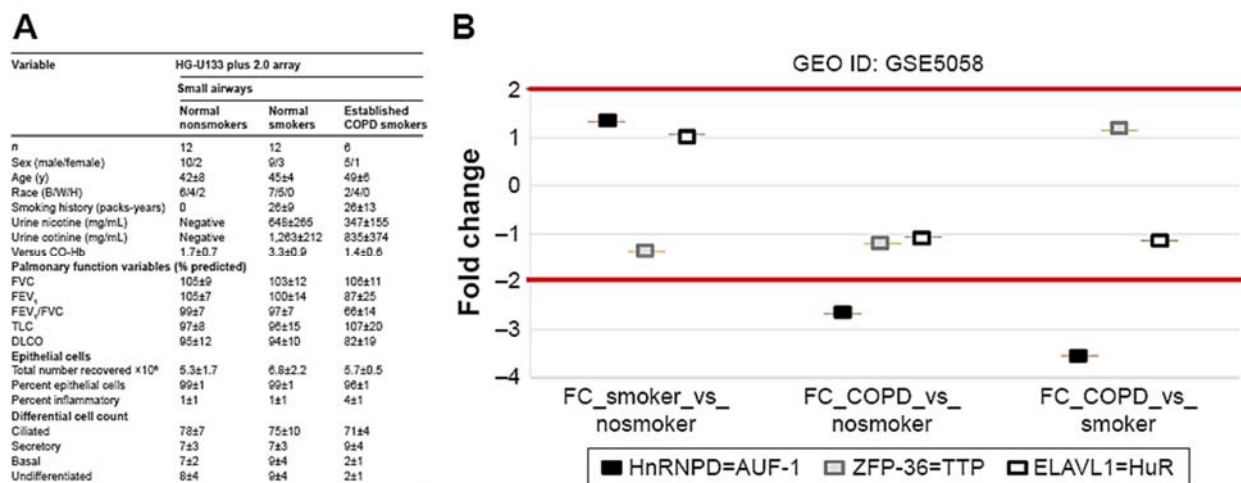
Figure 7. Differential expression of RNA-binding proteins in transcriptomic analysis of primary human airway epithelial cells. Expression of AUF-1, TTP, and HuR (corresponding gene names indicated in legend) was investigated in the GEO database GSE5058.36 (A) Clinical characteristics of study population where epithelial cells were collected by bronchial brushing. Reprinted from, *Cancer Res*, 2018; 66(22):10729–10740, Carolan BJ et al, Up-regulation of Expression of the Ubiquitin Carboxyl-Terminal Hydrolase L1 Gene in Human Airway Epithelium of Cigarette Smokers, with permission from AACR.36 (B) Scatterplot showing FC for RBP expression between smokers vs nonsmoker controls, COPD vs nonsmokers, and COPD vs smoker controls (left to right). FCs for RBPs were set at ≥ 2.0 with a false discovery rate of ≤ 0.05. **Abbreviations:** HuR, human antigen R; TTP, tristetraprolin; AUF-1, AU-rich element-binding factor 1; FC, fold change; RBP, RNA-binding protein.
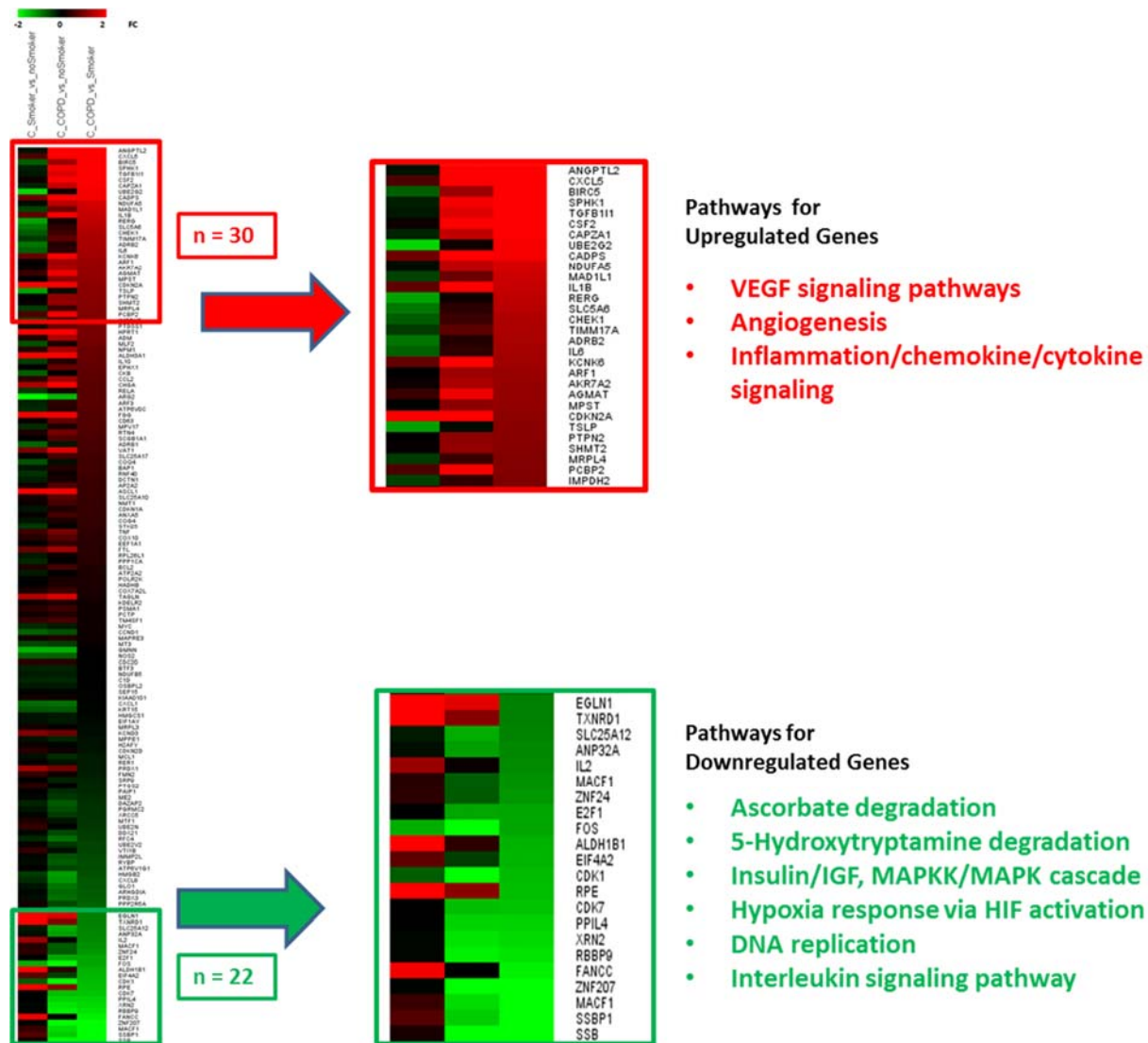
Figure 8. Expression of AUF-1-dependent genes in airway epithelial gene array database GSE5058. (A) Heatmap showing FC of 152 annotated AUF-1-dependent genes investigated in the GEO database GSE5058, comparing expression from left to right: smokers vs nonsmoker controls; COPD vs nonsmokers; COPD vs smoker controls. Enlarged heatmaps show 30 upregulated and 22 downregulated genes displaying a FC > 2.0 in COPD vs smoker controls. **(B)** Results of genome ontology analysis indicating the main pathways related to the expressed genes according to NCBI Panther tool. **Abbreviations:** AUF-1, AU-rich element-binding factor 1; FC, fold change.

Discussion

This study provides for the first time the expression profile of RBPs chiefly regulating inflammatory responses – HuR, TTP, and AUF-1 – in the lower airways of patients with COPD, a chronic lung inflammatory disease. In particular, immunohistochemical analysis showed that the expression of AUF-1 was selectively decreased in the bronchial, but not in the bronchiolar, epithelium from patients with stable COPD compared to control smokers, while HuR and TTP expression levels were comparable between groups in both bronchial and lung tissues. Importantly, the selective loss of AUF-1 in epithelium was confirmed by unbiased search in a primary bronchial epithelial gene array database derived from bronchial brushings of COPD patients and controls with similar clinical characteristics. In contrast, expression of RBP transcripts did not differ in PBMCs of stable COPD compared to control smokers, suggesting that AUF-1 downregulation, rather than systemic,[34] may be related to airway-specific conditions.

Bronchial epithelium is an early and key contributor to the pathogenesis of COPD[48] although at variance with asthma, its functional activity in stable COPD patients is less characterized, with most studies focused on the role of mucus-secreting epithelial cells and on epithelial stem cells[13] Inhaled cigarette smoke, pollutants, and irritants activate epithelial innate immune responses via TLR and DAMPS, producing both barrier alteration and triggering recruitment of immune cells and their activation through the release of chemotactic and proinflammatory mediators. This gene expression program is largely mediated at transcriptional level by activation of NF-κB, documented in the bronchial epithelium of mild/moderate stable COPD patients and, to a lesser extent, in control smokers in comparison with control nonsmokers.[49]. In the same disease context, our study uncovers the potential contribution of altered posttranscriptional gene regulatory mechanisms in mediating defective response to oxidative stress and inflammation in COPD, suggested by decreased levels of the RBP AUF-1 in ex vivo and in vitro experiments. Very few studies so far investigated AUF-1 in models of human lung inflammation. In vitro, cytosolic levels of AUF-1 increased significantly in primary airway epithelial cells infected with human rhinovirus, concomitant with a decreased expression of CXCL10,[50] while cigarette smoke-induced upregulation of CXCL8 was not AUF-1-dependent.[51] Recently, decreased levels of AUF-1 mRNA were found in bronchoalveolar lavage cells and PBMC of patients with sarcoidosis, another chronic inflammatory lung disease.[52] The epithelial-specific loss of AUF-1 observed in COPD subjects in our study suggests that lower AUF-1 levels may become determinants of non-resolving inflammation, by altering the RNP complexes necessary for coordinate degradation of epithelial transcripts involved in the inflammatory response.

Importantly, the selective loss of AUF-1 in epithelium was reproducible in vitro by exposure of BEAS-2B cells to established COPD/oxidative stress models such as CSE, which provides both a proinflammatory trigger and an oxidant overload stimulation;[39] stimulation with H2O2 did not change AUF-1 levels, suggesting selectivity in this response. Cytomix, a cytokine association representing the Th1-skewed airway milieu in

COPD,[53] instead reproduced CSE effect and was associated with a concomitant upregulation of known AUF-1 targets such as IL-6, CCL2, CXCL1, and CXCL8.[3,33,54] The pleiotropic cytokine IL-6 is also expressed in airway epithelium and is found in increased amounts in the sputum, exhaled breath, BAL fluid of patients with COPD,[55] in particular following exacerbations as well as in plasma, as important biomarkers of systemic inflammation.[35,55,56] Importantly, AUF-1 binds to AU-rich elements in IL-6 mRNA and promotes its degradation.[57] The chemokine CCL2 is a potent monocyte, T-cell, and mast cell chemoattractant and a basophil activator expressed by alveolar macrophages and T cells, and is overexpressed in airway epithelial cells in COPD.[58,59] Levels of the chemokine CCL2 are increased in the sputum and in the BAL fluid of patients with COPD.[19,20] Involvement of CCL2 in macrophage and mast cell recruitment in the lung is supported by several experimental mouse models of inflammation and emphysema, constituting an attractive therapeutic target.[20] Although well known to be regulated posttranscriptionally in airway epithelium by TTP and HuR,[60] association of CCL2 mRNA with AUF-1 has not been yet fully characterized; similarly, direct association of AUF-1 with other epithelial genes relevant to COPD pathogenesis overexpressed upon cytomix treatment, such as CCL5, CXCL10, and CXCL11, remains to be studied.

In our study, upregulation of IL-6, CCL2, and the entire chemokine/cytokine profile induced by cytomix in BEAS-2B cells was recapitulated, but without further modification, following siRNA-mediated silencing of AUF-1. This result does not yet clarify to what extent, and how, AUF-1 could be deemed necessary for cytokine upregulation in this model. First, limitations of the experimental setting – such as achieving only partial knockdown of AUF-1 protein and/or near-maximal stimulation of epithelial response by cytomix – may have hindered the uncovering of AUF-1 function in this model. Furthermore, the majority of the transcripts coding for the cytokine/chemokine profile induced by cytomix – including CCL2 and IL-6 mRNA – are dynamically regulated by multiple ARE-binding proteins, including TTP and HuR,[23,29,40,60] as well as by miRNA working either in cooperation or in competition, contextually to signaling-driven environmental changes.[3,4] Proteomic analysis of transcript-associated RNPs, models of AUF-1 overexpression, and binding site mutational studies will be necessary to further probe AUF-1 role in epithelial responses and in COPD. Moreover, stimulus-induced posttranslational mechanisms, such as promotion of ubiquitination,[61,62] may be regulating AUF-1 protein levels and require definition, also as potential means of modulating AUF-1-mediated gene regulation.

Further support to a role for AUF-1 in shaping epithelial gene expression in COPD is provided by the significant changes found, in the bronchial epithelial GEO database, in the global expression of a compiled list of bona fide AUF-1 mRNA targets[21,40,44] – including IL6 and CCL2 – within the COPD array samples compared to controls, concomitant with the loss of AUF-1 expression detected in the same data set. Genome ontology analysis of AUF-1-regulated gene expression profile in COPD samples indicates a potentially significant impact of this RBP in the pathogenesis of stable COPD through coordinate regulation of genes

involved in inflammation and angiogenesis, alteration of DNA repair, defective response to hypoxia and oxidative stress, and altered metabolism of serotonin – which is increased in COPD patients and linked to exposure to cigarette smoke.[13,63,64] Taken together, these findings suggest the occurrence of AUF-1-driven PTR in COPD according to a ribonomic paradigm, whereby transcripts structurally related by sharing RBP recognition motifs are co-regulated by a core RBP – likely shaping a specific RNP configuration – according to their participation to a specific function.[65]

The marginal yet consistent changes in HuR and TTP levels in our in vitro systems holds further investigation, rather than rule out their participation to epithelial gene regulation in COPD. In primary and transformed airway epithelial cultures, upon cytokine challenge, HuR functions as a positive regulator of mRNA stability for multiple chemokines, while TTP limits the half-life of inflammatory transcripts and mediates glucocorticoid-induced gene regulation – indicating their potential role in integrated posttranscriptional gene control, yet to be fully characterized in lung inflammatory diseases where airway epithelial responses are pathogenic. Furthermore, similarities in binding sites and partially overlapping mRNA target pools indicate major complexity of the interplay among TTP, HuR, and AUF-1, as well as with other ncRNA species participating to RNP complexes,[4,40,66] warranting further studies to understand how pathogenic immune responses in the lung ultimately rely on altered RBP-mediated control of mRNA decay and translation.

Increasing knowledge on how immune responses rely on PTR is likely to yield a strong rationale to evaluate PTR mechanisms for therapeutic intervention. Indeed, a major limitation in the current treatment of stable COPD patients is the reduced anti-inflammatory efficacy of glucocorticoids,[14] indicating a major unmet need for therapeutic approaches able to override this limitation. The development of high-throughput screening methods for RNP interactions and generation of small-molecule inhibitors for lung cancer[67–70] indicates that uncovering PTR mechanisms in COPD may also sustain the development of new anti-inflammatory strategies, potentially transferable to other chronic lung inflammatory diseases.

References

1. Anderson P. Post-transcriptional regulons coordinate the initiation and resolution of inflammation. *Nat Rev Immunol*. 2010;10(1):24–35.

2. Gerstberger S, Hafner M, Tuschl T. A census of human RNA-binding proteins. *Nat Rev Genet*. 2014;15(12):829–845.

3. Chowdhury S, Dijkhuis A, Steiert S, Lutter R. IL-17 attenuates degradation of ARE-mRNAs by changing the cooperation between AU-binding proteins and microRNA16. *PLoS Genet*. 2013;9(9):e1003747.

4. Tiedje C, Ronkina N, Tehrani M, et al. The p38/MK2-driven exchange between tristetraprolin and HuR regulates AU-rich element-dependent translation. *PLoS Genet*. 2012;8(9):e1002977.

5. Abdelmohsen K, Kuwano Y, Kim HH, Gorospe M. Posttranscriptional gene regulation by RNA-binding proteins during oxidative stress: implications for cellular senescence. *Biol Chem*. 2008;389(3):243–255.

6. Kirkham PA, Caramori G, Casolari P, et al. Oxidative stress-induced antibodies to carbonyl-modified protein correlate with severity of chronic obstructive pulmonary disease. *Am J Respir Crit Care Med*. 2011;184(7):796–802.

7. Caramori G, Casolari P, Cavallesco GN, Giuffrè S, Adcock I, Papi A. Mechanisms involved in lung cancer development in COPD. *Int J Biochem Cell Biol*. 2011;43(7):1030–1044.

8. Fallahi M, Amelio AL, Cleveland JL, Rounbehler RJ. CREB targets define the gene expression signature of malignancies having reduced levels of the tumor suppressor tristetraprolin. *PLoS One*. 2014;9(12):e115517.

9. Giaginis C, Alexandrou P, Tsoukalas N, et al. Hu-antigen receptor (HuR) and cyclooxygenase-2 (COX-2) expression in human non-small-cell lung carcinoma: associations with clinicopathological parameters, tumor proliferative capacity and patients' survival. *Tumour Biol*. 2015;36(1):315–327.

10. Muralidharan R, Panneerselvam J, Chen A, Zhao YD, Munshi A, Ramesh R. HuR-targeted nanotherapy in combination with AMD3100 suppresses CXCR4 expression, cell growth, migration and invasion in lung cancer. *Cancer Gene Ther*. 2015;22(12):581–590.

11. Juan Y, Haiqiao W, Xie W, et al. Cold-inducible RNA-binding protein mediates airway inflammation and mucus hypersecretion through a post-transcriptional regulatory mechanism under cold stress. *Int J Biochem Cell Biol*. 2016;78:335–348.

12. Baker JR, Vuppusetty C, Ito K, Barnes P, Yasuo K. RNA-binding protein HuR inhibits the expression of sirtuin-1 in patients with COPD. Paper presented at: *European Respiraory Journal*. 2017. Epub 2017 Dec 6.

13. Caramori G, Kirkham P, Barczyk A, di Stefano A, Adcock I. Molecular pathogenesis of cigarette smoking-induced stable COPD. *Ann N Y Acad Sci*. 2015;1340:55–64.

14. Barnes PJ, Burney PG, Silverman EK, et al. Chronic obstructive pulmonary disease. *Nat Rev Dis Primers*. 2015;1:15076.

15. Barnes PJ. Immunology of asthma and chronic obstructive pulmonary disease. *Nat Rev Immunol*. 2008;8(3):183–192.

16. Caramori G, Adcock IM, Casolari P, et al. Unbalanced oxidant-induced DNA damage and repair in COPD: a link towards lung cancer. *Thorax*. 2011;66(6):521–527.

17. Cosio MG, Saetta M, Agusti A. Immunologic aspects of chronic obstructive pulmonary disease. *N Engl J Med*. 2009;360(23):2445–2454.

18. Ito K, Barnes PJ. COPD as a disease of accelerated lung aging. *Chest*. 2009;135(1):173–180.

19. Barnes PJ. The cytokine network in asthma and chronic obstructive pulmonary disease. *J Clin Invest*. 2008;118(11):3546–3556.

20. Caramori G, di Stefano A, Casolari P, et al. Chemokines and chemokine receptors blockers as new drugs for the treatment of chronic obstructive pulmonary disease. *Curr Med Chem*. 2013;20(35):4317–4349.

21. Moore AE, Chenette DM, Larkin LC, Schneider RJ. Physiological networks and disease functions of RNA-binding protein AUF-1. *Wiley Interdiscip Rev RNA*. 2014;5(4):549–564.

22. Anderson P. Post-transcriptional control of cytokine production. *Nat Immunol*. 2008;9(4):353–359.

23. Stoecklin G, Tenenbaum SA, Mayo T, et al. Genome-wide analysis identifies interleukin-10 mRNA as target of tristetraprolin. *J Biol Chem*. 2008;283(17):11689–11699.

24. Hamilton T, Novotny M, Pavicic PJ, et al. Diversity in post-transcriptional control of neutrophil chemoattractant cytokine gene expression. *Cytokine*. 2010;52(1–2):116–122.

25. Keene JD. RNA regulons: coordination of post-transcriptional events. *Nat Rev Genet*. 2007;8(7):533–543.

26. Srikantan S, Gorospe M. HuR function in disease. *Front Biosci*. 2012;17(1):189–205.

27. Sanduja S, Blanco FF, Young LE, Kaza V, Dixon DA. The role of tristetraprolin in cancer and inflammation. *Front Biosci*. 2012;17:174–188.

28. White EJ, Brewer G, Wilson GM. Post-transcriptional control of gene expression by AUF-1: mechanisms, physiological targets, and regulation. *Biochim Biophys Acta*. 2013;1829(6–7):680–688.

29. Tiedje C, Diaz-Muñoz MD, Trulley P, et al. The RNA-binding protein TTP is a global post-transcriptional regulator of feedback control in inflammation. *Nucleic Acids Res*. 2016;44(15):7418–7440.

30. Raineri I, Wegmueller D, Gross B, Certa U, Moroni C. Roles of AUF-1 isoforms, HuR and BRF1 in ARE-dependent mRNA turnover studied by RNA interference. *Nucleic Acids Res*. 2004;32(4):1279–1288.

31. Taylor GA, Carballo E, Lee DM, et al. A pathogenetic role for TNF alpha in the syndrome of cachexia, arthritis, and autoimmunity resulting from tristetraprolin (TTP) deficiency. *Immunity*. 1996;4(5):445–454.

32. Lu JY, Sadri N, Schneider RJ. Endotoxic shock in AUF-1 knockout mice mediated by failure to degrade proinflammatory cytokine mRNAs. *Genes Dev*. 2006;20(22):3174–3184.

33. Sadri N, Schneider RJ. AUF-1/Hnrnpd-deficient mice develop pruritic inflammatory skin disease. *J Invest Dermatol*. 2009;129(3):657–670.

34. Agustí A, Faner R. Systemic inflammation and comorbidities in chronic obstructive pulmonary disease. *Proc Am Thorac Soc*. 2012;9(2):43–46.

35. Bradford E, Jacobson S, Varasteh J, et al. The value of blood cytokines and chemokines in assessing COPD. *Respir Res*. 2017;18(1):180.

36. Carolan BJ, Heguy A, Harvey BG, Leopold PL, Ferris B, Crystal RG. Up-regulation of expression of the ubiquitin carboxyl-terminal hydrolase L1 gene in human airway epithelium of cigarette smokers. *Cancer Res*. 2006;66(22):10729–10740.

37. Marwick JA, Caramori G, Casolari P, et al. A role for phosphoinositol 3-kinase delta in the impairment of glucocorticoid responsiveness in patients with chronic obstructive pulmonary disease. *J Allergy Clin Immunol*. 2010;125(5):1146–1153.

38. Fan J, Ishmael FT, Fang X, et al. Chemokine transcripts as targets of the RNA-binding protein HuR in human airway epithelium. *J Immunol*. 2011;186(4):2482–2494.

39. Yanagisawa S, Baker JR, Vuppusetty C, et al. The dynamic shuttling of SIRT1 between cytoplasm and nuclei in bronchial epithelial cells by single and repeated cigarette smoke exposure. *PLoS One* . 2018;13(3):e0193921.

40. Yoon JH, de S, Srikantan S, et al. PAR-CLIP analysis uncovers AUF-1 impact on target RNA fate and genome integrity. *Nat Commun*. 2014;5:5248.

41. Tominaga K, Srikantan S, Lee EK, et al. Competitive regulation of nucleolin expression by HuR and miR-494. *Mol Cell Biol*. 2011;31(20):4219–4231.

42. dal Col J, Dolcetti R. GSK-3beta inhibition: at the crossroad between Akt and mTOR constitutive activation to enhance cyclin D1 protein stability in mantle cell lymphoma. *Cell Cycle*. 2008;7(18):2813–2816.

43. Casolaro V, Fang X, Tancowny B, et al. Posttranscriptional regulation of IL-13 in T cells: role of the RNA-binding protein HuR. *J Allergy Clin Immunol*. 2008;121859(4):853–859.

44. Mazan-Mamczarz K, Kuwano Y, Zhan M, et al. Identification of a signature motif in target mRNAs of RNA-binding protein AUF-1. *Nucleic Acids Res*. 2009;37(1):204–214.

45. Howe EA, Sinha R, Schlauch D, Quackenbush J. RNA-Seq analysis in MeV. *Bioinformatics*. 2011;27(22):3209–3210.

46. Mi H, Huang X, Muruganujan A, et al. PANTHER version 11: expanded annotation data from Gene Ontology and Reactome pathways, and data analysis tool enhancements. *Nucleic Acids Res*. 2017;45(D1):D183–D189.

47. Bourgeois JS, Jacob J, Garewal A, Ndahayo R, Paxson J. The Bioavailability of Soluble Cigarette Smoke Extract Is Reduced through Interactions with Cells and Affects the Cellular Response to CSE Exposure. *PLoS One* . 2016;11(9):e0163182.

48. Gao W, Li L, Wang Y, et al. Bronchial epithelial cells: the key effector cells in the pathogenesis of chronic obstructive pulmonary disease? *Respirology*. 2015;20(5):722–729.

49. di Stefano A, Caramori G, Oates T, et al. Increased expression of nuclear factor-kappaB in bronchial biopsies from smokers and patients with COPD. *Eur Respir J*. 2002;20(3):556–563.

50. Spurrell JC, Wiehler S, Zaheer RS, Sanders SP, Proud D. Human airway epithelial cells produce IP-10 (CXCL10) *in vitro* and *in vivo* upon rhinovirus infection. *Am J Physiol Lung Cell Mol Physiol*. 2005;289(1):L85–L95.

51. Hudy MH, Proud D. Cigarette smoke enhances human rhinovirus-induced CXCL8 production via HuR-mediated mRNA stabilization in human airway epithelial cells. *Respir Res*. 2013;14:88.

52. Navratilova Z, Novosadova E, Hagemann-Jensen M, et al. Expression Profile of Six RNA-Binding Proteins in Pulmonary Sarcoidosis. *PLoS One* . 2016;11(8):e0161669.

53. Ricciardolo FL, Caramori G, Ito K, et al. Nitrosative stress in the bronchial mucosa of severe chronic obstructive pulmonary disease. *J Allergy Clin Immunol*. 2005;116(5):1028–1035.

54. Sirenko OI, Lofquist AK, Demaria CT, Morris JS, Brewer G, Haskill JS. Adhesion-dependent regulation of an A+U-rich element-binding activity associated with AUF-1. *Mol Cell Biol*. 1997;17(7):3898–3906.

55. di Stefano A, Caramori G, Barczyk A, et al. Innate immunity but not NLRP3 inflammasome activation correlates with severity of stable COPD. *Thorax*. 2014;69(6):516–524.

56. Bhowmik A, Seemungal TA, Sapsford RJ, Wedzicha JA. Relation of sputum inflammatory markers to symptoms and lung function changes in COPD exacerbations. *Thorax*. 2000;55(2):114–120.

57. Paschoud S, Dogar AM, Kuntz C, Grisoni-Neupert B, Richman L, Kühn LC. Destabilization of interleukin-6 mRNA requires a putative RNA stem-loop structure, an AU-rich element, and the RNA-binding protein AUF-1. *Mol Cell Biol*. 2006;26(22):8228–8241.

58. de Boer WI, Sont JK, van Schadewijk A, Stolk J, van Krieken JH, Hiemstra PS. Monocyte chemoattractant protein 1, interleukin 8, and chronic airways inflammation in COPD. *J Pathol*. 2000;190(5):619–626.

59. Traves SL, Culpitt SV, Russell RE, Barnes PJ, Donnelly LE. Increased levels of the chemokines GROalpha and MCP-1 in sputum samples from patients with COPD. *Thorax*. 2002;57(7):590–595.

60. Panganiban RP, Vonakis BM, Ishmael FT, Stellato C. Coordinated post-transcriptional regulation of the chemokine system: messages from CCL2. *J Interferon Cytokine Res*. 2014;34(4):255–266.

61. Laroia G, Sarkar B, Schneider RJ. Ubiquitin-dependent mechanism regulates rapid turnover of AU-rich cytokine mRNAs. *Proc Natl Acad Sci U S A*. 2002;99(4):1842–1846.

62. Laroia G, Schneider RJ. Alternate exon insertion controls selective ubiquitination and degradation of different AUF-1 protein isoforms. *Nucleic Acids Res*. 2002;30(14):3052–3058.

63. Lau WK, Li X, Yeung DS, Chan KH, Ip MS, Mak JC. The involvement of serotonin metabolism in cigarette smoke-induced oxidative stress in rat lung *in vivo*. *Free Radic Res*. 2012;46(11):1413–1419.

64. To M, Yamamura S, Akashi K, et al. Defect of adaptation to hypoxia in patients with COPD due to reduction of histone deacetylase 7. *Chest*. 2012;141(5):1233–1242.

65. Keene JD. The globalization of messenger RNA regulation. *Natl Sci Rev*. 2014;1(2):184–186.

66. Sedlyarov V, Fallmann J, Ebner F, et al. Tristetraprolin binding site atlas in the macrophage transcriptome reveals a switch for inflammationresolution. *Mol Syst Biol*. 2016;12(5):868.

67. Wu X, Lan L, Wilson DM, et al. Identification and validation of novel small molecule disruptors of HuR-mRNA interaction. *ACS Chem Biol*. 2015;10(6):1476–1484.

68. Yang WY, Gao R, Southern M, Sarkar PS, Disney MD. Design of a bioactive small molecule that targets r(AUUCU) repeats in spinocerebellar ataxia 10. *Nat Commun*. 2016;7:11647.

69. Alonso N, Guillen R, Chambers JW, Leng F. A rapid and sensitive high-throughput screening method to identify compounds targeting protein-nucleic acids interactions. *Nucleic Acids Res*. 2015;43(8):e52.

70. Wang Z, Bhattacharya A, Ivanov DN. Identification of Small-Molecule Inhibitors of the HuR/RNA Interaction Using a Fluorescence Polarization Screening Assay Followed by NMR Validation. *PLoS One* . 2015;10(9):e0138780.

Supplementary materials

Scoring system for immunohistochemistry in the bronchial rings

The immunostaining for all the RBPs studied was scored in the bronchial epithelium, as previously described.[1] Briefly, immunostained cells in the bronchial epithelium lined over the epithelial basement membrane were counted in several nonoverlapping high-power fields until the whole specimen was examined. As previous studies have shown that lung carcinogenesis may be associated per se with changes in RBP expression,[2,4–6] we deliberately avoided measuring the area of bronchial surface epithelium involved with squamous metaplasia and preneoplastic lesions of the bronchial epithelium. Results of the single immunohistochemistry are expressed as the area of stained bronchial surface epithelium to total bronchial epithelium area and as the area of reactive glands to total bronchial submucosal glands area, measured by computerized image analysis. Group data were expressed as mean and standard error of the mean (SEM).

Scoring system for immunohistochemistry in the peripheral lung

Staining analysis was performed as previously published.[3] A bronchiole was taken to be an airway with no cartilage and glands in its wall. According to a validated method,[3] the number of bronchiolar epithelial cells with positive staining (nuclear and/or cytosolic) was expressed as a percentage of the total number of epithelial cells counted in each bronchiolar section and the number of positively stained endoalveolar macrophages was expressed as a percentage of the total cells with the morphological appearance of alveolar macrophages counted inside of the alveoli. Group data were expressed as mean and standard error of the mean (SEM).

Supplementary Table and Figure

Table S1 Study population providing peripheral blood mononuclear cells (PBMC)

Participants	N	Age, years	Sex	Smoking history	Pack-years	FEV$_1$ % pred	FEV$_1$/FVC%
Smokers	4	53.5 (9.3)	2 M/2 F	4 current	31 (11.2)	105.8 (11.4)	78.6 (1.3)
COPD	5	73.8 (7.5)*	4 M/1 F	1 current 4 ex	39.6 (10)	59.8 (21.0)	52.9 (10.5)*

Notes: Predicted FEV$_1$% and FEV$_1$/FVC% are post-bronchodilator values. M, male; F, female. Data expressed as mean (SD). *$P<0.01$ compared to smokers.

Table S1 Study population providing peripheral blood mononuclear cells (PBMC). Predicted FEV1% and FEV1/FVC% are post-bronchodilator values. M, male; F, female. Data expressed as mean (SD). *$P < 0.01$ compared to smokers.
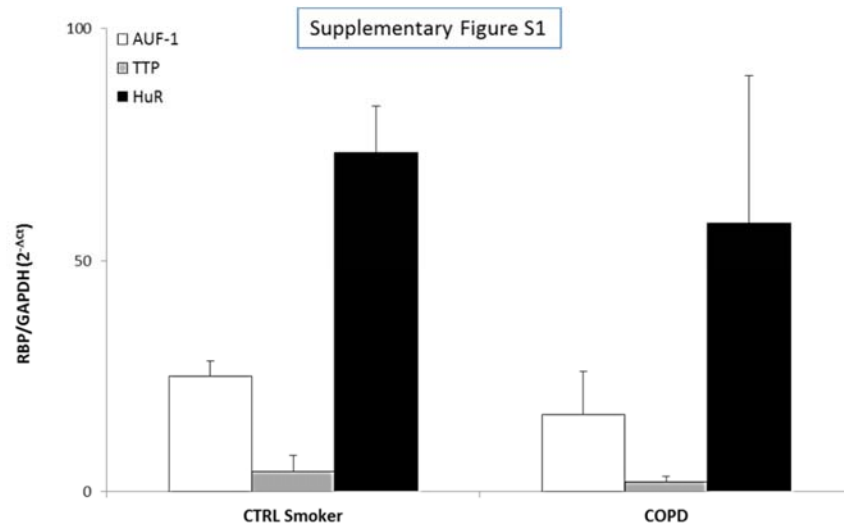
Figure S1. Expression of RBP mRNA in PBMC of COPD patients and control smokers. Real-time PCR analysis for RBP mRNA in PBMC of control smokers (n=4) and COPD patients (n=5) (Table S1). Data are mean ± SEM of RBP mRNA normalized to GAPDH mRNA and expressed as fold over GAPDH (ctrl) (as $2^{-\Delta Ct}$).

Abbreviations: RBP, RNA-binding protein; PBMC, peripheral blood mononuclear cell; SEM, standard error of mean.
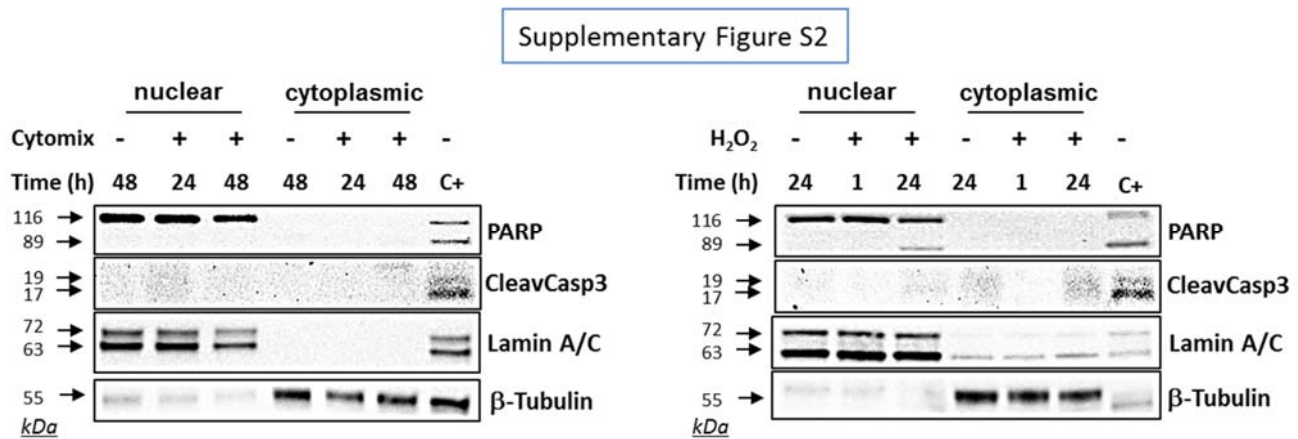
Figure S2. Evaluation of treatment-induced apoptosis in BEAS-2B cells. Western blot analysis of PARP and cleaved Caspase 3 expression in nuclear and cytoplasmic lysates obtained from BEAS-2B cells exposed to cytomix (left panel) and 200 μM (right panel) for the indicated times. Only the full-length bands of PARP and Caspase 3 were detectable in experimental samples, excluding treatment-induced apoptosis. Positive control (C+) is whole cell lysate of gefitinib-treated H1975 NSCLC cell line. Representative immunoblots of n=3 independent experiments are shown. Lamin A/C and tubulin are shown as nuclear and cytoplasmic loading controls, respectively. **Abbreviation**: NSCLC, non-small-cell lung cancer.
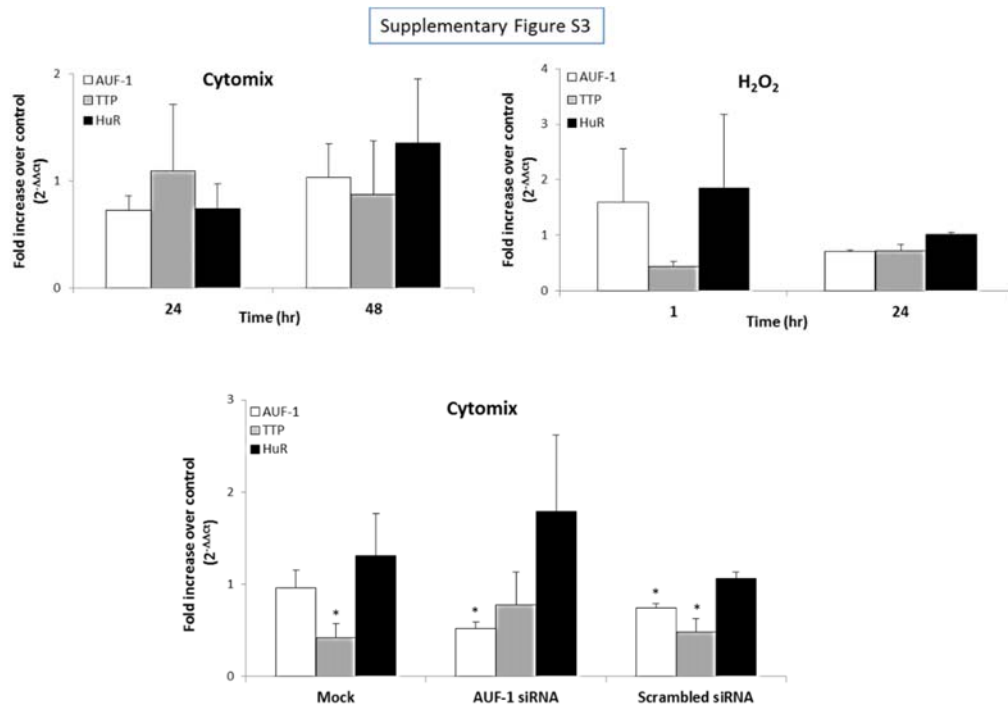
Figure S3. Expression of RBP mRNA in BEAS-2B cells. Real-time PCR analysis for RBP mRNA in nontransfected BEAS-2B cells stimulated with (**A**) cytomix and (**B**) hydrogen peroxide (200 M for the indicated times (mean ± SEM of n=3). (**C**) RBP mRNA in BEAS-2B cells stimulated 48 hours with cytomix following transfection with mock (F = Fugene), siRNA for AUF-1, scrambled siRNA (mean ± SEM of n=4). RBP mRNA was normalized to housekeeping mRNA levels and expressed as fold over corresponding unstimulated controls ($2^{-\Delta Ct}$). *$P < 0.05$ versus controls.
Abbreviations: AUF-1, AU-rich element-binding factor 1; RBP, RNA-binding protein; SEM, standard error of mean.
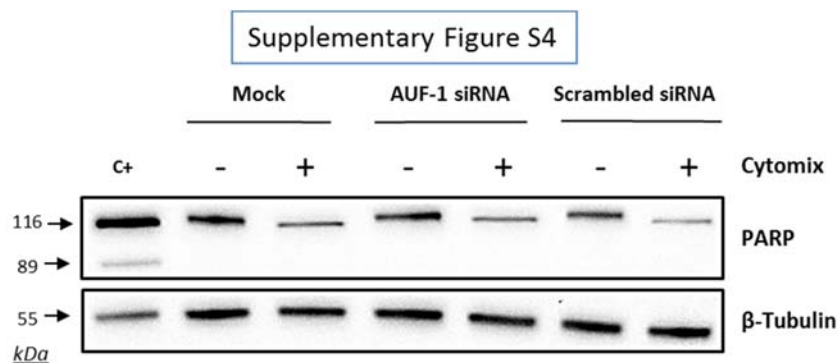
Figure S4. Evaluation of treatment-induced apoptosis in BEAS-2B cells following AUF-1 silencing. Western blot analysis of PARP expression in whole cell lysates obtained from BEAS-2B cells untreated and stimulated 48 hours with cytomix following transfection with AUF-1 siRNA, scrambled siRNA, and mock transfection (Fugene) (mean ± SEM of n=4). Positive control (Ctrl) showing cleaved PARP protein band is whole cell lysate of gefitinib-treated H1975 NSCLC cell line. Representative immunoblots of n=3 independent experiments are shown. β-Tubulin is shown as loading control. **Abbreviations:** AUF-1, AU-rich element-binding factor 1; NLF, normal lung function; SEM, standard error of mean; NSCLC, non-small-cell lung cancer.

Supplementary Material - References

1. Caramori G, Casolari P, Di Gregorio C, et al. MUC5AC expression is increased in bronchial submucosal glands of stable COPD patients. *Histopathology*. 2009;55(3):321–331.

2. Lafzi A, Kazan H. Inferring RBP-Mediated Regulation in Lung Squamous Cell Carcinoma. *PLoS One*. 2016;11(5):e0155354.

3. Caramori G, Adcock IM, Casolari P, et al. Unbalanced oxidant-induced DNA damage and repair in COPD: a link towards lung cancer. *Thorax*. 2011;66(6):521–527.

4. Fallahi M, Amelio AL, Cleveland JL, Rounbehler RJ. CREB targets define the gene expression signature of malignancies having reduced levels of the tumor suppressor tristetraprolin. *PLoS One* . 2014;9(12):e115517.

5. Giaginis C, Alexandrou P, Tsoukalas N, et al. Hu-antigen receptor (HuR) and cyclooxygenase-2 (COX-2) expression in human non-small-cell lung carcinoma: associations with clinicopathological parameters, tumor proliferative capacity and patients' survival. *Tumour Biol*. 2015;36(1):315–327.

6. Muralidharan R, Panneerselvam J, Chen A, Zhao YD, Munshi A, Ramesh R. HuR-targeted nanotherapy in combination with AMD3100 suppresses CXCR4 expression, cell growth, migration and invasion in lung cancer. *Cancer Gene Ther*. 2015;22(12):581–590.

b. **Study# 2**

Posttranscriptional gene regulatory networks in chronic airway inflammatory diseases: *in silico* mapping of RNA-binding proteins expression in airway epithelium

Luca Ricciardi[1], Giorgio Giurato[1], Domenico Memoli[1], Ilaria Salvato[1], Maria Assunta Crescenzi[1], Alessandro Vatrella[1], Alessandro Weisz[1], Gaetano Caramori[2], Vincenzo Casolaro[1] and Cristiana Stellato[1]

[1] Department of Medicine, Surgery and Dentistry '*Scuola Medica Salernitana*', University of Salerno, Salerno, Italy ;

[2] Pulmonary Unit, Department of Biomedical Sciences, Dentistry, Morphological and Functional Imaging (BIOMORF), University of Messina, Messina, Italy

Full manuscript to be submitted

Abstract

Background and Aim. Aberrant changes in messenger RNA (mRNA) turnover and translation rates are important means by which posttranscriptional gene regulation (PTR) contributes to inflammation. RNA-binding proteins (RBPs) chiefly coordinate these processes but their pathogenic role in chronic lung inflammatory diseases is partially characterized. We aim at evaluating the expression of a curated list of mRNA-binding RBPs (mRBPs) in selected transcriptomic GEO databases of primary airway epithelium isolated in lung inflammatory diseases. We hypothesize that global changes in mRBPs expression can be used to infer their putative pathogenetic roles and identify novel disease-related regulatory networks.

Methods. We evaluated the expression of 692 mRBPs, selected from a published census [Nat Rev Genet. 2014;15:829], in microarray databases originated from epithelial cells obtained by bronchial brushings of stable COPD patients (C), smokers (S), non-smokers (NS) as controls with normal lung function (n=6/12/12 each) [Gene Expression Omnibus (GEO) repository ID: GSE5058, Cancer Res. 2006;66:10729] and of severe asthma patients (SA) and control subjects (C) (n=6/12 each) [GEO ID: GSE63142, Am J Respir Crit Care Med. 2014;90,1363]. Fluorescence intensity data from individual datasets were extracted and normalized on the medians for fold change (FC) comparison of expression among groups. FCs were set at $\geq |1.5|$ with a false discovery rate (FDR) of ≤ 0.05. Pearson correlation maps for correlated expression changes and heatmaps were generated using tMEV tools v4_9_0.45. Gene Ontology (GO) was performed with Ingenuity Pathway Analysis (IPA) tool.

Results. Significant mRBP gene expression was detected for S/NS, COPD/NS and COPD/S comparisons (n genes = 41, 391, 382, respectively). Of those, 32% of genes changed by FC $\geq |1.5|$ in S/NS but more than 60% in COPD/NS and COPD/S (n=13, 267, 257, respectively). Interestingly, the majority of genes were downregulated (FC ≤ -1.5) in COPD/NS (n=194, 73%) and COPD/S (n=202, 79%) while only 31% were downregulated in S/NS (n=4). Correlation analysis identified discrete clusters of co-expressed mRBP genes. GO analysis revealed significant enrichments in canonical pathways both specific and shared among the comparisons. Unexpectedly, no significant mRBPs modulation was found in the SA patients compared to controls.

Conclusions. Characterization of epithelial mRBPs expression in stable COPD and SA reveals a COPD-specific global downregulation of RBPs shared by a subset of control smokers, and a significant impact on relevant pathways involved in COPD pathogenesis. Further functional studies are necessary to understand how PTR participates to chronic inflammatory lung disease process and whether it can be targeted therapeutically.

Introduction

RNA-binding proteins (RBPs) are key regulatory factors in post-transcriptional gene regulation (PTGR) involved in the maturation, stability, transport and degradation of cellular RNAs. RBP convey PTGR by binding to conserved regulatory elements shared by subsets of transcripts and by directing the bound targets towards cytoplasmic sites of translation or decay.[1] Importantly, RBPs exert their function as part of ribonucleoprotein (mRNP) complexes, constituted by proteins and noncoding RNAs, such as microRNAs.[2] Through stimulus-dependent cues, changes in mRBP composition ultimately determine the rate of target mRNA stability and translation. Therefore, understanding RBP function in disease models requires a larger evaluation of co-expression and regulatory scenarios, shaped by disease-driven triggers and signalling.

For human cancer the occurrence of aberrant RBP expression, along with altered RNA turnover and translation rates have been characterized in preclinical models, identified in human disease and further probed with *in silico* approaches,[3,4] leading to the identification of this class of regulators as novel disease biomarkers and as targets for small molecule-based therapeutics.[5-7] Similar studies in human chronic inflammatory diseases are lagging behind, despite ample knowledge of deregulated PTGR in inflammatory responses by *in vitro* studies and the strong inflammatory phenotypes obtained in some of the knock-out animal models.[8,9] This knowledge chasm is also present for lung diseases, despite the strong link between chronic inflammatory diseases such as Chronic obstructive pulmonary disease (COPD) and some lung cancer types[10] and the extensive overlap of RBP-regulated genes contributing to both disease process.[11]

Airway epithelium is a major driver in the development of inflammatory lung diseases such as asthma and COPD. Deregulated epithelial responses are a main therapeutic target of inhaled corticosteroids (ICS), the mainstay anti-inflammatory drug class for asthma symptom control (www.ginasthma.org) and for treating exacerbations in COPD (www.goldcopd.org). Involvement of RBPs in airway epithelial responses to inflammatory stimuli and glucocorticoid treatment has been well characterized *in vitro*[12-15] but awaits evidence from patient-based studies. To this end, we recently identified loss of the RBP AUF-1 in airway epithelial cells of patients with stable COPD compared to normal smokers.[16]

We hypothesized that global changes in mRNA-binding RBPs (mRBP) expression may occur in chronic inflammatory airways diseases, such as severe asthma and COPD and that identification of these changes can be used to infer their putative pathogenetic roles as disease-related regulatory networks, as in cancer.[17] On these bases, we set out to evaluate the expression profile of a curated gene list of mRBPs in selected transcriptomic GEO databases derived from airway epithelium isolated from bronchial brushings of phenotyped patients affected by COPD, bronchial asthma and relative control populations. Through gene ontology analysis we identified several pathways impacted by the RBP profiles and evaluated their relevance to disease pathogenesis; finally, we searched for coregulated RBP expression in the disease-regulated mRBPs.

In airway epithelial samples from COPD patients, this approach identified a global downregulation of RBP expression that was shared by a subset of smoker control subjects; changes in mRBP expression impacted

several biological pathways also involved in several aspects of COPD pathogenesis; finally, at least four groups of coregulated RBPs were identified. Importantly, airway epithelial mRBP expression was found to be much less regulated in patients with severe asthma.

Methods

Sample selection and data processing. We selected the following two trascriptomic databases generated from human airway epithelial cells obtained by bronchial brushings, downloaded from the Gene Expression Omnibus (GEO) public repository of high-throughput gene expression data (Figure 1A):

- **GEO ID: GSE5058**. Stable COPD patients (C), Smokers (S) and Non-Smokers (NS) as controls with normal al lung function (NLF) (n=6/12/12, respectively);[18]

- **GEO ID: GSE63142**. Patients with severe Asthma (SA), control subjects (C) (n=6/12 respectively, randomly selected from databes to match number of cases considered in GSE5058).[19]

The Affymetrix Human Genome U133 Plus 2.0 Array platform was used for the first study while the severe asthma study was performed using Agilent-014850 Whole Human Genome Microarray 4x44K G4112F. Fluorescence intensity data from individual datasets (raw data) were extracted and processed applying the standard Affimetrix MAS5 algorithm to calculate the fluorescence of the single probes compared to the fluorescence background. MAS5 values with $p < 0.05$ were considered for further analysis. Data were then normalized by the medians to calculate fold change (FC) expression among groups; only those showing a False Discovery Rate (FDR) ≤ 0.05 in each clinical sample comparison were considered. As genes are represented on the array platforms by multiple probes spanning different transcript portions, only genes with consistency across probes $\geq 67\%$ were considered for final analysis.

The analysis first identified statistically significant genes regardless of fold change value, which were denominated <u>D</u>ifferentially <u>E</u>xpressed <u>G</u>enes (DEG). Then, FCs threshold was set at $\geq |1.5|$ for identification of genes denominated <u>S</u>ignificant FC/<u>D</u>ifferentially <u>E</u>xpressed <u>G</u>enes (SDEG) as in standard array analysis. A curated gene list of mRNA-binding RBPs (mRBPs) published in a recent general census of RNA-binding proteins[20] was downloaded and searched in the final files (Figure 1B), producing a list of mRBPs regulated in disease state vs. controls (Figure 1C).

Generation of Venn diagram analysis for overlapping/unique gene lists was performed using Venny 2.1.[21] Pearson correlation matrix generation was produced using R version 3.6.2. Pearson correlation maps for mRBPs expression changes and heatmaps were generated using tMEV tools v4_9_0.45.[22,23]

Gene Ontology (GO). GO analysis was performed with Ingenuity Pathway Analysis (IPA) software on microarray probes of RBPs identified as DEG. The significance values for the canonical pathways is calculated by Fisher's exact test right-tailed. The prediction of activation or inhibition of Canonical Pathways was calculated by z-score[24] as follows:

$$z - score = \frac{(\sum Upregulated) - (\sum Downregulated)}{\sqrt{N}}$$

Statistical analysis. Statistical analysis was performed using GraphPad Prism 5 (*GraphPad Software Inc.*).
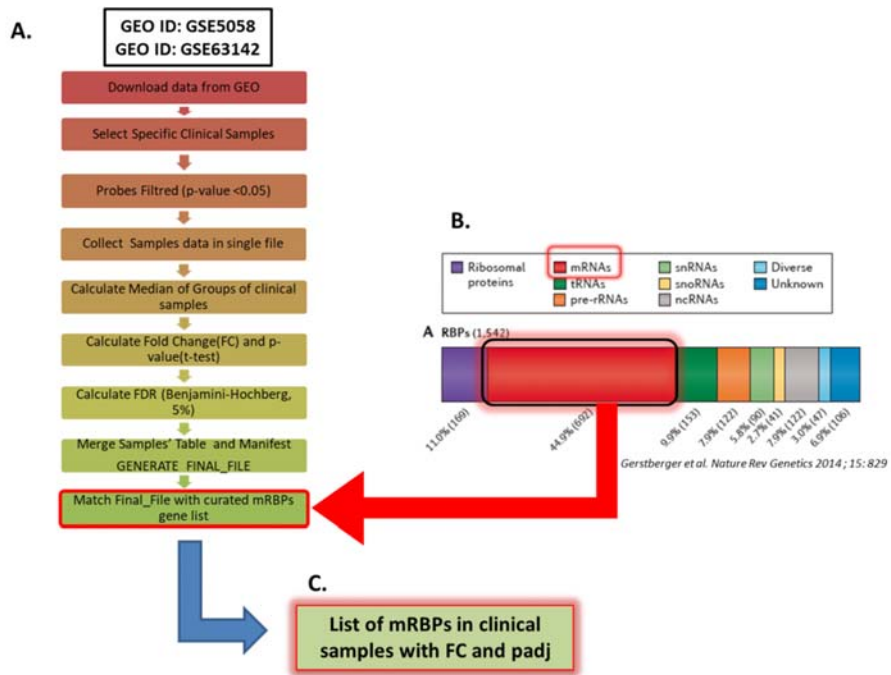
Figure 1. Methodological flowchart of data extraction from GEO databases and search of a curated list of mRNA-binding proteins (mRBPs) for expression profiling in airway epithelium transcriptomic studies in COPD and severe asthma. A. Flowchart for data analysis of the trascriptomic datasets obtained in the Gene Expression Omnibus (GEO) public database; B. A curated gene list of mRNA-binding RBPs (mRBPs) was downloaded by a census of RNA-binding proteins[20] as the dataset to search for in the GEO datasets; C. The search generated a list of differentially regulated mRBPs in clinical samples (see Methods for details).

Results

Expression profile of mRBPs in airway epithelial transcriptomic database of patients with stable COPD compared to non-smoker and smoker control subjects.

The mRBPs gene list was searched in the GSE5058 dataset to identify disease-dipendent mRBP gene expression in patients with moderate to severe COPD compared to control groups, clinically phenotyped as shown (Figure 2A). Comparisons of expression levels for the smoking control group vs. non-smoking control group dataset (S/NS) and of COPD patients vs. both NS and S group datasets (COPD/NS, COPD/S) were performed. The number of regulated mRBP genes is reported along with corresponding array probes, which detect different fragments of each gene sequence and generate the fluorescence intensity raw data. We first calculated regulated genes with statistically significant changes *regardless* of fold change (FC) value: these were defined as Differentially Expressed Genes (DEG) (Figure 2B).
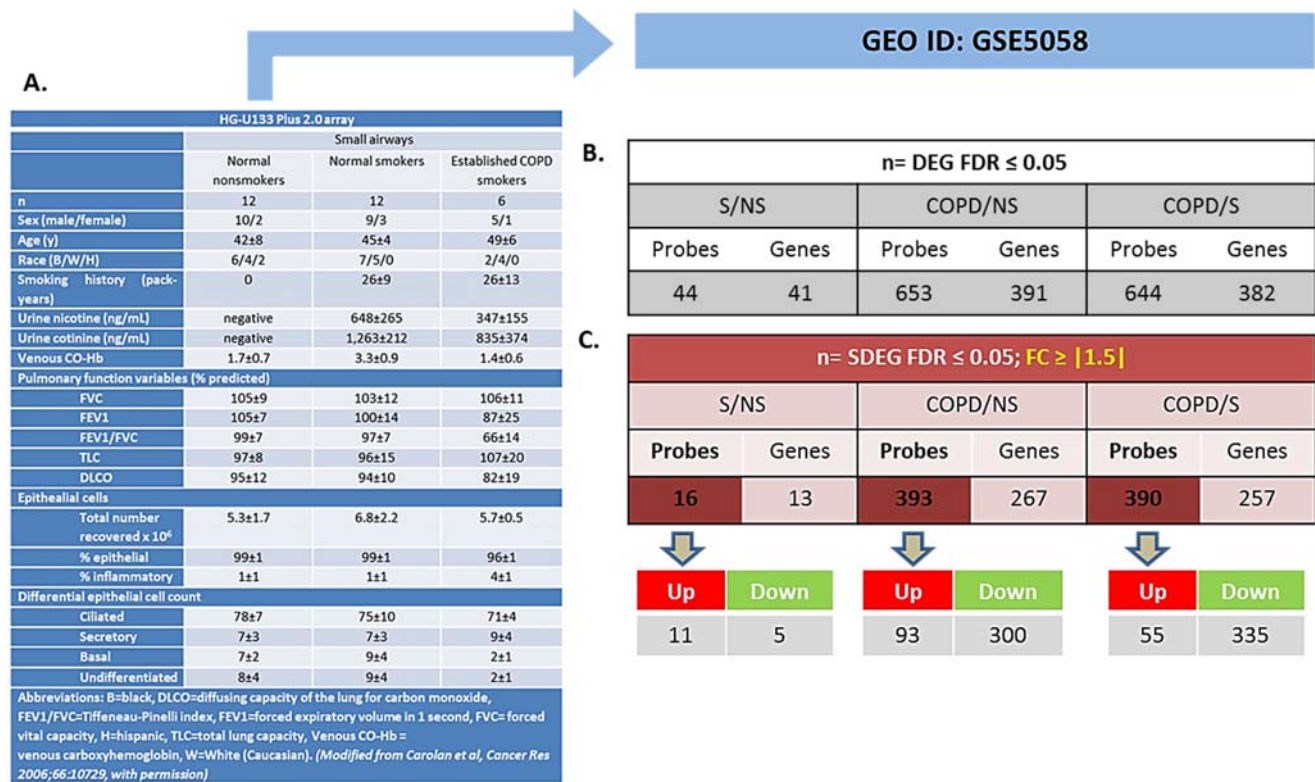
Figure 2. Regulated mRBP expression in Small Airway Epithelial Transcriptomics in stable COPD. (A.) Clinical and spirometric phenotyping of COPD smoker patients (COPD), nonsmokers (NS) and smokers (S) with normal lung function (NLF) as control cohorts providing airway epithelial cells by bronchial brushings for trascriptomic analysis reported in GEO GSE5058[18] utilized in this study for mRBP expression analysis. (B., C.) For each gene, multiple probes spanning different gene regions are represented on array platforms. Panels show the numbers of mRBP probes and corresponding genes obtained after p-value filtering. B. Statistically significant, Differentially Expressed mRBP Genes, regardless of fold change value (DEG) and C. Statistically Significant/Differential Expressed mRBP Genes with

differential expression set at $\geq |1.5|$ (SDEG) obtained comparing datasets from S versus NS, COPD versus S and versus NS. Number of Up- or down-regulated SDEG probes are shown below.

These data revealed an overall greater expression of mRBPs in COPD patients versus both NS and S control groups, about 9-fold higher than that triggered by smoke exposure alone. The mRBP genes displaying a statistically significant FC value $\geq |1.5|$ were further selected and denominated <u>S</u>ignificant FC/<u>D</u>ifferentially <u>E</u>xpressed <u>G</u>enes (SDEG) (Figure 2C). Approximately 70% of the mRBP DEG genes were included in this category when COPD samples were compared to both control samples (COPD/NS, COPD/S), while 30% of S/NS DEG genes were upregulated over this threshold. A small number of genes were excluded from further computing for probe discordance $\geq 67\%$ (n=30/267, 11% for COPD/NS; 10/257 for COPD/S, 3%). The SDEG profiles indicate that the majority of mRBP genes in COPD were downregulated compared to both controls (n=194/267, 73% for COPD/NS; n=202/257, 79% for COPD vs S) while in S/NS only 30% (n=4/13) were downregulated (Figure 3). Table 1 lists the main functions, published or described in GeneCards[25] for mRBPs SDEG with the highest numerical FC value in COPD vs both control groups.
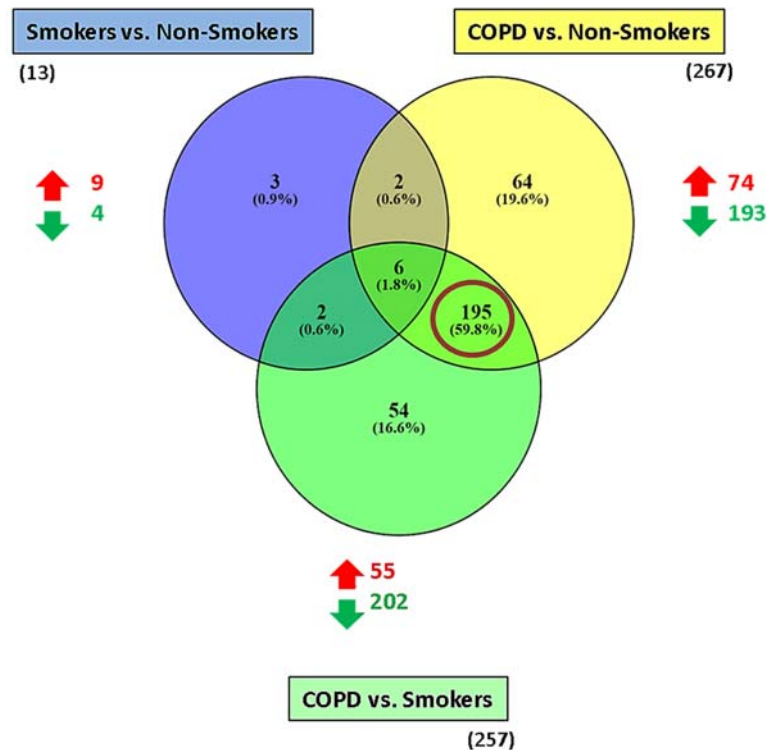
Figure 3. mRBP SDEG genes in small airway epithelium of stable COPD patients versus non-smoking and smoking control subjects: unique and overlapping regulated expression. Venn diagram generated with Venny 2.1[21], showing selective and shared mRBPs SDEG genes (FDR ≤ 0.05; FC $\geq |1.5|$) among the three comparisons. Total number of up-and down-regulated mRBPs for each comparison are shown by red/green arrows; total number in parenthesis. Red circle highlights the predominant number of SDEG differentially expressed in COPD, regardless the smoking status of controls.

The three gene groups (NS/S, COPD/NS, COPD/S) were intersected to identify both unique and overlapping mRBP expression profiles. As shown in the Venn's diagram (Figure 3), 195 SDEG genes are shared between the COPD patients vs both NS and S groups, pointing at a distinctive mRBP signature driven by COPD beyond the active exposure to cigarette smoke.

Using the larger DEG lists, the three gene sets were then analysed by IPA software probing changes in the categories of canonical pathways (Figure 4). Five out of eight canonical pathways impacted by COPD were shared by comparisons to NS and S groups (Figure 4A). Calculation of the z-score parameter yielded a predictive assessment of the downstream effect - activation or inactivation - exerted by the identified RBP profile on the metabolic pathways (Figure 4B). Table 2 lists the mRBPs involved for each comparison shown in Figure 4B.
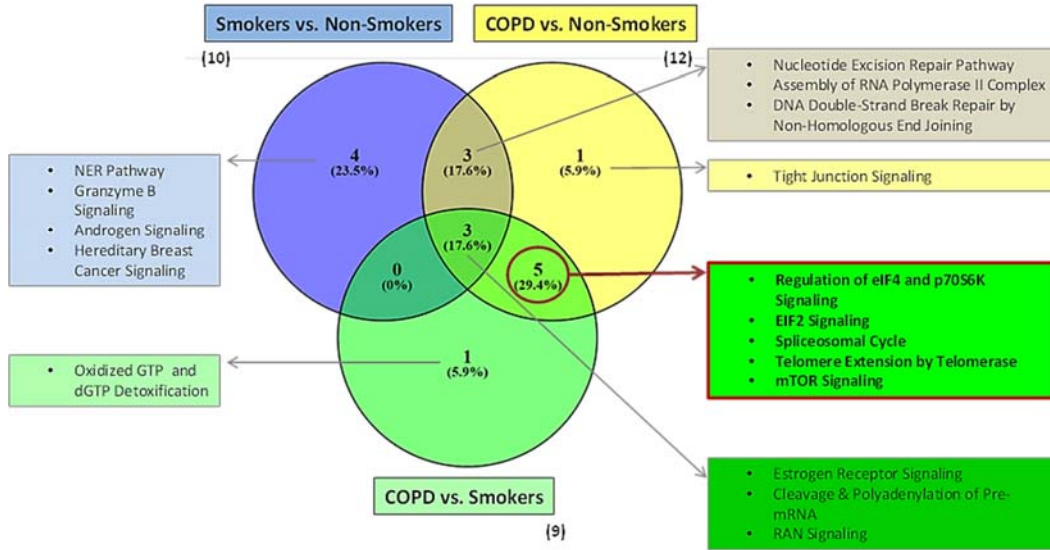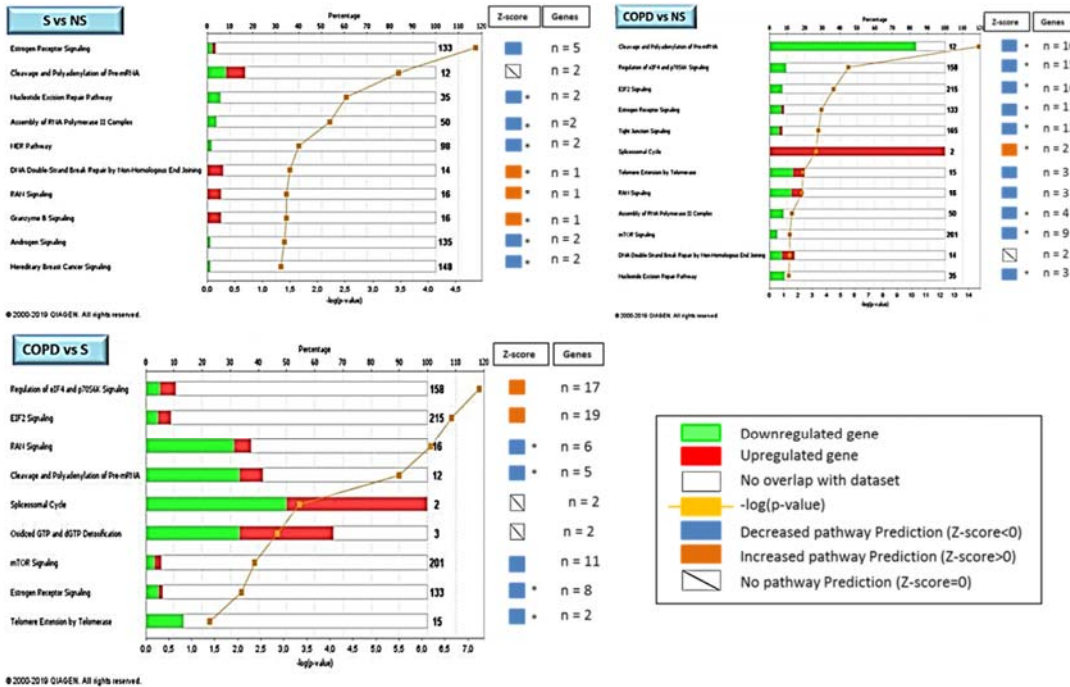
Figure 4. Genome Ontology analysis of mRBPs expression in small airway epithelium of stable COPD patients versus non-smoking and smoking control subjects: involvement in established COPD pathogenic pathways. Ingenuity Pathway Analysis (IPA) of mRBP DEGs in COPD GSE5058 Dataset. **A.** Venn diagram showing selective and shared canonical pathways among the group comparisons calculated on DEGs by Ingenuity Pathway Analysis (IPA). In evidence (red lined rectangle) the pathways enriched in COPD versus both NS and S control groups. B. Canonical pathways (bargraphs) of DEG identified for the indicated group comparisons. The Z-score predicts pathway repression or activation (see Methods); n= number of regulated mRBP genes involved for each pathway (listed in Table 2). * z-score ≥ |1|

Table 1. Regulated RBPs in COPD versus normal non-smokers and smokers: selected list with known functions. (References in Supplementary Materials).

Gene	Complete Name	FC$_{COPD}$ vs S	FC$_{COPD}$ vs NS	Main Functions	Refs
FUS	FUS RNA Binding Protein	-34.63	-37.5	Involved in pre-mRNA splicing and the export of fully processed mRNA to the cytoplasm	26
				Maintenance of genomic integrity and mRNA/microRNA processing	27
THRAP3	Thyroid Hormon Receptor Associated Protein 3	-33.54	-31.58	Enhances the transcriptional activation mediated by PPARG cooperatively with HELZ2	28
				Acts as a coactivator of the CLOCK-ARNTL heterodimer	29
				Involved in response to DNA damage	28
DDX17	DEAD-Box Helicase 17	-31.04	-46.27	RNA helicase	30
				pre-mRNA splicing, alternative splicing, ribosomal RNA processing and miRNA processing, transcription regulation	31-34
				Splicing of mediators of steroid hormone signaling pathway	35
				Synergizes with TP53 in the activation of the MDM2 promoter; may also coactivate MDM2 transcription through a TP53-independent pathway	36-38
				Coregulates SMAD-dependent transcriptional activity during epithelial-to-mesenchymal transition	33
				Plays a role in estrogen and testosterone signaling pathway	35,37-39
				Promotes mRNA degradation mediated by the antiviral zinc-finger protein ZC3HAV1	40
SCAF11	SR-Related CTD Associated Factor 11	-14.4	-12.7	Plays a role in pre-mRNA alternative splicing by regulating spliceosome assembly	41
STRAP	Serine/Threonine Kinase Receptor Associated Protein	-10.8	-8.22	Plays a catalyst role in the assembly of small nuclear ribonucleoproteins (snRNPs), the building blocks of the spliceosome	42
				Negatively regulates TGFβ signaling	42
				Positively regulates the PDPK1 kinase activity	42
RBM14	RNA Binding Motif Protein 14	-7.36	-6.31	General nuclear coactivator, and an RNA splicing modulator. Isoform 1 may function as a nuclear receptor coactivator.Isoform 2, functions as a transcriptional repressor	43
				Plays a role in the regulation of DNA virus-mediated innate immune response by assembling into the HDP-	44

				RNP complex, a complex that serves as a platform for IRF3 phosphorylation	
BCLAF1	Bcl-2-Associated Transcription Factor1	-7.32	-4.13	Regulation of apoptosis interacting with BCL2 proteins	45
ILF3	Interleukin Enhancer Binding Factor 3	-6.33	-4.61	Forms a heterodimer with ILF2, required for T-cell expression of IL-2	46
				Post transcriptional regulation of mRNA binding to poly-U elements and AU-rich elements (AREs) in the 3'-UTR of target mRNA	47
				Participates in the innate antiviral response	48,49
				Plays an essential role in the biogenesis of circRNAs	49
SFSWAP	Splicing Factor SWAP	-5.81	-3.34	Regulates the splicing of fibronectin and CD45 genes	50
RBM25	RNA Binding Motif Protein 25	-5.7	-4.16	Regulator of alternative pre-mRNA splicing	51
				Involved in apoptotic cell death through the regulation of the apoptotic factor BCL2L1 (proapoptotic isoform S, antiapoptotic isoform L)	51
DHX36	DEAH-Box Helicase 36	-4.96	-5.31	Enhance the deadenylation and decay of mRNAs with 3'-UTR AU-rich elements (ARE-mRNA)	52
				Multifunctional ATP-dependent helicase that unwinds G-quadruplex (G4) structures	53-56
				Plays a role in genomic integrity. Converts the G4-RNA structure present in TREC into a double-stranded RNA	54,57-61
				Plays a role in the regulation of cytoplasmic mRNA translation and mRNA stability	62,63
				Plays a role in transcriptional regulation and post-transcriptional regulation	56,64,65
HNRNPA2B1	Heterogeneous Nuclear Ribonucleoprotein A2/B1	-4.91	-4.63	Associates with nascent pre-mRNAs, packaging them into hnRNP particles and drive them into transcription, pre-mRNA processing, RNA nuclear export, subcellular location, mRNA translation and stability of mature mRNAs.	66
				Involved in transport of specific mRNAs to the cytoplasm in oligodendrocytes and neurons recognizing binding the A2RE or the A2RE11 sequence motifs present on some mRNAs.	67
				Specifically binds single-stranded telomeric DNA sequences, protecting telomeric DNA repeat against endonuclease digestion	68
				Involved in the transport of HIV-1 genomic RNA out of the nucleus, to the MTOC, and then from the MTOC to the cytoplasm: acts by specifically recognizing and binding the A2RE sequence motifs present on HIV-1 genomic RNA.	68

Gene	Name	Col3	Col4	Function	Ref
CCAR1	Cell Division Cycle And Apoptosis Regulator 1	-2.79	-2.93	Plays a role in cell cycle progression and/or cell proliferation	69,70
				p53 coactivator	71
NR0B1	Nuclear Receptor Subfamily 0 Group B Member 1	1.57	3.31	Acts as a dominant-negative regulator of transcription which is mediated by the retinoic acid receptor	72
				Functions as an anti-testis gene by acting antagonistically to Sry	72
				Have a role in the development of the embryo and in the maintenance of embryonic stem cell pluripotency	72
RBPMS	RNA-Binding Protein With Multiple Splicing	1.77	1.4	pre-mRNA maturation (binds to poly(A) RNA)	73,74
				Required to increase TGFB1/Smad-mediated transactivation	74
HDLBP	High Density Lipoprotein Binding Protein	1.91	2.53	Regulates excess cholesterol levels in cells	75
				Induces heterochromatin formation	75
MATR3	Matrin 3	2	3.3	Plays a role in the regulation of DNA virus-mediated innate immune response by assembling into the HDP-RNP complex, a complex that serves as a platform for IRF3	44
DHX30	DExH-Box Helicase 30	2.18	2.45	Assembly of the mitochondrial large ribosomal subunit	76,77
				Required for optimal function of the zinc-finger antiviral protein ZC3HAV1	78
				Involved in nervous system development differentiation	78

A2RE=21 nucleotide hnRNP A2 response element, A2RE11=11-nucleotide subsegment of the A2RE, ARE=AU Rich Elements, ARNTL=Aryl Hydrocarbon Receptor Nuclear Translocator Like, circRNA=circular RNA, CLOCK=Circadian Locomoter Output Cycles Protein Kaput, HELZ2=Helicase With Zinc Finger 2, hnRNP=heteronuclear ribonucleoprotein, IL-2=Interleukin2, IRF3=Interferon Regulatory Factor 3, MDM2=Proto-oncogene MDM2, miRNA=micro RNA, MTOC=microtubule organizing center, NONO=Non-POU Domain Containing Octamer Binding, PDPK1=3-Phosphoinositide Dependent Protein Kinase 1, rRNA=ribosomal RNA, SMAD=small mother against decantaplegic, TGFβ=Transforming Growth Factor β, TP53=Tumor Protein 53, TREC=telomerase RNA template component, ZC3HAV1=Zinc Finger CCCH-Type Containing Antiviral 1.

Table 2. GO analysis by IPA indicating canonical pathways in which RBP enrichment is significant for each comparison (a., b., c.), with predicted functional outcome indicated by Z-score (See Methods for details), and RBP molecules involved. Highlighted in yellow are the five pathways associated with COPD vs. both controls.

2a. S/NS				
Ingenuity Canonical Pathways	**p-value**	**z-score**	**Prediction**	**Molecules**
Estrogen Receptor Signaling	1.38E-05	-0.44	inhibition	PRKDC,NR0B1,SPEN,POLR2H, POLR2L
Cleavage and Polyadenylation of Pre-mRNA	3.47E-04	0	0	CPSF2,CPSF6
Nucleotide Excision Repair Pathway	3.02E-03	-1.41	inhibition	POLR2H,POLR2L
Assembly of RNA Polymerase II Complex	6.03E-03	-1.41	inhibition	POLR2H,POLR2L
NER Pathway	2.19E-02	-1.41	inhibition	POLR2H,POLR2L
DNA Double-Strand Break Repair by Non-Homologous End Joining	3.24E-02	1	activation	PRKDC
RAN Signaling	3.63E-02	1	activation	TNPO1
Granzyme B Signaling	3.63E-02	1	activation	PRKDC
Androgen Signaling	3.98E-02	-1.41	inhibition	POLR2H,POLR2L
Hereditary Breast Cancer Signaling	4.68E-02	-1.41	inhibition	POLR2H,POLR2L
2b. COPD/NS				
Ingenuity Canonical Pathways	**p-value**	**z-score**	**Prediction**	**Molecules**
Cleavage and Polyadenylation of Pre-mRNA	2E-15	-3.16	inhibition	PAPOLA,CPSF2,CPSF6,CSTF1,NUDT21,CPSF1,CSTF2,CPSF3,CSTF3,CPSF4
Regulation of eIF4 and p70S6K Signaling	2.88E-06	-3.87	inhibition	EIF2B4,PAIP2,EIF3E,EIF4G1,EIF2B2,EIF4E,EIF3M,EIF3G,EIF1,EIF3B,EIF3A,EIF2B1,EIF3L,EIF1AX,EIF3K
EIF2 Signaling	3.02E-05	-4	inhibition	EIF2B4,EIF3E,EIF4G1,EIF2B2,EIF4E,EIF3,EIF3G,PTBP1,EIF1,EIF3,HNRNPA1,EIF2B,EIF3A,EIF3L,EIF1AX,EIF3K
Estrogen Receptor Signaling	0.000209	-2.11	inhibition	PRKDC,DDX5,THRAP3,SPEN,NR0B1,POLR2H,GTF2F1,HNRNPD,RBFOX2,POLR2K,POLR2L

Tight Junction Signaling	0.000363	-1.73	inhibition	CPSF2,CPSF6,CSTF1,NUDT21,CPSF1,CSTF2,YBX3,CPSF3,SYMPK,SAFB,CSTF3,CPSF4
Spliceosomal Cycle	0.000501	1.41	activation	U2AF1/U2AF1L5,U2AF2
Telomere Extension by Telomerase	0.004169	-0.57	inhibition	HNRNPA1,XRCC6,HNRNPA2B1
RAN Signaling	0.005129	-0.57	inhibition	KPNB1,RANBP2,TNPO1
Assembly of RNA Polymerase II Complex	0.025704	-2	inhibition	POLR2H,GTF2F1,POLR2K,POLR2L
mTOR Signaling	0.038019	-3	inhibition	EIF3G,EIF3B,EIF3A,EIF3E,EIF4G1,EIF4E,EIF3L,EIF3M,EIF3K

2c. COPD/S

Ingenuity Canonical Pathways	p-value	z-score	Prediction	Molecules
Regulation of eIF4 and p70S6K Signaling	5.75E-08	0.24	activation	EIF2B4,EIF4G3,PAIP2,EIF3E,EIF4G1,EIF2B2,EIF4E,EIF3M,EIF3G,EIF1,EIF3B,PAIP1,EIF3A,EIF2B5,EIF1AX,EIF3L,EIF3K
EIF2 Signaling	2.24E-07	0.22	activation	EIF2B4,EIF4G3,EIF3E,EIF4G1,EIF2B2,EIF4E,EIF3M,EIF3G,PTBP1,EIF1,EIF3B,HNRNPA1,EIF5,PAIP1,EIF3A,EIF2B5,EIF1AX,EIF3,EIF3K
RAN Signaling	6.46E-07	-1.63	inhibition	KPNB1,RANBP2,TNPO1,RAN,XPO1,IPO5
Cleavage and Polyadenylation of Pre-mRNA	3.16E-06	-1.34	inhibition	PAPOLA,CPSF2,CSTF1,NUDT21,CSTF3
Spliceosomal Cycle	0.000468	0	0	U2AF1/U2AF1L5,U2AF2
Oxidized GTP and dGTP Detoxification	0.00138	0	0	DDX6,RUVBL2
mTOR Signaling	0.004365	-0.30	inhibition	EIF3G,EIF3B,EIF3A,EIF4G3,EIF3,EIF4G1,EIF3L,EIF4E,EIF3M,EIF4B,EIF3K
Estrogen Receptor Signaling	0.008318	-1.41	inhibition	PRKDC,THRAP3,NR0B1,SPEN,HNRNPD,GTF2F1,POLR2K,POLR2
Telomere Extension by Telomerase	0.040738	-1.41	inhibition	HNRNPA1,HNRNPA2B1
Regulation of eIF4 and p70S6K Signaling	5.75E-08	0.242536	activation	EIF2B4,EIF4G3,PAIP2,EIF3E,EIF4G1,EIF2B2,EIF4E,EIF3M,EIF3G,EIF1,EIF3B,PAIP1,EIF3A,EIF2B5,EIF1AX,EIF3L,EIF3K

We then selected the gene set obtained for the comparison COPD/S (n=409 SDEG probes) to perform an unsupervised clustering analysis of each subject's mRBP expression profile for the three groups (NS, S, COPD), using Pearson's hierarchical clusters/complete linkage method. Results were represented in a heatmap generated with the T-MeV software (Figure 5).[22,23] As expected, the heatmap clearly showed how the expression of mRBPs appears predominantely diminished compared to NS and most of S subjects; interestingly, it also identified in the S group a subset of four subjects displaying an expression profile highly homologous to the one identified in COPD patients (Figure 5A). This similarity was confirmed by performing unsupervised cluster analysis for both genes and subjects using an Euclidean distance metrics (Figure 5B). This analysis confirmed that the RBP expression profile of this S subgroup indeed clustered with the samples from COPD patients.
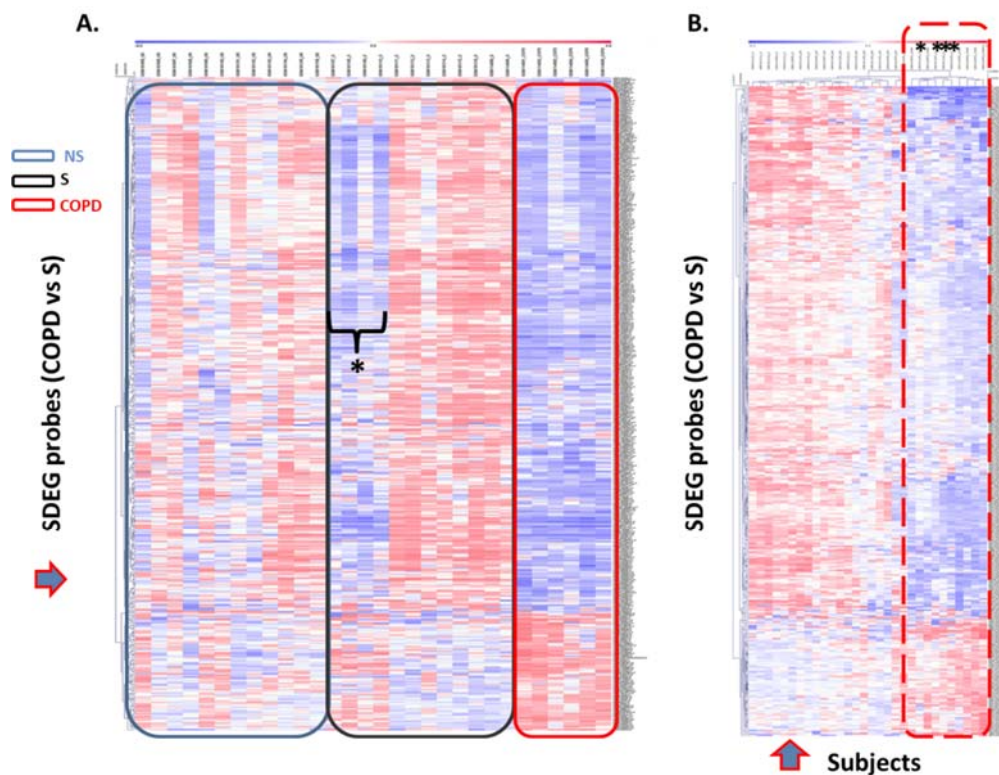
Figure 5. Unsupervised gene cluster analysis across the individual samples from GSE5058 dataset identifies selective global mRBPs repression in COPD patients shared by a subset of smoker controls. A. Unsupervised clustering analysis applied to (blue arrow) SDEG probe list identified in COPD/S (n=409). Heatmap shows SDEG probes' fluorescence intensity value (blue < 0, reduced: red > 0, increased). The data were normalized on the median and log$_2$-trasformed for relative fold changes. B. Unsupervised clustering analysis applied to both SDEG probe list and individual samples (blue arrows). Asterisks indicate the SDEG profiles of four smokers with NLF, clustering with those of COPD patients indicated by the dotted line.

As mRBPs exert their function by dinamically assembling in RNP complexes, the same gene dataset (n=409 SDEG identified in COPD/S) was searched for RBPs with correlated expression, which may indicate disease-driven, coordinated target regulation. Pearson correlation map showed at least five highly correlated mRBP clusters (r ≥ 0.70) (Figure 6A). In particular, cluster 3 included 40 genes (Table S1), among which IPA analysis identified enrichment of genes involved in RAN signalling, IL-15 expression, telomere extension (Figure 6B). Importantly, included in this cluster is *HNRNPD*, coding for the RBP AUF-1 we previously identified as repressed in small airway epithelium of COPD patients compared to smoker controls.[16] Figure 6C shows normalized fold changes across the three groups for eight representative mRBPs, including *HNRNPD*, contained in cluster 3.
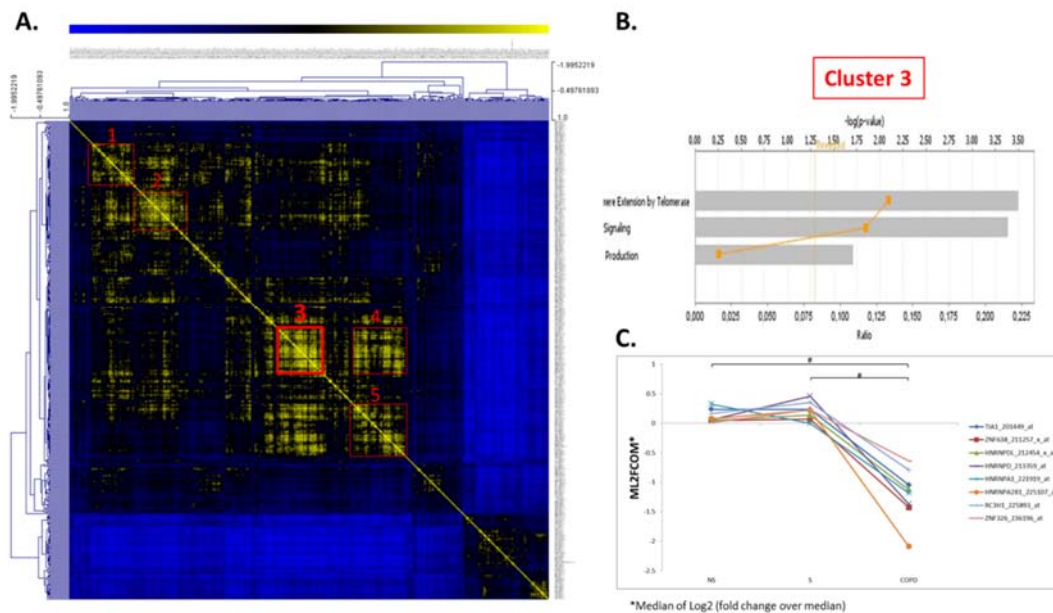
Figure 6. Correlation map identifies groups of coexpressed RBPs in COPD. A. Pearson Correlation maps of SDEG probe list (n=409 in COPD/S) across all samples, with R value set as (r ≥ 0.7) identifies at least five clusters of coexpressed mRBPs (red squares). **B.** GO analysis of cluster 3 (n=42 SDEG). **C.** Expression of selected mRBPs coexpressed in cluster 3. [#] p-value ≤ 0.05

Expression profile of mRBPs in bronchial epithelium of patients with severe asthma compared to control subjects.

Transcriptomic data in airway epithelium from bronchial brushing of patients with severe asthma (SA) and healthy controls (HCs) were searched for mRBP expression using the same methodology (Figure 1). We randomly extracted from the GSE63142 dataset[19] the same number of patients of the GSE5058 COPD dataset (n= 6 SA, n=12 HCs). Clinical characteristics of the full study groups are shown in Figure 7A. Only 30 probes (corresponding to 29 genes) were differentially expressed (DEG) in SA vs. HCs (listed in Table S2), but none of the DEG genes changed by at least 50% compared with HCs, thus none was cathegorized as SDEG (FDR ≤ 0.05; FC ≥ |1.5|) (Figure 7b and C).

Figure 7A table:

	HCs	SA	p-value
Age, mean ± SD	32±12	45±11	<0,0001
Sex, M/F	12/14	16 / 35	0,61
Race, W/AA/O	18/5/3	31 / 14 / 3	0,43
BMI, median (25-75th quartile)	24 (22-30)	32 (26-37)	0,006
FEV1% predicted (mean ± SEM)	94±9	56±20	<0,0001
Atopy, yes/no	16/10	39/8	0,08
IgE, median (25-75th quartile), IU/ml	59 (11-132)	104 (26-434)	0,042
Blood eos, median (25-75th quartile), %	2 (2-3)	3 (1-5)	0,14
FE_{NO}, median (25-75th quartile), ppb	20 (13-37)	37 (21-63)	0,043

AA=African American; BMI=Body Mass Index; eos=eosinophils; F=female; FE_{NO}=fraction of exhaled nitric oxide; HCs=healthy controls; M=male; O=other; SA=severe asthma; SD=standard deviation; W=caucasian. Significant p-value according to Bonferroni test p<0.05. (from Modena et al. Am J Respir Crit Care Med 2014, with permission)

A. GEO ID: GSE63142

B. padj < 0.05

SA/C	
Probes	Genes
30	29

C. n= SDEG padj< 0.05; FC ≥ |1.5|

SA/C	
Probes	Genes
0	0

Figure 7. mRBP expression in airway epithelium of patients with severe asthma and healthy controls. A. Clinical, spirometric and peripheral blood parameters of HC and SA cohorts providing airway epithelial cells by bronchial brushings for trascriptomic analysis reported in GEO GSE63142[19], utilized in this study for analysis of mRBP expression. B. List of DEG and C. SDEG obtained by data analysis (as described in Methods and Figure 1).

Discussion

In our initial study,[16] a search in a transcriptome database from bronchial brushings of COPD patients versus normal smokers and non-smokers controls confirmed the altered RBP pattern we identified by IHC in COPD patients vs. control subjects, consisiting of selected downregulation of the RBP AUF-1. In the present study, substantial changes in global mRBP gene expression were identified in the same gene array database. Changes were largely due to relative downregulation of mRBP expression, a feature that was found also in a subset of control smokers.

The list of RBPs we chose for this study[20] has been created by annotation of proteins as RBPs mainly by domain search, considering known RNA binding domains [among 800 domains extracted from the protein family (Pfam) database], or proteins known as validated partners of RNP complex. The human genome was searched for protein-coding genes bearing RBDs using specific statistical probability models and futher manual curation, which led to a final census of 1,542 RBPs. Of relevance, the biological functions of a third of these proteins is unknown or minimally defined at least in human disease, some of which we found as differently regulated in COPD patients - such as DEAD/DEAH box helicases.

The DEAD-box RNA helicase, DDX17 was among the top downregulated mRBP in COPD and its role is not yet defined in this disease. DDX17 is a nucleocytoplasmic shuttling factor that functions as RNA helicase and is involved in transcription, splicing and miRNA processing. Several studies indicate its involvement in antiviral responses: in a recent study, a significant decrease in DDX17 was found in transcriptional signature to vaccination to H1N1 influenza virus in human subjects, which correlated with antibody titer and IFN-γ production by T-cells.[79] Upregulated DDX17 expression has been reported to be associated with resistance to the tyrosine kinase inhibitor drug, gefitinib in non-small cell lung cancer (NSCLC) cells.[80] We also found as significantly downregulated the $3'-5'$ DEAH-box helicase DHX36, also known as RHAU (RNA helicase associated with AU-rich element).[46] In addition to regulating the transport and half-life of ARE-bearing mRNAs, it has a role in the mechanisms of preservation of genome integrity and in the maintenance of telomeres. In particular, DHX36 assists the activity of the TERT (Telomerase Reverse Transcriptase) enzyme.[56-61] As helicase, DHX36 unwinds parallel G-quadruplex structures formed in DNA and RNA. Interestingly, a recent study indicates that ablation of DHX36 results in increased SG formation and protein kinase R (PKR/EIF2AK2) phosphorylation, indicating that DHX36 is involved in resolution of cellular stress at the level of SG.[81] Moreover, in rat alveolar epithelial cells DHX36 downregulates epithelial sodium channel (ENaC) mRNA stability by binding with TIAR-1 to the transcript 3'-UTR.[82]

Pathway analysis may assist in directing further studies on a scale larger than single-gene analysis, in particular when exploring relatively uncharted pathways. In our study, two pathways significantly impacted by mRBP changes are well recognized as pathogenetic components of COPD: the signaling pathways coordinated by the kinase mTOR (Mechanistic Target Of Rapamycin) and the expression/activity of the telomerase enzyme.[83-87] Telomerase is an enzyme complex that reverse-transcribes an integral RNA template

in order to add short DNA repeats at the 3'-ends of telomeres. In our study, the mRBPs HnRNPA1 and HnRNPA2B were downregulated SDEG in COPD and this profile was predicted by IPA to inhibit telomere extension by telomerase. Furthermore, these two RBPs were coexpressed in cluster 3 (Figure 6), along with another known TERT-regulating factor, AUF-1,[88] which we validated as downregulated RBP at protein level by immunohistochemistry in COPD patients vs. controls.[16] Coexpression is often found among RBPs that participate to common posttranscriptional pathways; therefore, the novel mRBP clusters we identified (as cluster 3, Table S1) can be used as starting point to infer mRBP putative regulatory roles and identify coordinated expression of targets.[20]

Early studies established that hnRNP-A1, hnRNP-A2, and hnRNP-B1 proteins can interact with telomeres and are products of two different genes (*HNRNPA1* and *HNRNPA2B1*) but display similar structures (two RRMs and four RGG motifs in each).[89] The mRBP hnRNP A1 is the best characterized and found to be associated with human telomeres *in vivo*;[90] depletion of hnRNP A/B proteins in human embryonic kidney 293 cell extracts greatly reduced telomerase activity, which was rescued by addition of recombinant hnRNP A1.[90] Recently, a large study conducted in a group of 576 patient with moderate-to-severe COPD found a significant relationship of absolute telomere length, measured by PCR in DNA from peripheral blood samples, with several clinical parameters such as quality of life, number of exacerbations, and mortality.[91] These evidence suggest that shorter leukocyte telomere lengths could be evaluated as a biomarker for clinical outcomes in COPD. Depletion in COPD of this RBP crucial for telomere length, therefore, may have a role in supporting this clinical phenotype.

Quite strikingly, no significant differential mRBP expression was found in the database derived from bronchial brushings of severe asthma patients versus healthy controls. We rerun the search including the entire database (n = 56 SA and 27 HCs) with almost identical results (data not shown). This could be due to the different triggers and inflammatory features of severe asthma, in which activation, rather that expression, of mRBPs (see Introduction) may be critically involved in modulating epithelial responses, or can be due to a wider spectrum of disease endotypes present in the studied population. More studies will be necessary to validate this important negative finding.

There are several limitations also to the results obtained for the COPD database, the main one being the small number of subjects included. In support of our findings, this patient and control cohort did have statistical power to support the findings of the original study;[18] it is nevertheless necessary to evaluate another independent population with larger number of subjects. Moreover, it is possible that other RBPs with less defined domains have been left out of the compiled list.

Overall, the COPD-related mRBP profile found in our study suggests post-transcriptional control of epithelial gene expression as substantial, yet understudied process possibly contributing to key pathogenic mechanisms in COPD. In-depth characterization of proteins dynamically interacting with mRNAs is necessary to understand how PTGR participates to the disease process – and whether it can be targeted therapeutically.

Therefore, creating a map of RBP expression is a necessary first step to then analyze epithelial mRNA-bound proteome and potential changes in disease. Focused functional analysis and validating proteomic experiments will be needed to validate the coexpression of mRBPs and to address whether expression of mRBP targets, when known, in the COPD epithelial transcriptome database would show alterations consistent with – and dependent from - the documented changes of mRBPs expression.

References

1. Keene JD. RNA regulons: coordination of post-transcriptional events. *Nat Rev Genet.* 2007;8(7):533-543.

2. Gehring NH, Wahle E, Fischer U. Deciphering the mRNP Code: RNA-Bound Determinants of Post-Transcriptional Gene Regulation. *Trends Biochem Sci.* 2017;42(5):369-382.

3. Hitti E, Bakheet T, Al-Souhibani N, et al. Systematic Analysis of AU-Rich Element Expression in Cancer Reveals Common Functional Clusters Regulated by Key RNA-Binding Proteins. *Cancer Res.* 2016;76(14):4068-4080.

4. Pereira B, Billaud M, Almeida R. RNA-Binding Proteins in Cancer: Old Players and New Actors. *Trends Cancer.* 2017;3(7):506-528.

5. Wang Z, Bhattacharya A, Ivanov DN. Identification of Small-Molecule Inhibitors of the HuR/RNA Interaction Using a Fluorescence Polarization Screening Assay Followed by NMR Validation. *PLOS ONE* . 2015;10(9):e0138780.

6. Hong S. RNA Binding Protein as an Emerging Therapeutic Target for Cancer Prevention and Treatment. *J Cancer Prev.* 2017;22(4):203-210.

7. Patial S, Blackshear PJ. Tristetraprolin as a Therapeutic Target in Inflammatory Disease. *Trends Pharmacol Sci.* 2016;37(10):811-821.

8. Taylor GA, Carballo E, Lee DM, et al. A Pathogenetic Role for TNFα in the Syndrome of Cachexia, Arthritis, and Autoimmunity Resulting from Tristetraprolin (TTP) Deficiency. *Immunity.* 1996;4(5):445-454.

9. Lu JY, Sadri N, Schneider RJ. Endotoxic shock in AUF-1 knockout mice mediated by failure to degrade proinflammatory cytokine mRNAs. *Genes Dev.* 2006;20(22):3174-3184.

10. Durham AL, Adcock IM. The relationship between COPD and lung cancer. *Lung Cancer.* 2015;90(2):121-127.

11. Khabar KSA. Post-transcriptional control during chronic inflammation and cancer: a focus on AU-rich elements. *Cell Mol Life Sci.* 2010;67(17):2937-2955.

12. Ishmael FT, Fang X, Galdiero MR, et al. Role of the RNA-Binding Protein Tristetraprolin in Glucocorticoid-Mediated Gene Regulation. *J Immunol.* 2008;180(12):8342-8353.

13. Ishmael FT, Fang X, Houser KR, et al. The human glucocorticoid receptor as an RNA-binding protein: global analysis of glucocorticoid receptor-associated transcripts and identification of a target RNA motif. *J Immunol.* 2011;186(2):1189-1198.

14. Fan J, Ishmael FT, Fang X, et al. Chemokine transcripts as targets of the RNA-binding protein HuR in human airway epithelium. *J Immunol.* 2011;186(4):2482-2494.

15. Stellato C. Glucocorticoid actions on airway epithelial responses in immunity: Functional outcomes and molecular targets. *J Allergy Clin Immunol.* 2007;120(6):1247-1263.

16. Ricciardi L, Col JD, Casolari P, et al. Differential expression of RNA-binding proteins in bronchial epithelium of stable COPD patients. *Int J Chron Obstruct Pulmon Dis.* 2018;13:3173-3190.

17. Kechavarzi B, Janga SC. Dissecting the expression landscape of RNA-binding proteins in human cancers. *Genome Biol.* 2014;15(1):R14.

18. Carolan BJ, Heguy A, Harvey BG, Leopold PL, Ferris B, Crystal RG. Up-regulation of expression of the ubiquitin carboxyl-terminal hydrolase L1 gene in human airway epithelium of cigarette smokers. *Cancer Res.* 2006;66(22):10729-10740.

19. Modena BD, Tedrow JR, Milosevic J, et al. Gene expression in relation to exhaled nitric oxide identifies novel asthma phenotypes with unique biomolecular pathways. *Am J Respir Crit Care Med.* 2014;190(12):1363-1372.

20. Gerstberger S, Hafner M, Tuschl T. A census of human RNA-binding proteins. *Nat Rev Genet.* 2014;15:829.

21. Oliveros JC. VENNY. An interactive tool for comparing lists with Venn Diagrams. 2007. Available at: http://bioinfogp.cnb.csic.es/tools/venny/index.html.

22. Howe E, Holton K, Nair S, Schlauch D, Sinha R, Quackenbush J. MeV: MultiExperiment Viewer. In: Ochs MF, Casagrande JT, Davuluri RV, eds. *Biomedical Informatics for Cancer Res.* 2010:267-277.

23. Saeed AI, Sharov V, White J, et al. TM4: A Free, Open-Source System for Microarray Data Management and Analysis. *BioTechniques.* 2003;34(2):374-378.

24. Walter W, Sanchez-Cabo F, Ricote M. GOplot: an R package for visually combining expression data with functional analysis. *Bioinformatics.* 2015;31(17):2912-2914.

25. Stelzer G, Rosen N, Plaschkes I, et al. The GeneCards Suite: From Gene Data Mining to Disease Genome Sequence Analyses. *Curr Protoc Bioinformatics.* 2016;54(1):1.30.31-31.30.33.

26. Yamaguchi A, Takanashi K. FUS interacts with nuclear matrix-associated protein SAFB1 as well as Matrin3 to regulate splicing and ligand-mediated transcription. *Sci Rep.* 2016;6(1):35195.

27. Baechtold H, Kuroda M, Sok J, Ron D, Lopez BS, Akhmedov AT. Human 75-kDa DNA-pairing Protein Is Identical to the Pro-oncoprotein TLS/FUS and Is Able to Promote D-loop Formation. 1999;274(48):34337-34342.

28. THRAP3 Gene - GeneCards | TR150 Protein | TR150 Antibody. Available at: https://www.genecards.org/cgi-bin/carddisp.pl?gene=THRAP3&keywords=thrap3.

29. Lande-Diner L, Boyault C, Kim JY, Weitz CJ. A positive feedback loop links circadian clock factor CLOCK-BMAL1 to the basic transcriptional machinery. *Proc Natl Acad Sci U S A.* 2013;110(40):16021-16026.

30. DDX17 Gene - GeneCards | DDX17 Protein | DDX17 Antibody. Available at: https://www.genecards.org/cgi-bin/carddisp.pl?gene=DDX17&keywords=ddx17.

31. Hönig A, Auboeuf D, Parker MM, O'Malley BW, Berget SM. Regulation of Alternative Splicing by the ATP-Dependent DEAD-Box RNA Helicase p72. *Mol Cell Biol.* 2002;22(16):5698-5707.

32. Dardenne E, Pierredon S, Driouch K, et al. Splicing switch of an epigenetic regulator by RNA helicases promotes tumor-cell invasiveness. *Nat Struct Mol Biol.* 2012;19(11):1139-1146.

33. Dardenne E, Polay Espinoza M, Fattet L, et al. RNA Helicases DDX5 and DDX17 Dynamically Orchestrate Transcription, miRNA, and Splicing Programs in Cell Differentiation. *Cell Rep.* 2014;7(6):1900-1913.

34. Germann S, Gratadou L, Zonta E, et al. Dual role of the ddx5/ddx17 RNA helicases in the control of the pro-migratory NFAT5 transcription factor. *Oncogene.* 2012;31(42):4536-4549.

35. Samaan S, Tranchevent L-C, Dardenne E, et al. The Ddx5 and Ddx17 RNA helicases are cornerstones in the complex regulatory array of steroid hormone-signaling pathways. *Nucleic Acids Res.* 2013;42(4):2197-2207.

36. Shin S, Janknecht R. Concerted activation of the Mdm2 promoter by p72 RNA helicase and the coactivators p300 and P/CAF. *J Cell Biochem.* 2007;101(5):1252-1265.

37. Mooney SM, Grande JP, Salisbury JL, Janknecht R. Sumoylation of p68 and p72 RNA Helicases Affects Protein Stability and Transactivation Potential. *Biochemistry.* 2010;49(1):1-10.

38. Mooney SM, Goel A, D'Assoro AB, Salisbury JL, Janknecht R. Pleiotropic Effects of p300-mediated Acetylation on p68 and p72 RNA Helicase. *J Biol Chem.* 2010;285(40):30443-30452.

39. Dutertre M, Gratadou L, Dardenne E, et al. Estrogen Regulation and Physiopathologic Significance of Alternative Promoters in Breast Cancer. *Cancer Res.* 2010;70(9):3760-3770.

40. Chen G, Guo X, Lv F, Xu Y, Gao G. p72 DEAD box RNA helicase is required for optimal function of the zinc-finger antiviral protein. *Proc Natl Acad Sci U S A.* 2008;105(11):4352-4357.

41. SCAF11 Gene - GeneCards |SCAF11 Protein | SCAF11 Antibody. Available at: https://www.genecards.org/cgi-bin/carddisp.pl?gene=SCAF11#publications.

42. STRAP Gene - GeneCards | STRAP Protein | STRAP Antibody. Available at: https://www.genecards.org/cgi-bin/carddisp.pl?gene=STRAP&keywords=strap.

43. Iwasaki T, Chin WW, Ko L. Identification and Characterization of RRM-containing Coactivator Activator (CoAA) as TRBP-interacting Protein, and Its Splice Variant as a Coactivator Modulator (CoAM). *J Biol Chem.* 2001;276(36):33375-33383.

44. Morchikh M, Cribier A, Raffel R, et al. HEXIM1 and NEAT1 Long Non-coding RNA Form a Multi-subunit Complex that Regulates DNA-Mediated Innate Immune Response. *Mol Cell.* 2017;67(3):387-399.e385.

45. BCLAF1 Gene - GeneCards | BCLF1 Protein | BCLF1 Antibody. Available at: https://www.genecards.org/cgi-bin/carddisp.pl?gene=BCLAF1&keywords=BCLAF1.

46. ILF3 Gene - GeneCards | ILF3 Protein | ILF3 Antibody [Internet]. Available at: https://www.genecards.org/cgi-bin/carddisp.pl?gene=ILF3&keywords=ilf3.

47. Tran H, Schilling M, Wirbelauer C, Hess D, Nagamine Y. Facilitation of mRNA Deadenylation and Decay by the Exosome-Bound, DExH Protein RHAU. *Mol Cell.* 2004;13(1):101-111.

48. Harashima A, Guettouche T, Barber GN. Phosphorylation of the NFAR proteins by the dsRNA-dependent protein kinase PKR constitutes a novel mechanism of translational regulation and cellular defense. *Genes Dev.* 2010;24(23):2640-2653.

49. Li X, Liu C-X, Xue W, et al. Coordinated circRNA Biogenesis and Function with NF90/NF110 in Viral Infection. *Mol Cell.* 2017;67(2):214-227.e217.

50. SFSWAP Gene - GeneCards | SFSWA Protein | SFSWA Antibody. Available at: https://www.genecards.org/cgi-bin/carddisp.pl?gene=SFSWAP&keywords=sfswap.

51. RBM25 Gene - GeneCards | RBM25 Protein | RBM25 Antibody. Available at: https://www.genecards.org/cgi-bin/carddisp.pl?gene=RBM25&keywords=rbm25.

52. DHX36 Gene - GeneCards | DHX36 Protein | DHX36 Antibody. Available at: https://www.genecards.org/cgi-bin/carddisp.pl?gene=DHX36&keywords=dhx36.

53. Vaughn JP, Creacy SD, Routh ED, et al. The DEXH Protein Product of the DHX36 Gene Is the Major Source of Tetramolecular Quadruplex G4-DNA Resolving Activity in HeLa Cell Lysates. *J Biol Chem.* 2005;280(46):38117-38120.

54. Chalupníková K, Lattmann S, Selak N, Iwamoto F, Fujiki Y, Nagamine Y. Recruitment of the RNA Helicase RHAU to Stress Granules via a Unique RNA-binding Domain. *J Biol Chem.* 2008;283(50):35186-35198.

55. Lattmann S, Giri B, Vaughn JP, Akman SA, Nagamine Y. Role of the amino terminal RHAU-specific motif in the recognition and resolution of guanine quadruplex-RNA by the DEAH-box RNA helicase RHAU. *Nucleic Acids Res.* 2010;38(18):6219-6233.

56. Giri B, Smaldino PJ, Thys RG, et al. G4 Resolvase 1 tightly binds and unwinds unimolecular G4-DNA. *Nucleic Acids Res.* 2011;39(16):7161-7178.

57. Lattmann S, Stadler MB, Vaughn JP, Akman SA, Nagamine Y. The DEAH-box RNA helicase RHAU binds an intramolecular RNA G-quadruplex in TERC and associates with telomerase holoenzyme. *Nucleic Acids Res.* 2011;39(21):9390-9404.

58. Booy EP, Meier M, Okun N, et al. The RNA helicase RHAU (DHX36) unwinds a G4-quadruplex in human telomerase RNA and promotes the formation of the P1 helix template boundary. *Nucleic Acids Res.* 2012;40(9):4110-4124.

59. Booy EP, McRae EKS, McKenna SA. Biochemical Characterization of G4 Quadruplex Telomerase RNA Unwinding by the RNA Helicase RHAU. *Methods Mol Biol.* 2015;1259:125-135.

60. Sexton AN, Collins K. The 5′ Guanosine Tracts of Human Telomerase RNA Are Recognized by the G-Quadruplex Binding Domain of the RNA Helicase DHX36 and Function To Increase RNA Accumulation. *Mol Cell Biol.* 2011;31(4):736-743.

61. Meier M, Patel TR, Booy EP, et al. Binding of G-quadruplexes to the N-terminal Recognition Domain of the RNA Helicase Associated with AU-rich Element (RHAU). *J Biol Chem.* 2013;288(49):35014-35027.

62. Booy EP, Howard R, Marushchak O, et al. The RNA helicase RHAU (DHX36) suppresses expression of the transcription factor PITX1. *Nucleic Acids Res.* 2013;42(5):3346-3361.

63. Nie J, Jiang M, Zhang X, et al. Post-transcriptional Regulation of Nkx2-5 by RHAU in Heart Development. *Cell Rep.* 2015;13(4):723-732.

64. Huang W, Smaldino PJ, Zhang Q, et al. Yin Yang 1 contains G-quadruplex structures in its promoter and 5′-UTR and its expression is modulated by G4 resolvase 1. *Nucleic Acids Res.* 2011;40(3):1033-1049.

65. Newman M, Sfaxi R, Saha A, Monchaud D, Teulade-Fichou M-P, Vagner S. The G-Quadruplex-Specific RNA Helicase DHX36 Regulates p53 Pre-mRNA 3′-End Processing Following UV-Induced DNA Damage. *J Mol Biol.* 2017;429(21):3121-3131.

66. He Y, Smith R. Nuclear functions of heterogeneous nuclear ribonucleoproteins A/B. *Cell Mol Life Sci.* 2009;66(7):1239-1256.

67. Munro TP, Magee RJ, Kidd GJ, et al. Mutational Analysis of a Heterogeneous Nuclear Ribonucleoprotein A2 Response Element for RNA Trafficking. *J Biol Chem.* 1999;274(48):34389-34395.

68. HNRNPA2B1 Gene - GeneCards | HNRNPA2B1 Protein | HNRNPA2B1 Antibody. Available at: https://www.genecards.org/cgi-bin/carddisp.pl?gene=HNRNPA2B1.

69. Rishi AK, Zhang L, Boyanapalli M, et al. Identification and Characterization of a Cell Cycle and Apoptosis Regulatory Protein-1 as a Novel Mediator of Apoptosis Signaling by Retinoid CD437. *J Biol Chem.* 2003;278(35):33422-33435.

70. Seo W-Y, Jeong BC, Yu EJ, et al. CCAR1 promotes chromatin loading of androgen receptor (AR) transcription complex by stabilizing the association between AR and GATA2. *Nucleic Acids Res.* 2013;41(18):8526-8536.

71. CCAR1 Gene - GeneCards | CCAR1 Protein | CCAR1 Antibody. Available at: https://www.genecards.org/cgi-bin/carddisp.pl?gene=CCAR1&keywords=ccar1.

72. NR0B1 Gene - GeneCards | NR0B1 Protein | NR0B1 Antibody [Internet]. Available at: https://www.genecards.org/cgi-bin/carddisp.pl?gene=NR0B1&keywords=NR0B1.

73. Sun Y, Ding L, Zhang H, et al. Potentiation of Smad-mediated transcriptional activation by the RNA-binding protein RBPMS. *Nucleic Acids Res.* 2006;34(21):6314-6326.

74. Teplova M, Farazi TA, Tuschl T, Patel DJ. Structural basis underlying CAC RNA recognition by the RRM domain of dimeric RNA-binding protein RBPMS. *Q Rev Biophys.* 2016;49:e1.

75. HDLBP Gene - GeneCards | VIGLN Protein | VIGLN Antibody. Available at: https://www.genecards.org/cgi-bin/carddisp.pl?gene=HDLBP&keywords=HDLBP.

76. Antonicka H, Shoubridge Eric A. Mitochondrial RNA Granules Are Centers for Posttranscriptional RNA Processing and Ribosome Biogenesis. *Cell Rep.* 2015;10(6):920-932.

77. Lessel D, Schob C, Küry S, et al. De Novo Missense Mutations in DHX30 Impair Global Translation and Cause a Neurodevelopmental Disorder. *Am J Hum Genet..* 2017;101(5):716-724.

78. DHX30 Gene - GeneCards | DHX30 Protein | DHX30 Antibody. Available at: https://www.genecards.org/cgi-bin/carddisp.pl?gene=DHX30&keywords=DHx30.

79. Skibinski DAG, Jones LA, Zhu YO, et al. Induction of Human T-cell and Cytokine Responses Following Vaccination with a Novel Influenza Vaccine. *Sci Rep.* 2018;8(1):18007.

80. Li K, Mo C, Gong D, et al. DDX17 nucleocytoplasmic shuttling promotes acquired gefitinib resistance in non-small cell lung cancer cells via activation of β-catenin. *Cancer Lett.* 2017;400:194-202.

81. Sauer M, Juranek SA, Marks J, et al. DHX36 prevents the accumulation of translationally inactive mRNAs with G4-structures in untranslated regions. *Nat Commun.* 2019;10(1):2421.

82. Migneault F, Gagnon F, Pascariu M, et al. Post-Transcriptional Modulation of aENaC mRNA in Alveolar Epithelial Cells: Involvement of its 3' Untranslated Region. *Cell Physiol Biochem.* 2019;52(5):984-1002.

83. Ito K, Barnes PJ. COPD as a Disease of Accelerated Lung Aging. *Chest.* 2009;135(1):173-180.

84. Barnes PJ. Senescence in COPD and Its Comorbidities. *Annu Rev Physiol..* 2017;79(1):517-539.

85. Houssaini A, Breau M, Kebe K, et al. mTOR pathway activation drives lung cell senescence and emphysema. *JCI Insight.* 2018;3(3).

86. Bozkus F, Guler S, Sımsek S. Serum Telomerase Levels and COPD Exacerbations. *Respir Care.* 2016;61(3):359.

87. Mercado N, Ito K, Barnes PJ. Accelerated ageing of the lung in COPD: new concepts. *Thorax.* 2015;70(5):482.

88. Pont Adam R, Sadri N, Hsiao Susan J, Smith S, Schneider Robert J. mRNA Decay Factor AUF-1 Maintains Normal Aging, Telomere Maintenance, and Suppression of Senescence by Activation of Telomerase Transcription. *Mol Cell.* 2012;47(1):5-15.

89. Shishkin SS, Kovalev IL, Pashintseva VN, Kovaleva AM, Lisitskaya K. Heterogeneous Nuclear Ribonucleoproteins Involved in the Functioning of Telomeres in Malignant Cells. *Int J Mol Sci.* 2019;20(3).

90. Zhang Q-S, Manche L, Xu R-M, Krainer AR. hnRNP A1 associates with telomere ends and stimulates telomerase activity. *RNA.* 2006;12(6):1116-1128.

91. Jin M, Lee EC, Ra SW, et al. Relationship of Absolute Telomere Length With Quality of Life, Exacerbations, and Mortality in COPD. *CHEST*. 2018;154(2):266-273.

Supplementary material

Table S1. mRBPs list of Cluster 3 in COPD patients (COPD) versus no smoker (NS) and Smoker (S) comparisons in the GSE5058 database. FC = Fold change; FDR = False Discovery Rate. The red text denotes an FDR ≤ 0.05. Bold characters denote an FC value ≤ -1.5 (green) and FC value ≥ 1.5 (red), respectively.

Gene Symbol	Probe ID	FC S vs NS	FC COPD vs NS	FC COPD vs S	FDR S vs NS	FDR COPD vs NS	FDRC COPD vs S
SCAF11	1570507_at	-1.09	**-3.15**	**-2.88**	0.467129	0.014375	0.0275015
SF3B1	201071_x_at	1.04	**-1.84**	**-1.91**	0.499574	0.0046634	0.0121703
TIA1	201449_at	1	**-2.41**	**-2.42**	0.491093	0.0149244	0.031216
RANBP2	201712_s_at	1.11	**-1.93**	**-2.15**	0.36093	0.0137568	0.0114609
RANBP2	201713_s_at	1.17	**-1.6**	**-1.88**	0.319399	0.0450322	0.0230986
UPF2	203519_s_at	-1.05	**-2.52**	**-2.4**	0.404338	0.0053674	0.0188686
WBP4	203599_s_at	1.31	-1.18	**-1.54**	0.265744	0.0628788	0.0232771
SRSF10	204299_at	-1.21	**-2.49**	**-2.07**	0.376659	0.0242595	0.0468013
DZIP1	204557_s_at	-1.05	**-2.66**	**-2.54**	0.354549	0.0156042	0.0190971
CLK4	210346_s_at	-1.1	**-2.62**	**-2.37**	0.399698	0.0021015	0.0199102
ZNF638	211257_x_at	1.02	**-2.78**	**-2.82**	0.395084	0.0021378	0.0150037
PNN	212036_s_at	-1.17	**-4.93**	**-4.21**	0.399274	0.0045727	0.0254254
HNRNPDL	212454_x_at	1.07	**-2.19**	**-2.33**	0.482769	0.0113383	0.0297528
TNPO1	212635_at	1.14	**-1.77**	**-2.01**	0.486699	0.0304605	0.0202625
SREK1	212721_at	1.08	**-2.59**	**-2.81**	0.487995	0.0150868	0.0319828
FUBP1	212847_at	1.06	**-1.85**	**-1.96**	0.402346	0.0243383	0.0281825
YTHDC2	213077_at	-1.04	**-1.81**	**-1.74**	0.467076	0.0451012	0.0332428
HNRNPD	213359_at	1.32	**-2.69**	**-3.56**	0.491093	0.0408363	0.0488046
PPWD1	213483_at	1.05	**-1.94**	**-2.04**	0.41731	0.0150868	0.0224045
FUBP1	214093_s_at	1.3	**-3.21**	**-4.17**	0.407856	0.008399	0.0141766
SRSF7	214141_x_at	1.12	**-2.07**	**-2.32**	0.482769	0.0003094	0.0133373
CLK1	214683_s_at	-1.07	**-3.78**	**-3.55**	0.342525	0.0040844	0.025705
SLTM	217828_at	1.06	**-1.64**	**-1.75**	0.492836	0.0274489	0.0397468
CAPRIN2	218456_at	-1.24	**-2.21**	**-1.78**	0.304049	0.0021378	0.0353238
LUC7L3	220044_x_at	1.01	**-2.36**	**-2.38**	0.47383	0.0164155	0.0181931
SFPQ	221768_at	1.01	**-5.11**	**-5.18**	0.39481	0.0067192	0.0275965
ANGEL2	221826_at	-1.01	**-1.7**	**-1.68**	0.496762	0.0027824	0.0221826
HNRNPA1	221919_at	-1.26	**-2.83**	**-2.26**	0.234404	0.0053674	0.0388807
DHX36	223140_s_at	1	**-1.72**	**-1.72**	0.479051	0.020492	0.0180915
ZRANB2	223716_s_at	1.22	**-2.29**	**-2.78**	0.346255	0.0360208	0.0188656
TNRC6A	224705_s_at	-1.02	**-3.19**	**-3.14**	0.381743	0.0036641	0.025705
NUFIP2	224938_at	1.01	**-1.89**	**-1.91**	0.423526	0.0300288	0.0162441
HNRNPA2B1	225107_at	1.11	**-4.43**	**-4.91**	0.487983	0.0114244	0.0251596
RC3H1	225893_at	1.14	**-1.94**	**-2.21**	0.491755	0.0132038	0.0308894
HELZ	225910_at	-1.22	**-1.94**	**-1.59**	0.44806	0.0113383	0.0311165
MSI2	226134_s_at	1.04	**-1.66**	**-1.72**	0.492836	0.0209936	0.0150271
SRSF1	226419_s_at	1.05	**-2.16**	**-2.26**	0.411642	0.0090966	0.0428733
PPIL4	226472_at	-1.11	**-2.25**	**-2.03**	0.496762	0.0113383	0.0115967
TPR	228709_at	-1.03	**-2.02**	**-1.95**	0.484297	0.0090674	0.0223358
RBM26	229433_at	1.23	**-1.84**	**-2.26**	0.403047	0.0164155	0.0278978
SREK1	235611_at	1.07	**-1.5**	**-1.61**	0.346146	0.1361973	0.0467
ZNF326	236196_at	1.17	**-1.57**	**-1.83**	0.371045	0.0396157	0.0332428
DZIP1L	239785_at	-1.1	**-2.12**	**-1.92**	0.367387	0.0140181	0.0453026

Table S2. List of mRBPs DEG genes in severe asthma (SA) versus healthy controls (HCs) (GSE63142 database). FC = Fold change; FDR = False Discovery Rate. The red text denotes an FDR ≤ 0.05.

Gene Symbol	Probe ID	FC	FDR
ADAD1	A_23_P41514	-1.02	0.04198
AFF4	A_24_P394408	-1.04	0.040722
CXorf23	A_24_P841677	-1.04	0.043031
DHX35	A_23_P5945	1.12	0.040722
ELAVL2	A_24_P933037	-1.05	0.043031
ELAVL3	A_23_P218492	-1.05	0.015611
FASTKD1	A_23_P307624	1.02	0.043031
FMR1	A_24_P93967	-1.03	0.043031
FXR1	A_32_P16954	1.03	0.040722
GTPBP1	A_23_P103120	-1.03	0.044604
HNRNPCL1	A_24_P136161	-1.07	0.04198
IREB2	A_24_P188005	-1.03	0.040722
LUZP4	A_23_P96611	-1.03	0.048486
PCF11	A_23_P116578	-1.03	0.040722
PLRG1	A_24_P268856	1.03	0.043031
RAVER2	A_23_P74215	1.04	0.043031
RBM46	A_23_P404575	1.06	0.04387
RBM47	A_24_P921660	-1.04	0.043031
RBMX	A_32_P56392	-1.06	0.040722
RBPMS2	A_23_P100056	1.04	0.040722
RPUSD4	A_24_P318073	1.02	0.040722
SF1	A_24_P925158	-1.06	0.040722
SMG6	A_23_P4014	-1.04	0.040722
SRSF12	A_32_P456318	1.03	0.040722
TNPO2	A_24_P44891	-1.04	0.043031

UPF3A	A_32_P226567	-1.05	0.040722
WIBG	A_24_P917612	1.02	0.043031
YBX1	A_23_P34767	1.03	0.018585
YBX1	A_32_P218989	1.03	0.040722
ZNF638	A_32_P15211	-1.05	0.048486

c. **Study# 3:**

Posttranscriptional regulation of airway epithelial responses:

identification of airway epithelial transcripts as targets of RNA-binding protein AUF-1

Luca Ricciardi[1], Giorgio Giurato[1], Domenico Memoli[1], Assunta Sellitto[1], Jessica Dal Col[1], Maria Assunta Crescenzi[1], Ilaria Salvato[1], Alessandro Weisz[1], Gaetano Caramori[2], Cristiana Stellato[1]

[1]Department of Medicine, Surgery and Dentistry *'Scuola Medica Salernitana'*, University of Salerno, Baronissi (SA), Italy

[2]Department of Biomedical Sciences, Dentistry and Morphological and Functional Imaging (BIOMORF), Respiratory Medicine Unit, University of Messina, Messina, Italy

Study Ongoing

Abstract

Background and Aim. RNA-binding proteins (RBP) coordinate PTGR by binding to conserved sequences of targeted mRNAs. The majority of genes expressed in immune and structural cells in chronic lung inflammation are susceptible to RBP-mediated regulation, yet the role of RBPs in this setting remains elusive. We previously documented significant loss of the RBP AUF-1 in airway epithelium of patients with stable COPD compared to smokers with normal lung function, reproducing AUF-1 downregulation in human airway epithelial cell line upon challenge with cigarette smoke extract. On these basis, the present study aims at identifying AUF-1-targeted genes to better understand the contribution of this RBP to epithelial-driven responses in chronic inflammatory airway diseases, such as COPD.

Methods. Cytoplasmic lysates of human bronchial epithelial cell line BEAS-2B were extracted using procedures that preserve mRNA-protein complexes. RNA immunoprecipitation (RIP) using specific anti-AUF-1 antibody (Ab) and isotype-matched IgG control Ab was followed by high-throughput sequencing of bound RNA (RIP-Seq) to identify AUF-1-bound target RNAs. RNA-Seq statistical and data anlysis were performed using DESeq2. RNAs with Enrichment Factor (EF) $\geq$ 1.5 and False Discovery Rate (FDR) $\leq$ 0.05 were used in subsequent analyses. Gene Ontology (GO) was performed with Ingenuity Pathway Analysis (IPA) software. Sequence motifs were determined by comparison with <u>S</u>equence & <u>S</u>tructure <u>M</u>otif enrichment <u>A</u>nalysis for <u>R</u>anked RNA da<u>T</u>a generated from *In Vivo* binding experiments (SMARTIV). Protein-RNA binding sites were predicted with catRAPID upon submission of amino acid sequence of p45[AUF-1].

Results. RIP-Seq analysis identified n = 494 AUF-1-bound mRNAs in cytoplasmic lysates from unstimulated BEAS-2B cells. A shared GC motif was the most enriched binding site identified computationally in the 3'UTR among the experimentally defined AUF-1 targets. Initial *in silico* validation revealed significant agreement of the experimental dataset with computationally predicted AUF-1 targets also expressed in BEAS-2B prior to IP. A search in the GSE5058 transcriptomic database of primary airway epithelial cells obtained from bronchial brushings of COPD patients and relative controls (Cancer Res. 2006;66:10729) indicated significant changes in expression levels (FC value $\geq$ │1.5│, FDR $\leq$ 0.05) of experimentally derived AUF-1 targets versus non smokers and smoker controls. Based on these evidence, ongoing experiments are set to validate a list of AUF-1 targets from our RIP-Seq dataset that are deregulated in primary cells of COPD patients, by examining their expression profile and mRNA stability upon inflammatory challenge (cytomix, cigarette smoke extract) and changes upon AUF-1 silencing.

Conclusions. AUF-1 may regulate the coordinate expression of subsets of epithelial genes that are functionally related by their participation in pathogenis pathways of COPD. Identification of these genes and of AUF-1 role in their deregulated expression will expose the role of this RBP as regulatory determinant in epithelial responses, and pave the way for evaluation of its value as therapeutic target or as disease biomarker.

Introduction

RNA-binding proteins (RBPs) critically regulate the processing, transport and cytoplasmic fate of mRNA by forming ribonucleoprotein complex (mRNPs) in posttranscriptional gene regulation (PTGR) processes. They regulate transcript stability and translation by recognizing of specific *cis*-elements present on the 3'-Untranslated Region (3'-UTR) on mRNAs targets, determining the rate of protein output in fundamental processes like cell cycle, proliferation and stress responses.[1,2]

AUF-1 belongs to a family of ubiquitously expressed proteins that mediate the stabilization or decay of mRNA targets *(see also Introduction, paragraph 3b)*. Four isoforms of AUF-1 are described and originate from the alternative splicing of a single mRNA transcript, which determines their different molecular weight: p37[AUF-1], p40[AUF-1], p42[AUF-1], p45[AUF-1].[3] Different expression levels and nucleocytoplasmic distribution were correlated with their different structural features. Mouse models lacking AUF-1 allowed to identify the role of this RBP in numerous human diseases, such as breast cancer and melanoma.[4] Importantly, mice lacking AUF-1 have a strong inflammatory phenotype. They spontaneously develop an age-dependent, chronic pruritic inflammatory skin dermatitis highly resembling atopic dermatitis, characterized by enhanced dermal infiltration of inflammatory cells, reduced wound healing and elevated serum IgE levels. In addition, *AUF-1^{-/-}* T cells and macrophages have increased expression of inflammatory cytokines, such as IL-2, TNF-α, and IL-1β.[5] Recent evidence from our group indicates a significantly diminished expression of AUF-1 in the airway epithelium of patients with stable COPD compared to control smoking subjects, a finding also reproduced *in vitro* by challenge of the airway epithelial cell line BEAS-2B with cigarette smoke extract and cytomix.[6] To date, the identity of AUF-1 mRNA targets in airway epithelium and the relevance of AUF-1-dependent epithelial gene expression still remains poorly characterized, along with AUF-1 role in the epithelial response to triggers and mediators involved in COPD pathogenesis.

On this basis we used unstimulated BEAS-2B, in which AUF-1 levels were preserved, to identify by RIP-seq, for the first time, AUF-1-bound mRNA in human airway epithelium and to estimate what type of transcripts would be impacted by its loss. Future experiments will be needed to verify – in AUF-1 KO and control cells as well as in experiments of phenotype rescue - the modulation of the identified targets following either CSE or Cytomix stimulation, as well as characterize AUF-1 regulation, using assays of mRNA stability and translational control.

The present study has identified for the first time an AUF-1-bound mRNA pool in the bronchial epithelial BEAS-2B cell line using RNA immunoprecipitation and high-throughput sequencing (RIP-Seq); ongoing experiments are currently validating and characterizing the role of AUF-1 regulation for the expression of a selected number of AUF-1-bound mRNAs.

Methods

RNA immunoprecipitation and sequencing (RIP-Seq) assay (Figure 1). RNA immunoprecipitation (RIP) is an antibody (Ab)-based technique developed to study the interaction between an RBP and its endogenous targets.[7] After generating cytosolic cell extracts under conditions that preserved the integrity of RNP complexes, the RBP of interest is immunoprecipitated with an RBP-specific Ab (and an isotype-matched, non specific Ab as control) together with its associated RNA. After RNA purification, bound transcripts (mRNAs and non-coding RNAs) are identified trough sequencing.
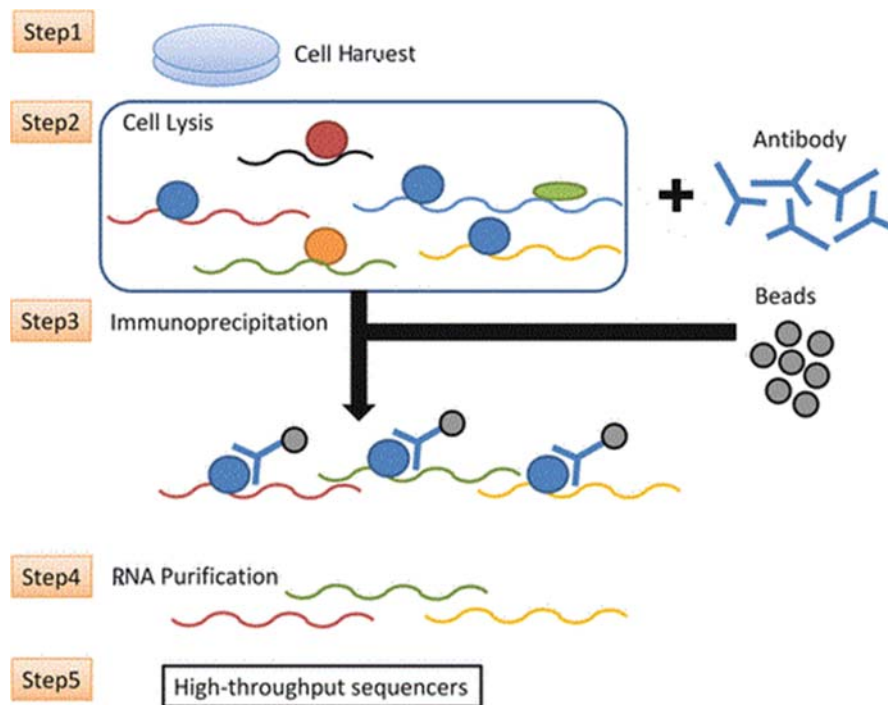
Figure 1. Schematic of RIP-Seq protocol. Cells are harvested (Step 1) and then lysed with polysome lysis buffer. The cytosolic extract is incubated with specific anti RBP/isotype-matched control for specific immunoprecipitation (IP) of the protein and its associated targets (Step 2). Bound RNA is then purified with magnetic beads (Step 4) and analyzed by high throughput sequencing (Step 5).[8]

Cell culture. The human BEAS-2B cell line (*ATCC*) was cultured in DMEM/Ham's F12 (*EuroClone*) supplemented with 5% heat-inactivated FBS (*EuroClone*), 2 mM L-glutamine (*Lonza*), penicillin (100 U/ml) - streptomycin (100 mg/ml) (*Lonza*) and 0.2% fungizone (*EuroClone*).[9] BEAS-2B bronchial epithelial cells are non-cancerous and immortalized through transformation with SV40 adenovirus. Cells were plated in T-175 flasks and harvested at 80% confluency. At least 10^8 cells were used for each condition for the IP experiments.

Cell viability. The cells were harvested using trypsin/EDTA (*Lonza*), counted and their viability was verified with the Trypan Blue exclusion test (*EuroClone*). Cell viability was $\geq$ 90% at harvest in all conditions.

Cytosolic protein extraction and RIP. Cytosolic fractions were collected after lysing BEAS-2B cells with polysome lysis buffer, as described.[10] The buffer components were: 10 mM HEPES pH 7.0, 100 mM KCl, 5 mM $MgCl_2$, 0.5% NP40, 1 mM DTT, 100 U/ml RNase out, 400 µM Vanadyl-Ribonucleoside Complex, 1X Protease Inhibitors. An aliquot of cytosolic extract (10% of total) was taken as Input. For IP with anti-AUF-1 Ab (HPA004911, *Atlas Antibodies*), 2 mg of cytosolic extract were incubated at 4 °C overnight with 4 µg of antibody. For control IP, IgG isotype (02-6102, *Thermo Fisher Scientific*) was used at the same conditions. Then, 100 µl of pre-blocked magnetic beads (*Dynabeads*, Thermofisher) were added and the incubation was continued at 4 °C for 4 h.

Total RNA extraction. Total RNA pools bound to AUF-1/control Ab were extracted adding TriFast reagent (*EuroClone*) directly to the washed beads, following the manufacturer's instructions. The size distribution of each RNA sample was assessed by running a 1 µl aliquot on an Agilent High Sensitivity RNA chip using an Agilent Technologies 2100 Bioanalyzer (*Agilent Technologies*). The concentration of each RNA sample was determined by using a Quant-IT RNA Assay Kit-High Sensitivity and a Qubit Fluorometer (*Life Technologies*).

Sequencing. Total RNA was used for the preparation of the sequencing library. Library preparation was performed as described[11]. Briefly, 1 µg of RNA Input and 300 ng of AUF-1- and Ctrl Ab-IP RNA were used as the starting material for sequencing library preparation from three independent experiments. Indexed triplicate libraries were prepared with a TruSeq Stranded Total RNA (*Illumina Inc.*). The qualitys of the libraries was evaluated by 2100 Bioanalyzer (*Agilent*) and Qubit dsDNA HS Assay Kit (*Thermo Fisher Scientific*). Libraries were sequenced at a concentration of 3 pM/lane (paired-end, 2 × 75 cycles) on a NextSeq 500 (*Illumina Inc.*).

Alignment to the human genome and quantification of gene signal. The Cutadapt software was used to remove the adapter sequences[12]. The quality of the sequenced reads was assessed by evaluating several factors such as the quality score, the presence of k-mers, the balance of the GC percentage, and an appropriate quality cutoff was set on these bases. Raw sequence files (.fastq files) were checked using FastQC software[13] after adapter trimming, as described[11]. The Human transcriptome and genome (assembly hg38) was used as a reference for the alignment, which was performed using STAR version 2.7.[14]

RIP-Seq data analysis. Feature-count was used to compute gene-level read counts.[15] Transcript per million (TPM) was computed using RSEM.[16] The R bioconductor package DESeq2 was used to test the differential expression of genes from RNA-Seq data[17]. The normalized sequencing data were compared with each other in order to avoid the unbalancing of the libraries, in terms of numbers of sequenced reads and other variables given by sequencing. Therefore, only the transcripts with significant differential expression greater than, or equal to, the chosen cutoff were considered. Only the genes whose read count was ≥ 10 in all samples were

considered. RNAs showing Enrichment Factor (EF) ≥ 1.5 and False Discovery Rate (FDR) ≤ 0.05 computed according to Benjamini–Hochberg were considered for further analysis.

Prediction of binding motifs. The p45[AUF-1] sequence from NCBI was used for analysis with CatRAPID algorithm.[18] The list of coding and non-coding targets of AUF-1 protein was filtered for Discriminative Power (DP). Enrichment ratios for every transcript in each of RIP-Seq experiments were log transformed. Graphics visualization was elaborated with R version 3.6.2 [19]. Prediction of binding motifs of AUF-1 was identified with Sequence & Structure Motif enrichment Analysis for Ranked RNA data generated from *in vivo* binding experiments (SMARTIV)[20,21].

Genome Ontology (GO) and pathway analyses. Gene Ontology (GO) was performed with Ingenuity Pathway Analysis (IPA) software[22].

For each Canonical Pathway, the z-score was calculated as described by Walter et al.[23] to predict the degree of activation or inhibition:

$$z-score = \frac{(\sum Up-regulated) - (\sum Down-regulated)}{\sqrt{N}}$$

Heatmaps and Pearson correlation matrices for correlated expression changes were generated using tMEV.

Statistical analysis. Data from Western blot densitometry were analyzed using Student's paired *t*-testA probability $p \leq 0.05$ was considered significant. Statistical analysis was performed using GraphPad Prism 5 (*GraphPad Software Inc.*). For statistical analyses, FDR was used (see "RIP-Seq data analysis" paragraph).

Results

Cytosolic extracts of BEAS-2B cells (n=3) were isolated and subjected to RIP (see Methods). AUF-1- and IgG control-associated RNAs were immunoprecipitated (IP AUF-1, IP IgG), along with a No-Ab IP to evaluate potential non-specific interactions during IP procedure. Input samples (Input) for each condition were also collected for the sequencing analysis. Western Blot analysis of the protein fraction (Figure 2) revealed a high level of enrichment in IP AUF-1 compared to IP IgG, No-Ab IP and unbound fractions (Unbounds) controls.
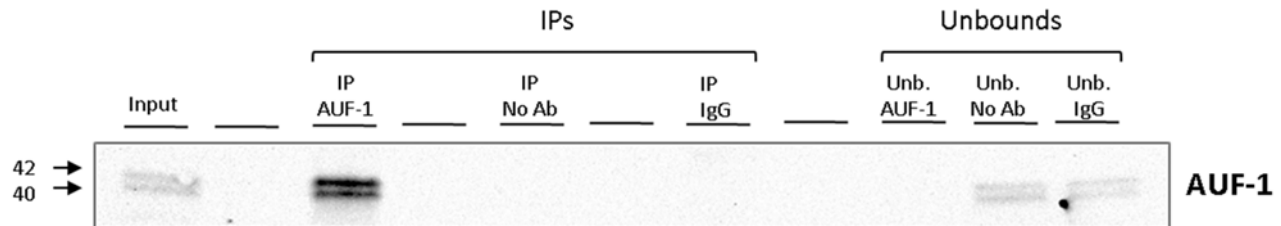
Figure 2. Representative Western Blot analysis (n=3) showing selective AUF-1 IP compared to controls. The Input samples (Input) were incubated with both AUF-1 and IgG antibodies (AUF-1 IP and IgG IP, respectively) and then immunoprecipitated with magnetic beads. An additional antibody-free control sample (no Ab) was performed.

Immunoprecipitated RNAs were fragmented and converted to complementary DNA (cDNA) after adaptor ligations, and then sequenced on an *Illumina* platform. An average of 27466311, 36765708 and 25288124 reads were obtained from the Input, AUF-1 IP and IgG IP libraries, respectively. Despite differences in total read numbers due to the low amount of Input cDNA, the IPs consistently yielded many more mappable reads than did the controls. Principal component analysis (PCA) showed that one of the biological replicates was discordant respect to the other two samples. For this reason, based on PCA results only two of the three original experiments were considered for further analysis (Figure 3).
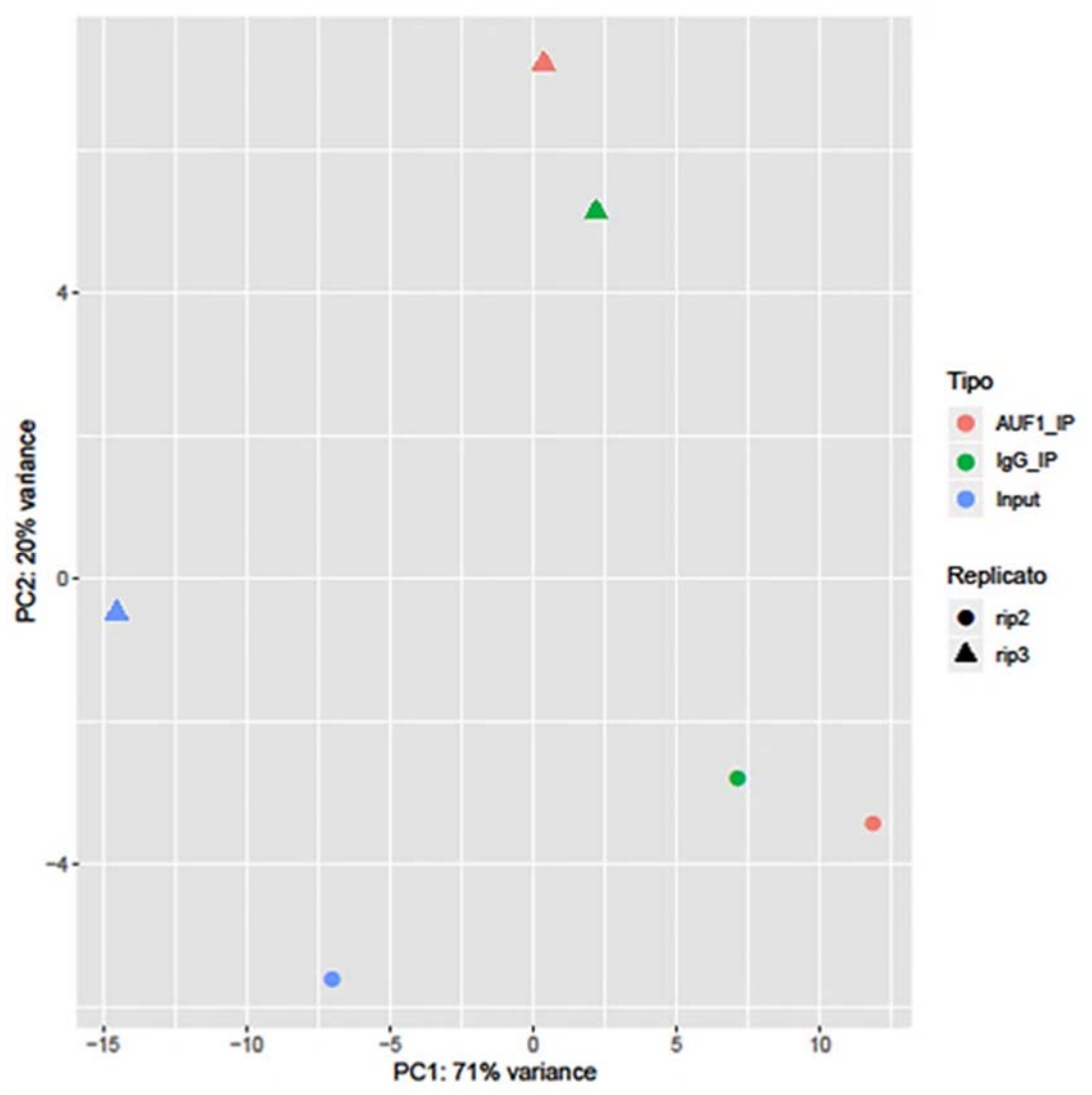
Figure 3. Principal component analysis (PCA) based on gene enrichment profile after sequencing, considering the two biological replicates of the AUF-1 IP, IgG IP and Input samples. The two principal components (PC) variables are shown on the two axes of the graph.

After normalization (see Methods) a total of 12,727 transcripts were expressed in the cell line in Input samples. Enrichment analysis was set with EF ratio vs Input at ≥ 1.5 and FDR ≤ 0.05.

To visualize the enrichment data, each sequenced transcript in the Input sample versus the IP samples were plotted. The scatter plot was constructed using the log-transformed and normalized read numbers (Figure 4).
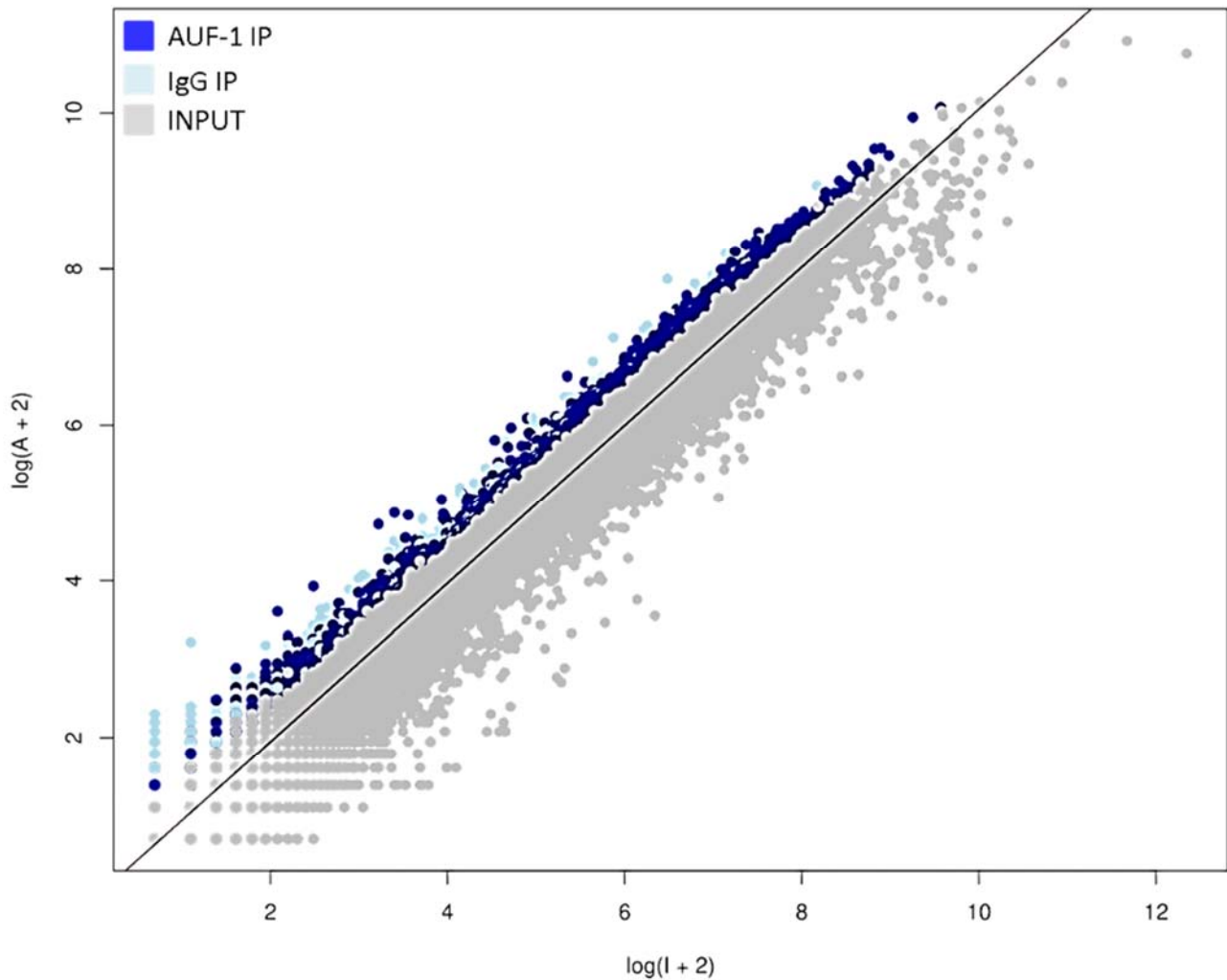
Figure 4. Scatter plot of RIP-Seq data. Read counts for AUF-1 IP, IgG and Input controls were normalized and log-transformed. Dark blue and light blu dots represent enriched AUF-1 IP and IgG targets (EF≥1.5 and FDR≤0.05), respectively. Gray dots represent background (Input). X and Y represent $\log_2$ read count in Input (X) and AUF-1 IP (Y).

With this cutoff, 1078 transcripts resulted as significantly immunoprencipitated in AUF-1 IP and 1149 transcripts in IgG IP samples. Subsequently, these transcripts were crossed (Figure 5) and overlapping targets were excluded. Only 494 AUF-1 IP-specific transcripts were therefore considered for further analysis. Table 1 lists the genes coding for the top ten AUF-1-bound transcripts by enrichment value; full list in Table S1).
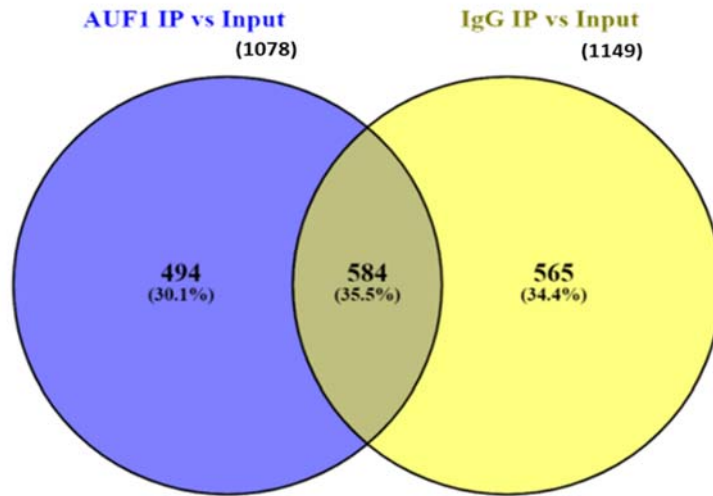
Figure 5. Venn diagram showing specific and common enriched transcript targets by comparison of AUF-1 IP-enriched and IgG-IP enriched vs Input (EF $\geq$ 1.5 and FDR $\leq$ 0.05).

For these selected targets, the average of reads enrichment was, as expected, significantly higher in AUF-1 IP compared to the Input and to IgG IP, while no difference in mean reads enrichment was found between the IgG IP and the Input (Figure 6).
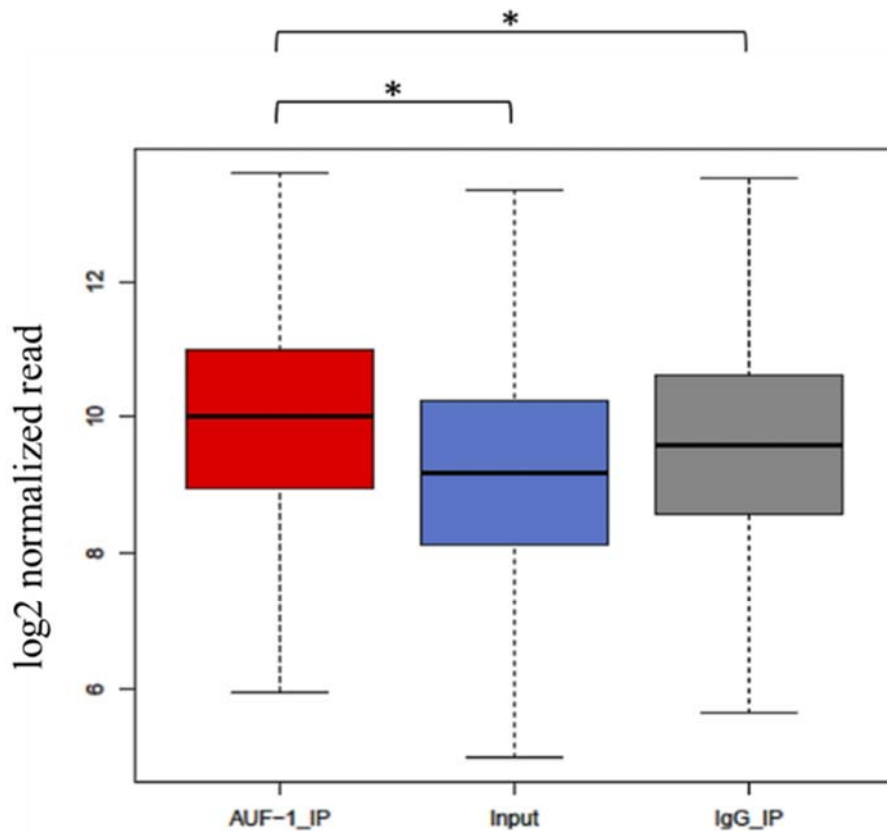
Figure 6. Boxplot showing the average enrichment of the 494 AUF-1 transcript targets in Input, AUF-1 IP and IgG IP samples. The average of the enrichment of the two biological replicates for each condition have been considered. Y represents the $\log_2$ of the normalized read count. *p-value $\leq$ 0.05(Student's t-test).

Table 1. Top ten genes with highest fold enrichment (FE, AUF-1 IP vs Input) in RIP-Seq experiments. Full list (n=494) in Supplementary Table S1.

GENE_SYMBOL	Complete Name	FE	FDR	Main Functions	Refs
PRR36	Proline Rich 36	5,73	0,020203	Unknown function	24
GLIS2	GLIS Family Zinc Finger 2	4,95	0,00745	Transcription factor	25,26
ZNF385A	Zinc Finger Protein 385A	4,4	5,15E-05	Zinc finger protein	27
TCF7L1	Transcription Factor 7 Like 1	4,14	0,003217	Mediator of Wnt signaling pathway	28-30
PIANP	PILR Alpha Associated Neural Protein	3,52	0,000871	Ligand for the paired immunoglobin-like type 2 receptor alpha	31,32
MBD6	Methyl-CpG Binding Domain Protein 6	3,42	2,49E-09	Binds to heterochromatin	33
MUC1	Mucin 1, Cell Surface Associated	3,37	1,81E-06	Binds to oligosaccharides by the extracellular domain	34-36
FOXP4	Forkhead Box P4	3,27	7,46E-05	Trascriptor factor	37,38
KDM6B	Lysine Demethylase 6B	3,2	0,000139	Lysine-specific demethylase	39,40
FBRSL1	Fibrosin Like 1	3,09	0,000336	Unknown function	41

The AUF-1-bound transcript pool (n=494 genes) was then subjected to computational analysis to map the main biological pathways putatively impacted by AUF-1 regulation and to identify the conserved binding elements through which the RBP binds.

Gene Ontology analysis showed several Canonical Pathways (CPs) involving the recognized AUF-1 regulated genes, such as cell growth and proliferation, gene expression modulation and corticosteroid response (Table 2 and S2).

Table 2. Selected list of significant Canonical Pathways (CPs) of AUF-1 targets obtained by IPA.

❖ **Ingenuity Canonical Pathways:**
❖ Glucocorticoid Receptor Signaling
❖ PPARα/RXRα Activation
❖ FAK Signaling
❖ Inosine-5'-phosphate Biosynthesis II
❖ Protein Ubiquitination Pathway
❖ PAK Signaling
❖ p53 Signaling
❖ EGF Signaling
❖ 2-ketoglutarate Dehydrogenase Complex
❖ TGF-β Signaling
❖ RAN Signaling
❖ HGF Signaling
❖ Clathrin-mediated Endocytosis Signaling
❖ CXCR4 Signaling
❖ Estrogen Receptor Signaling
❖ Synaptogenesis Signaling Pathway
❖ SAPK/JNK Signaling
❖ GNRH Signaling
❖ Actin Cytoskeleton Signaling
❖ TCA Cycle II (Eukaryotic)
❖ FGF Signaling
❖ IL-9 Signaling

❖ Hereditary Breast Cancer Signaling
❖ PDGF Signaling
❖ TNFR1 Signaling
❖ Signaling by Rho Family GTPases
❖ Assembly of RNA Polymerase I Complex
❖ Role of Tissue Factor in Cancer
❖ B Cell Receptor Signaling
❖ Molecular Mechanisms of Cancer
❖ IL-17A Signaling in Airway Cells
❖ CD40 Signaling
❖ ErbB Signaling
❖ CCR3 Signaling in Eosinophils
❖ Circadian Rhythm Signaling
❖ GM-CSF Signaling
❖ DNA Double-Strand Break Repair by Non-Homologous End Joining
❖ DNA Methylation and Transcriptional Repression Signaling
❖ ERK/MAPK Signaling
❖ Nitric Oxide Signaling in the Cardiovascular System
❖ Gα12/13 Signaling
❖ Human Embryonic Stem Cell Pluripotency
❖ IL-23 Signaling Pathway
❖ Estrogen-Dependent Breast Cancer Signaling
❖ Superpathway of Methionine Degradation

The interaction of AUF-1 with its target mRNAs has been shown to be mediated predominantly by motifs located in the 3′-UTR of the transcripts.[4,42-44] Therefore, we focused our analysis of enriched elements to the 3-′UTR of the bound targets. We screened the 494 epithelial AUF-1 targets for the occurrence of motifs using the SMARTIV tool. A group of 6 candidate motifs was derived from the experimental dataset but one motif in particular, mostly comprising GC nucleotides had the highest frequency of hits over the entire SMARTIV database (Figure 7).
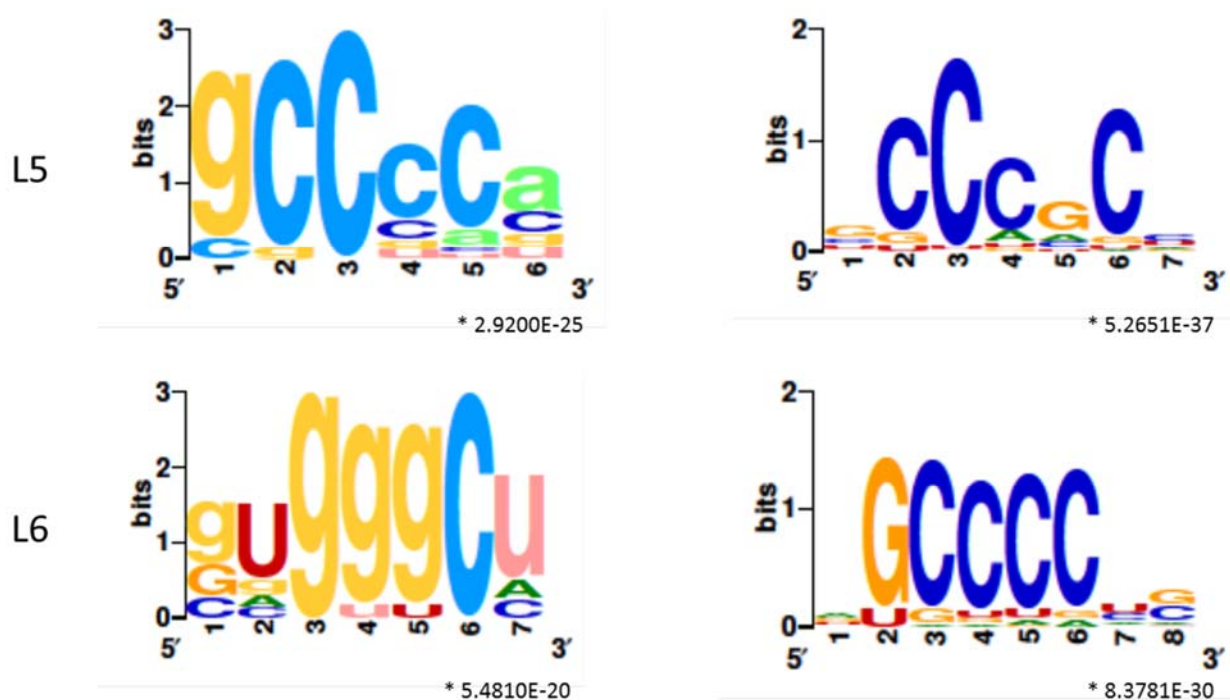
Figure 7. k-mer length 5 and 6 graphic logo generated by SMARTIV tool (see Methods) representing the probability matrix of the AUF-1 motif, showing the relative frequency of each nucleotide for each position within the motif sequence. The motif is originated from the experimental data set (n=494 AUF-1 transcripts) fobtained rom the RIP-Seq study. Upper and lower case alphabets show the secondary structure prediction (A,G,C,U for unpaired nucleotides and a,g,c,u for paired nucleotides). * p-value ≤ 0.05 [according to minimum hypergeometric statistical approach (mmHG)].

As a first validation approach, a list of genome-wide AUF-1 target transcripts (n= 3367) was derived *in silico* through the catRAPID tool (see Methods) choosing a DP ≥ 0.75 and TPM ≥ 0.5 as thresholds. From this list, only those expressed in the Input samples were selected and then compared with the experimental dataset. This approach identified 123 transcripts present in the Input dataset, of which 70 were shared with the transcripts of the RIP-Seq experimental dataset. Among these genes some transcripts of particular interest have emerged, such as Histone deacetylase 2 (HDAC2), a deacetylase critically involved in the suppression of inflammatory gene transcription (Figure 8).[45,46]
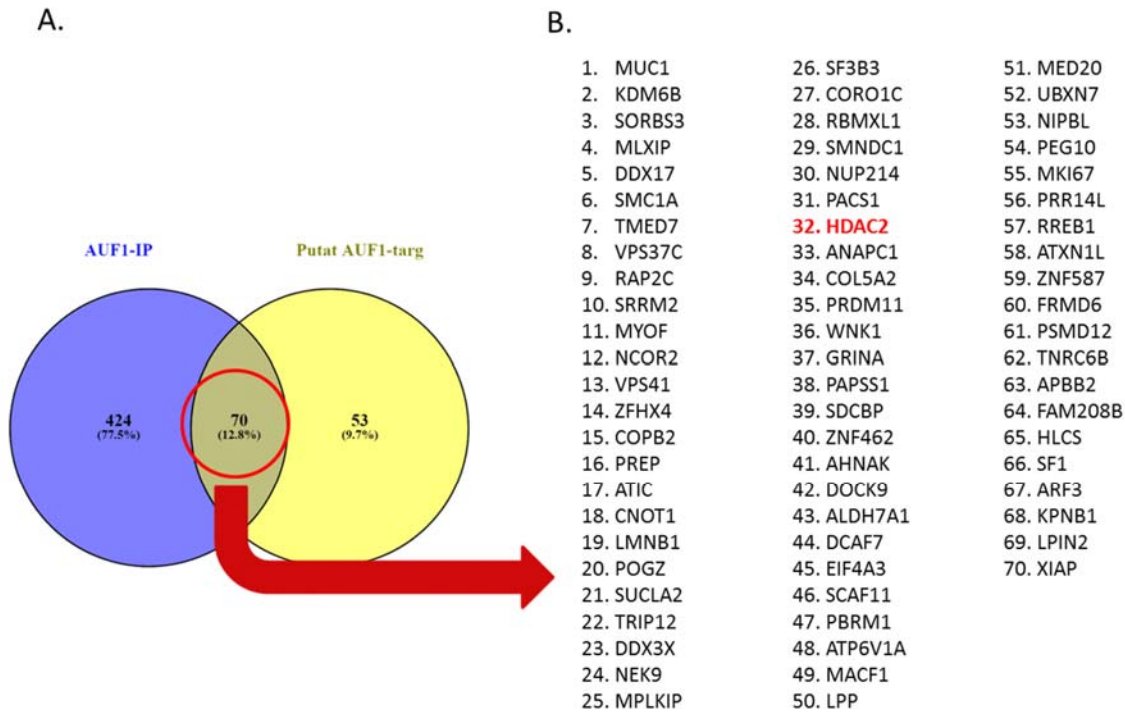
Figure 8. A. Venn diagram showing the crossing of AUF-1 IP dataset from RIP-Seq (blue) and putative AUF-1 targets obtained from Catrapid prediction (yellow). B. List of transcripts shared by the two lists. In red HDAC2, a gene of known interest for COPD pathogenesis, as example.

On these bases we are currently pursuing validation experiments in BEAS-2B cells, where we plan to confirm AUF-1 binding through RIP experiments associated to single-gene PCR and evaluate the impact of AUF-1 regulation through gene ablation, mRNA stability assays and other approaches. To gain a stronger biological rationale for the targets to choose for validation, we consulted again the GEO GSE5058 database, originally used to confirm loss of AUF-1 in airway epithelial cells obtained from COPD patients, to look for regulated expression of our 494 experimentally identified AUF-bound mRNAs.[47,48] We identified 450 of these transcripts as present in this database: considering significant changes in expression levels (FC value $\geq$ |1.5|, FDR $\leq$ 0.05) a number of them were indeed regulated: n= 19/450 (4.22%) in Smoker versus Non Smoker controls, 219/450 (49%) in COPD patients versus NS and 154/450 (34%) in COPD patients versus S. Table 3 shows selection of targets regulated in primary epithelium, as found in GEO GSE5058 database, listed according to the enrichment found in the RIP-Seq experiments. Based on this ranking, we will primarily select genes that resulted upregulated in conditions of AUF-1 loss, such as GLIS, FOXP4, IL-17R and HDAC2 (not shown in table, EF 1.7), examine their expression profile and mRNA stability upon inflammatory challenge (cytomix, cigarette smoke extract) and evaluate changes upon AUF-1 silencing. We will then consider other models of potential regulation by AUF-1 for downregulated genes (for example, translational repression). Lastly - and in support of this approach for choosing targets to validate experimentally – we found in GEO

GSE5058 that AUF-1 also targets 22 mRBPs (Table 4) differentially expressed in COPD vs. controls and that the top-upregulated RBP, ZFP36L2 is indeed a known target of AUF-1.[49]

Table 3. AUF-1 targets (listed as multiple probes covering different gene parts) derived by RIP-Seq analysis in BEAS-2B cells, ranked by Enrichment Factor (EF) ≥ 2.5 (column on the right, AUF-1 RIP targets) and their regulation in airway epithelium of COPD patients (COPD) versus no smoker (NS) and Smoker (S), derived from the GSE5058 database (Column on the right, GSE5058). FC = Fold change; FDR = False Discovery Rate, ER = Enrichment Factor. The red text denotes a statistically significant FDR ≤ 0.05. Bold characters denote an FC value ≤ -1.5 (green) and FC value ≥ 1.5 (red), respectively.

GeneName	Probe_ID	FC_S_vs_NS	FC_COPD_vs_NS	FC_COPD_vs_S	FDR_S_vs_NS	FDR_COPD_vs_NS	FDR_COPD_vs_S	EF_AUF1_vs_Input	FDR_AUF1_vs_Input
				GSE5058				AUF-1 RIP targets	
GLIS2	223378_at	-1.46	1.22	1.78	0.08928887	0.34273354	0.02071707	4.95	0.007449735
ZNF385A	226111_s_at	-1.20	1.68	2.02	0.42790438	0.00832359	0.11451765	4.4	0.0000515
TCF7L1	221016_s_at	-1.96	-1.78	1.10	0.00179558	0.00859051	0.24310109	4.14	0.003217425
MBD6	227833_s_at	-1.23	-1.20	1.02	0.10973763	0.12561105	0.32883218	3.42	2.49E-09
MBD6	226076_s_at	-1.91	-1.48	1.28	0.05469724	0.0726062	0.31316592	3.42	2.49E-09
MUC1	207847_s_at	-1.00	1.34	1.34	0.48110505	0.10555101	0.14564064	3.37	0.00000181
MUC1	213693_s_at	1.06	1.54	1.46	0.42097727	0.00149968	0.01571835	3.37	0.00000181
MUC1	211695_x_at	-1.36	1.29	1.76	0.42497027	0.09019573	0.08370628	3.37	0.00000181
FOXP4	227120_at	-1.19	1.72	2.06	0.47507268	0.03508035	0.06495909	3.27	0.0000746
KDM6B	213146_at	-1.35	-1.52	-1.12	0.40275949	0.08157529	0.24325563	3.2	0.000139227
KDM6B	1556067_a_at	-1.06	1.16	1.23	0.47013913	0.33964143	0.30437591	3.2	0.000139227
KDM6B	41387_r_at	-1.11	1.36	1.52	0.40152041	0.03324808	0.04793452	3.2	0.000139227
KDM6B	41386_i_at	-1.39	1.13	1.58	0.10632632	0.29301486	0.02344987	3.2	0.000139227
FBRSL1	225704_at	-1.51	-1.03	1.47	0.04256702	0.4412191	0.02811713	3.09	0.00033594
FBRSL1	225703_at	-1.96	-1.26	1.56	0.02550564	0.1913082	0.06703669	3.09	0.00033594
C1orf226	227019_at	-1.16	1.51	1.75	0.33595935	0.09780266	0.060771	2.86	0.039358298
CRTC1	207159_x_at	-1.11	1.37	1.52	0.43611132	0.34352464	0.27191588	2.73	0.001313828
ATXN2L	207798_s_at	1.47	-3.37	-4.96	0.40041597	0.15341746	0.10274981	2.6	1.37E-08
ATXN2L	201806_s_at	-1.45	-1.74	-1.20	0.35801664	0.23105094	0.42019401	2.6	1.37E-08
RNF44	203286_at	-1.18	1.16	1.38	0.29603832	0.0602814	0.07373776	2.6	0.000146243
KIAA1522	224746_at	-1.19	-1.03	1.16	0.3382488	0.39210982	0.37875129	2.58	1.23E-08
IL17RD	227997_at	-1.04	1.26	1.31	0.3604282	0.23841446	0.17006415	2.58	0.026678426
IL17RD	229263_at	1.51	3.64	2.40	0.48259696	0.04187032	0.04958724	2.58	0.026678426

Table 4. List of mRBPs (listed as probes covering different gene parts) found as significantly enriched in AUF-1 RIP-Seq, ranked by Enrichment Factor (EF) ≥ 1.5 (column on the right, AUF-1 RIP targets) and their regulation in airway epithelium of COPD patients (COPD) versus no smoker (NS) and Smoker (S), derived from the GSE5058 database (Column on the right, GSE5058). Note that upregulated ZFP36L2 is a known target of AUF-1. FC = Fold change; FDR = False Discovery Rate, ER = Enrichment Factor. The red text denotes a statistically significant FDR ≤ 0.05. Bold characters denote an FC value ≤ -1.5 (green) and FC value ≥ 1.5 (red), respectively.

GeneName	Probe_ID	FC_S_vs_NS	FC_COPD_vs_NS	FC_COPD_vs_S	FDR_S_vs_NS	FDR_COPD_vs_NS	FDR_COPD_vs_S	EF_AUF1_vs_Input	FDR_AUF1_vs_Input
DDX17	213998_s_at	-1.49	-46.27	-31.04	0.404338	0.0140181	0.0278978	2.13	0.00000631
DDX17	230180_at	1.17	-13.61	-15.92	0.352592	0.0001584	0.0254254	2.13	0.00000631
SON	201085_s_at	-1.03	-2.56	-2.49	0.499255	0.0017621	0.0232771	1.98	0.000718917
SRRM2	208610_s_at	-1.2	-4.28	-3.57	0.241551	0.0028941	0.0092905	1.96	0.0000829
SRRM2	1554671_a_at	1.39	-1.24	-1.73	0.230395	0.2456353	0.0490928	1.96	0.0000829
DHX36	223139_s_at	-1.07	-5.31	-4.96	0.38121	0.0004195	0.0030576	1.94	0.009783615
DHX36	223138_s_at	1.08	-2.58	-2.79	0.479051	0.0005561	0.0102221	1.94	0.009783615
DHX36	223140_s_at	1	-1.72	-1.72	0.479051	0.020492	0.0180915	1.94	0.009783615
DHX36	1559039_at	1.05	1.95	1.85	0.367387	0.0053674	0.0278978	1.94	0.009783615
SF3B4	209044_x_at	-1.33	1.13	1.51	0.157765	0.3772207	0.0379235	1.88	0.004953468
HNRNPM	200072_s_at	-1.01	-1.58	-1.56	0.338265	0.0009265	0.0161679	1.84	0.010043351
CNOT1	1554052_at	1.15	-2.07	-2.39	0.397312	0.0140181	0.0245646	1.82	0.000346861
G3BP2	206383_s_at	1.22	-1.44	-1.75	0.230395	0.0243383	0.0323169	1.78	0.002331774
G3BP2	208840_s_at	1.13	-1.46	-1.65	0.186348	0.0395403	0.0102221	1.78	0.002331774
YTHDC2	1568680_s_at	1.49	-2.24	-3.34	0.14654	0.0007806	0.0241358	1.77	0.045855155
YTHDC2	213077_at	-1.04	-1.81	-1.74	0.467076	0.0451012	0.0332428	1.77	0.045855155
DDX3X	212515_s_at	1.23	-2.09	-2.58	0.375965	0.025486	0.0190971	1.75	0.018266402
DDX3X	212514_x_at	1.29	-1.54	-1.98	0.189196	0.0474536	0.0345498	1.75	0.018266402
DHX40	222574_s_at	1.18	-1.84	-2.17	0.247381	0.0045273	0.0137857	1.74	0.019458974
EIF4G3	1554310_a_at	1.34	-1.28	-1.71	0.142925	0.2878268	0.0499241	1.66	0.005624005
EIF4G3	201935_s_at	1.56	1.03	-1.52	0.010468	0.0919914	0.0323119	1.66	0.005624005
RBM15	1555760_a_at	-1.09	-1.71	-1.57	0.379516	0.0057604	0.0152375	1.65	0.026375426
ZFP36L2	201369_s_at	-1.09	2.08	2.27	0.275643	0.0224596	0.0143254	1.65	0.042907908
SCAF11	209376_x_at	1.13	-12.7	-14.4	0.382279	0.0000081	0.0142029	1.64	0.031544378
SCAF11	213850_s_at	1.26	-4.84	-6.11	0.365262	0.0000272	0.0171338	1.64	0.031544378
RANBP2	201711_x_at	1.57	-2.64	-4.15	0.186498	0.0008907	0.017659	1.64	0.019228686
SCAF11	1570507_at	-1.09	-3.15	-2.88	0.467129	0.014375	0.0275015	1.64	0.031544378
RANBP2	201712_s_at	1.11	-1.93	-2.15	0.36093	0.0137568	0.0114609	1.64	0.019228686
SETX	201965_s_at	1.3	-1.56	-2.02	0.146125	0.0166961	0.0155975	1.64	0.018608842
RANBP2	201713_s_at	1.17	-1.6	-1.88	0.319399	0.0450322	0.0230986	1.64	0.019228686
SCAF11	225336_at	-1.01	-1.89	-1.87	0.43975	0.0265162	0.0275015	1.64	0.031544378
SETX	201964_at	1.1	-1.68	-1.85	0.253103	0.0041782	0.0092905	1.64	0.018608842
SETX	232229_at	1.7	-1.06	-1.8	0.126396	0.3128	0.0282626	1.64	0.018608842
RANBP2	226922_at	1.11	-1.55	-1.71	0.375965	0.0483165	0.0286315	1.64	0.019228686
SCAF11	235579_at	-1.04	-1.6	-1.54	0.390845	0.0172984	0.0390701	1.64	0.031544378
SYNCRIP	209024_s_at	1.68	-2.16	-3.64	0.106247	0.0005547	0.0092905	1.57	0.048276717
TNRC6B	229036_at	1.26	-2.93	-3.7	0.253541	0.0007262	0.0107368	1.55	0.026787535
TNRC6B	228998_at	-1.05	-2.53	-2.4	0.467076	0.0071551	0.0245646	1.55	0.026787535
TNRC6B	213254_at	1.22	-1.29	-1.57	0.14654	0.0586954	0.0175076	1.55	0.026787535
TNRC6B	1558142_at	1.02	1.79	1.76	0.187295	0.008306	0.0200034	1.55	0.026787535
SF1	210172_at	-1.78	-9.07	-5.09	0.218881	0.0244725	0.0269621	1.54	0.020991399
KPNB1	208974_x_at	-1.15	-2.28	-1.98	0.496762	0.0002102	0.0142154	1.53	0.037058081
PUM2	201493_s_at	-1.04	-1.75	-1.68	0.311061	0.0021999	0.0204315	1.51	0.031875996
PUM2	216221_s_at	-1.05	-1.73	-1.65	0.140212	0.0014364	0.0106904	1.51	0.031875996

References

1. Glisovic T, Bachorik JL, Yong J, Dreyfuss G. RNA-binding proteins and post-transcriptional gene regulation. *FEBS Lett.* 2008;582(14):1977-1986.

2. Barreau C, Paillard L, Osborne HB. AU-rich elements and associated factors: are there unifying principles? *Nucleic Acids Res.* 2005;33(22):7138-7150.

3. White EJF, Matsangos AE, Wilson GM. AUF-1 regulation of coding and noncoding RNA. *Wiley Interdiscip Rev RNA.* 2017;8(2):e1393.

4. Moore AE, Chenette DM, Larkin LC, Schneider RJ. Physiological networks and disease functions of RNA-binding protein AUF-1. *Wiley Interdiscip Rev RNA.* 2014;5(4):549-564.

5. Sadri N, Schneider RJ. AUF-1/Hnrnpd-Deficient Mice Develop Pruritic Inflammatory Skin Disease. *J Investig Dermatol Symp Proc.* 2009;129(3):657-670.

6. Ricciardi L, Dal Col J, Conti V, et al. Differential expression of RNA-binding proteins in airway epithelium in chronic lung inflammation. *Allergy.* 2017;42(S103)::3–127.

7. Gagliardi M, Matarazzo MR. RIP: RNA Immunoprecipitation. *Methods Mol Biol.* 2016: 1480:73-86.

8. Mimura I, Nangaku M. Next-Generation Sequencing (NGS) in Biomarker Discovery and Applications in Nephrology. *Biomarkers in Kidney Disease.* 2015:1-21.

9. Fan J, Ishmael FT, Fang X, et al. Chemokine transcripts as targets of the RNA-binding protein HuR in human airway epithelium. *J Immunol.* 2011;186(4):2482-2494.

10. Keene JD, Komisarow JM, Friedersdorf MB. RIP-Chip: the isolation and identification of mRNAs, microRNAs and protein components of ribonucleoprotein complexes from cell extracts. *Nat Protoc.* 2006;1(1):302-307.

11. Tarallo R, Giurato G, Bruno G, et al. The nuclear receptor ERbeta engages AGO2 in regulation of gene transcription, RNA splicing and RISC loading. *Genome Biol.* 2017;18(1):189.

12. Martin M. Cutadapt removes adapter sequences from high-throughput sequencing reads. *EMBnet J.* 2011;17(1):3.

13. Andrews S. FastQC: a quality control tool for high throughput sequence data. 2010; http://www.bioinformatics.babraham.ac.uk/projects/fastqc.

14. Dobin A, Davis CA, Schlesinger F, et al. STAR: ultrafast universal RNA-seq aligner. *Bioinformatics.* 2013;29(1):15-21.

15. Liao Y, Smyth GK, Shi W. featureCounts: an efficient general purpose program for assigning sequence reads to genomic features. *Bioinformatics.* 2014;30(7):923-930.

16. Li B, Dewey CN. RSEM: accurate transcript quantification from RNA-Seq data with or without a reference genome. *BMC Bioinformatics.* 2011;12(1):323.

17. Love MI, Huber W, Anders S. Moderated estimation of fold change and dispersion for RNA-seq data with DESeq2. *Genome Biol.* 2014;15(12):550.

18. Agostini F, Zanzoni A, Klus P, Marchese D, Cirillo D, Tartaglia GG. catRAPID omics: a web server for large-scale prediction of protein-RNA interactions. *Bioinformatics.* 2013;29(22):2928-2930.

19. R: Avaible at: https://www.r-project.org/

20. Polishchuk M, Paz I, Yakhini Z, Mandel-Gutfreund Y. SMARTIV: combined sequence and structure de-novo motif discovery for in-vivo RNA binding data. *Nucleic Acids Res.* 2018;46(W1):W221-W228.

21. Polishchuk M, Paz I, Kohen R, Mesika R, Yakhini Z, Mandel-Gutfreund Y. A combined sequence and structure based method for discovering enriched motifs in RNA from in vivo binding data. *Methods.* 2017;118-119:73-81.

22. Kramer A, Green J, Pollard J, Jr., Tugendreich S. Causal analysis approaches in Ingenuity Pathway Analysis. *Bioinformatics.* 2014;30(4):523-530.

23. Walter W, Sanchez-Cabo F, Ricote M. GOplot: an R package for visually combining expression data with functional analysis. *Bioinformatics.* 2015;31(17):2912-2914.

24. https://www.genecards.org/cgi-bin/carddisp.pl?gene=PRR36 PG-GPPPAAa.

25. Attanasio M, Uhlenhaut NH, Sousa VH, et al. Loss of GLIS2 causes nephronophthisis in humans and mice by increased apoptosis and fibrosis. *Nat Genet.* 2007;39(8):1018-1024.

26. Jetten AM. GLIS1–3 transcription factors: critical roles in the regulation of multiple physiological processes and diseases. *Cell Mol Life Sci.* 2018;75(19):3473-3494.

27. https://www.genecards.org/cgi-bin/carddisp.pl?gene=ZNF385A ZAGZAPZAAAa.

28. Murphy M, Chatterjee SS, Jain S, Katari M, DasGupta R. TCF7L1 Modulates Colorectal Cancer Growth by Inhibiting Expression of the Tumor-Suppressor Gene EPHB3. *Sci Rep.* 2016;6(1):28299.

29. Shan J, Shen J, Wu M, et al. Tcf7l1 Acts as a Suppressor for the Self-Renewal of Liver Cancer Stem Cells and Is Regulated by IGF/MEK/ERK Signaling Independent of β-Catenin. *S tem Cells.* 2019;37(11):1389-1400.

30. Sierra RA, Hoverter NP, Ramirez RN, et al. TCF7L1 suppresses primitive streak gene expression to support human embryonic stem cell pluripotency. *Development.* 2018;145(4):dev161075.

31. https://www.genecards.org/cgi-bin/carddisp.pl?gene=PIANP PGPPPAAa.

32. Kogure A, Shiratori I, Wang J, Lanier LL, Arase H. PANP is a novel O-glycosylated PILRα ligand expressed in neural tissues. *Biochem Biophys Res Commun.* 2011;405(3):428-433.

33. https://www.genecards.org/cgi-bin/carddisp.pl?gene=MBD6 MGMPMAAa.

34. Milara J, Díaz-Platas L, Contreras S, et al. MUC1 deficiency mediates corticosteroid resistance in chronic obstructive pulmonary disease. *Respir Res.* 2018;19(1):226.

35. Nath S, Mukherjee P. MUC1: a multifaceted oncoprotein with a key role in cancer progression. *Trends Mol Med.* 2014;20(6):332-342.

36. Kato K, Lillehoj EP, Lu W, Kim KC. MUC1: The First Respiratory Mucin with an Anti-Inflammatory Function. *J Clin Me.* 2017;6(12).

37. Kim J-H, Hwang J, Jung JH, Lee H-J, Lee DY, Kim S-H. Molecular networks of FOXP family: dual biologic functions, interplay with other molecules and clinical implications in cancer progression. *Mol Cancer.* 2019;18(1):180.

38. Co M, Anderson AG, Konopka G. FOXP transcription factors in vertebrate brain development, function, and disorders. *Wiley Interdiscip Rev Dev Biol.* 2020;n/a(n/a):e375.

39. Wijayatunge R, Liu F, Shpargel KB, et al. The histone demethylase Kdm6b regulates a mature gene expression program in differentiating cerebellar granule neurons. *Mol Cell Neurosci.* 2018;87:4-17.

40. Burchfield JS, Li Q, Wang HY, Wang R-F. JMJD3 as an epigenetic regulator in development and disease. *TInt J Biochem Cell Biol.* 2015;67:148-157.

41. https://www.genecards.org/cgi-bin/carddisp.pl?gene=FBRSL1 FGFPFAAa.

42. Yoon JH, De S, Srikantan S, et al. PAR-CLIP analysis uncovers AUF-1 impact on target RNA fate and genome integrity. *Nat Commun.* 2014;5:5248.

43. Wagner BJ, DeMaria CT, Sun Y, Wilson GM, Brewer G. Structure and Genomic Organization of the Human AUF-1 Gene: Alternative Pre-mRNA Splicing Generates Four Protein Isoforms. *Genomics.* 1998;48(2):195-202.

44. Zucconi BE, Wilson GM. Assembly of Functional Ribonucleoprotein Complexes by AU-rich Element RNA-binding Protein 1 (AUF-1) Requires Base-dependent and -independent RNA Contacts. *J Biol Chem.* 2013;288(39):28034-28048.

45. Fang W-F, Chen Y-M, Lin C-Y, et al. Histone deacetylase 2 (HDAC2) attenuates lipopolysaccharide (LPS)-induced inflammation by regulating PAI-1 expression. *J Inflamm.* 2018;15(1):3.

46. Barnes PJ. Role of HDAC2 in the Pathophysiology of COPD. *Annu Rev Physiol.* 2009;71(1):451-464.

47. Carolan BJ, Heguy A, Harvey BG, Leopold PL, Ferris B, Crystal RG. Up-regulation of expression of the ubiquitin carboxyl-terminal hydrolase L1 gene in human airway epithelium of cigarette smokers. *Cancer Res.* 2006;66(22):10729-10740.

48. Ricciardi L, Col JD, Casolari P, et al. Differential expression of RNA-binding proteins in bronchial epithelium of stable COPD patients. *Int J Chron Obstruct Pulmon Dis.* 2018;13:3173-3190.

49. Kedar VP, Zucconi BE, Wilson GM, Blackshear PJ. Direct binding of specific AUF-1 isoforms to tandem zinc finger domains of tristetraprolin (TTP) family proteins. *J Biol Chem.* 2012;287(8):5459-5471.

Table S1. Experimental targets list of the RIP-Seq (n=494). EF = Enrichment Factor, FDR = False Discovery Rate

GENE_SYMBOL	EF	FDR	GENE_SYMBOL	EF	FDR	GENE_SYMBOL	EF	FDR
PRR36	5,73	0,020203	DIO2	1,77	0,007614	PDE1C	1,6	0,010379
GLIS2	4,95	0,00745	DOCK4	1,77	0,017798	PKM	1,6	0,028566
ZNF385A	4,4	5,15E-05	ERC1	1,77	0,009031	QSER1	1,6	0,032528
TCF7L1	4,14	0,003217	ERF	1,77	0,013416	UBXN7	1,6	0,009406
PIANP	3,52	0,000871	MCM10	1,77	0,026995	ZNF281	1,6	0,043779
MBD6	3,42	2,49E-09	MTR	1,77	0,007964	ABL2	1,59	0,011266
MUC1	3,37	1,81E-06	NOL11	1,77	0,044104	C2CD3	1,59	0,029498
FOXP4	3,27	7,46E-05	POLR1A	1,77	0,028233	CLASP1	1,59	0,023914
KDM6B	3,2	0,000139	POM121	1,77	0,006086	FN1	1,59	0,031621
FBRSL1	3,09	0,000336	TRERF1	1,77	0,005063	ICE1	1,59	0,025196
C1orf226	2,86	0,039358	TRPS1	1,77	0,02826	LRPPRC	1,59	0,048861
AP001972.5	2,84	0,032884	TSPYL1	1,77	0,001935	NIPBL	1,59	0,029242
STX1B	2,83	0,012534	YTHDC2	1,77	0,045855	NRIP1	1,59	0,015232
CRTC1	2,73	0,001314	ARFGEF3	1,76	0,025196	PAK2	1,59	0,010016
AL513165.1	2,66	0,034496	CSTF2T	1,76	0,020999	PHF20	1,59	0,023516
ATXN2L	2,6	1,37E-08	DDX1	1,76	0,029098	RGP1	1,59	0,017329
RNF44	2,6	0,000146	DMXL1	1,76	0,003715	TAF2	1,59	0,047451
IL17RD	2,58	0,026678	FASTKD2	1,76	0,042233	UBR4	1,59	0,010492
KIAA1522	2,58	1,23E-08	TRIP12	1,76	0,00196	ADAT1	1,58	0,037967
HIVEP3	2,47	0,000702	WDR47	1,76	0,024643	GLI3	1,58	0,034866
RNF165	2,46	0,026659	ACADM	1,75	0,010333	GNA12	1,58	0,037128
MNT	2,45	0,000654	ATG2B	1,75	0,003324	KPNA6	1,58	0,043402
BICRA	2,43	0,011555	BAG3	1,75	0,019395	MAP1B	1,58	0,025353
SYNPO	2,43	8,11E-07	DDX3X	1,75	0,018266	MAPK14	1,58	0,030753
RIN3	2,42	0,005946	ERCC6L	1,75	0,028489	NEU3	1,58	0,041545
ZBTB7A	2,42	0,001117	HSP90AA1	1,75	0,023752	PAN3	1,58	0,020557
AL158212.3	2,38	0,020718	MINPP1	1,75	0,042958	PEG10	1,58	0,017043
ZFHX2	2,37	0,04323	NEK9	1,75	0,015949	RFX7	1,58	0,022644
AL365181.3	2,3	0,004542	SYT16	1,75	0,044134	SIPA1L2	1,58	0,046799
ZNF697	2,3	0,043455	TOP2B	1,75	0,007066	SMAD3	1,58	0,014242
SORBS3	2,29	0,000841	WDR36	1,75	0,04438	THUMPD1	1,58	0,038338
AKAP12	2,27	0,000177	COPA	1,74	0,041701	TP53BP2	1,58	0,037967
LINC01963	2,25	0,011995	DHX40	1,74	0,019459	USP40	1,58	0,043165
ZNF555	2,25	0,002913	DMXL2	1,74	0,021561	BHLHE40	1,57	0,04742
PPP1R13L	2,24	0,000906	DOP1A	1,74	0,037632	CRYBG1	1,57	0,026855
NFIX	2,19	0,000846	EPG5	1,74	0,016524	MIEF1	1,57	0,032281
CREB3L1	2,18	0,038525	GIT2	1,74	0,013925	MKI67	1,57	0,021889
TGFB1	2,16	0,003603	KLHL24	1,74	0,013386	PAFAH1B1	1,57	0,011198
EGR1	2,15	0,00016	MPLKIP	1,74	0,024103	PJA2	1,57	0,04553
FRMD4B	2,15	0,047394	POLR3A	1,74	0,017697	PRR14L	1,57	0,01896
MLXIP	2,15	0,002861	PTK2B	1,74	0,037832	RAB11FIP1	1,57	0,020592
PER1	2,15	0,00825	SF3B3	1,74	0,027771	RREB1	1,57	0,042637

GENE_SYMBOL	EF	FDR	GENE_SYMBOL	EF	FDR	GENE_SYMBOL	EF	FDR
AC037459.3	2,14	0,032596	URB1	1,74	0,01869	STXBP1	1,57	0,02617
CRNKL1	2,14	0,005231	ADGRL1	1,73	0,023475	SYNCRIP	1,57	0,048277
DDX17	2,13	6,31E-06	BEND3	1,73	0,039406	TMPO	1,57	0,020991
RERE	2,13	2,14E-05	CORO1C	1,73	0,003582	AAK1	1,56	0,030407
AC012513.3	2,12	0,037906	CRKL	1,73	0,002197	ATXN1L	1,56	0,039925
CPNE8	2,11	0,019199	EED	1,73	0,028789	DICER1	1,56	0,026375
SMC1A	2,09	0,000554	FBXO11	1,73	0,017493	GBF1	1,56	0,039763
UBR5	2,09	1,57E-05	GCH1	1,73	0,020541	GJA1	1,56	0,043402
FAM98B	2,07	0,002364	IREB2	1,73	0,004428	PCNX1	1,56	0,024485
SF3A2	2,07	0,004451	PAICS	1,73	0,002123	PXN	1,56	0,023271
CAMTA2	2,06	0,004478	RBMXL1	1,73	0,012451	ZNF587	1,56	0,035882
NFATC2IP	2,06	4,41E-05	RNF111	1,73	0,039845	ANKRD17	1,55	0,049895
SVEP1	2,06	0,010826	SMNDC1	1,73	0,014471	ARHGEF7	1,55	0,045818
WDR3	2,06	0,007161	CHD1	1,72	0,022644	FRMD6	1,55	0,019485
ZXDA	2,06	0,033232	FAM222B	1,72	0,033972	MECP2	1,55	0,045722
CDC42EP1	2,05	0,003648	MAMLD1	1,72	0,020665	PSMD12	1,55	0,035743
POLR1B	2,05	0,001552	NPEPPS	1,72	0,012968	RBPJ	1,55	0,028668
SCARNA7	2,05	0,001451	NUP214	1,72	0,032662	TFCP2	1,55	0,046532
TMEM178B	2,05	0,017907	PACS1	1,72	0,0035	TNRC6B	1,55	0,026788
LIG4	2,04	0,012687	PLS3	1,72	0,027236	TUBGCP4	1,55	0,042235
NPTXR	2,03	0,016856	PTPN14	1,72	0,001692	APBB2	1,54	0,020718
YLPM1	2,03	0,0003	AP1G1	1,71	0,005593	CAND1	1,54	0,049007
FAM120C	2,02	0,013125	CPSF7	1,71	0,004825	FAM208B	1,54	0,02591
IRS2	2,01	0,003319	DNAJC13	1,71	0,011256	HIF1AN	1,54	0,021424
BCL3	2	0,016054	MED12	1,71	0,00733	HLCS	1,54	0,045645
DAGLA	2	0,017176	MIB1	1,71	0,003195	NSD3	1,54	0,023881
RAB14	2	0,000195	NHLRC2	1,71	0,013803	SF1	1,54	0,020991
SUPT16H	2	0,009683	RAB3B	1,71	0,001753	ARF3	1,53	0,024611
TMED7	2	0,001526	RALGAPB	1,71	0,012032	ARHGAP21	1,53	0,030715
ZMIZ2	2	0,003344	RAPH1	1,71	0,002963	HPS3	1,53	0,035819
ZNF888	2	0,027102	STK35	1,71	0,008742	KMT2A	1,53	0,035849
CBX5	1,99	6,46E-05	ZBTB10	1,71	0,016877	KPNB1	1,53	0,037058
SAMD9L	1,99	0,019229	DNMBP	1,7	0,030715	LPIN2	1,53	0,035849
VPS37C	1,99	0,01312	DOCK5	1,7	0,002992	NR2C2	1,53	0,036826
ZNF221	1,99	0,033232	GPATCH8	1,7	0,020406	PSME4	1,53	0,023595
COL12A1	1,98	0,002492	HDAC2	1,7	0,017493	SMARCC1	1,53	0,043732
HNRNPH2	1,98	0,009816	PDCD4	1,7	0,019496	SWAP70	1,53	0,029709
MARCKS	1,98	0,00108	WDR11	1,7	0,026166	TNKS2	1,53	0,028566
NECTIN1	1,98	0,003359	ABCD3	1,69	0,013297	VPS26A	1,53	0,049267
SMC3	1,98	0,006401	ANAPC1	1,69	0,011066	XIAP	1,53	0,038949
SMG8	1,98	0,005702	COL5A2	1,69	0,026243	ZNF609	1,53	0,025731
SON	1,98	0,000719	DYNC1H1	1,69	0,011245	BMPR2	1,52	0,044307
HSD17B4	1,97	0,012356	FAM160A1	1,69	0,030753	GLG1	1,52	0,049989
RAP2C	1,97	0,001002	HEATR6	1,69	0,031621	MICAL2	1,52	0,023687
TET3	1,97	0,00108	KIAA1109	1,69	0,013803	PPP3CA	1,52	0,029034

GENE_SYMBOL	EF	FDR	GENE_SYMBOL	EF	FDR	GENE_SYMBOL	EF	FDR
BRD4	1,96	0,001236	SAMD4B	1,69	0,012752	BPTF	1,51	0,03306
POM121C	1,96	0,000586	VIRMA	1,69	0,024321	NEDD4L	1,51	0,037268
SRRM2	1,96	8,29E-05	ATP6V1B2	1,68	0,024643	PUM2	1,51	0,031876
TOP1	1,96	0,007066	CTNNA1	1,68	0,037269	RBM12	1,51	0,048281
AL031587.5	1,95	0,011276	DDX46	1,68	0,033733	USP13	1,51	0,032808
EPN1	1,95	0,005678	DNMT1	1,68	0,045856	VPS13D	1,51	0,044307
MAST4	1,95	0,04438	FBXO38	1,68	0,046632	DOCK1	1,5	0,032698
MYOF	1,95	0,001451	GLCCI1	1,68	0,021442	PDPR	1,5	0,045776
DHX36	1,94	0,009784	MAST3	1,68	0,022542			
NCOR2	1,94	0,01749	MYO6	1,68	0,045818			
SLFN11	1,93	0,002032	NF1	1,68	0,006862			
TMEM8B	1,93	0,030496	SRGAP1	1,68	0,014568			
ACTR6	1,92	0,038294	TEAD3	1,68	0,023595			
FOXJ2	1,92	0,001315	TUG1	1,68	0,010064			
NATD1	1,92	0,007202	USP14	1,68	0,026166			
NUP160	1,92	0,024106	WNK1	1,68	0,003319			
PSAT1	1,92	0,004771	BLMH	1,67	0,011218			
VPS41	1,92	0,002647	GRINA	1,67	0,014701			
ZFHX4	1,92	0,000304	ITPR2	1,67	0,037847			
ADAMTSL4	1,91	0,015213	MYO1E	1,67	0,044752			
EIF5B	1,91	0,013755	NOL9	1,67	0,023025			
ELFN2	1,91	0,022742	NT5DC3	1,67	0,00686			
TRIP4	1,91	0,028566	PAK4	1,67	0,044413			
CCDC120	1,9	0,048041	PAPSS1	1,67	0,048926			
DCAF1	1,9	0,007427	PIKFYVE	1,67	0,007311			
LEMD3	1,9	0,007714	RAP1GAP2	1,67	0,028754			
MCCC2	1,9	0,009406	TRAF6	1,67	0,029498			
USP9X	1,9	0,000813	ZNF148	1,67	0,006623			
BRWD3	1,89	0,001032	APOBEC3C	1,66	0,023025			
COL4A6	1,89	0,048614	APOOL	1,66	0,030843			
DDX20	1,89	0,024583	ATXN1	1,66	0,017697			
EFTUD2	1,89	0,018566	CYB5RL	1,66	0,04387			
MYO5A	1,89	0,000363	DDHD1	1,66	0,018784			
PLAGL1	1,89	0,007338	EIF4G3	1,66	0,005624			
SART3	1,89	0,004504	LRBA	1,66	0,010908			
GRAMD1B	1,88	0,012766	MAP3K9	1,66	0,031094			
SF3B4	1,88	0,004953	MAVS	1,66	0,027521			
TRIM13	1,88	0,00447	MED13	1,66	0,004775			
CEBPZ	1,87	0,006399	N4BP2	1,66	0,044454			
CLTC	1,87	0,004478	SDCBP	1,66	0,011202			
COPB2	1,87	0,018715	TCEAL9	1,66	0,016357			
GEMIN5	1,87	0,027269	TRIM14	1,66	0,014761			
NKRF	1,87	0,016649	ZNF462	1,66	0,006012			
PLAGL2	1,87	0,002967	AHNAK	1,65	0,004293			
AR	1,86	0,009351	DOCK9	1,65	0,009985			
GTF3C1	1,86	0,012556	MTHFR	1,65	0,043674			

GENE_SYMBOL	EF	FDR	GENE_SYMBOL	EF	FDR
KLHL28	1,86	0,024761	NARS	1,65	0,049028
MTHFD1	1,86	0,022111	NIF3L1	1,65	0,026166
NCAPD3	1,86	0,007964	PDS5B	1,65	0,017191
NPRL3	1,86	0,011963	PFKFB2	1,65	0,048243
PIK3R4	1,86	0,020724	PHIP	1,65	0,037967
WDR7	1,86	0,013386	RANBP6	1,65	0,04022
AASDH	1,85	0,042012	RBM15	1,65	0,026375
ANKFY1	1,85	0,00301	SRP54	1,65	0,049409
CHD9	1,85	0,001472	TBL1X	1,65	0,026678
CTPS1	1,85	0,007537	TULP3	1,65	0,036366
DLST	1,85	0,001575	ZFP36L2	1,65	0,042908
FBXO30	1,85	0,004943	ALDH7A1	1,64	0,014021
MDGA1	1,85	0,043779	CBLL1	1,64	0,048504
TRIM5	1,85	0,018156	CCDC82	1,64	0,043851
ZNF607	1,85	0,025731	DCAF7	1,64	0,010168
AARS	1,84	0,011116	EIF4A3	1,64	0,034914
ARID2	1,84	0,002333	FAM168A	1,64	0,006668
HNRNPM	1,84	0,010043	KIF24	1,64	0,028489
MMP24OS	1,84	0,005863	MDN1	1,64	0,041353
NEURL1B	1,84	0,002201	PML	1,64	0,023736
PREP	1,84	0,005009	PRMT6	1,64	0,048848
PRICKLE2	1,84	0,005593	RANBP2	1,64	0,019229
PROSER3	1,84	0,011712	SCAF11	1,64	0,031544
AC004943.2	1,83	0,043402	SETX	1,64	0,018609
FAM160B1	1,83	0,003045	TAF1	1,64	0,01499
FIGN	1,83	0,005163	TANC2	1,64	0,004497
SEC24D	1,83	0,01381	ZBED5	1,64	0,045056
THRA	1,83	0,009064	MPHOSPH8	1,63	0,042752
ATIC	1,82	0,011266	MYNN	1,63	0,048625
CAMK1D	1,82	0,009148	PALLD	1,63	0,00675
CNOT1	1,82	0,000347	PBRM1	1,63	0,014761
IBA57	1,82	0,040616	SBNO1	1,63	0,013508
KBTBD7	1,82	0,040506	SEMA3A	1,63	0,026078
RECQL	1,82	0,030015	ZNF765	1,63	0,033282
RNF20	1,82	0,030753	ZNF845	1,63	0,045805
RPAP3	1,82	0,020991	ZSWIM6	1,63	0,012968
VAPB	1,82	0,000414	ATP6V1A	1,62	0,042774
ZNF219	1,82	0,035867	ERCC6	1,62	0,028489
CRYBG3	1,81	0,019199	MAP3K1	1,62	0,024063
LMNB1	1,81	0,00929	METTL16	1,62	0,01558
NACC2	1,81	0,009609	MPP5	1,62	0,019258
PIK3C2A	1,81	0,005266	NCOR1	1,62	0,02023
RUNX3	1,81	0,032767	SELENON	1,62	0,016313
ZBTB21	1,81	0,004685	SIK3	1,62	0,019111
BMS1	1,8	0,033384	SPATA13	1,62	0,049615
DLD	1,8	0,012046	SRPRA	1,62	0,022284

GENE_SYMBOL	EF	FDR	GENE_SYMBOL	EF	FDR
PLRG1	1,8	0,033329	BIRC6	1,61	0,028575
POGZ	1,8	0,001353	HELLS	1,61	0,031652
ZNF106	1,8	0,000631	IGF1R	1,61	0,016693
ZNF551	1,8	0,021424	LIG3	1,61	0,032138
AMIGO2	1,79	0,027058	MACF1	1,61	0,014615
ASXL2	1,79	0,002797	MAT2A	1,61	0,038683
DENND4C	1,79	0,015438	NCOA6	1,61	0,016198
MYORG	1,79	0,042896	PDP1	1,61	0,026678
NHS	1,79	0,034874	RTCB	1,61	0,042896
TSC22D4	1,79	0,024377	RUNX1	1,61	0,021062
CCNK	1,78	0,018413	SPRED2	1,61	0,0298
DOCK7	1,78	0,042714	TSC22D2	1,61	0,020438
G3BP2	1,78	0,002332	USP34	1,61	0,009784
SEC23IP	1,78	0,037567	DDX21	1,6	0,043779
SUCLA2	1,78	0,015724	FTO	1,6	0,049895
TOPORS	1,78	0,014124	LPP	1,6	0,013544
UBR3	1,78	0,016497	MED20	1,6	0,032051
WDFY3	1,78	0,001371	NAV2	1,6	0,027014

Table S2. Full list of significant Canonical Pathways (CP) obtained by IPA of 494 AUF-1 targets identified by RIP-Seq.

1. TR/RXR Activation
2. Paxillin Signaling
3. RANK Signaling in Osteoclasts
4. Glucocorticoid Receptor Signaling
5. PPARα/RXRα Activation
6. FAK Signaling
7. Folate Transformations I
8. Germ Cell-Sertoli Cell Junction Signaling
9. RAR Activation
10. Inosine-5'-phosphate Biosynthesis II
11. Protein Ubiquitination Pathway
12. Renin-Angiotensin Signaling
13. Mitotic Roles of Polo-Like Kinase
14. PAK Signaling
15. p53 Signaling
16. EGF Signaling
17. 2-ketoglutarate Dehydrogenase Complex
18. Lysine Degradation II
19. Lysine Degradation V
20. TGF-β Signaling
21. RAN Signaling
22. HGF Signaling
23. Clathrin-mediated Endocytosis Signaling
24. Rac Signaling
25. CXCR4 Signaling
26. Estrogen Receptor Signaling
27. Role of NFAT in Cardiac Hypertrophy
28. Integrin Signaling
29. Synaptogenesis Signaling Pathway
30. SAPK/JNK Signaling
31. GNRH Signaling
32. Chronic Myeloid Leukemia Signaling
33. Actin Cytoskeleton Signaling
34. Mouse Embryonic Stem Cell Pluripotency
35. Role of Osteoblasts, Osteoclasts and Chondrocytes in Rheumatoid Arthritis
36. TCA Cycle II (Eukaryotic)
37. FGF Signaling
38. Leucine Degradation I
39. Renal Cell Carcinoma Signaling
40. Reelin Signaling in Neurons
41. Osteoarthritis Pathway
42. IL-9 Signaling
43. Hereditary Breast Cancer Signaling
44. PDGF Signaling
45. Purine Nucleotides De Novo Biosynthesis II
46. TNFR1 Signaling
47. Acute Myeloid Leukemia Signaling
48. Signaling by Rho Family GTPases
49. Assembly of RNA Polymerase I Complex
50. Role of Tissue Factor in Cancer
51. B Cell Receptor Signaling
52. Molecular Mechanisms of Cancer
53. IL-17A Signaling in Airway Cells
54. CD40 Signaling
55. ErbB Signaling
56. CCR3 Signaling in Eosinophils
57. Circadian Rhythm Signaling
58. GM-CSF Signaling
59. Aryl Hydrocarbon Receptor Signaling
60. DNA Double-Strand Break Repair by Non-Homologous End Joining
61. Amyotrophic Lateral Sclerosis Signaling
62. DNA Methylation and Transcriptional Repression Signaling
63. ERK/MAPK Signaling
64. Nitric Oxide Signaling in the Cardiovascular System
65. Gα12/13 Signaling
66. Human Embryonic Stem Cell Pluripotency
67. IL-23 Signaling Pathway
68. Neuropathic Pain Signaling In Dorsal Horn Neurons
69. Choline Degradation I
70. Sulfate Activation for Sulfonation
71. Angiopoietin Signaling
72. Estrogen-Dependent Breast Cancer Signaling
73. Superpathway of Methionine Degradation
74. Cardiac Hypertrophy Signaling

d. Final considerations: study limitations and future directions

Study limitations.

In this thesis we set to characterize the expression profile of mRBPs in two major human chronic lung inflammatory diseases – COPD and bronchial asthma – and evaluate their functional role in models of disease pathogenesis. The limits of the studies performed pertain both to the general approach as well as to specific problems encountered along the use of experimental procedures: as we aimed at integrating different laboratory techniques and bioinformatic tools, we often found ourselves facing problems that concerned both specific protocols at the bench as well as aspects of the *in silico* analysis.

- ✓ First of all, the limited number of patients enlisted in the first and second study indicates the need to examine a larger sample number in independent patient/control cohorts.
- ✓ A deeper clinical characterization of the study populations would help the identification of potential links between phenotypic characteristics and molecular signatures. In particular, for both the first and second study we have no data for COPD patients regarding alpha-1-antitrypsin deficiency, length of smoking history or time from smoking cessation, history of exacerbation; in the second study for bronchial asthma, we have no information on smoking status or severe asthma phenotype (es. eosinophilic vs. neutrophilic, associated with obesity, etc); the evaluation of patients with milder asthma could also be important to add, for example to confirm a potential role of RBP modulation by glucocorticoid therapy so far identified in human airway epithelium *in vitro*;
- ✓ Future studies may include the inclusion of well-phenotyped subjects with other respiratory diseases, including idiopathic pulmonary fibrosis and sarcoidosis, which are associated with distinct inflammatory responses;
- ✓ In our first study, the incomplete silencing of the AUF-1 protein we achieved should be overcome through the development of cells with stable loss of AUF-1 gene. To this end, CRISPR-Cas9 technique could be used to develop airway epithelial KO cell line, in which perform RNA-seq to gain a deeper characterization of AUF-1-related transcriptomic changes in this cell type.
- ✓ The use of human primary bronchial epithelial cells will be necessary also for *in vitro* studies, to validate and expand the knowledge on the expression of RBPs found in human samples.
- ✓ In the third study, discrepancy in PCA analysis among the three biological replicates of immunoprecipitation experiments in BEAS-2B cells may due to the use of cells of different passages, or by the different lot of anti-AUF1 antibody used. The use of bioinformatic tools capable of removing the batch effect may be considered.

Future directions.

Studies on the biology of the RBPs regulating the fate of protein-coding RNAs, both at basic level and increasingly in translational settings, indicate the powerful impact of these regulatory factors in coordinating the expression of multiple genes participating to a disease process. On these basis, our general aim is to identify the role of RBP-dependent gene regulation in chronic lung inflammatory responses. Much of this aim is still being tested by work in progress, and the discussed limitations we encountered so far are contributing to improve the design of our upcoming studies and shape future directions. Following are mayor points we intend to pursue:

1. Studies in patients and controls: studies in independent patient/control COPD and SA cohorts with larger sample number, with deeper clinical characterization of the study populations. Moreover, biopsy samples could be interrogated more in depth by setting up newly developed, single-cell techniques, such as single cell sequencing, *in situ* imaging and proteome profiling. These techniques could help identify, directly in human samples, the type and state of epithelial cell most involved, and provide proteome-wide information on protein states and interactions occurring in vivo in disease states vs. controls.

2. Studies in vitro: in the short term, in vitro studies will address, for the third study in progress, validation of AUF-1-bound targets followed by functional characterization of AUF-1 regulation using dedicated gene KO and phenotype rescue cellular models. Using medium- throughput screenings of reporter constructs bearing AUF-1 targets 3'-UTRs, we could probe for the first time a disease-derived, functionally verified pool of transcripts coordinately regulated in sequence-specific fashion by an RBP. This set can be probed by compound libraries for drug screening in appropriate assays. On medium term, development of tissue-specific transgenic/KO animal models will be desirable. For the second study, validation of the observed RBP expression patterns will be pursued in our BEAS-2B *in vitro* challenge models, as well as characterization of RBP coexpression patterns will be our next task.

3. Studies in silico:

a. The use of more sophisticated metadata and bioinformatics tools, such as GSVA, to corroborate the analysis done so far and in larger datasets we need to analyze to confirm the RBP-associated gene signatures we found so far;

b. Our search for RBP role in COPD and SA transcriptomic databases will need to be conducted also for the growing body of non-conventional RBPs. For the second study, in fact, we probed the airway epithelial transcriptome in COPD and SA datasets using a list of RBPs selected on the basis of canonical RBDs (Gerstberger et al Nat Rev Genet 2014). However, further investigations will need expand the study to other RBPs that contain no conventional RBDs (Hentze Nat Rev Mol Cell Biol 2018), which have been increasingly identified in human RNA interactome studies. Like canonical RBPs, these RBPs also have

RNA binding activity but hold several functions, such enzymatic activity in different metabolic pathways or in RNA-modification; their role in human epithelial biology is currently unknown.

c. the significant differences between COPD and SA RBP profiles will need to be further defined. One aspect to be investigated could be whether in SA there are changes related more to RBP binding rather than changes in RBP levels. This entails the study of RBP interactome rather than that of expression levels, concurrent with whole proteome, as well as consideration of assays probing RBP PTMs in human samples or cell lines.

Overall, validation RBP-associated targets and RBP profiles and characterization of functional outcomes will allow to study how altered post-transcriptional processes shape epithelial cell phenotype, how they contribute to disease or altered response to treatment, and whether this alteration can be used as a biomarker or targeted for therapeutics. It is our hope that on the long term, preclinical evidences may be translated to clinical research on severe asthma and COPD and conceptually transferable to other chronic inflammatory lung diseases.